

1978

Petrogenesis Of Some Peralkaline And Non-peralkaline Post-tectonic Granites In The Arabian Shield, Kingdom Of Saudi Arabia

Abdulaziz A. Radain

Follow this and additional works at: <https://ir.lib.uwo.ca/digitizedtheses>

Recommended Citation

Radain, Abdulaziz A., "Petrogenesis Of Some Peralkaline And Non-peralkaline Post-tectonic Granites In The Arabian Shield, Kingdom Of Saudi Arabia" (1978). *Digitized Theses*. 1119.
<https://ir.lib.uwo.ca/digitizedtheses/1119>

This Dissertation is brought to you for free and open access by the Digitized Special Collections at Scholarship@Western. It has been accepted for inclusion in Digitized Theses by an authorized administrator of Scholarship@Western. For more information, please contact tadam@uwo.ca, wlsadmin@uwo.ca.

 National Library of Canada

Cataloguing Branch
Canadian Theses Division

Ottawa, Canada
K1A 0N4

Bibliothèque nationale du Canada

Direction du catalogage
Division des thèses canadiennes

NOTICE

The quality of this microfiche is heavily dependent upon the quality of the original thesis submitted for microfilming. Every effort has been made to ensure the highest quality of reproduction possible.

If pages are missing, contact the university which granted the degree.

Some pages may have indistinct print especially if the original pages were typed with a poor typewriter ribbon or if the university sent us a poor photocopy.

Previously copyrighted materials (journal articles, published tests, etc.) are not filmed.

Reproduction in full or in part of this film is governed by the Canadian Copyright Act, R.S.C. 1970, c. C-30. Please read the authorization forms which accompany this thesis.

**THIS DISSERTATION
HAS BEEN MICROFILMED
EXACTLY AS RECEIVED**

AVIS

La qualité de cette microfiche dépend grandement de la qualité de la thèse soumise au microfilmage. Nous avons tout fait pour assurer une qualité supérieure de reproduction.

S'il manque des pages, veuillez communiquer avec l'université qui a conféré le grade.

La qualité d'impression de certaines pages peut laisser à désirer, surtout si les pages originales ont été dactylographiées à l'aide d'un ruban usé ou si l'université nous a fait parvenir une photocopie de mauvaise qualité.

Les documents qui font déjà l'objet d'un droit d'auteur (articles de revue, examens publiés, etc.) ne sont pas microfilmés.

La reproduction, même partielle, de ce microfilm est soumise à la Loi canadienne sur le droit d'auteur, SRC 1970, c. C-30. Veuillez prendre connaissance des formules d'autorisation qui accompagnent cette thèse.

**LA THÈSE A ÉTÉ
MICROFILMÉE TELLE QUE
NOUS L'AVONS REÇUE**

PETROGENESIS OF SOME PERALKALINE AND NON-PERALKALINE
POST-TECTONIC GRANITES IN THE ARABIAN SHIELD,
KINGDOM OF SAUDI ARABIA

by

Abdulaziz A.M. Radain

Department of Geology

Submitted in partial fulfillment
of the requirements for the degree of
Doctor of Philosophy

Faculty of Graduate Studies
The University of Western Ontario
London, Ontario
March, 1978

© Abdulaziz A.M. Radain 1978

بِسْمِ اللَّهِ الرَّحْمَنِ الرَّحِيمِ

الحمد لله رب العالمين

والصلاة والسلام على سيدنا محمد وآله

بسم

الحمد لله رب العالمين

والصلاة والسلام على سيدنا محمد وآله

ABSTRACT

Four post-tectonic granitic plutons occur within a northerly trending rectangle 60 x 47 km at the northeast corner of the Southern Hijaz quadrangle in the Precambrian Arabian Shield, 470 km northeast of Jeddah, Saudi Arabia. The area is between latitudes 23°21'N and 23°52'N, and longitudes 40°55'E and 41°26'E.

Field, petrographical and geochemical studies of these plutons support a division of them into two main groups:

1. Non-peralkaline granites which include calc-alkaline Albari granite, and the peraluminous Alse-Hairah granite and biotite granite of the Hadb-Aldyaheen complex. Granites of this group are 600 to 650 m.y. old, are hypidiomorphic in texture, and consist primarily of oligoclase, microperthite, quartz and biotite. Mineralogically and chemically they are comparable to normal calc-alkaline granites and to young granites throughout the Arabian Shield. Their origin is attributed to partial melting of lower crust above a subduction zone with some mixing of crustal material and andesitic magma derived from subducted material.

2. Peralkaline granites which include the granite porphyry and riebeckite granite of the Hadb-Aldyaheen ring complex and the riebeckite granite of Jabal Sayid.

8

Granites of this group are 505 to 570 m.y. old, are high-level magmatic intrusions, and constitute the last granitic phase of the Pan-African thermal event and the development of the Arabian Shield. There is a notable absence of any contemporaneous mafic plutons. These granites are hypidior-morphic to porphyric in texture; riebeckite and aegirine are the principal mafic minerals. The plagioclase is almost pure albite and the K-feldspar is microcline (Or 96%) and microcline-perthite. Late growth and recrystallization of microcline and quartz in the riebeckite granites are evident. Chemically, they have large SiO_2 and total Fe, and small Ca, Mg and Al abundances, Na_2O , K_2O are not abnormally abundant for granitic rocks. In general major element oxides do not vary systematically with increasing SiO_2 , D.I. and D.I. + ac + ns. There is a significant enrichment in Nb, Zr, Y and Rb and depletion in Ba and Sr relative to crustal averages and to normal granites. Distribution of most trace elements except Ba and Sr is erratic, and no trends relative to major element distribution or the alkalinity index (A.I.) are evident. Values of ^{18}O are + 10% to + 16 ‰, which are considerably greater than the + 8‰ of the associated older non-peralkaline granite. However, although spatially related, the peralkaline granites appear to be unrelated genetically to older non-peralkaline granites of the area.

The present data exclude a genesis of the peralkaline granites by magmatic differentiation alone. Rather, origin of these granites is attributed to contamination of extremely differentiated granitic magma derived by partial melting of the continental crust and late stage metasomatism by residual fluid. Contamination was accomplished by either massive influx of ^{18}O rich sediments or hot saline water, but the available information does not permit distinction between the two.

ACKNOWLEDGEMENTS

I would like to gratefully acknowledge the support of the King Abdulaziz University which generously provided financial support for this study. I am deeply grateful to Dr. A.O. Nasseef whose encouragement is responsible for my completion of this work. Particular thanks goes to my thesis supervisor, Professor W.S. Fyfe, who was a constant source of help during the course of research and writing. I would like, also, to thank Dr. R.W. Hodder who provided continuous encouragement and invaluable advice. I am also grateful to Dr. R. Kerrich who carried out the oxygen isotope analyses; R.L. Barnett who did the electron microprobe analyses, and also Dr. H. Hunter for his assistance in the whole rock analyses and John Forth for preparation of thin sections. Mrs. Judy Blackwell did the typing.

I wish at this time to remember my mother, who provided a particular sense of purpose to my work, but unfortunately did not live to see it completed.

TABLE OF CONTENTS

	Page
CERTIFICATE OF EXAMINATION.....	ii
ABSTRACT.....	iii
ACKNOWLEDGEMENTS.....	vi
TABLE OF CONTENTS.....	vii
LIST OF FIGURES AND PLATES.....	xi
LIST OF TABLES.....	xvi
CHAPTER 1 - INTRODUCTION.....	1
1.1 General Statement.....	1
1.2 Statement of the Problem.....	2
1.3 Location and Access.....	3
1.4 Previous Work.....	3
1.5 Techniques of Present Study.....	6
CHAPTER 2 - THE ARABIAN SHIELD.....	7
2.1 General Statement.....	7
2.2 Structure.....	7
2.3 General Stratigraphy.....	10
2.4 Tectonism and Plutonism.....	15
CHAPTER 3 - THE YOUNGER GRANITES IN THE NORTHEAST CORNER OF THE SOUTHERN HIJAZ QUADRANGLE.....	23
3.1 General Statement.....	23
3.2 Albari Granite.....	26

	Page
3.2.1 Geologic Setting.....	26
3.2.2 Petrography.....	33
History of Crystallization.....	37
3.3 Alse-Hairah Granite.....	38
3.3.1 Geologic Setting.....	38
3.3.2 Petrography.....	41
History of Crystallization.....	48
3.4 Jabal Sayid Riebeckite Granite.....	49
3.4.1 Geologic Setting.....	50
3.4.2 Petrography.....	56
3.5 Hadb-Aldyaheen Ring Complex.....	62
3.5.1 Geologic Setting.....	62
3.5.2 Biotite Granite.....	66
3.5.2.1 Petrography.....	66
3.5.3 Microgranite.....	69
3.5.3.1 Petrography.....	70
3.5.4 Granite Porphyry.....	73
3.5.4.1 Petrography.....	75
3.5.5 Riebeckite Granite.....	84
3.5.5.1 Petrography.....	91
 CHAPTER 4 - PETROCHEMISTRY.....	 101
4.1 General Statement.....	101
4.2 Chemical Classification.....	102
4.2.1 Albari Granite.....	102
4.2.2 Alse-Hairah Granite.....	103
4.2.3 Jabal Sayid Riebeckite Granite.....	103
4.2.4 Hadb-Aldyaheen Ring Complex.....	104

	Page
4.3 Major Element Abundances.....	108
4.3.1 Albari Granite.....	108
4.3.2 Alse-Hairah Granite.....	112
4.3.3 Jabal Sayid Riebeckite Granite.....	115
Summary.....	121
4.3.4 Hadb-Aldyahéen Ring Complex.....	122
Summary.....	125
4.4 Trace Element Abundances.....	137
4.4.1 General Statement.....	137
4.4.2 Rubidium.....	137
4.4.3 Niobium.....	150
4.4.4 Zirconium.....	155
4.4.5 Yttrium.....	160
4.4.6 Barium and Strontium.....	163
4.4.7 Summary.....	172
CHAPTER 5 - OXYGEN ISOTOPE AND FLUID INCLUSION.....	174
5.1 Oxygen Isotope Relations.....	174
5.2 Fluid Inclusion.....	176
Results.....	176
CHAPTER 6 - PETROGENESIS, TECTONICS AND	
CONCLUSIONS.....	179
6.1 General Statement.....	179
6.2 Tectonic Model.....	187
APPENDIX A - METHODS.....	196

	Page
APPENDIX B - ELEMENT ABUNDANCES.....	205
APPENDIX C - MICROPROBE ANALYSES.....	213
BIBLIOGRAPHY.....	230
VITA.....	246

LIST OF FIGURES AND PLATES

Figure	Description	Page
1	Location Map.....	4
2	Generalized geologic map of the Arabian Shield..	9
3	Geologic Framework of the Arabian Peninsula.....	12
4	Generalized geologic map of Southern Hijaz Quadrangle.....	23
5	Satellite photograph of the Four Plutons.....	25
6	Geologic map of Albari granite.....	27
7	Modal classification of Albari granite.....	35
8	Geologic map of Alse-Hairah granite.....	40
9	Modal classification of Alse-Hairah granite.....	45
10	Geologic map of Jabal Sayid riebeckite granite..	51
11	Modal classification of Jabal Sayid granite.....	59
12	Geologic map of Hadb-Aldyaheen ring complex.....	63
13	Modal classification of rocks forming Hadb- Aldyaheen complex.....	83
14	Normative classification of the rocks of the four plutons.....	105
15	Normative classification of the rocks of the four plutons.....	106
16	Alkalinization index diagram for Albari granite.	107
17	Harker silica variation diagram for Albari granite.....	110

Figure	Description	Page
18	Fe total, Mg and Ca against felsic index for Albari and Alse-Hairah granite.....	111
19	Harker silica variation diagram for Alse-Hairah granite.....	114
20	Harker silica variation diagram for Jabal Sayid granite.....	117
21	Total alkalies against SiO_2 for the granitic rocks from the four plutons.....	119
22	Differentiation index against SiO_2 , CaO, Fe_2O_3 for Albari, Alse-Hairah and Jabal Sayid granites.....	119
23	Differentiation index against Na_2O , K_2O	120
24	Harker silica variation diagram for the biotite granite and microgranite of Hadb-Aldyaheen.....	123
25	Harker silica variation diagram of Hadb-Aldyaheen granite porphyry.....	126
26	Harker silica variation diagram of Hadb-Aldyaheen riebeckite granite.....	130
27	Differentiation index against SiO_2 , CaO, Fe total for Albari granite and granites of Hadb-Aldyaheen ring complex.....	132
28	Differentiation index against Na_2O , K_2O and Al_2O_3	133
29	Differentiation index plus (ac)+(ns) against SiO_2 , CaO, Fe total for Jabal Sayid riebeckite	

Figure	Description	Page
	granite and rocks forming Hadb-Aldyaheen ring complex.....	134
30	Differentiation index plus $(ac) + (ns)$ against Na_2O , K_2O and Al_2O_3	135
31	K against Rb for granitic rocks of the four plutons.....	146
32	K/Rb against A.I. for granitic rocks of the four plutons.....	147
33	K/Rb against D.I. for granitic rocks of the four plutons.....	149
34	Nb against Na for Jabal Sayid granite and the rocks of Hadb-Aldyaheen ring complex.....	151
35	Nb against A.I.....	152
36	Nb against TiO_2 for the granitic rocks from the four plutons.....	154
37	Zr against SiO_2 for the granitic rocks from the four plutons.....	156
38	Zr against A.I. for the granitic rocks from the four plutons.....	157
39	Y against A.I. for Jabal Sayid granite and the rocks of Hadb-Aldyaheen ring complex.....	159
40	Y against Zr.....	160
41	Sr against Ca for the granitic rocks from the four plutons.....	164
42	Sr against Rb.....	165

Figure	Description	Page
43	Ba against Sr for Albari and Alse-Hairah granites.....	166
44	Ba against Sr for Hadb-Aldyaheen ring complex rocks.....	167
45	Ba/Sr against A.I. for Jabal Sayid granite and rocks of Hadb-Aldyaheen ring complex.....	168
46	Ba, Sr and Rb against SiO ₂ for Albari, Alse-Hairah and Hadb-Aldyaheen biotite granites.....	170
47	Ba, Sr and Rb against SiO ₂ for Jabal Sayid granite and rocks of Hadb-Aldyaheen ring complex.....	171
48	A schematic tectonic model.....	189

Plate	Description	Page
1.	Figures showing the geologic features of thin section photographs of Albari granite.....	32
2	Figures showing the geologic features and thin section photographs of Alse-Hairah granite.....	43
3.	Figures showing the geologic features of Jabal Sayid riebeckite granite.....	54
4	Thin section photographs of Jabal Sayid riebeckite granite.....	61

Plate	Description	Page
5	Figures showing the geologic features of Hadb-Aldyaheen ring complex.....	72
6	Thin section photographs of the microgranite and the granite porphyry of Hadb-Aldyaheen ring complex.....	77
7	Thin section photographs of the granite porphyry of Hadb-Aldyaheen ring complex.....	80
8,9	Figures showing the geologic features of the riebeckite granite of Hadb-Aldyaheen ring complex.....	86, 90
10,11	Handspecimen and thin section photographs of the riebeckite granite of Hadb-Aldyaheen ring complex.....	94, 99

LIST OF TABLES

Table	Description	Page
1	PreCambrian formations, tectonism, plutonism and volcanism in the Arabian Shield.....	11
2	Stratigraphy, orogenic events and plutonic rocks, Southern part of the Arabian Shield.....	17
3	Modal composition of Albari Granite.....	34
4	Modal composition of Alse-Hairah Granite.....	44
5	Modal composition of Jabal Sayid riebeckite granite.....	58
6	Modal composition of Hadb-Aldyaheen biotite granite.....	68
7	Modal composition of Hadb-Aldyaheen granite porphyry.....	81
8	Modal composition of Hadb-Aldyaheen riebeckite granite.....	92
9	Average chemical composition of Albari granite..	109
10	Average chemical composition of Alse-Hairah granite.....	113
11	Average chemical composition of Jabal Sayid riebeckite granite.....	116
12	Average chemical composition of Hadb-Aldyaheen biotite granite and microgranite.....	124
13	Average chemical composition of Hadb-Aldyaheen granite porphyry.....	127

Table	Description	Page
14	Average chemical composition of Hadb-Aldyaheen riebeckite granite.....	129
15	Average trace element abundances of Albari granite.....	138
16	Average trace element abundances of Alse-Hairah granite.....	139
17	Average trace element abundances of Hadb-Aldyaheen biotite granite and microgranite.....	140
18	Average trace element abundances of Hadb-Aldyaheen granite porphyry.....	141
19	Average trace element abundances of Hadb-Aldyaheen riebeckite granite.....	142
20	Average trace element abundances of Jabal Sayid riebeckite granite.....	143
21	Average trace element abundances for the four plutons and Taylor's averages.....	144
22	Oxygen isotope analysis.....	175
23	Average major element abundances of Jabal Sayid granite and rocks of Hadb-Aldyaheen ring complex.....	180
24	Average trace element abundances of Jabal Sayid granite and rocks of Hadb-Aldyaheen ring complex.....	182
25	Comparison between the Nigerian Younger granites and peralkaline granites of Southern Hijaz Quadrangle.....	184

CHAPTER 1

INTRODUCTION

1.1 General Statement

The Kingdom of Saudi Arabia is 2,150,000 km² in area; roughly a quarter of this is the Arabian Shield which is part of the Arabian-Nubian Shield, a geological entity of more than 2 million km² that extends through the Arabian Peninsula, northern Somalia, Ethiopia, Sudan and Egypt. The Arabian Shield consists approximately of 40% plutonic rocks which intrude basement gneiss and volcanic and volcano-clastic rocks.

The basement is overlain by volcanic rocks which are dominantly basaltic. These are overlain by a thick series of andesitic volcanic rocks, with rhyolite appearing at the top. This layered sequence concludes with Late Precambrian to Early Paleozoic units in which the proportion of sedimentary rocks increases upward and rhyolite gives way to minor andesite and basalt. The regional metamorphism is green schist facies (Brown, 1972; Schmidt and others, 1973; Greenwood and others, 1976).

Plutonic rocks, which appear in part to be the intrusive equivalents of volcanic rocks, cover an age range

of 490 to 1,100 m.y. Most are 520 to 620 m.y. old (Brown, 1972; Fleck et al., 1976), or synchronous with the Pan African orogeny (Brown, 1970, 1972; Clifford, 1967, 1968, 1970; Black and Girod, 1970). These rocks can be grouped into 5 phases of plutonic activity at 960, 800, 785, 650 to 600 and 570 to 550 m.y. ago (Greenwood et al., 1976). The earlier phases are primarily dioritic rocks which have calcic affinities whereas later phases are dominantly granodiorite to granite in composition with calc-alkalic affinity. However, a subordinate number of the late phases have alkalic and peralkalic modal trends and mineralogy (Brown et al., 1962; Brown, 1972; Greenwood and Brown, 1973).

This thesis is concerned with the late phases of plutonic activity, post tectonic, and 490 to 600 m.y. old and hence in the age range of the Pan-African orogeny. They appeared from previous work to be irregular stocks to small batholiths, circular plugs, cone sheets and ring structure and tabular bodies within faults. They are essentially calc-alkalic, alkalic and peralkalic.

1.2 Statement of the problem

The purpose of this thesis is threefold:

- 1) A documentation of the geology, petrography and chemistry of the late phase granitic rocks in the Northeast corner of the Southern Hijaz quadrangle.

2) A conclusion as to the genesis of these late phase granitic rocks in the Arabian Shield.

3) A conclusion as to the cause of peralkalic compositions for some plutons of this late phase of granitic magmatism.

1.3 Location and Access

The four granitic plutons with which we are concerned in this thesis are one unit on the 1:500,000 scale geological map of Southern Hijaz quadrangle (Brown et al., 1962). They are within a northerly trending rectangle about 60 km long and 47 km wide; between latitudes 23.21°N and 23.52°N , and longitudes 40.55°E and 41.26°E . The area is at an altitude of 950-1,000 m at the northeast corner of the Southern Hijaz quadrangle in the western part of the Precambrian, Arabian Shield, Kingdom of Saudi Arabia (Fig. 1). It is accessible throughout the year from Jeddah by driving along the Jeddah-At Taif highway, taking a turn off 40 km from At Taif, north of the At-Taif-Ar Riyadh highway, onto the Ushayrah-Mahd adh Dhahab road, a total distance of about 470 km, of which 230 km is paved road, and 240 km is desert track. The north part of the area is about two hours by road from Al Madinah. Numerous trails, over which jeeps can pass, are found throughout the area.

1.4 Previous Work

In 1960, Brown and Jackson summarized the results

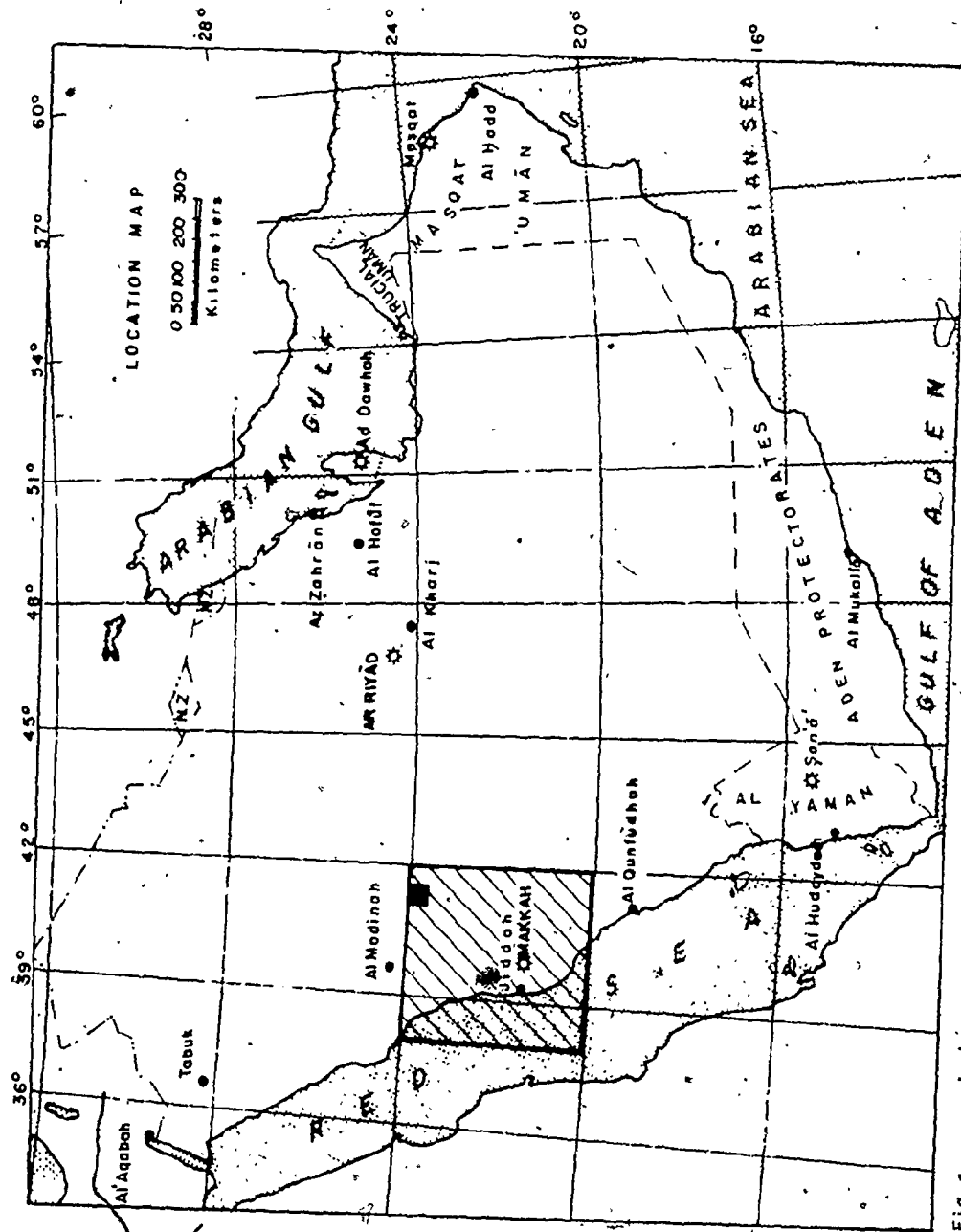


Fig 1 Index map of ARABIAN PENINSULA showing location of the southern HIJAZ quadrangle and the area mapped within that quadrangle

of early geologic mapping in the Arabian Shield published as reconnaissance geologic maps at a scale of 1:500,000 during the interval 1956-1963. Brown and others (1962) published the first geological map of the Southern Hijaz quadrangle (Map I-210A) at the scale of 1:500,000. They listed the basic stratigraphic divisions for Precambrian units in the quadrangle and the area studied within this quadrangle. In 1963 a compiled geologic map of the Arabian Peninsula was published by the U.S.G.S. and ARAMCO at a scale of 1:2,000,000. In 1971, the Directorate General of Minerals Resources (DGMR) in Jeddah, Saudi Arabia, published two bulletins (No 5 and 6). Bulletin No 5 was concerned with mineral resources of the Southern Hijaz quadrangle by Goldsmith, in which he briefly described the fluorite deposits and radioactive minerals associated with pegmatite veins of Jabel Sayid and the Hadb-Aldyaheen Complex. In Bulletin 6, Goldsmith and Kouter included a 1:50,000 scale map of the Umm Ad Damar and Mahd adh Dhahab areas and the Albari and Hadb-Aldyaheen Plutons were described in a general way. Brown (1972) published the only tectonic map of the Arabian Peninsula at a scale of 1:4,000,000 (Map AP-2). Schmidt and others (1973) published a report on the stratigraphy and tectonism of the south part of the Arabian Shield (Bulletin No 8). The DGMR (1973) published a bulletin on the petrology and chemical analysis of selected plutonic rocks from the Arabian Shield by W.R. Greenwood and G.F. Brown (Bulletin No 9).

Part of the thesis area, including the Albari and Alse-Hairah Plutons, was described in two reports published by the Bureau de Recherches Geologiques et Minieres (BRGM) (Dottin, 1974; Dottin et al., 1975). Greenwood et al. (1976), described late Proterozoic cratonization in the south part of the Arabian Shield. This paper was one of the first modern attempts at a tectonic synthesis of the Shield. In 1976, Fleck et al. published the first paper on the K-Ar geochronology of the Arabian Shield.

All the above publications include some general aspects of the thesis area. However, no detailed work on any of the plutons investigated in this thesis, had been done previously.

1.5 Techniques of Present Study

The thesis is based on detailed geological mapping of four plutons. Field work was done during February through May, 1976 when 200 samples were collected, mostly from the granitic rocks.

Petrographic studies were done on 100 samples. Whole rock, and some trace element analyses were completed on 90 granitic rocks. X-ray fluorescence and other analytical techniques used in laboratory investigations are outlined in Appendix A.

CHAPTER 2

THE ARABIAN SHIELD

2.1 General Statement

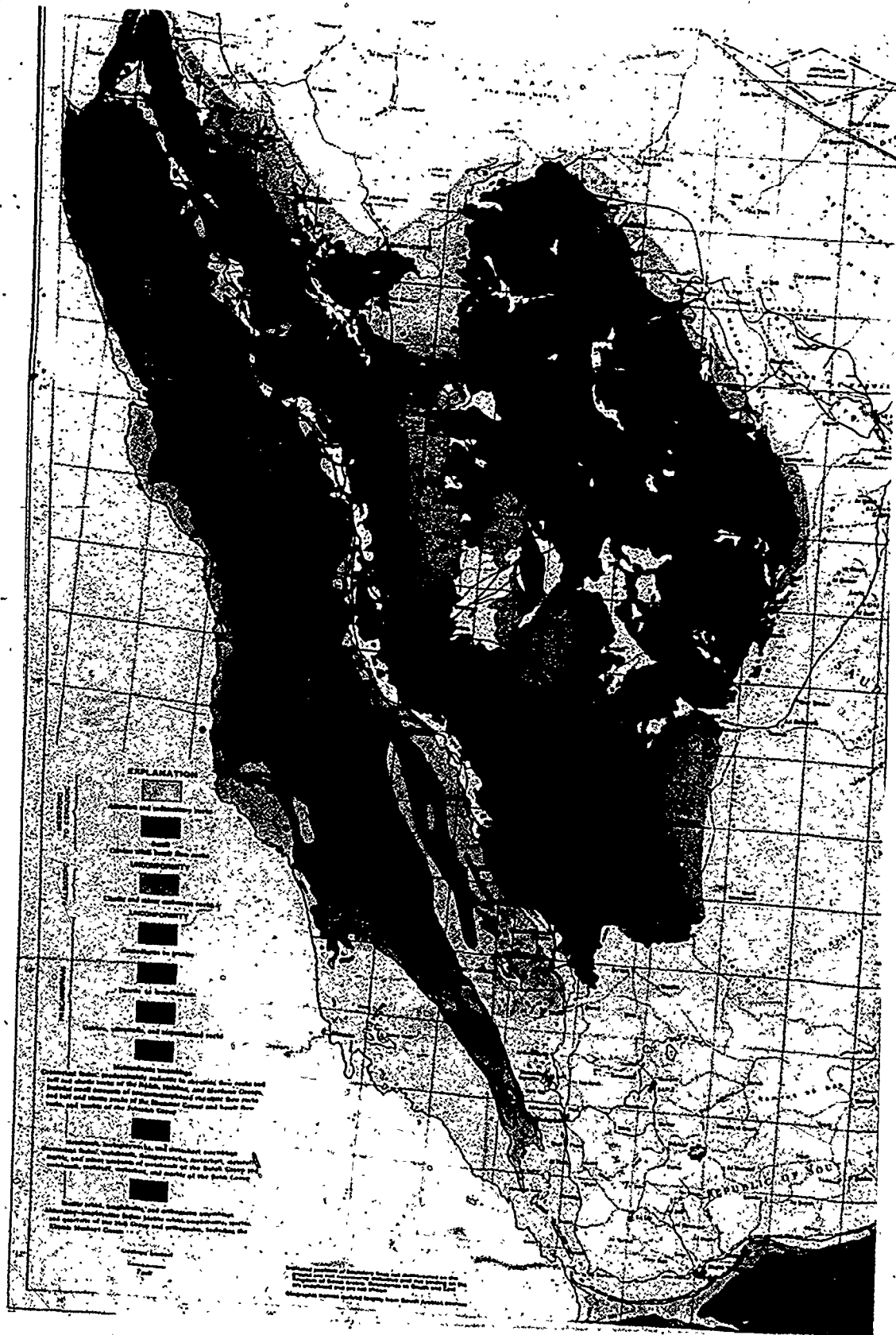
The Kingdom of Saudi Arabia has an area of 2,150,000 km² of which approximately a quarter is occupied by the Arabian Shield. The Arabian Shield extends from the Red Sea coast for distances ranging from 50 to 700 km eastward. The Precambrian Arabian Shield covers an area of about 541,060 km², and is a pseudotrapizoidal (Fig. 2). It consists of Precambrian to early Paleozoic rocks, partly overlain by younger sedimentary rocks, Tertiary to Quaternary basalt and alluvium.

2.2 Structure

The Arabian Shield has been divided by Brown (1960) into three physiographic provinces or belts:

1. The Scarp Mountains extend from the alluvium of the coastal plain to the tip of the Hijaz Plateau and is between 40 and 140 km wide. Height and ruggedness tend to decrease northward.
2. The Hijaz Plateau is a dissected, elevated and tilted peneplain which slopes northeast away from a maximum height

Figure 2. Generalized geologic map of the Arabian
Shield. Kingdom of Saudi Arabia
(scale 1:4,000,000) Greenwood et al.,
1974. U.S.G.S, Jeddah.



of 3130 m near Abha to the vast desert plain of Najd.

3. The Najd Pediplain is the coalescing pediment and desert plain east of the Hijaz Plateau which is interrupted only here and there by isolated inselbergs of Precambrian rocks.

Paleozoic and Mesozoic sedimentary rocks, mostly sandstone, limestone, transgress the crystalline shield from the east (Fig. 3).

Major faults in the Shield trend northwest in the north and east parts, whereas to the south a north and northeasterly trend is dominant. The most prominent fracture system is the left lateral Najd wrench fault system which traverses the Shield in a northwest direction (Fig. 2 and 3).

2.3 General Stratigraphy

Eight Precambrian to Early Paleozoic stratigraphic units have been suggested for the entire Arabian Shield, six in the south part of the Shield and two, the youngest units, in the north part of the Shield (Table 1) (Schmidt et al., 1973). They overlie a basement gneiss complex called the Khamis Mushayt Gneiss. It consists of coarse-grained, banded orthogneiss derived from diorite, quartz diorite, granodiorite and granite, migmatite and lesser amounts of paragneiss, paraschist and amphibolite. Rocks are regionally metamorphosed to amphibolite facies and locally to granulite facies.

Table 1. Precambrian-Cambrian tectonic history of southern Arabian Shield (Schmidt et al., 1973).

DEPOSITIONAL UNITS	* TECTONIC EPISODES	PLUTONIC ROCKS (millions of years)	RADIOMETRIC AGES (millions of years)
Jubaylah Group	Najd wrench faulting Northwest-southeast, left-lateral shear zones	Granite to granodiorite and subordinate syenite; late- and postfaulting	520
Shammar Group	<u>Shammar depression</u> Basins formed penecontemporaneously with Shammar volcanism	Granite to granodiorite;	560
Murdama Group	<u>Bishah orogeny</u> Folding about north-south axes and slight metamorphism of rocks of the Murdama Group. Continued north-south wrench faulting	Granite to granodiorite and subordinate syenite	570
Halaban Group	<u>Hijaz orogeny</u> Folding and lower-greenschist-facies metamorphism of Jiddah and Halaban rocks. Extensive north-south left-lateral wrench faulting during volcanism and folding. Emplacement of gneiss domes	Diorite and quartz diorite to granite plutonism related to Jiddah-Halaban volcanism. Subordinate gabbro. Intrusion perhaps related to north-south wrench faulting	665
Jiddah Group	<u>Tihama orogeny</u>	Plutonism not recognized	1,000
Bahah Group	Folding and generally greenschist-facies metamorphism of Baish and Bahah rocks		
Baish Group	<u>Asir tectonism</u>		
Hali Group	Folding and metamorphism of Hali rocks, chiefly to amphibolite facies.	Tonalite; ultimately orthogneiss	
Khamis Mushayt Gneiss	<u>Basement tectonism (inferred)</u> Migmatites and quartzofeldspathic gneisses possibly older than the Hali rocks. Basement tectonism not distinguished from Asir tectonism		

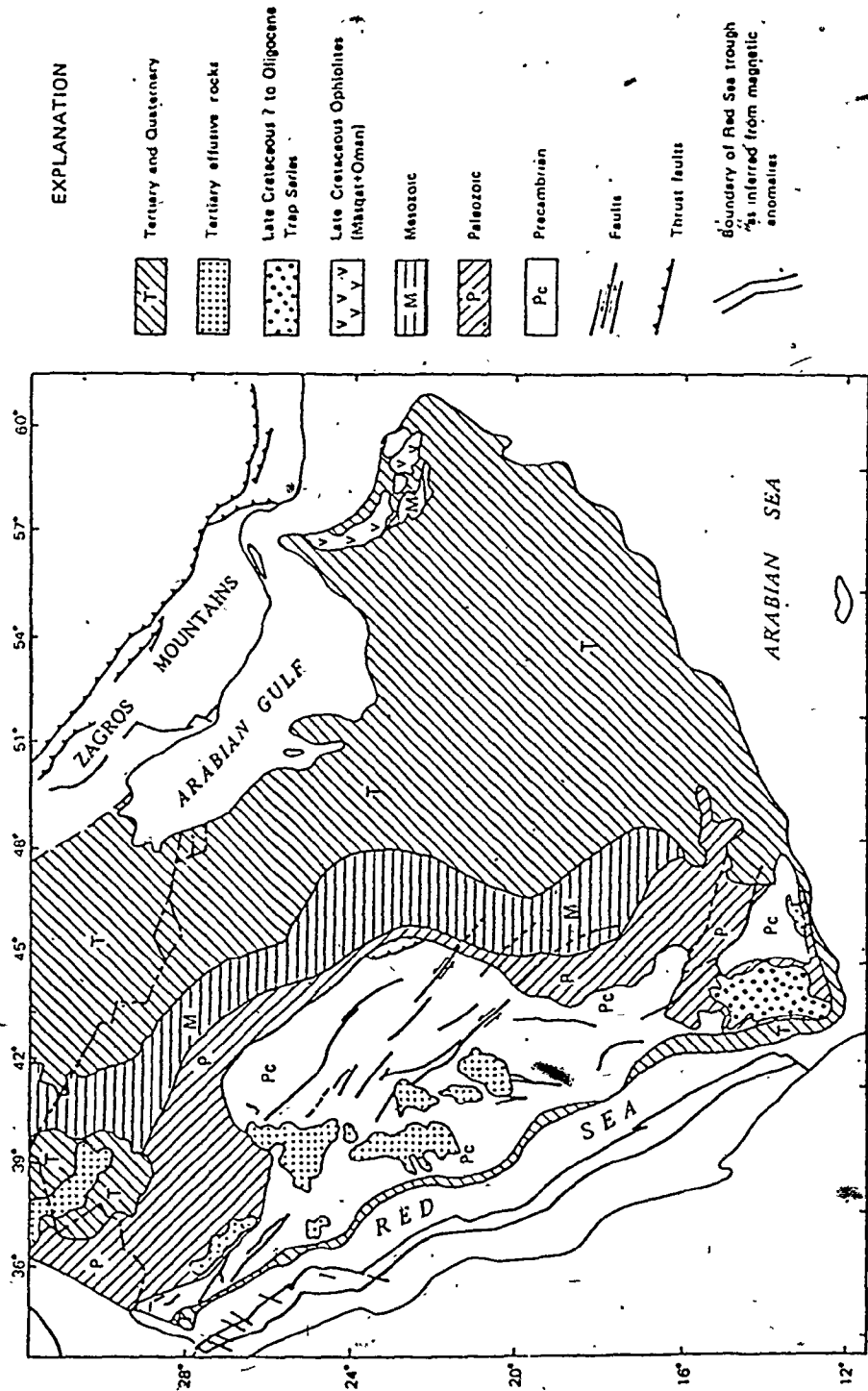


Figure 3 - Geologic framework of the Arabian Peninsula, after USGS, 1972.

The chronological order of the eight units from the oldest to youngest is: Hali Group, Baish Group, Bahah Group, Jiddah Group, Ablah Group, Halaban Group, Murdama Group, Shammar Group and Jubaylah Group (Table 1).

1. The Hali Group is thick sections of quartz biotite garnet schist with amphibolite. Metamorphism is of amphibolite facies. Hali rocks have been intensively tectonized. The relation between Khamis Mushayt Gneiss and Hali Group is not clear. Greenwood et al. (1976), considers rocks of Khamis Mushayt gneiss and Hali Group to be highly metamorphosed equivalents of the Biash and Bahah Groups and plutonic rocks which intrude them.

2. The Baish Group overlies the Hali Group and is greenstone consisting predominantly of mafic metavolcanic rocks intercalated with agglomerates, tuffs and detrital beds. The metamorphic grade is greenschist facies. Most of the Biash rocks are intensely deformed. The regional relationship between Hali rocks and Baish rocks suggests an original major unconformity.

3. The Bahah Group overlies the Biash Group and is a thick section of metasedimentary rocks, mostly, quartz-chlorite-sericite schist which is metamorphosed bedded siltstone, mudstone, siliceous shale and fine-grained sandstone. They are regionally metamorphosed to greenschist facies.

4. The Jiddah Group unconformably overlies the Biash and Bahah Group and consists mainly of red to green andesitic agglomerate, flow breccia, tuff and dacite as well as less abundant basalt flows, pillow lava and basaltic tuff. They are regionally metamorphosed to greenschist facies.

5. The Ablah Group (Table 2) is essentially andesitic and dacitic volcanic rocks. It is regarded as a separate unit between the Jiddah Group and the overlying Halaban Group by Greenwood, et al. (1976) (Table 2).

6. The Halaban Group is metavolcanic and meta-sedimentary rocks. It is subdivided into three main parts: a predominantly clastic lower part, a predominantly andesitic middle part, and an upper part of silicic flows and pyroclastic rocks. The lower Halaban is thick green conglomerate, sandstone and siltstone of largely andesitic volcanic derivation. The middle Halaban is green, massive, and commonly deuterically altered flows, agglomerate, breccia, tuff, and detrital rocks of andesitic composition as well as subordinate but locally thick basaltic rocks. The upper Halaban is green to buff rhyolitic and trachytic flows and pyroclastic rocks, including ignimbritic flows. The Halaban Group is metamorphosed to the greenschist facies.

The Halaban Group is estimated to be at least 10,000 m thick near Halaban in the central part of the Shield (Brown and Jackson, 1960). The group is characterized by rapid lateral and vertical facies variations typical of environments near volcanic sources (Greenwood et al., 1975).

7. The Murdama Group unconformably overlies the Halaban Group and older rocks. A thick marble is characteristic of the upper part of the Murdama Group. The lower part is thick massive conglomerate containing red and gray granitic and andesitic cobbles and boulders derived from underlying rocks. The sandstone and siltstone middle part contains several thick andesitic breccia flows and tuffaceous units. This suggests a continental shallow-water origin for much of the Murdama. The Murdama Group contains the youngest, and in general, the least deformed and least metamorphosed rocks in the south part of the Arabian Shield.

8 and 9. The Shammar and Jubaylah Groups are the youngest groups recognized in the Arabian Shield. They are not metamorphosed. The Shammar Group is mainly rhyolite and minor clastic rocks and the Jubaylah Group is mainly clastic rocks with minor volcanic rocks.

2.4 Tectonism and Plutonism

In an interpretation made by Schmidt et al., 1973, the occurrence of four major tectonic episodes was indicated by observed and presumed angular unconformities in the south part of the Shield. The Asir Tectonism was regarded as the oldest tectonic episode for which there is clear evidence. During the Asir Tectonism, rocks of the Hali Group and Khamis Mushayt Gneiss were intensely deformed and metamorphosed, in contrast to the greenschist facies of metamorphism in the Biash and younger groups.

The Biash and Bahah Groups and older rocks together are considered to have been deformed and metamorphosed during the Tihama Orogeny. Extrusion of voluminous and widespread basaltic lavas of the Baish Group is considered to signify an abrupt change in the evolution of the Shield and possibly the beginning of the Tihama Orogeny. Similarly the change from the basaltic volcanism of the Biash Group to the andesitic volcanism and dioritic plutonism of the Jiddah and Halaban Group marks a significant change and the beginning of the Hijaz Orogeny which is a series of tectonic events characterized by north-trending wrench faults and compressional folds, plutonism, and volcanism.

The Najd Fault System, which enters the northeast of the south part of the Shield, is prominent northwest-trending shear zones with left lateral displacements.

More recent interpretations by Greenwood et al., (1976) of the southern part of the Shield omit the Asir Orogeny on the grounds that the Khamis Mushayt Gneiss and the Hali Group are at least partly metamorphosed equivalents of younger groups and plutons. They also suggest that the Shield was affected by one tectonic cycle, the Hijaz tectonic cycle which they divided into three main episodes (Table 2).

First Episode: This began with deposition of tholeiitic basalt and basaltic andesite of the Biash and Bahah Groups, followed or accompanied by the Jiddah Group whose composition generally falls in the alkali-olivine-basalt

Table 2. Stratigraphy, orogenic events and plutonic rocks in the southern part of the Arabian Shield (Greenwood et al., 1976).

UNITS	PRINCIPAL LAYERED ROCKS	OROGENIC EVENTS	PLUTONIC ROCKS
THIRD EPIISODE	Murdama Group	BISHAH - Folds and faults; faults; northerly trends; greenschist metamorphism	Granite and quartz monzonite (570-550 Ma)
THIRD EPIISODE	UNCONFORMITY		
THIRD EPIISODE	Halaban Group	YAFIKH - Folds and faults; northerly trends; green-schist metamorphism	Quartz monzonite (650-600 Ma)
SECOND EPIISODE	UNCONFORMITY-?-		
SECOND EPIISODE	Ablah Group	RANYAH - Folds and faults; northerly and northeasterly trends; late transverse shears; greenschist, amphibolite, and granulite metamorphism	Injection gneiss (785 Ma)
SECOND EPIISODE	UNCONFORMITY		
SECOND EPIISODE	Jiddah Group	AQIQ - Folds and faults; northerly trends; green-schist metamorphism	Second dioritic series (800 Ma)
SECOND EPIISODE	Bahah Group		
SECOND EPIISODE	Baish Group		
FIRST EPIISODE			
FIRST EPIISODE			First dioritic series (960 Ma)

HJAZ TECTONIC CYCLE

field. This episode was terminated by the Aqiq orogeny. During this orogeny rocks of the first episode were deformed, metamorphosed to greenschist facies and post-tectonically intruded by gabbro to quartz diorite batholiths at about 960 m.y. This is the first diorite series with an initial $\text{Sr}^{87}/\text{Sr}^{86}$ ratio of about 0.7029 (Greenwood, 1976).

Second Episode: This began with unconformable deposition of clastic and volcanic rocks of the Ablah Group. This group and older rocks were deformed and metamorphosed to greenschist facies and intruded by batholiths of gabbro to trondjemite composition of the second diorite series during the Ranyah orogeny at about 800 m.y. Initial $\text{Sr}^{87}/\text{Sr}^{86}$ ratio of rocks of the second dioritic series is about 0.7028. The Ranyah orogeny climaxed with syntectonic intrusions of injection gneiss at about 785 m.y. That is, after intrusion of the second diorite series. The second diorite intrusion has initial $\text{Sr}^{87}/\text{Sr}^{86}$ ratios of 0.7028 in the southern Shield area and 0.7035 to the northeast. The Ranyah orogeny appears to have been accompanied or overlapped in time by deposition of clastic and volcanic rocks of the Halaban Group. Rocks of the Halaban Group were folded, faulted, metamorphosed to greenschist facies and intruded by plutons from gabbro to granite in composition during the Yafikh Orogeny, from about 650-600 m.y. ago. The $\text{Sr}^{87}/\text{Sr}^{86}$ initial ratios are 0.7035 for granodiorite to granite plutons of this orogeny (Greenwood, et al., 1976).

Third Episode: This began with the unconformable deposition of the Murdama Group on metamorphosed Halaban Group and older layered rocks. The Bishah Orogeny terminated this episode and deformed and metamorphosed the Murdama Group and older rocks to greenschist facies. Granitic plutons were intruded about 550 m.y. ago.

The northwest trending Najd fault system is about 540-510 m.y. old and cuts across the south part of the Shield to truncate older north trending structures produced during the Hijaz tectonic cycle. There is a lack of regionally significant volcanic and sedimentary deposits associated with the formation of the Najd fault system. In the north-central Shield, the Najd fault system is a 300 km wide zone of major and many minor shear zones that extend southeast across the entire Arabian Shield. It is considered to be in part contemporaneous with deposition of the Shammar and Jubaylah Groups. Upper Precambrian and Cambrian granite plutons were intruded along the northwest trending Najd fault system at about the time of cessation of fault movement (B.R.G.M., 1976).

In 1976, R.J. Fleck and others concluded that, the Arabian Peninsula was affected by an orogenic event between 510 and 610 m.y. ago, and they correlated this event with the Pan-African orogeny in east Africa. They also concluded that during the last part of this 510 to 610 m.y. period, left lateral strike slip faulting occurred along a set of north-west trending fracture zones, whose composite displacement may be as much as 240 km.

The application of modern type-motions to the Arabian Shield has been taken into consideration very recently by a number of workers (Greenwood and Brown, 1973; Greenwood et al., 1976; Al-Shanti and Mitchell, 1975; Bakor et al., 1976; Nasseef and Gass, 1977; Gass, 1977; Marzouki and Fyfe, 1977; Neary et al., 1976).

Greenwood and Brown (1973) related their findings of an increase in the ratio $K_2O/K_2O + Na_2O$, accompanied by an increase in the proportion of granite to diorite exposure, from the southwest to the northwest, to a possible eastward dipping subduction zone. Later this hypothesis was developed by Greenwood et al. (1976) in which the southern part of the Shield was identified as a cratonized intraoceanic island arc and they confirmed the northwest trend and eastward dipping subduction zone for the proposed island arc. Similar studies have been carried out in the northern part of the Arabian Shield (Bakor, 1973, 1976; Neary, 1974), the eastern desert of Egypt (Garson and Shalaby, 1974) and NE Sudan (Neary et al., 1976; Gass, 1977). All these studies called for the cratonization of oceanic island arc systems. Along with these types of studies, other workers were looking for basic-ultrabasic and possibly ophiolitic suites associated in the region (Bakor, 1973; Bakor et al., 1976; Neary, 1974; Garson and Shalaby, 1974). On the basis of petrographic and geochemical data, Bakor et al. (1976) identified the basic and ultrabasic complex of Jabal Al-Wask as an ophiolite suite

formed in a back-arc environment. Furthermore, several ultrabasic zones lying in NW-SE zones across western Arabia and northeast Africa separated by a granitic basement are believed to be formed by cratonization of island arcs (Bakor et al., 1976). These ultrabasic zones are sutures between these arcs and they represent lithosphere remnant of back arc seas.

CHAPTER 3

THE YOUNGER GRANITES IN THE NORTHEAST CORNER OF THE SOUTHERN HIJAZ QUADRANGLE

3.1 General Statement

Granitic plutons in the northeast corner of the Southern Hijaz quadrangle (Fig. 4) are $535 \pm$ m.y. by Rb/Sr isotope ratios (Geological map of Southern Hijaz quadrangle [I-210A], scale of 1:500,000 [Brown et al., 1962]) and in 1972, Brown considered them as part of the post-tectonic intrusions with ages of 490-600 m.y. Potassium-argon age determinations by the Geophysics Department at the University of Western Ontario on granitic rocks in the northeast corner of the Southern Hijaz Quadrangle, indicate ages of 500-650 m.y. This thesis divides these granitic intrusions into 4 types according to texture, composition and mode of emplacement:

- 1) Medium-grained calc-alkalic granite of Albari (650 m.y.)
- 2) Coarse-grained alkalic granite of Alse-Hairah.
- 3) Medium-grained per-alkalic riebeckite granite of Jabal Sayid (500 m.y.).

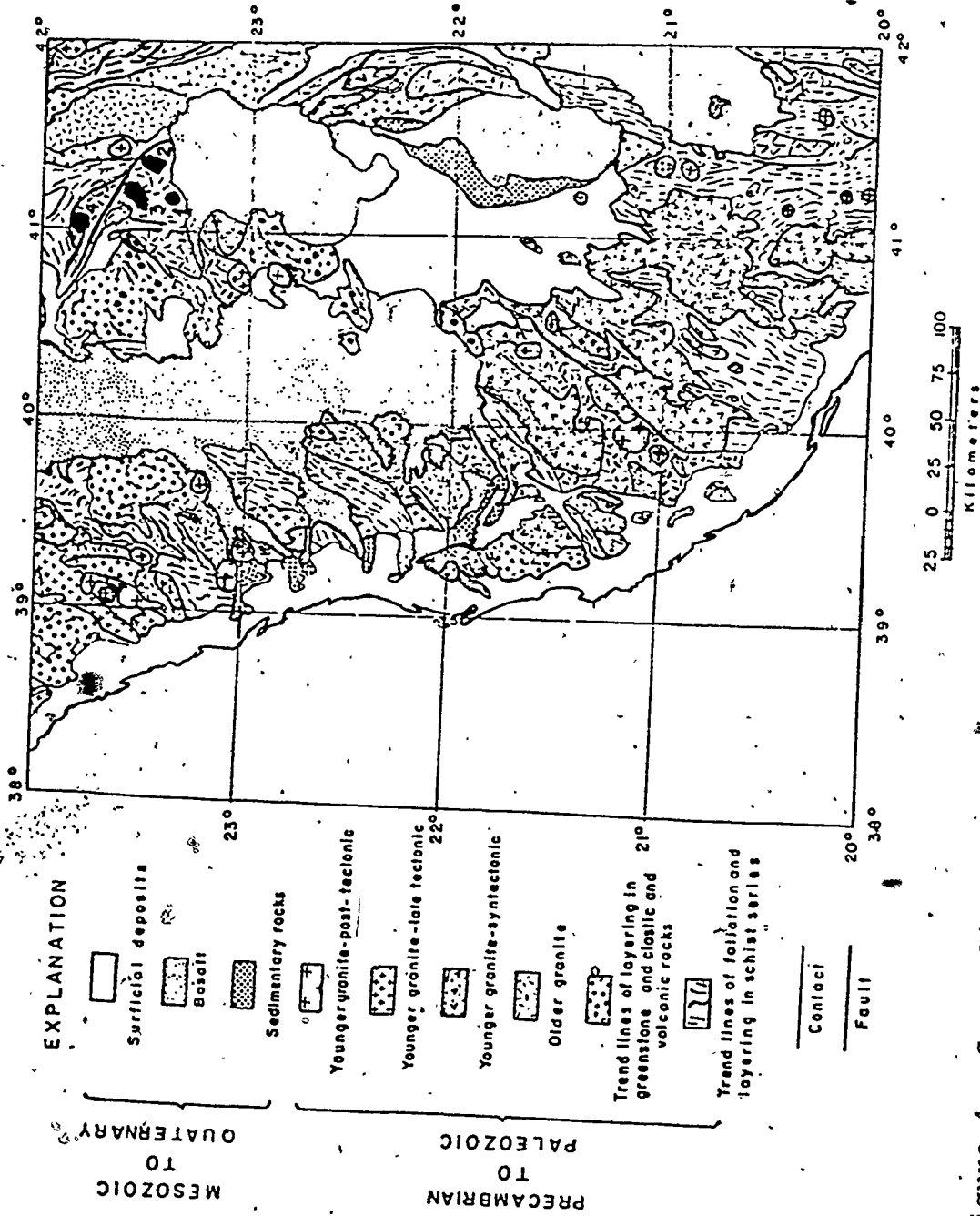
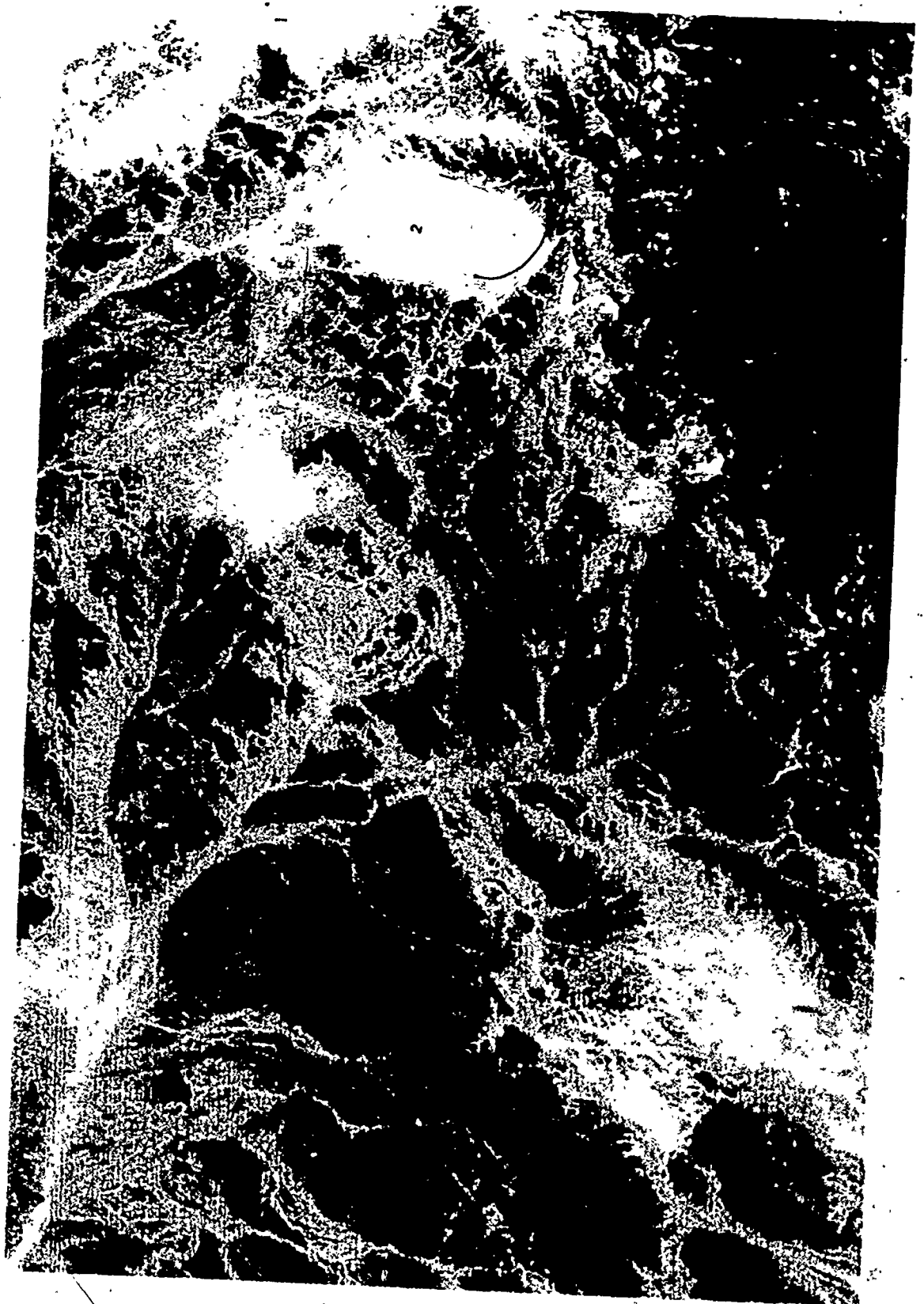


Figure 4. Generalized geological map of Southern Hijaz quadrangle, with the locations of granitic plutons discussed in the text (after U.S.G.S.)
 1 - Albari, 2 - Alse-Hairah, 3-Hadb-Aldyaheen, 4- Jabal Sayid

Figure 5. Satellite photograph of the area includes the four plutons which are the subject of this thesis.

1. Albari Pluton
2. Alse-Hairah Pluton
3. Hadb-Aldyaheen ring complex
4. Southern part of Jabal Sayid Riebeckite granite



- 4) Medium-grained-porphyrific peralkaline and non-peralkaline granites of the Hadb-Aldyaheen ring complex (557-573 m.y.).

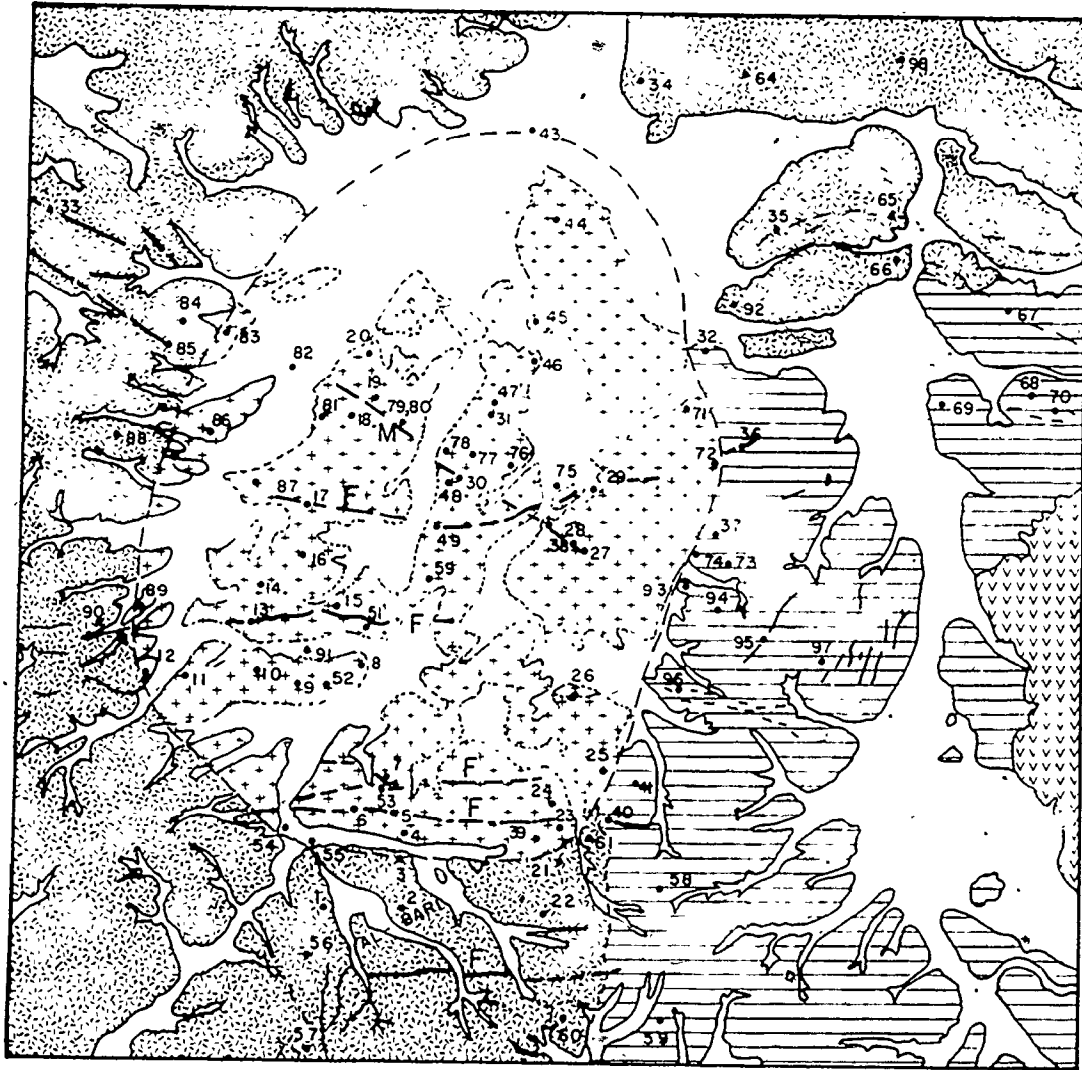
3.2 Albari Granite

This pluton is between latitude $23^{\circ}.20'N$ and $23^{\circ}.24'N$ and longitude $41^{\circ}.9'E$ and $41^{\circ}.11'E$. It is about 30 km southeast of the ancient gold mine of Madh-adh-Dhahab and about 300 km north of the town of At-Taif:

3.2.1 Geologic Setting

The Albari pluton crops out as an oval body, approximately 4.6 km long and 3.4 km wide (Fig. 6). The country host rocks surrounding this pluton are, in order of abundance quartz diorite, diorite and locally, a muscovite garnet granite. The quartz diorite is coarse, gray to dark gray to green in colour and forms hills of spheroidal weathering outcrop. Mafic mineral content is variable and there are locally gabbroic and dioritic and more rarely, leucocratic phases. Constituent minerals are oligoclase-andesine, quartz and green hornblende with chlorite and epidote common where the rock is foliated. Quartz diorite grades to granodiorite through the appearance of microcline perthite. Similarly the quartz diorite grades into gabbro by increase in hornblende content especially along local faults within the quartz diorite. There are also pegmatitic phases with large

FIG.6. GEOLOGIC MAP OF ALBARI GRANITE



0 1/2 Km

Scale: 1 30,000 Km

EXPLANATION

-  Wadi Alluvium
-  Recent Volcanism
-  Fine-Medium Grained Biotite Granite
-  Muscovite Granite and Granodiorite
-  Diorite, Quartz Diorite and Gabbro
-  M - Mafic Dike, F - Felsic Dike

amphipoles near shear zones. General trend of shearing is N55 to 65W/70 to 80NE. Similar trends are emphasized by numerous micro-diorite dykes which form steep elongated hills.

Muscovite granite is only found in small outcrops on the east southeast side of the map area of Albari Granite (Fig. 6). It is a medium-grained rock, commonly foliated with the foliation striking N50W and dipping 80NE. In many places, this rock is almost pegmatitic, and aplitic differentiates have also been observed. The muscovite granite consists of cataclastic quartz, microcline, perthite, oligoclase, muscovite, sericite, chlorite, garnet and epidote; in some places the rock contains a pink mica called lepidolite. In the pegmatitic phase, many of these components are absent, and there is only quartz, microcline and large flakes of muscovite, generally with large garnet crystals. The rock is cut by several microdiorite dykes striking N20 to 25E and dipping 90° and N70W dipping 90°. Two major sets of joints strike N20W and dip vertical or strike N75E and dip 70N.

The Albari granite pluton:

The Albari granite is exposed as spheroidal outcrops and rubble over a flat area of about 15.6 square kilometers (Plate 1a). Most of the pluton sub-outcrops beneath a skin of sand and fine decomposed granite. On the weathered surface, the rock is gray to white, gray or yellow reddish-gray, depending on its degree of weathering. Fresh rock is

massive, crystalline medium to fine-grained equigranular and a remarkably homogenous mixture of feldspar, quartz and biotite, except in marginal facies on the west side where it contains a few crystals of amphibole. Fine-grained mafic inclusions occur in many places particularly in the southwest part of the pluton, and near the contact with the dioritic country rocks. Most of these inclusions are oblate, spheroid, or discoid, ranging from 5 to 30 cm in diameter (Plate 1b). They consist of fine-grained andesine laths, green hornblende, biotite, minor quartz and chlorite, and accessory magnetite and epidote. Minerals in the mafic inclusions are similar to those in the fine-grained diorite of the country rocks. Contact of inclusions with enclosing granite is generally sharp, except in a few instances where the inclusion is immediately surrounded by a granite with abnormally large dark mineral content. In general, the inclusions are structureless and have no preferred orientation.

The contact between the Albari granite and the country rocks is commonly covered by alluvial sands and gravels. Most observed contacts are sharp although no decrease in grain size was noticeable. The pluton is discordant to the regional trend of foliation in the country rocks. Its western contact appears to be rather regular with few apophyses extending into the country rocks. A conspicuous foliation with general trend parallel to the contact within the granite is noticeable at few localities along the west margin of the pluton (Plate 1c). The contact is

mostly vertical, or dipping outward. At the south and west margins particularly a mixed rock is present. This is of intermediate colour index and has a composition between the granite and the diorite country rocks.

The contact between the Albari pluton and the muscovite granite is not clear and occurs across a fine-grained rock, which seems to belong to the muscovite granite rather than the Albari granite. A notable feature along all contacts between the Albari granite and the country rocks, is the lack of any obvious evidence of contact metamorphism.

The pluton is cut by rhyolite dykes, dark microdiorite dykes and rare small quartz veins. Microdiorite dykes which are the oldest, generally trend N60W which is the same trend as they have in surrounding country rocks. These dykes are fine to very fine-grained in texture, black to dark green in colour, jointed and very commonly fragmented by fractures which give them a zig-zag appearance in the field. They have a microgranular texture with hypidiomorphic saussuritized plagioclase, mainly andesine, hornblende which is commonly chloritic, and interstitial quartz. Rhyolite dykes are localized mainly in the south half of the pluton, forming reddish and yellowish brown hills. These dykes are more recent than microdiorite dykes and have an east strike. They consist of very fine-grained to vitreous rock which locally contains subhedral quartz phenocrysts. Only a few grains of potassic feldspar appear in the groundmass. Some of the rhyolite dykes in the middle of the pluton are sheared

PLATE 1

Albari Granite

- a) Spheroidal outcrops of Albari pluton.
- b) Mafic inclusions enclosed by Albari granite.
- c) Foliated granite of Albari along the contact.
- d) Rhyolite dyke (in the middle) and microdiorite dykes cutting Albari granite.
- e) Thin-section of Albari granite showing a string microperthite, zoned plagioclase, quartz and biotite. (Cross nicols, X16)
- f) Zoned plagioclase. (Cross nicols, X16)
- g) Oscillatory normal zoning of the plagioclase.
(Cross nicols, X25)

PLATE 1



and bounded on both sides by unshaped microdiorite dykes (plate 1d). Both dykes, the microdiorite and the rhyolite dykes penetrate the surrounding country rocks.

3.2.2 Petrography

The rock has a hypidiomorphic granular texture in which the predominant mineral is euhedral to subhedral plagioclase. This is accompanied by irregular interstitial quartz and rarer anhedral crystals of K-feldspar. The main mafic mineral is biotite. Hornblende was noted in some samples. Accessory minerals include iron ore mainly as pyrite, apatite, sphene, and rare zircon.

Modal composition of 8 representative samples are given in Table 3, and modal classification of this granite is shown in Figure 7. The plagioclase forms 36.9 to 53.6 percent of the mode. It is subhedral to euhedral tabular crystals with a grain size from 1 to 3 mm in length and 0.2 - 0.8 mm wide. Plagioclase crystals are generally twinned according to the albite law and combined carlsbad and albite twinning and oscillatory normal zoning is generally well developed (Plate 1f, g). The mineral is andesine An_{30} to An_{50} , and rims of An_{17} to An_{28} (see Appendix C, Table 1c). It has sericite along cracks and in the cores of grains and some crystals are wholly occupied by sericite and clay minerals. Inclusions of pyrite, magnetite, apatite, biotite, and quartz were commonly observed (Plate 1f). Myrmekite

Table 3. Modal composition of Albari granite

Sample No.	K- feldspar	Plag:	Quartz	Biotite	Horn- blende	Acc
Alb 4A	12.99	44.37	34.53	7.08	-	1.03
11 6A	7.05	50.51	35.27	5.09	-	1.26
Alb 10	2.56	49.43	37.31	8.66	-	2.04
Alb 13A	5.37	45.88	40.28	7.03	-	1.44
Alb 16	3.18	53.65	36.01	5.28	0.04	1.84
Alb 20	10.20	38.98	41.83	5.65	1.34	2.00
Alb 23	13.11	41.69	33.11	7.8	2.36	1.73
Alb 30	18.86	36.93	34.15	7.03	1.03	2.00
Range	2.56- 18.86	36.93- 53.65	32.15- 41.83	5.28- 8.66	0.04- 2.36	1.03- 2.04
Average	9.42	45.18	36.31	6.80	0.6	1.67

ALBARI MASSIF GRANITE

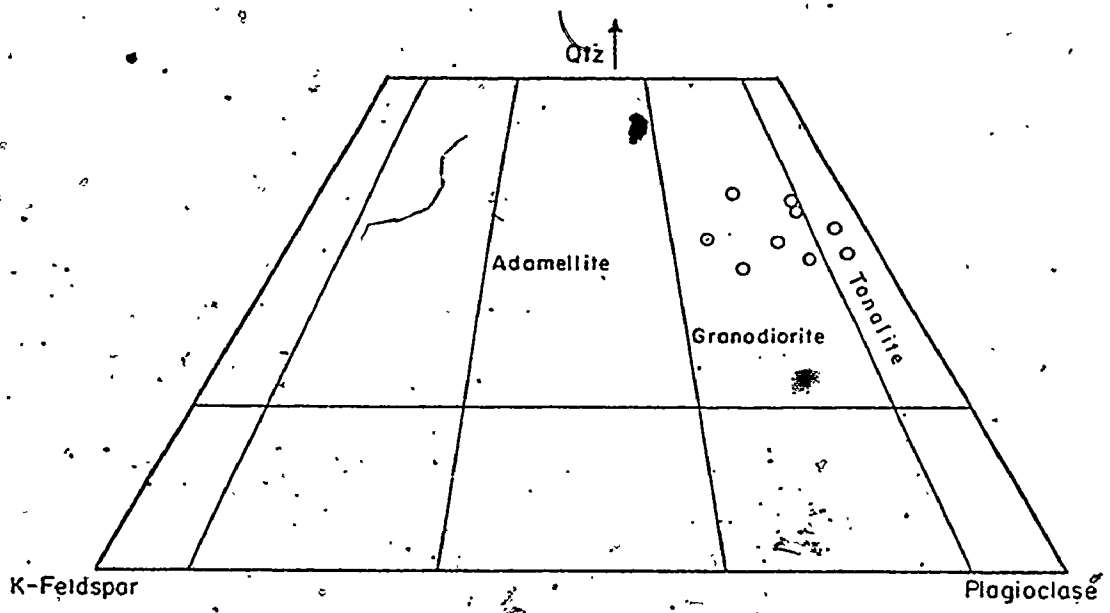


Figure 7. Modal classification of Albari granitic rocks (Streckeisen, 1967).

texture along the margins of some of the plagioclase and perthite grains was noted.

Quartz makes up from 42 to 32 percent of the rock. It occurs mainly as anhedral grains 2 to 0.5 mm in diameter occupying interstitial positions between early formed minerals. Large grains are irregularly fractured and filled with sericite. Some enclose early formed phases. Small grains of quartz with rounded outline are enclosed in perthite, plagioclase and biotite crystals perhaps representing an early formed quartz. Moderate undulose extension is common.

K-feldspar as microperthite forms 3 to 18 percent of the modal composition, occurring mostly as large anhedral grains with irregular boundaries, ranging in size from 3 to 0.5 mm long and 1 to 0.2 mm wide. Sericite and clay minerals occupy some sites, but in general the perthite is much less altered than the plagioclase (Plate 1e). Inclusions of plagioclase with irregular boundaries and more sodic rims in some instances with myrmakite growth along the margins, biotite, and less frequently, iron ore and apatite. Biotite is the major mafic mineral and is about 5 to 8.5 percent of the rock occurring as a tabular crystal, elongated flakes and needles. They measure 4 to 0.3 mm in length and 1 to 0.2 mm in width. It is commonly altered, either completely or partly to green or berlin blue chlorite. Euhedral apatite and pyrite are common as inclusions, and less frequently rounded quartz, sphene and zircon.

Hornblende accounts for as much as 2 percent and occurs as greenish brown, ragged prismatic crystals to 0.4 mm. in diameter. It is commonly partly altered to biotite, sphene, and iron ore.

Accessory minerals are iron oxides, apatite and sphene and very rarely zircon. They are 1 to 2 percent of the mode. Pyrite is euhedral to subhedral in grains up to 0.2 mm in diameter. It is almost always associated with biotite, particularly the more chloritic grains and it is commonly the pyrite that is altered to hematite. Apatite occurs as prisms or needles as an inclusion in biotite, and, less commonly, in feldspar. Sphene is mainly in the form of granules, and less commonly as wedge-shaped grains associated with biotite and hornblende. It rims biotite and the iron oxide grains in some instances.

History of Crystallization:

Grain relationships suggest that the first minerals to crystallize from the magma were iron ore, zircon and some apatite and sphene, as they are included in all other minerals—especially biotite. Accessory minerals were followed by the crystallization of andesine and biotite. Andesine reacted with the melt to give rise to reaction rims of oligoclase. The presence of normal zoning suggests that crystallization of plagioclase was not continuous. Biotite started to crystallize contemporaneously with plagioclase or not long thereafter. Potash feldspar as microperthite began to form following biotite and before all the plagioclase was

completely crystallized. The presence of small inclusions of biotite and plagioclase suggests that late crystallization of potash feldspar occurred. Quartz was the last mineral to form as it is interstitial. It began to crystallize during the last stage of the K-feldspar formation and, therefore, micrographic growth of quartz and microperthite are commonly noted. The small rounded crystals of quartz ^{are} forming embayments in the feldspar and ^{are} considered to be earlier stages and the first generation of quartz. Some of the sphene and rare epidote are most likely secondary deuteric minerals. Sericitization of feldspar is probably a near surface hydrothermal event.

3.3 Alse-Hairah Granite

This pluton is between lat. $23^{\circ}.25N$ and $23^{\circ}.32N$ and long. $41^{\circ}.20E$ and $41^{\circ}.24E$. It is about 15 km northeast of the Albari Pluton and immediately at the north edge of Harrat Al Kishb.

3.3.1 Geologic Setting:

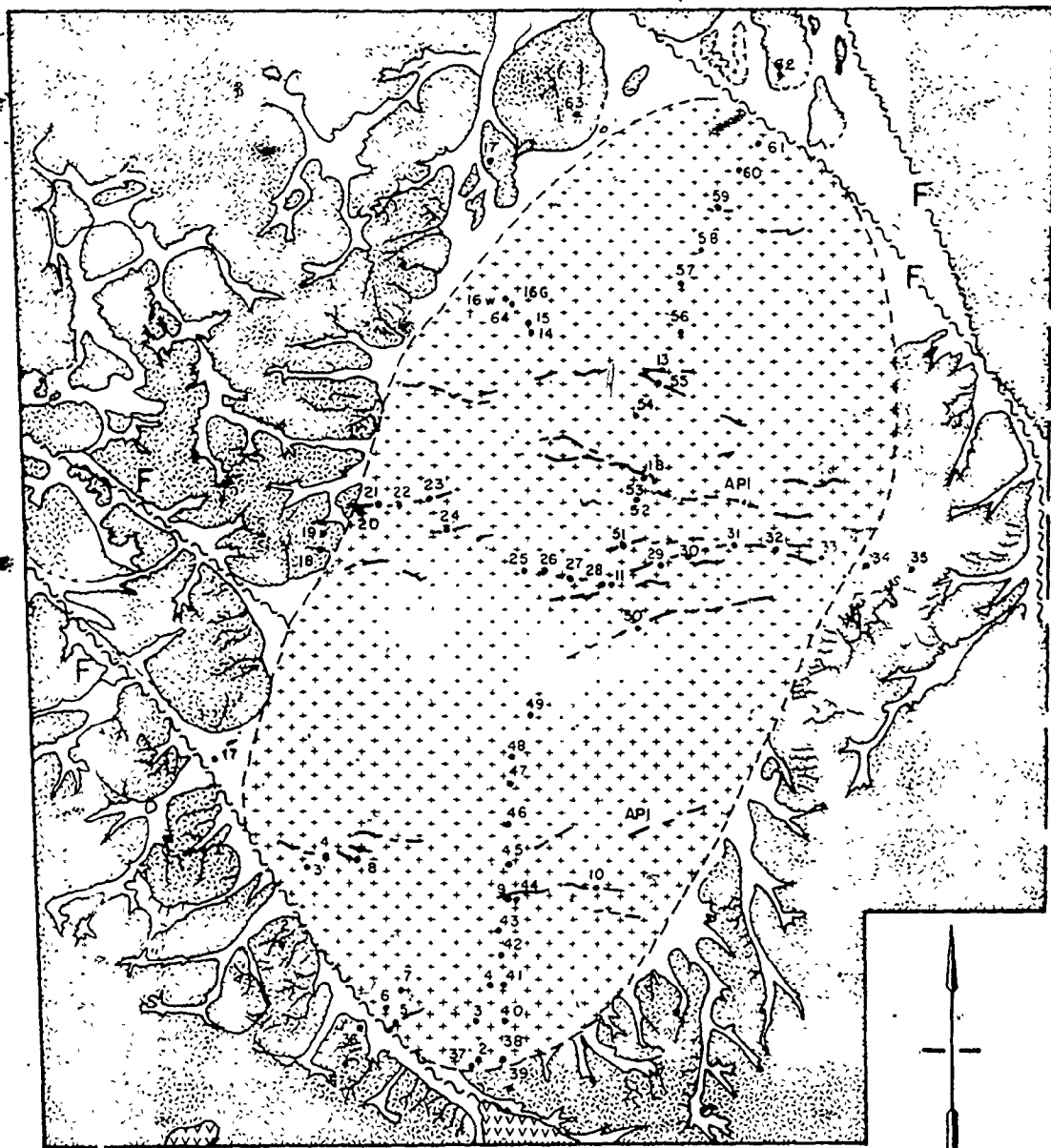
Alse-Hairah granite crops out in an elliptical body, with a long axis of about 15.3 km in a northeast direction and a short axis averaging 7.4 km long (Fig. 8). It is intrusive into quartz diorite, diorite and gabbroic rocks similar to those that host the Albari granite. The granite occupies a depression and the rock is almost always

weathered. At its margins the granite surface rises slightly above the general level of the interior of the mass. Outcrops are rare and a large part of the body is covered by white or pink sand and coarse grained decomposed granite from which here and there flat slabs emerge. More rarely, to the north, it is characterized by debris and common east strike (Plate 2a). It is surrounded by low hills of older quartz diorite, diorite and gabbro.

Where the granite is exposed, it is pink, coarse-grained and porphyritic with rapakivi texture in places (Plate 2b). Fresher exposures occur in the northern part of the pluton where the rock has a slight foliation with a general strike of north-northeast. In hand specimen this foliation is difficult to recognize. Pink potash feldspar phenocrysts have a preferred orientation parallel to the foliation in these outcrops. The marginal-border zone of the pluton is finer-grained rock with more quartz and less biotite than rock of the interior of the pluton.

Where observed, the contact with diorite country rock is sharp. The dip of the contact is difficult to determine because of scanty and weathered exposures along the borders, but in general it is vertical or steeply dipping outward. Many apophyses of fine-grained granite were observed extending into the surrounding country rock (Plate 2c). The contact in the northeast and southwest part of the pluton are faulted and emphasized by two main wadis. Many mafic

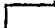

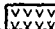

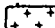

FIG. 8. GEOLOGIC MAP OF ALSE-HAIRAH GRANITE



0 1/2 1 Km

Scale 1 30,000 Km

EXPLANATION

- | | |
|--|--|
|  Wadi Alluvium |  Diorite, Granodiorite and Gabbro |
|  Recent Volcanism |  Fault |
|  Coarse-Grained Biotite Granite |  API Aplite, Microgranite Dikes |

inclusions, and a few felsic inclusions, were observed in the central part of the pluton. They are subangular to subrounded in shape, vary in size from 5 cm to one meter. Mafic inclusions consist of small grains of plagioclase, hornblende, biotite, chlorite and lesser quartz. The smaller inclusions are somewhat oriented parallel to the general direction of the slightly foliated enclosing granite, but large inclusions are of random orientation. Contact of these inclusions with the granite is generally sharp. Large phenocrysts of potash feldspar occur near the margins of these inclusions (Plate 2d).

3.3.2 Petrography:

The main mass of Alse-Hairah granite is a very coarse-grained buff-reddish coloured rock, in which large grains of pink feldspar, up to 2 cm in diameter are surrounded by smaller grains of quartz, feldspar and biotite. Rapakivi texture is very common. Samples from the margins are finer-grained with more quartz and less modal biotite than the central part. All samples from the main mass have a porphyritic, hypidiomorphic granular texture in which large sub-hedral to anhedral crystals of perthite are surrounded by smaller crystals of plagioclase, perthite, quartz and biotite.

Modal composition of nine representative samples is given in Table 4, and modal classification of this granite is shown in Figure 9.

The main alkali feldspar is string perthite, and less commonly, anti-perthite, which is the intergrowth of potash

PLATE 2

Alse-Hairah Granite

- a) Flat slabs outcrops of Alse-Hairah Pluton.
- b) Hand specimen of Alse-Hairah granite with rapakivi texture.
- c) Apophyses of fine grained granite extending into the diorite country rocks.
- d) Mafic inclusion, within the granite, has a potash feldspar phenocrysts close to their contact with the granite.
- e) Microperthite dark gray, biotite, plagioclase with slight alteration, quartz and apatite of Alse-Hairah granite. (Cross nicols, X16)
- f) Microperthite replaced by sodic plagioclase rapakivi texture; euhedral sphene crystal with magnetite and apatite. (Cross nicols, X16)
- g) Slightly altered plagioclase, euhedral sphene crystal.
- h) Sodic plagioclase replacing microcline perthite. (Cross nicols, X25)

PLATE . 2



Table 4. Modal composition of Alse-Hairah granite

Sample	K-feldspar	plagioclase	quartz	biotite	Accessory Minerals
Als 4	32.87	30.17	29.53	4.85	2.58
Als 3	40.59	38.21	16.38	3.04	1.76
Als 7	41.50	35.33	16.54	3.64	2.99
Als 12	42.61	17.43	32.25	4.36	3.35
Als 13A	38.38	21.36	36.46	2.56	1.24
Als 14	36.50	19.07	35.35	6.5	2.58
Als 15	31.24	32.96	38.03	4.16	2.61
Als 16	38.79	26.86	30.41	2.11	1.83
Als 11B	43.88	29.21	20.07	3.70	3.14
Range	31.24- 43.88	17.43- 38.21	16.38- 38.03	2.11- 6.5	1.24- 3.35
Average	38.48	26.84	28.34	3.88	2.45

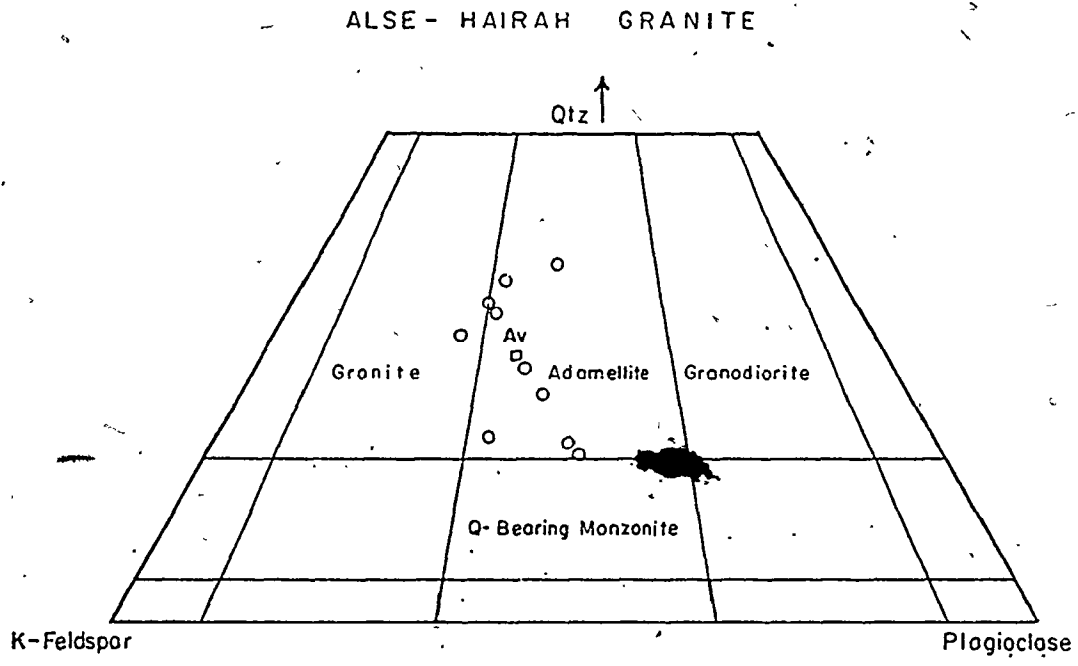


Figure 9. Modal classification of Alse-Hairah granite.

feldspar within a crystal of plagioclase (Plates 2e and h). The plagioclase of the antiperthite is oligoclase and the replacing phase is orthoclase or microcline. Both, perthite and antiperthite occur mostly as large subhedral and anhedral crystals of 1.5 cm to 5 mm long and 6 to 2 mm wide. They also occur as smaller grains 0.5 mm in diameter in the groundmass. Microcline, the less common form of K-feldspar here, is presented locally by few small, 0.2 mm, interstitial grains. All forms of alkali feldspar make up 31 to 44 percent of the mode (Table 4). String perthite phenocrysts are commonly mantled by oligoclase, a Rapakivi texture (Plate 2f). Inclusions of quartz, plagioclase with sodic rims and euhedral sphene are common. Less common are biotite and magnetite (Plate 2e and f). The perthite phenocrysts are slightly sericitic.

Plagioclase forms 17 to 38 percent of the rock. Most of it occurs as subhedral elongated crystals from 5 to 0.7 mm long and 1.5 to 0.4 mm wide. It also occurs as smaller grains 0.3 mm long and 0.15 mm wide enclosed in perthite phenocrysts, large grains of quartz or as interstitial grains in the groundmass. Twinning, according to albite and carlsbad laws, are very notable among most of the plagioclase grains. The plagioclase has the composition of sodic oligoclase An_{12} to An_{16} (Appendix C, Table 26). Plagioclase is almost always sericitic. Few plagioclase crystals are zoned. Many enclose inclusions of quartz, sphene, iron

ore and biotite (Plate 2g). Myrmekitic intergrowths are abundant, normally as small inclusions in perthite phenocrysts or in between plagioclase and perthite crystals.

Quartz occurs mainly as large interstitial crystals from 1 to 6 mm in diameter. Quartz forms about 16 to 38 percent of the mode. Large crystals are commonly cracked and broken (Plate 2f), and they have strong undulose extinction indicating some sort of deformation after crystallization. Inclusions of small grains of feldspar, sphene, biotite and apatite are commonly found within the large quartz grains.

Biotite is the major mafic constituent, and occurs as isolated prismatic crystals and as smaller ragged flakes, some of which are poikilitically enclosed within the feldspar and quartz crystals. Biotite grains range in size from 1.5 to 0.3 mm long and 0.1 to 0.2 mm wide. It is 2 to 6.5 percent of the mode. Euhedral sphene, small prisms of apatite, quartz and iron ore grains are commonly as inclusions within the biotite. Some of the biotite is partly occupied by green chlorite and less commonly, replaced by quartz. Accessory minerals make up to 1.2 to 3.3 percent of the mode. Common accessories are sphene, iron ores, apatite and very rare zircon. These are mostly found inside the large crystals of major phases, particularly the biotite (Plate 2e, f and g).

History of Crystallization:

Accessory minerals, iron ore, sphene and apatite, were first to crystallize from the melt. They were followed by hornblende, which occurs as rare small grains in the groundmass or poikilitically enclosed by plagioclase. The first generation of biotite, which occurs as small crystals in the groundmass or poikilitically enclosed in the feldspars, appears to have crystallized after hornblende and some of the plagioclase. They were followed by the first generation of plagioclase as small anhedral grains followed by small microcline grains and the first generation of quartz. The first stage in the crystallization history must have been relatively short-lived as can be seen from small grain size of its crystals compared with later phenocrysts. During this stage, some sort of change in the crystallization environment has been introduced. This change may be caused by the enrichment in the hydrous phase introduction of heat of fluids from below, or a variety of other factors. In this new environment, the formation of minerals was renewed with the crystallization of larger biotite and plagioclase crystals. They were followed by crystallization of alkali feldspar in the form of perthite phenocrysts. Many of these crystals reacted with the melt to produce the Rapakivi texture with sodic oligoclase shells. Some of the K-feldspar exsolved from the plagioclase to produce the antiperthite. Quartz was the last mineral to separate from the melt, and it fills

interstitial spaces and replaces some of the rock constituents. It began to crystallize during the last stages of separation of perthite and, therefore, a micrographic growth of quartz and microperthite is common. Formation of some of the accessories results from disintegration of hornblende and the chloritization of biotite. The introduction of hydrothermal solutions was the main cause of alteration of the most minerals. This rock has had a post-consolidation deformation as evidenced by the presence of deformed and broken quartz with strong undulose extinction and also by the abundance of fractured plagioclase grains. The absence or impoverishment of the marginal zone in mafic minerals together with its enrichment in quartz, could have resulted from differentiation of the melt to produce a more silic margin. This could have been accomplished by assimilation of silica from the country rocks, or by a filter-press procession, which squeezed late-stage silica-rich fluids toward the margin.

3.4 Jabal Sayid Riebeckite Granite

The map area of this granite is between lat. $23^{\circ} 44'N$ and $23^{\circ} 58'N$, and long. $40^{\circ} 56'E$ and $41^{\circ} 3'E$, and is about 150 km southeast of the town of Al-Madinah, and 40 km northeast of the ancient gold mine of Madh-adh-Dhahab. The south part of this granite is about 25 km northwest of Hadb-Aldyaheen ring complex.

3.4.1 Geologic Setting

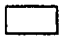
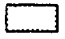
This granite (Fig. 10) is within an area about 10.5 km long and 6.5 km wide. It is bodies intruding granodiorite, diorite, red biotite granite and volcanic rocks of the Halaban Group. In the field this granite is characterized by its high standing ridges and sharp erosional peaks (Plate 3a). It is coarse to medium-textured with evenly distributed well-formed prisms and needles of riebeckite and aegirine about 1-0.5 by 2-5 mm which are partly aligned and sometimes sweep around quartz crystals (Plate 4a). Some of the needles were captured within the quartz crystals as inclusions. The rock is gray to white and contains transparent to translucent bipyramidal quartz crystals 5 mm in diameter, indicating that they crystallized as high temperature beta form (about 573°C). Small reddish patches of disseminated hematitic material within the feldspar are common. Occasionally a few fluorite crystals were observed. This is fairly massive, homogeneous and well-jointed in three main directions, N45 to 65E dipping 65 to 75SE, N and vertical and N50 to 70W dipping 70-80°S-Sw. Flat joints are well developed particularly in the high ridge of outcrops (Plate 3b). The granite is cut by few, slightly foliated reddish rhyolite dykes with a general east trend. No mafic dykes were observed. Many quartz-fluorite veins have been recognized in different localities cutting the granite, particularly in the central part of the

FIG.10.
GEOLOGIC MAP OF
JABAL SAYID GRANITE

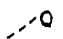
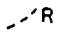
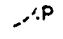
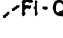
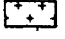
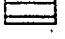
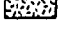
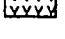
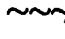


EXPLANATION

QUATERNARY

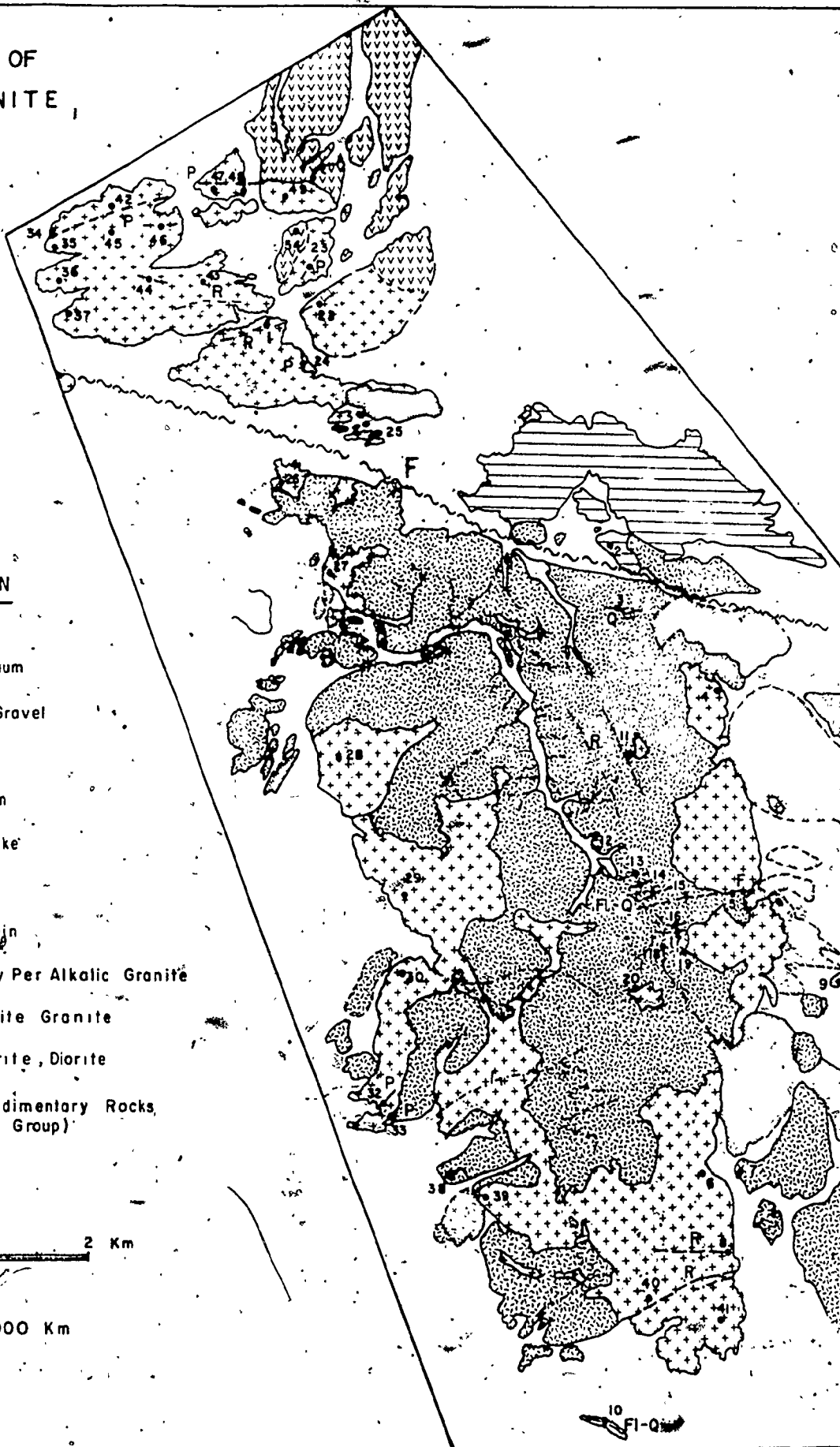
-  Wadi Alluvium
-  Sand and Gravel

PRECAMBRIAN

-  Quartz vein
-  Rhyolite dike
-  Pegmatite
-  Fluorite vein
-  White-Gray Per Alkalic Granite
-  Red Biotite Granite
-  Granodiorite, Diorite
-  Volcanosedimentary Rocks (Hulayfah Group)
-  Fault

0 1 2 Km

Scale: 1: 30,000 Km



mapped area (Plate 3c). The general trend of these veins is N80E to East. Pegmatitic granite and pegmatitic dykes and pockets were recognized in many places in this granite, especially along its north and east borders (Plate 3e, f). The granite also contains streaks and knots of pegmatite, a few meters long in which amphibole crystals have lengths of 10 to 25 cm (Plate 3d). Both the quartz fluorite veins and the pegmatites will be discussed later. The major structure in the area includes two major west-northwest, east-southeast faults. The southern margin of the granite abuts against Al-Aqiq faults; from the north it is offset northwestward along wadi Al-Hifer fault. Both faults parallel the major trend of the Najd fault system.

The contact between the granite of Jabal Sayid and the country rocks is sharp, and no pronounced decrease in the grain size was noticeable. Pegmatitic modification of the granite, and pegmatite dykes and pockets were developed along the north and east contacts. A few localized regions of contact metamorphism, limited to a few meters, have been recognized along the north contact where the granite is in contact with the volcanosedimentary rocks of Halaban group. The contact is everywhere vertical or steeply dipping outward. The contact zone and the granite itself are almost free of any inclusions of country rock.

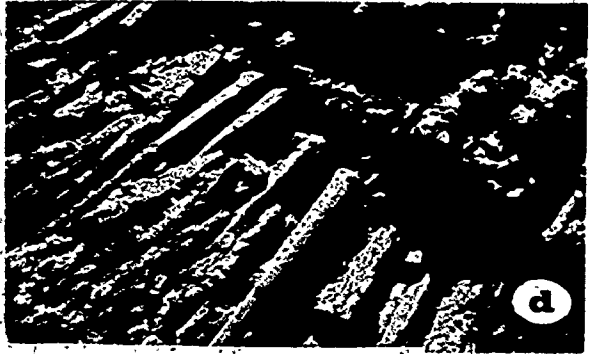
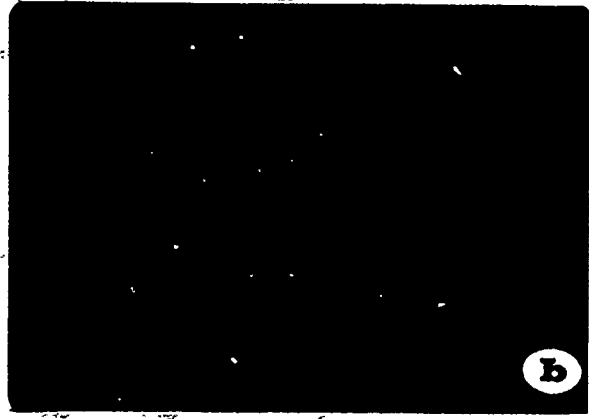
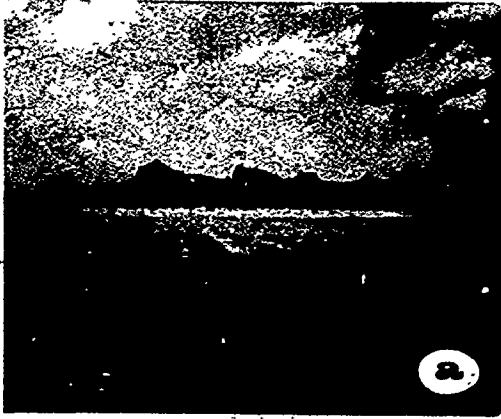
Pegmatitic dykes to 50 30 meters long and 30 cm to 1.5 meter thick and lenses up to 3 meters long and 6

PLATE 3

Jabal Sayid Riebeckite Granite

- a) A view, looking northwest of Jabal Sayid riebeckite granite.
- b) High standing ridges and sharp erosional peaks of Jabal Sayid riebeckite granite intruding the dioritic country rocks (dark gray).
- c) Quartz fluorite vein of Jabal Sayid.
- d) Pegmatite knots along the border of the granite in which amphibole crystals have lengths of 10 to 25 cm.
- e) Pegmatitic dyke with radioactive minerals along the north edge of Jabal Sayid riebeckite granite.
- f) Pegmatitic vein cutting the riebeckite granite of Jabal Sayid.

PLATE 3



meters thick, occur mainly along the east and north borders of the Jabal Sayid granite. They are quartz, microcline, hematite, zircon and radioactive minerals. Bouladon (1968) has described one of them as a zone of quartz feldspar and hematite surrounding a core of quartz with pockets of pink feldspar. All pegmatitic dykes and lenses have a distinctive reddish brown to dark brown colour. Some of the pegmatitic dykes are foliated and composed of quartz with few grains of feldspar and hematite with radioactive minerals.

Quartz-fluorite veins occur outside and within the granite of Jabal Sayid. The veins outside the main mass are not as well developed as those in the interior part. They are mostly quartz with fluorite and cryptocrystalline quartz filling fractures in the vein. The largest vein, which forms a pronounced ridge along the southern edge of the granite is about 60 meters long and about 1 meter wide, trends N70W and dips steeply to the northeast. The fluorite is not more than 5% by volume of the vein. Seven well developed veins occur at the central part of the granite. Most of these veins have banded structure where quartz bands alternate with those of fluorite. The veins each are 20-40 cm wide, with 20-50 meters strike length. The general strike is East to N70°E and dip is vertical. The fluorite is moderately hard, glassy, transparent to translucent, occurring commonly as crystalline masses. Colour varies between colourless, green, violet,

and purple, with pale green most prevalent. Veins are mainly in fissures that cut the granite or the country rock along the contact zone.

3.4.2 Petrography

The granite of Jabal Sayid is practically identical with the Hadb-Aldyaheen riebeckite granite which will be described later. Both rocks have the same appearance in hand specimens, the same mineralogy and the same texture. In detail they have minor differences as the following:

- 1) The relative proportions of the main constituents
- 2) The intensity of grains deformation and alteration.

These differences will be emphasized during the following brief petrographic description of Jabal Sayid granite.

The common texture is hypidiomorphic porphyritic, with large grains of quartz, K-feldspar, occasional phenocrysts of riebeckite and aegirine in a groundmass of albite laths and quartz grains. Quartz forms 40 to 56 percent of the mode. Large grains have ragged boundaries and are commonly fractured and sometimes fragmented with strong undulatory extinction (Plate 4e, f). Potash feldspar occurs as microcline and microcline exsolution perthite (Plate 4b, c, d). Both occur in 22 to 34 percent. The perthite form here is more dominant than microcline. The ratio of microcline to albite phase, by volume, in the perthite form is about 3:1.

Plagioclase, which is 10 to 16 percent of the mode, is present as albite An_0 - $An_{0.12}$ (Appendix C, Table 10c). Electron microprobe analyses of 35 plagioclase grains from 3 samples, including grains from the groundmass and grains which are enclosed by microcline and quartz grains (Plate 4d, g), indicate that all have the composition of albite with minor differences in the amount of K_2O and Fe_2O_3 content. The analytical results are listed in Appendix C. Aegirine is from 2.5 to 5 percent and is mainly long or short euhedral-subhedral prismatic shapes (Plate 4d, e). Some crystals are bent or fractured; many of the fractures are filled with quartz veins, indicating some sort of late deformation.

Riebeckite makes up 1 to 3 percent of the mode. It is very commonly altered either partly or completely to iron ore or to dark brown-dark green alteration products (Plate 4e, f). In many instances allanite and few sphene grains were found in the vicinity of the altered riebeckite grains. Riebeckite and aegirine have the same general characteristics as those of the riebeckite granite of Hadb-Aldyaheen, that is spongy texture, poikilitically enclosing albite laths, microcline, quartz and fluorite.

In terms of accessories, iron oxides, mainly hematite, are the most common accessories, accompanied by fluorite, allanite and locally, zircon are more abundant than in Hadb-Aldyaheen riebeckite granite. Hematite occurs

Table 5. Modal composition of Jabal Sayid riebeckite granite

Sample No.	Quartz	K-feldspar	Plagioclase	Aegirine	Riebeckite	Access.*
J5.13	49.1	28.88	11.88	5.2	3.12	1.82
J5.6	54.64	26.46	11.48	2.86	2.68	1.88
J5.20	54.10	22.66	13.54	3.65	2.30	3.74
J5.40	56.10	27.30	10.20	2.80	1.00	2.60
J5.43A	45.56	30.81	14.93	2.00	2.18	4.52
J5.26	40.82	34.14	16.39	2.58	1.97	4.1
J5.28	49.46	28.79	13.05	3.17	1.88	3.65
Range	40.82- 56.1	22.66- 34.14	10.2- 16.39	2.00- 5.2		
Average	49.46	28.79	13.05			

*Accessories include hematite, fluorite, allanite and zircon.

JABAL SAYID RIEBECKITE GRANITE

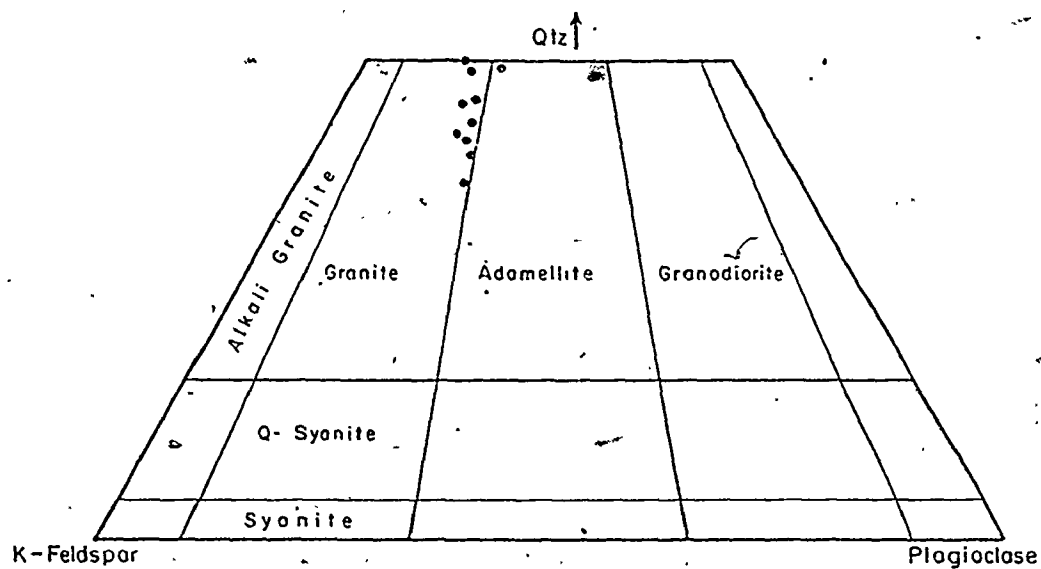


Figure 11. Modal classification of the riebeckite granite of Jabal Sayid.

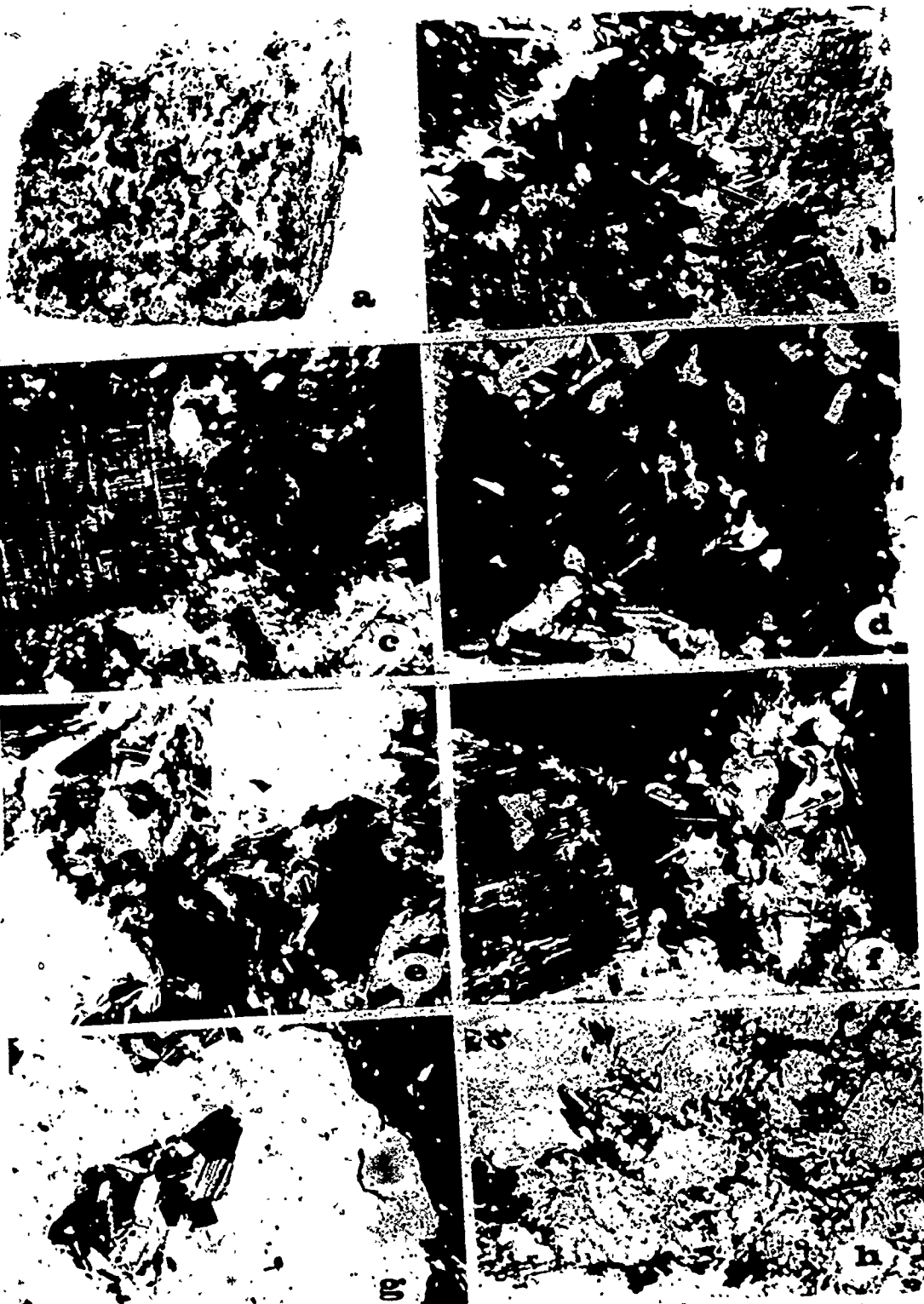
PLATE 4

Jabal Sayid Riebeckite Granite

Thin Sections

- a) Handspecimens of Jabal Sayid riebeckite granite.
- b) Twinned riebeckite, laths of albite and microcline crystals. (Cross nicols, X16)
- c) Riebeckite crystal (black) with spongy texture, poikilitically enclosing albite laths, microcline, quartz and fluorite; with microcline crystal (left) partly replaced by albite. (Cross nicols, X16)
- d) Microcline crystal with albite patches and well twinned albite laths; with fractured aegirine crystal (dark gray) enclosing albite laths and quartz grains. (cross nicols, X25)
- e) Albite laths surrounding the large quartz grains (white); euhedral aegirine crystal (dark gray) and riebeckite crystal (black) enclosing albite laths. (Cross nicols, X16)
- f) Albite laths enclosed by altered riebeckite crystal (black) and along the edge of quartz grains (dark gray) and by microcline. (Cross nicols, X25)
- g) Microcline, aegirine and albite laths are enclosed by quartz grains. (Cross nicols, X16)
- h) Hematite associated with the albite laths in the groundmass. (Plane polarized light, X25)

PLATE 4



either as an alteration product of riebeckite or as a well-crystallized grain associated with albite in the groundmass (Plate 4h). The seven modal analyses of Table 5 are plotted on the ternary diagram of Fig. 11. Most fall within the upper part of the granite field.

3.5 Hadb-Aldyaheen Ring Complex

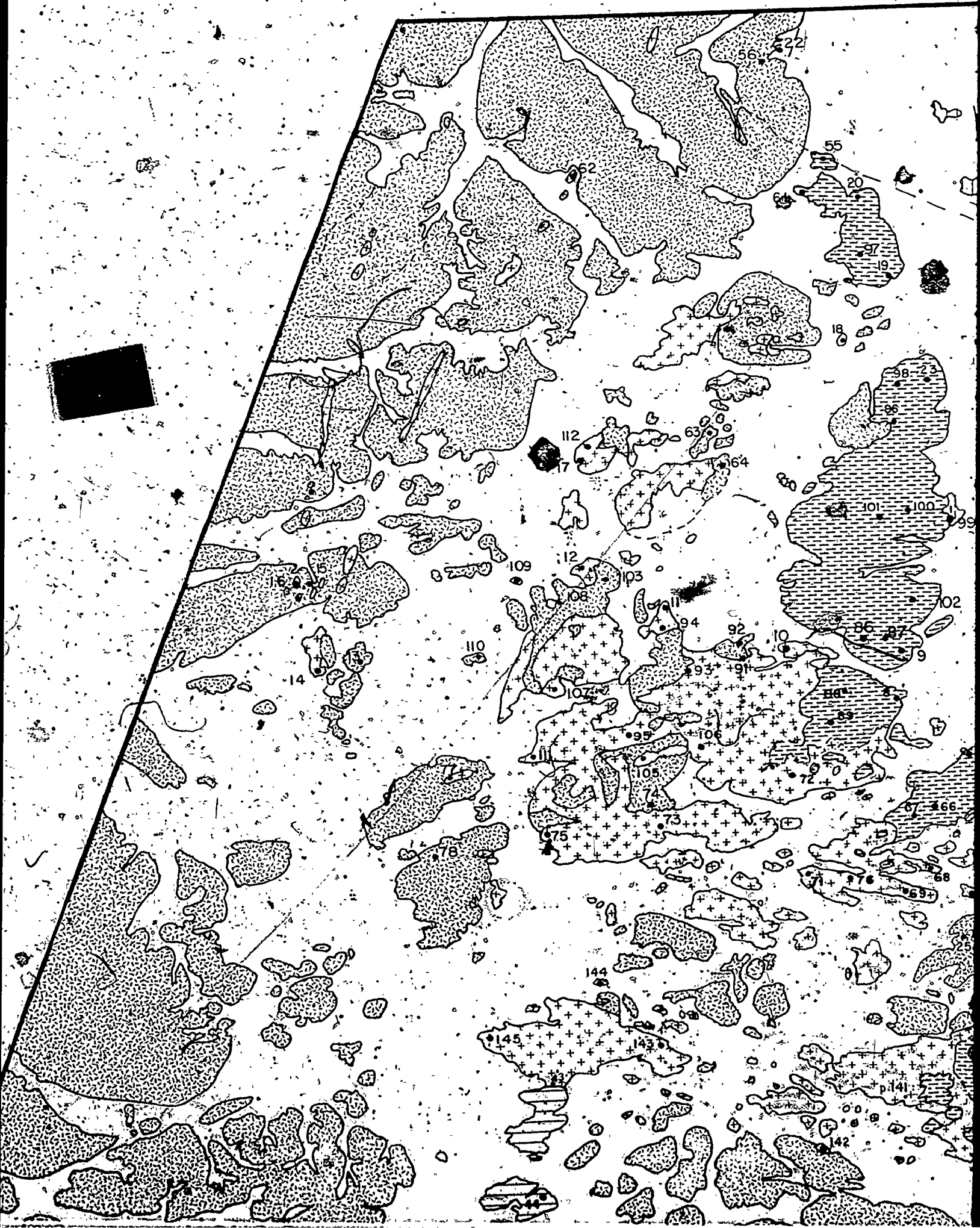
This complex is between lat. $23^{\circ}.30'N$ and $23^{\circ}37'N$ and long. $41^{\circ}7'E$ and $41^{\circ}15'E$, and is about 20 km north of the Albari Granite and about 30 km northeast of the ancient gold mine of Mahd-Adh-Dahab.

3.5.1 Geologic Setting (Fig. 12)

The Hadb-Aldyaheen ring complex occupies an area of about 117 square kilometers. It is oval in outline with longer and shorter axes measuring 11.5 and 10.2 kilometers. It is predominantly granitic rocks, rich in alkali feldspar and distinguished by the presence of riebeckite and aegirine as the main mafic minerals. It may therefore, be termed peralkaline.

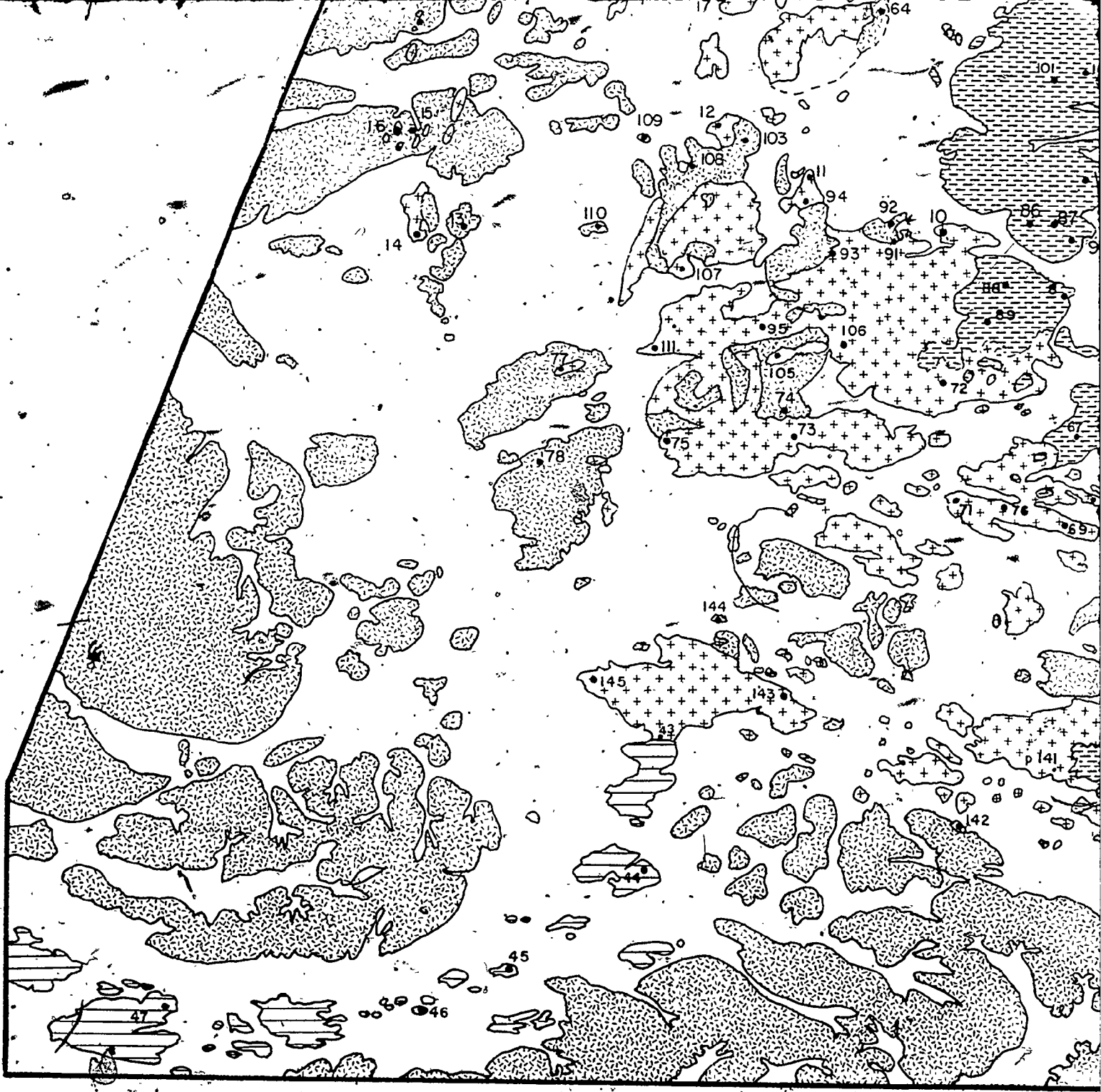
Because of the superior resistance of these granites to erosion, the ring complex of Hadb-Aldyaheen appears as a prominent massif rising well above the level plains (Plate 5a). The ring complex is of a simple general pattern. The separate granitic intrusions are arranged concentrically and clearly defined topographically. The

FIG. 12. GEOLOGIC MAP OF HAUB - ALU



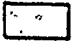


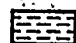
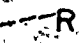




MAP OF HADB - ALDYAHEEN GRANITE COMPLEX





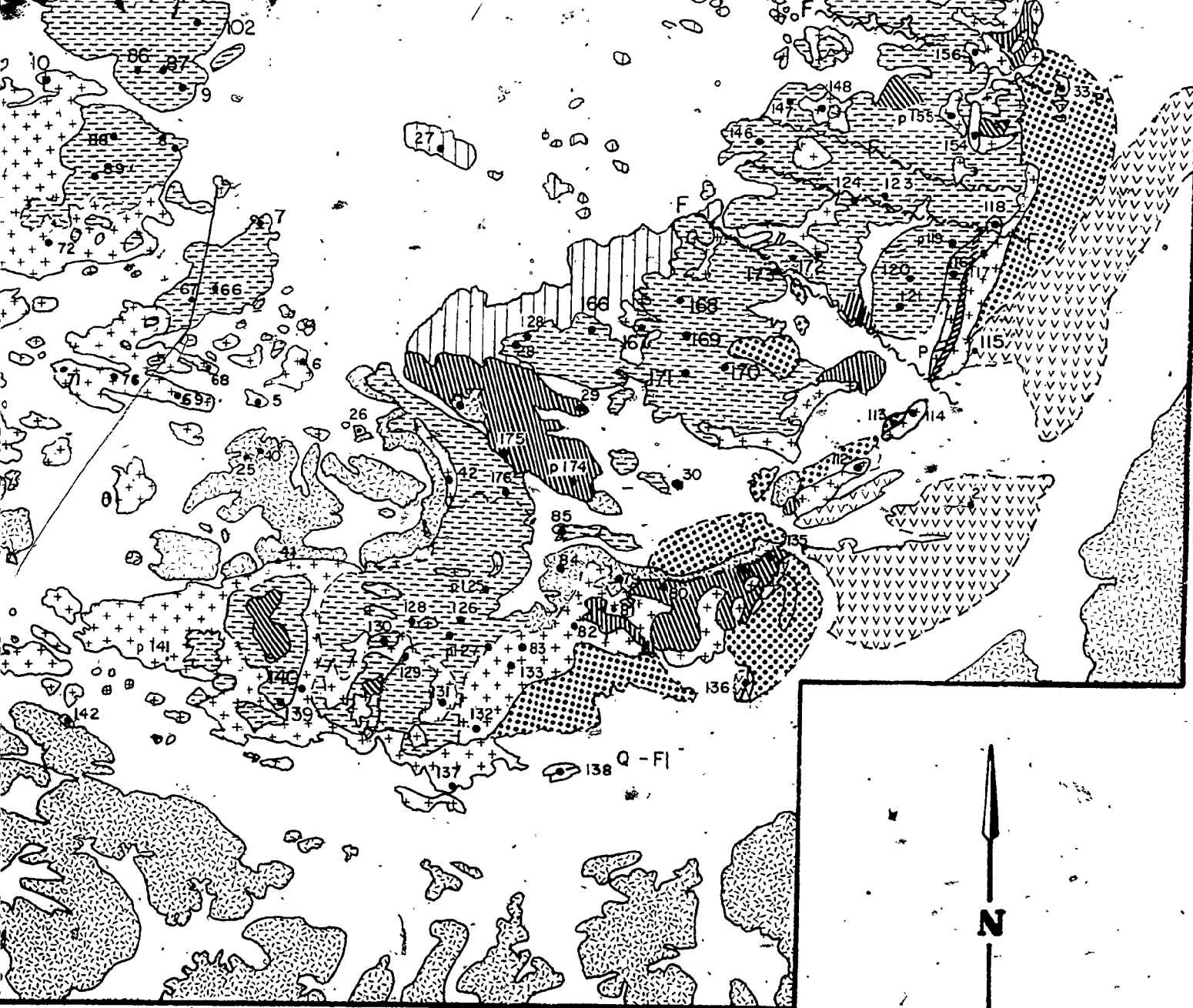
EXPLANATION



- | | | | |
|---|----------------------------|---|--------------------------------------|
|  | Wadi Alluvium |  | White-Gray Albite-Riebeckite Granite |
|  | Sand and Gravel |  | Reddish-Dark Gray Granite Porphyry |
|  | Sheared Rhyolitic Dike |  | Reddish-Micro Granite |
|  | Pegmatite and Quartz Veins |  | Biotite Granite |
|  | Quartz-Fluorite Vein | | |

0 2 Km

Scale: 1:30,000



Km
Scale: 1 : 30,000 Km

Albite-Riebeckite Granite
Dark Gray Granite Porphyry
Micro Granite
Granite

Red Biotite Granite
Granodiorite-Quartz Diorite-Diorite and Gabbro
Metamorphosed Volcanic Rocks
Fault



center of the complex is an oval-shaped biotite granite which forms low-lying, marshy ground (Plate 5c). Microgranite occurs mainly at the east side of the complex in the form of relatively small discontinuous pendants enclosed by granite porphyry. Granite porphyry is a ring dyke surrounding the west, east and south margins of the central biotite granite. The ring dyke consists of high hills on the east and west sides and relatively low hills at the south. The fourth unit is riebeckite granite which intrudes the granite porphyry and forms high standing ridges and sharp erosional peaks (Plate 8a). Outcrops of this granite determines the outline of the complex in that they occur along the outer margin of the granite porphyry in the form of a discontinuous ring dyke (Fig. 12). The rocks of the complex are well jointed in a roughly cubic pattern. Radial faults are also emphasized by vertical cliffs and steep-walled wadis. The relative ages of the rock members of Hadb-Aldyaheen complex are mainly based upon mapping.

A preliminary age of 500 m.y. was determined by R. Reesman, 1964, for galena in a small pegmatite within the complex (R. Goldsmith et al., 1971). K-Ar age determination of the granite porphyry and riebeckite granite indicate ages of 573 and 557 m.y. respectively (Geophysics Department, University of Western Ontario). Rocks of the complex discordantly cross-cut Precambrian quartz diorite, granodiorite and diorite. Quartz diorite

seems to be the main country rock which has least resistance to erosion and forms isolated groups of low hills and rarely continuous ranges (Plate 5b). They are dark-gray to greenish gray in colour, mostly medium-grained; fine and coarse varieties are present. Mafic mineral content varies from place to place but typical constituents are plagioclase of andesine and labradorite composition, green hornblende with or without quartz and K-feldspar. They also contain chlorite and epidote where they are cleaved and sheared.

Diorite country rock west of the complex is intruded by the red biotite granite as small isolated bodies. This granite adjoins the southern margin of the complex in the form of a semi-ring shaped mass. It is a medium to coarse grained, orange to reddish rock with scattered quartz and white plagioclase crystals set in a groundmass of finer-grained red potash feldspar and small clusters of biotite. The country rock also includes metamorphosed volcanic rocks in the mapped area, exposed at the east margin of the complex as small outcrops of low relief. The rocks surrounding the complex are considered to be regionally metamorphosed to green schist facies. The northeast side of the complex, slightly outside of the mapped area (Fig. 12), abuts against the major northwest striking Aqig fault which is part of Brown's (1960) Najd wrench-fault system.

3.5.2 Biotite granite

This granite occupies a central position in the complex, and forms an elliptical body in plan with long axis trending northeast. The rock is weathered, and topographically distinguished from other members of the complex (Plate 5c). The granite commonly occupies low-lying areas covered by gravels and blown sands. Where the rock is exposed, it is rubbly and weathered, although small less-weathered exposures occur in the south and northwest parts of the body. It is typically a medium-grained biotite granite; inward the rock becomes variably porphyritic in texture with light pink potash feldspar phenocrysts up to 1 cm in length and 1/2 cm in width. It is cut by two rhyolite dykes with a general trend of N60W (Plate 5a). These dykes cut the country rock, but their continuation into the surrounding granite porphyry is not certain. They are very similar to rhyolite dykes recognized in the Albari granite, south the complex. No basaltic dykes were observed. The contact with the surrounding granite porphyry is poorly exposed, and no reliable estimation of the attitudes can be made.

3.5.2.1 Petrography

This granite is gray to pinkish-gray in colour. It is massive, crystalline, medium-grained and locally has a porphyritic texture with phenocrysts of pinkish feldspar.

It has fairly uniform composition. The main constituents are white and pinkish feldspar, quartz and biotite. Under the microscope the texture is hypidiomorphic granular in which the predominant mineral is quartz, accompanied by euhedral to subhedral plagioclase and anhedral microperthite. The main mafic mineral is biotite. Accessory minerals include pyrite, sphene and apatite.

Plagioclase is the dominant feldspar, and is 32.8 to 36.5 percent of the mode (Table 6) as subhedral twinned grains of 0.3 to 3 mm long by 0.2 to 0.9 mm wide. It is oligoclase An_{14} to An_{24} and oscillatory zoning is well developed among many grains with rims of An_{14-20} and cores of An_{16-24} (Appendix C, Table 3c). Plagioclase crystals are commonly occupied by sericite, kaolinite and muscovite particularly in their cores. There are also inclusions of pyrite, biotite, apatite and quartz. Myrmekite intergrowths have been occasionally noted between plagioclase and perthite crystals.

Quartz is 34 to 40 percent of the mode. It occurs chiefly as interstitial grains up to 1.5 mm in diameter and as small grains 0.2 mm in diameter either in an interstitial position or poikilitically enclosed in large crystals of feldspar. Alkali feldspar is 20 to 23 percent of the mode. It is anhedral grains of microperthite interstitial between plagioclase grains. It is almost always of an exsolution type. Grain size is from 2 mm to 0.3 mm in diameter. Large

Table 6. Modal Composition of Hudb-Aldyaheen biotite granite.

Sample No.	Quartz	Plagioclase	K-Feldspar	Biotite	Chlorite	Access.
HD.22	34.77	36.5	20.31	6.04	1.27	1.11
HD.27	36.11	34.00	23.44	4.56	0.78	1.10
HD.28	40.11	32.85	21.56	3.31	0.53	1.64
Range	34.77- 40.11	32.85- 36.5	20.31- 23.49	3.31- 6.04	0.53- 1.27	1.1- 1.64
Average	36.99	34.45	21.77	4.64	0.86	1.28

phenocrysts to 1.2 cm long and 4 mm wide occur locally. The perthite grains are almost unaltered. The large microperthite crystals commonly enclose inclusions of plagioclase, biotite, quartz and opaque minerals.

Biotite makes up 3 to 6 percent of the mode. It occurs as a tabular crystal and larger flakes, forming lamellar aggregates. Grain size ranges from 0.2 mm to 1.5 mm long and 0.2 to 0.7 mm wide. Chlorite and sphene are common alteration products. Prisms of apatite, oxidized pyrite are the usual inclusions and less commonly, plagioclase and small quartz grains. The most abundant accessory minerals are pyrite, sphene and apatite. Pyrite and sphene are always associated with the biotite and some sphene grains form a reaction rim around oxidized pyrite grains.

3.5.3 Microgranite

The microgranite occurs mainly as pendants enclosed in the granite porphyry on the east side of the complex. In most instances this granite, with its reddish brown colour on weathered surface, is very difficult to recognize in the field because of its similarity to the reddish variety of the granite porphyry. In outcrops where microgranite is mixed with granite porphyry, the entire outcrop was mapped as microgranite where it is the dominant rock type in that particular outcrop. The contact zone between microgranite and granite porphyry is so confused

that there is no reliable determination of attitude. It appears that these two granites are close to each other in time. Age relationship between the microgranite and the biotite granite is uncertain.

3.5.3.1 Petrography

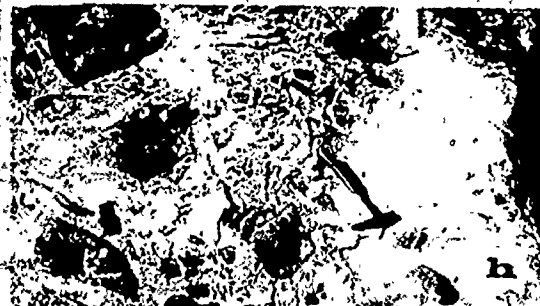
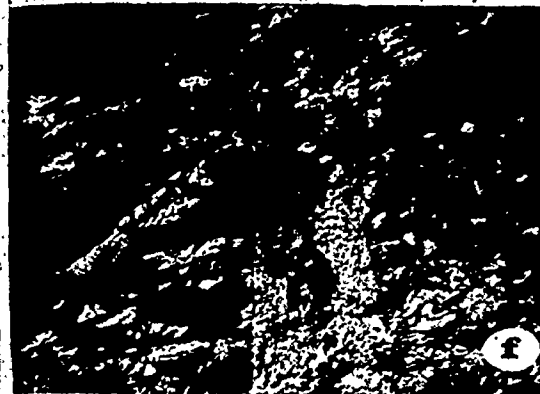
The microgranite has a remarkable uniformity of texture and composition. It is reddish to reddish-brown, with a finer grained 0.02 to 0.2 mm homogeneous groundmass and very few phenocrysts of pink-feldspar to 3 mm in diameter plus clots of fine-grained dark green minerals up to 2 mm in diameter. Occasional rounded quartz phenocrysts are also present and 2 to 3 mm in diameter. Most of the microgranite is very fine-grained and in this respect can resemble rhyolite. In thin section, phenocrysts of perthite, hornblende and clots of biotite and chlorite can be identified within (Plate 6a) quartz, plagioclase, K-feldspar as microperthite, biotite and hornblende. The plagioclase is clearly twinned and it is albite, An_0 to An_5 (Appendix C, Table 4c). The perthite phenocrysts are mainly of a replacement type 0.5 to 3 mm in diameter. They are slightly altered to sericite. Occasional hornblende and biotite phenocrysts (1-2 mm in diameter) were found. (Plate 6a), and they are as the rest of the hornblende and biotite in the rock are commonly altered to chlorite and iron ore. The common accessory minerals are sphene, magnetite, hematite and occasional apatite. Calcite occurs as a secondary mineral associated with the altered hornblende crystals.

PLATE 5

Habb-Aldyaheen Ring Complex

- a) Riebeckite granite forming the eastern margin of the ring complex.
- b) A view, looking east of the low hills of the dioritic country rocks.
- c) Sheared rhyolite dyke cutting the biotite granite in the central part of the complex.
- d) Apophyses of medium grained riebeckite granite cutting the granite porphyry.
- e) Sharp contact between the riebeckite granite (gray) and the granite porphyry (dark gray).
- f) Pegmatitic dyke with radioactive minerals cutting the granite porphyry along the eastern contact with the riebeckite granite.
- g) Flattened inclusions of granite porphyry within the riebeckite granite along the contact between the two.
- h) Rounded and subrounded inclusions of granite porphyry within the riebeckite granite.

PLATE 5.

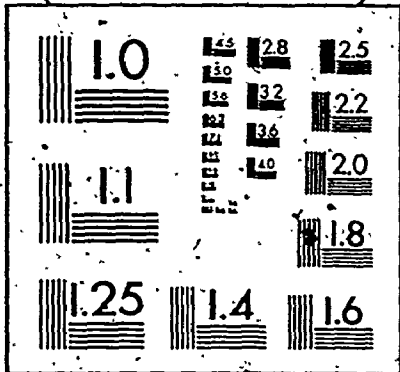


3.5.4 Granite Porphyry

Granite porphyry is the predominant unit forming the Hadb-Aldyaheen ring complex. It occurs as a large ring dyke, extending for 8 km with maximum thickness of 2 km, and almost completely surrounding the biotite granite of the inner part of the complex (Plate 5c). In plan, the outcrop is crescentic and thins out to the north. It is widest at the south end of the complex (Fig. 12). The resistance of the granite porphyry to erosion is less than that of the riebeckite granite and very much greater than that of any of the country rocks. The rock has variations of colour, ranging from various shades of gray to brown and reddish-brown. It has a porphyritic texture, and rarely has more than 25 percent phenocrysts of corroded crystals of bipyramidal quartz, pink feldspar and occasionally plagioclase. Heterogeneity of texture and colour becomes more pronounced at the margins.

The contact of the granite porphyry with the biotite granite is not exposed, although both rocks crop out within a few meters of each other. The contact between granite porphyry and riebeckite granite is exposed (Plate 5e) and in many places it is sharp, and irregular. It is generally vertical or dips steeply outward. Irregular apophyses of riebeckite granite penetrate the granite porphyry (Plate 5d). The riebeckite granite along some of the southwest contact is crowded with inclusions from the

2



4 5110 NIAUS BUC-711 11 2/68

granite porphyry. These inclusions are from 30 to 5 cm. in diameter and commonly subrounded to subangular in shape (Plate 5h). Some are progressively more flattened toward the contact, and the elongation is parallel to the contact (Plate 5g). The contact of this granite with the older dioritic country rocks is usually marked by a break in slope. The actual contact is sharp, and where measurable is observed to dip outward. Inclusions of country rocks are not found in this granite. Narrow elongate bodies and screens of older diorite are in many places enclosed between granite porphyry and riebeckite granite outcrops. The contact attitude of these bodies is not clear, but in general, appear to be dipping outwards.

Many pegmatites bearing radioactive materials occur in the complex, and most of them are associated with the granite porphyry outcrop (Plate 5f). Most are not true dykes, but rather are knots and lenticles in the granite porphyry, no more than 10 meters long with maximum thickness of about 1.5 meter. Nowhere do they penetrate older rocks and most are near the outer contact zone of the granite porphyry. They consist of quartz, potash feldspar crystals up to 3 cm in diameter with finer grained aggregates, about 1 to 2 mm, of quartz, K-feldspar, and dark minerals including zircon and permeated with earthy hematite. Most of them have been brecciated and filled with veins and vugs of quartz.

Joints are well developed in the granite porphyry. Beside the flat joints, four main sets of joints have been recognized with attitudes of strike N5E dip vertical, strike N20 to 30E, vertical dip, strike N60 to 70W dip 80°W and strike N55 to 65E dip 60° to 70°SE.

3.5.4.1 Petrography

This granite is hard, resistant rock, gray to pinkish-gray in colour although some of the darker granite porphyry contains an abundance of iron oxide which imparts a reddish colour to the weathered rock. Phenocrysts of pink gray feldspar and quartz are set in a dense ground-mass peppered with dark minerals. Mafic minerals as phenocrysts are very rare. Phenocrysts, generally accounts for 15 to 40 percent of the rock, rarely exceed 35 percent.

Potash feldspar phenocrysts 2 to 6 mm in diameter are most abundant in phenocrysts. They are subhedral or rounded in shape and are microcline microperthite. The proportion of albite lamellae is 15 to 45 percent. Some perthite phenocrysts have rims of albite about 0.5 to 1 mm thick (Plate 6f). Some are euhedral to subhedral, but most are smoothly rounded (Plate 6c). Myrmekite is common only in four samples and occurs mainly along the margins of perthite phenocrysts. A few perthites are slightly altered to sericite but in general, they are fresh (Plate 6c, f). In some samples perthite phenocrysts poikilitically

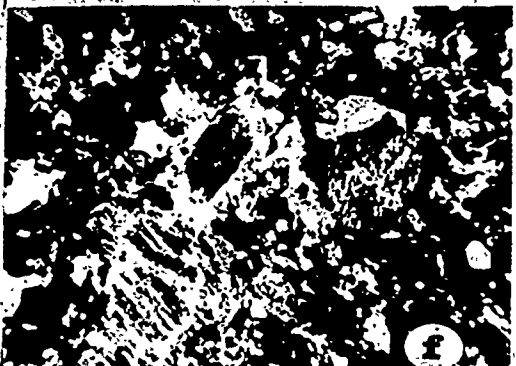
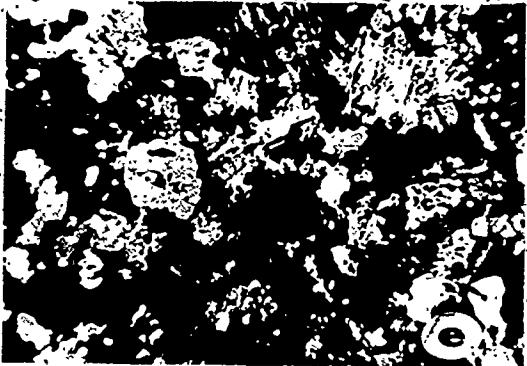
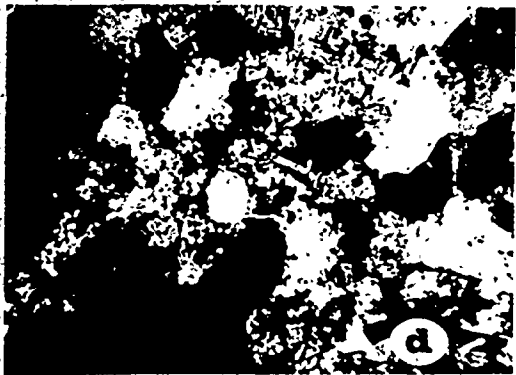
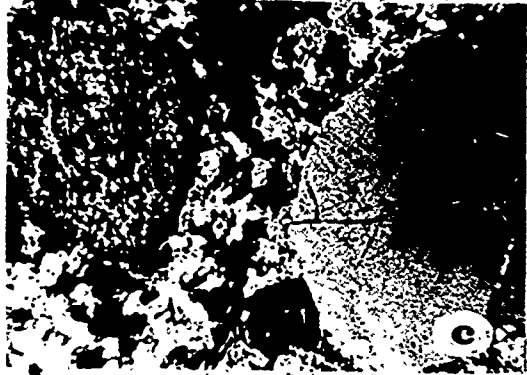
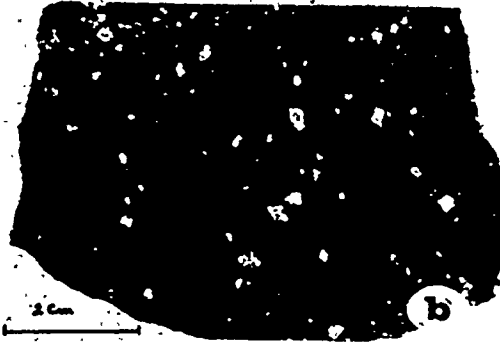
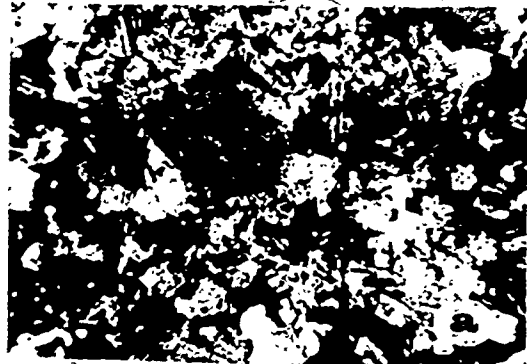
PLATE 6

Granite Porphyry of Hadb-Aldyaheen

Ring Complex (Thin Sections)

- a) Hornblende phenocrysts in the microgranite, with fine grained groundmass of quartz, plagioclase, biotite. (Cross nicols, X16)
- b) Handspecimen of the granite porphyry with K-spar and quartz phenocrysts.
- c) Rounded quartz and microperthite phenocrysts within a groundmass of fine grained quartz, albite microcline and riebeckite. (Cross nicols, X16)
- d) Corroded quartz phenocrysts (dark gray), albite and microcline appears in the groundmass. (Cross nicols, X16)
- e) Rounded quartz and rectangular microperthite phenocrysts. (Cross nicols, X16)
- f) Microperthite phenocrysts rimmed with albite. (Cross nicols, X16)

PLATE 6



enclose laths of albite and grains of quartz, fluorite and magnetite (Plate 7c). In one sample out of 35, small grains of brown biotite were formed as an inclusion in a perthite phenocryst.

Quartz phenocrysts are 2 to 5 mm in diameter, stubby, rounded bipyramidal crystals of beta or high temperature form. They are 5 to 15 percent of the rock. Many of them are cracked and in a few of them the fractures are occupied by fine grained groundmass minerals (Plate 6d). Undulose extinction is common.

The few phenocrysts of riebeckite average about 1.5 mm in length and 0.4 mm in width and have prismatic shape. Some are subrounded or compact clots of 0.2 mm grains. They are notably spongy and poikilitically enclosing numerous rounded-subrounded inclusions of quartz, albite, fluorite, sphene and a few small prisms of needles of apatite (Plate 7d, e, f). Few of the riebeckite phenocrysts are partly altered to iron oxide. In many instances, a disoriented 0.1 mm crystal of brown biotite was found in the middle of a riebeckite phenocryst (Plate 7d, e).

Groundmass accounts for 60 to 85 percent of the rock, is remarkably uniform and composed of perthite, quartz, riebeckite, aegirine, albite laths and a few biotite grains. Grain size is from 0.5 to 0.1 mm. Approximately half of the groundmass is microperthite with the same characteristic as the K-spar phenocrysts (Plate 6e). There are a few microcline grains in the groundmass (Plate 6d). Quartz grains

PLATE 7

- a) Euhedral quartz phenocryst and albite laths of the granite porphyry. (Cross nicols, X25)
- b) Myrmekite developed along border of the perthite phenocrysts. (Cross nicols, X25)
- c) Microperthite phenocrysts, with apatite and fluorite inclusions, small twinned riebeckite crystal. (Cross nicols; X25)
- d) Riebeckite phenocrysts, with spongy texture enclosing inclusions of albite, quartz and fluorite. (Plane polarized light, X25)
- e) Euhedral spongy crystal of riebeckite has biotite (dark gray) in the center and inclusions of albite and quartz (white). (Plane polarized light, X25)
- f) Spongy texture of riebeckite crystal with inclusions of euhedral apatite and fluorite grains. (Plane polarized light, X64)

PLATE 7

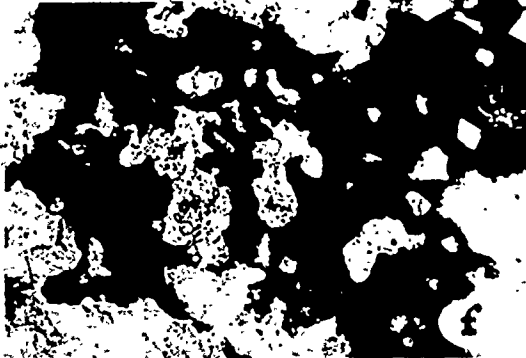
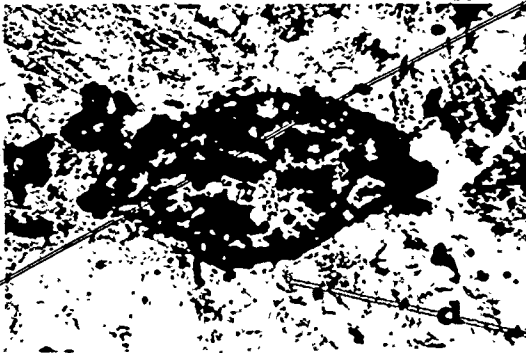
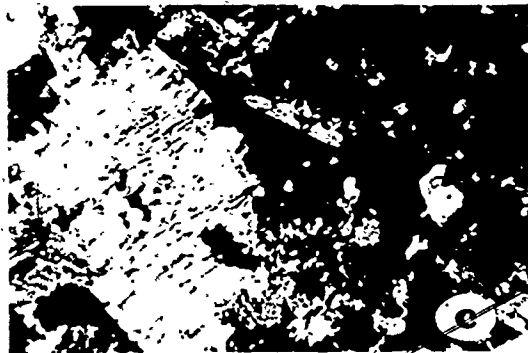
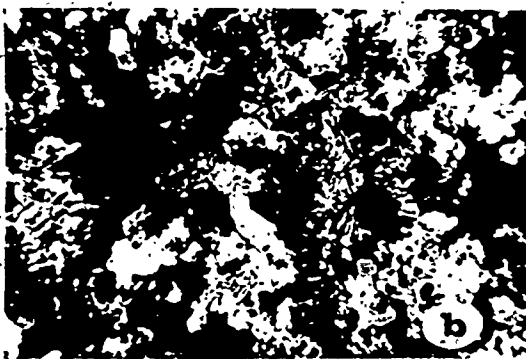


Table 7. Modal analyses of the granite porphyry of
Hadb-Aldyaheen ring complex.

Sample No.	K-feldspar	plagioclase	quartz	Riebeckite	aeqirine	Access.
HD 7	51.09	5.93	34.22	3.69	2.65	0.34
HD 9	47.01	10.28	33.29	3.64	3.58	2.21
HD 19A	57.36	2.22	27.04	3.88	7.75	1.08
HD 24	51.5	7.5	39.3	0.2	0.7	0.8
HD 147	44.12	11.09	34.85	4.11	3.11	2.72
Range	44.12- 57.36	2.22- 11.09	27.04- 39.3	0.2- 4.11	0.7- 7.75	0.8- 2.72
Average	50.216	7.40	33.74	3.10	3.56	1.43

are of varied shapes from rounded to angular. They are interstitial to feldspar grains.

Riebeckite in the groundmass is small interstitial grains with an average size not more than 0.2 mm, or as aggregates of 0.1 mm grains associated with grains of aegirine and biotite. Elongate or needle-like crystals of riebeckite were also observed. The riebeckite is always very pleochroic, with dark blue to greenish blue to yellowish-green. Aegirine accounts for 3 percent. It is usually intergrown or associated with riebeckite as individual small grains, or as aggregates of needles. Both riebeckite and aegirine have an interstitial position to feldspar indicating a late magmatic derivation. A few subhedral grains of plagioclase with a composition of albite $An_{0.14}$ to $An_{0.35}$ (Appendix C, Table 5c) occur in the groundmass.

Biotite grains, 0.1 mm in diameter occurs mostly as compact clots up to 1.5 mm long, consisting of disoriented grains occupying the core of riebeckite phenocrysts or in the vicinity of the relatively large grains of riebeckite and aegirine. Sphene, fluorite and apatite are the most common accessories. They usually are inside large crystals of the major phases, particularly riebeckite (Plate 7f). Zircon, magnetite, ilmenite and hematite are invariably present. Allanite is rare.

The modal analyses of Table 7, plotted on the triangular diagram of Figure 13, are mostly within the area of granite and alkali granite.

HADB-ALDYAHEEN RING COMPLEX

- ▲ Biotite Granite
- ▲ Microgranite
- Granite Porphyry
- Riebeckite Granite

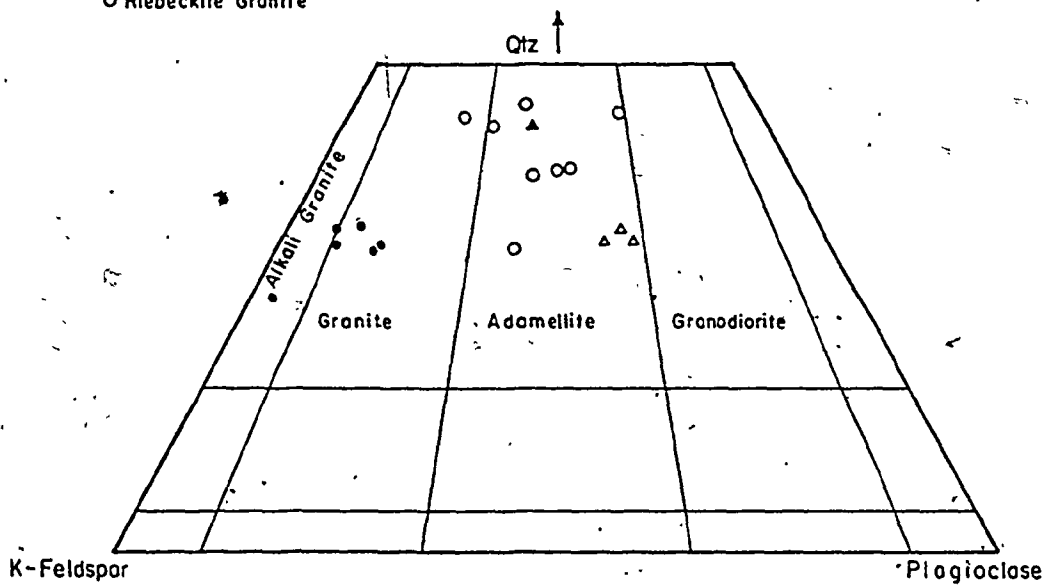


Figure 13. Modal classifications of the rocks forming the Hadb-Aldyaheen ring complex.

3.5.5 Riebeckite Granite

Riebeckite granite of the complex is less extensive than the granite porphyry and forms most of the complex's outer area (Plate 8a). It is a lenticular and arcuate intrusion with the general pattern of a disconnected ring dyke which follows the outer edge of the granite porphyry into which it is intrusive. The riebeckite granite is generally more extensive in the west half of the complex than the east half. Around the west edge of the complex, the riebeckite granite forms two narrow semi-ring dykes, 15 to 25 meters wide, which extend for a distance of about 7 to 8 km, convex toward the west. These dykes are very resistant to erosion, relative to the surrounding diorite country rock and appear as an arc of steep ragged hills separated from the main body of the complex by a wide screen of diorite country rocks. Contact between the riebeckite granite and country rock can be seen in several places and has an outward dip of 65 to 75 degrees.

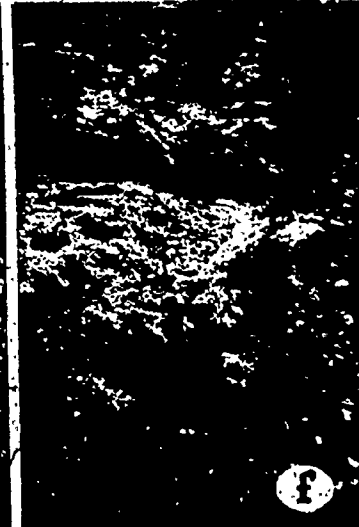
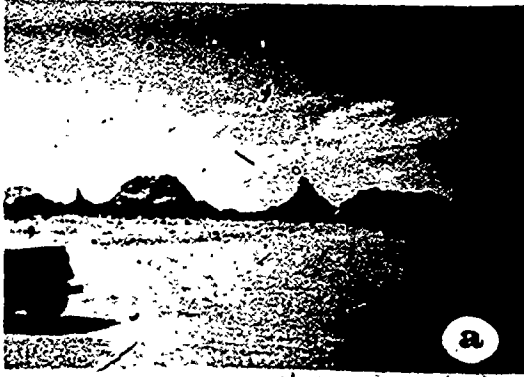
The riebeckite granite is gray-white in colour with transparent to translucent bipyramidal quartz crystals, some of which enclose small needles of riebeckite and aegirine (Plate 10b). Quartz grains are from 4-2 mm in diameter. The texture is medium grained porphyritic with evenly distributed well formed prisms and needles of riebeckite (2-6 x 0.5-2 mm) in a white groundmass of plagioclase, microcline and quartz (Plate 10a,b). Quartz

PLATE 8

Riebeckite Granite of Hadb-Aldyaheen Ring
Complex

- a) Sharp erosional peaks of the riebeckite granite, looking northeast.
- b) Moderately dipping outwards, sharp contact between the riebeckite granite (dark gray) and the diorite of the country rocks (black), looking north.
- c) Dipping outwards sharp contact between the red granite (gray) of the country rock, and the riebeckite granite (dark gray).
- d) Foliated riebeckite granite along the eastern contact with the diorite.
- e) Foliation direction of the riebeckite granite along the eastern contact.
- f) Narrow pegmatitic dykes developed within the granite along the southern contact with country rock quartz diorite.

PLATE 8



phenocrysts are 6 mm in diameter. Coarse and fine textures are also observed and heterogeneity of texture becomes more pronounced in the vicinity of the contact with a coarse texture mainly near the outer margin of the intrusion and fine-grained rock near the inner contact with the granite porphyry. Contact with the granite porphyry is sharp with riebeckite granite locally, chilled against granite porphyry. The exact attitude of the contact is not certain, but generally it is moderate to steeply dipping outwards. Many granite porphyry inclusions occur within the riebeckite granite. The contact between riebeckite granite and diorite country rock is not well exposed, but covered with boulders from the adjacent riebeckite granite but where it can be seen, it is nearly always knife-edge sharp and dipping moderately to steeply outward (Plate 8b). At a few localities, along the east edge, the granite has a foliation produced by orientation of riebeckite and feldspar crystals parallel to the contact. This may have resulted from flowage of melt before consolidation (Plate 8e). There is also a conspicuous foliation within the riebeckite granite at two localities along south-east contact (Plate 8d).

The contact with the older red biotite-granite at the south margin of the complex is sharp and dips moderately outward (Plate 8c). Pegmatite facies of the riebeckite granite occur along some of the contact zones, both as small dykes and knots (Plate 8f).

Knots and streaks of pegmatite, 2-5 meters long with a maximum width of 1 meter, in which the riebeckite and aegirine crystals attain lengths of 2 to 5 cm occur in many places away from the contacts (Plate 9a, b). Some of these streaks and knots have radioactive materials. In general, the radioactivity of the pegmatitic rocks here, is less than the pegmatites of Jabal Sayid. Unlike the similar riebeckite granite of Jabal Sayid, this granite rarely has a marginal pegmatite along its contact with the country rocks.

Fine to medium-grained green narrow dykes and sills of aegirine, riebeckite granite are abundant at the contacts, particularly along the southwest margin. They fill fractures in both the diorite and the riebeckite granite (Plate 9c, d), but do not extend far into the diorite country rock. Constituent minerals of dykes and sills are very similar to those of riebeckite granite but with more aegirine needles and more modal quartz, microcline and accessory sphene. Similar dykes were observed associated with the riebeckite granite of Jabal Sayid.

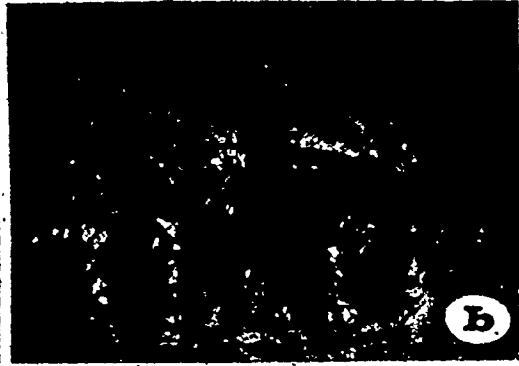
Inclusions of undoubtedly older diorite country rocks are very rare, except xenoliths of mappable dimensions (Plate 12). They mainly occur at the south half of the complex and their contacts with the granite are invariably knife-sharp, steeply dipping outward (Plate 9e). There is a narrow zone, not more than a few meters wide between xenoliths and enclosing granite in which diorite of the xenolith

PLATE 9

Riebeckite Granite of Hadb-Aldyaheen Ring Complex

- a) Pegmatitic streaks, in which the riebeckite and aegirine crystals attain lengths of 2 to 5 cm.
- b) Pegmatitic knots in the riebeckite granite.
- c) Medium grained green narrow dykes cutting the riebeckite granite.
- d) Fine-grained green dyke filling the fractures of the riebeckite granite along the southwest contact with the quartz diorite.
- e) Outward dipping sharp contact between the diorite xenolith (gray) and the riebeckite granite (dark gray).
- f) Jointed riebeckite granite along the eastern margin of the complex.

PLATE 9



is sheared, fine-grained, and chloritic. Riebeckite granite next to the xenolith has more model sphene than the average.

Joints are well developed in the riebeckite granite in a roughly cubic pattern (Plate 9f), and are more widely spaced than in the other granites of the complex. They make many vertical cliffs and steep-walled wadis. The general trends of the main sets of joints are strike N50 to 70E dip 70-80°NW, N20 to 40W dip vertical N60 to 70W dip vertical and EW dip vertical.

3.5.5.1 Petrography

The riebeckite is hypidiomorphic porphyritic (Plate 10a, b, c). Essential minerals are quartz, microcline and microcline-perthite, albite, riebeckite and aegirine. Accessories include sphene, fluorite, apatite, magnetite, hematite, zircon and allanite. Potash feldspar is 33 to 23 percent of the mode (Table 8) and occurs as microcline and microcline perthite in two main forms: (1) as large rectangular grains with irregular rims or as subrounded grains up to 0.9 to 2 mm in diameter (Plate 10c, d, f) and (2) as smaller anhedral grains, 0.1 mm to 0.3 mm in diameter in random orientations in the groundmass (Plate 11a, b). Microcline perthite is mainly of exsolution type and it is less abundant than the microcline. It consists of microcline with clear polysynthetic twinning, penetrated

Table 8. Modal analyses of the riebeckite granite of
Hadb-Aldeyaheen ring complex.

Sample No.	K-feldspar	Plagioclase	Quartz	Riebeckite	Aegirine	Access.
HD 4A	28.29	16.31	49.34	0.14	0.70	5.23*
HD 6	33.02	25.08	33.05	6.49	2.02	0.34
HD 10	26.96	22.17	42.61	5.33	2.06	0.87
HD 14	28.12	10.12	45.41	0.02	7.18	9.15*
HD 17B	13.45	26.54	46.59	5.25	5.73	2.44
HD 18A	23.52	17.46	50.56	7.61	-	0.85
HD 26	22.99	26.02	43.42	5.29	1.71	0.57
HD 150	22.83	24.29	42.65	6.67	2.19	1.37
Range	13.45- 33.02	10.12- 26.02	33.05- 50.56	0.02- 7.51	0.00 7.18	0.34- 2.44
Average	24.91	20.99	44.20	4.60	2.36	1.07

* Mainly iron ores

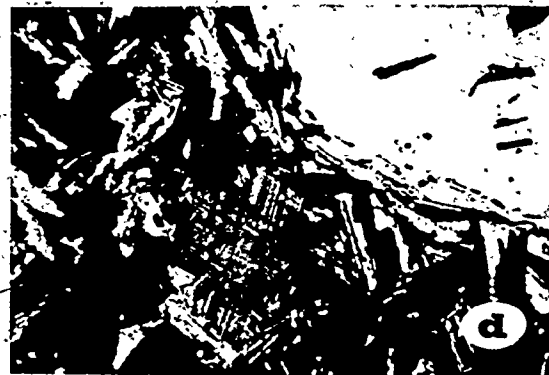
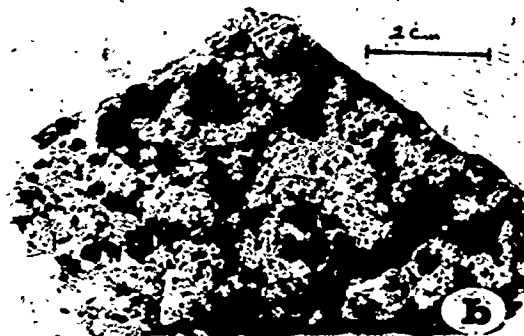
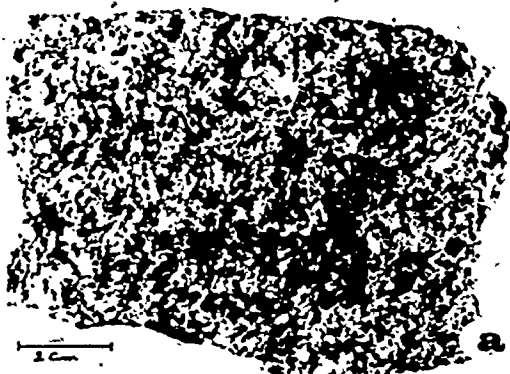
PLATE 10

Riebeckite Granite of Hadb-Aldyaheen

Ring Complex Thin Sections

- a) Handspecimen of riebeckite granite showing the euhedral grains of riebeckite.
- b) Handspecimen of coarse-grained riebeckite granite with pyramidal quartz phenocrysts.
- c) Subhedral rectangular microcline crystal surrounded by laths of albite. Euhedral aegirine crystals (black). (Cross nicols, X16)
- d) Albite laths enclosed and oriented along the margin of the large quartz grain. (Cross nicols, X16)
- e) Microcline porphyrite phenocrysts. (Cross nicols, X25)
- f) Fractured quartz grain (dark gray) enclosing albite laths. (Cross nicols, X25)

PLATE .10



6


by stringers or irregular patches of untwinned albite. The ratio of microcline to albite by volume is about 5:1, most of the time (Plate 11a). Both the microcline perthite and the microcline are enclosing many disoriented well twinned albite laths (Plate 10e, f) which have the character and composition of discrete albite laths in the groundmass (Appendix A, Table). Rounded quartz inclusions also occur. The K-feldspar minerals are clear and free of secondary minerals.

Quartz is 33 to 50 percent of this granite and it is the most abundant modal mineral. It is chiefly as rounded to subrounded interstitial phenocrysts up to 6 mm in diameter, and less commonly as small anhedral grains in the groundmass 0.1 to 0.04 mm in diameter. Some of it is poikilitically enclosed by riebeckite, aegirine and K-feldspar. Few of the large grains are fractured and partly fragmented, some enclose grains of microcline, albite, aegirine and riebeckite. Myrmekitic texture is not present, a point of distinction from the older granite porphyry.

Plagioclase is 11 to 26 percent of the mode and is albite with $An_{0.1}$ to $An_{0.15}$ (Appendix C, Table 6c). It is typically euhedral-subhedral, lath shaped, from 0.1 to 0.6 long by 0.05 to 0.2 mm wide. It occurs mainly in the groundmass and most of the laths in the near vicinity of the phenocrysts of K-feldspar or quartz are oriented parallel

to the phenocryst's borders (Plate 10c, d). Some of these laths are enclosed within the outer part of the quartz phenocrysts parallel to outlines of the enclosing crystal (Plate 10d and 11b). Also, many albite laths were found poikilitically enclosed by riebeckite and aegirine crystals (Plate 11b). The albite invariably has albite twinning although carlsbad twinning was occasionally noted; zoned crystals are absent. Smooth and ragged rims occur and most grains are typically fresh and free of inclusions. Some albite in the groundmass is associated or surrounded by well crystallized grains of hematite.

Some samples contain only aegirine, some only riebeckite, but the majority contain both and riebeckite is dominant. Riebeckite and aegirine crystals are always interstitial to feldspar and quartz. They are commonly spongy with poikilitic inclusions of rounded quartz, albite laths, microcline, fluorite and apatite (Plate 11b and c). Average amount of riebeckite is about 5 percent and occurs two ways: (1) mostly as large interstitial sieve crystals with general prismatic shape, 1-5 mm long by 0.3-1 mm wide. In detail their edges are ragged and appear to be molded on feldspar and quartz (Plate 11a). (2) Less commonly as small grains in the groundmass 0.2 - 0.2 mm in diameter. Riebeckite is always strongly pleochroic, many are twinned and some have a perfect amphibole cleavage. Few are partly altered to iron ore (Plate 10f).



Aegirine amounts to about 2.5 percent on average, and has four modes of occurrence:

1) It is intergrown with riebeckite. There is no regular pattern to these intergrowths and it is difficult to establish the order of crystallization. Aegirine is in the cores and around riebeckite borders (Plate 11b, e). In a few instances it is intergrown in parallel orientation with riebeckite (Plate 11c). This may be caused by fluctuating chemical conditions in the magma resulting in partial transformation of one mineral into the other. (2) Aegirine occurs as long subhedral, spongy prismatic crystals to 1 mm long and 0.2 mm wide. These crystals as the riebeckite, have inclusions of albite, quartz, fluorite, apatite and rarely zircon. (3) It also occurs as smaller euhedral short prismatic crystals not more than 0.2 mm in diameter, commonly with typical four or eight sided sections of pyroxenes; cleavage is prominent (Plate 11d). (4) Aegirine where more abundant relative to riebeckite, particularly in the rocks associated with contact zone, appears as fibrous aggregates to 0.2 mm long, or as dispersed wisps in the groundmass (Plate 11f).

Common accessory minerals are sphene, fluorite, apatite, magnetite, hematite, ilmenite and zircon, erratically distributed. Allanite is rare. In two samples, secondary sericite was identified as veins filling the fractures in some quartz phenocrysts. None of the accessories which have

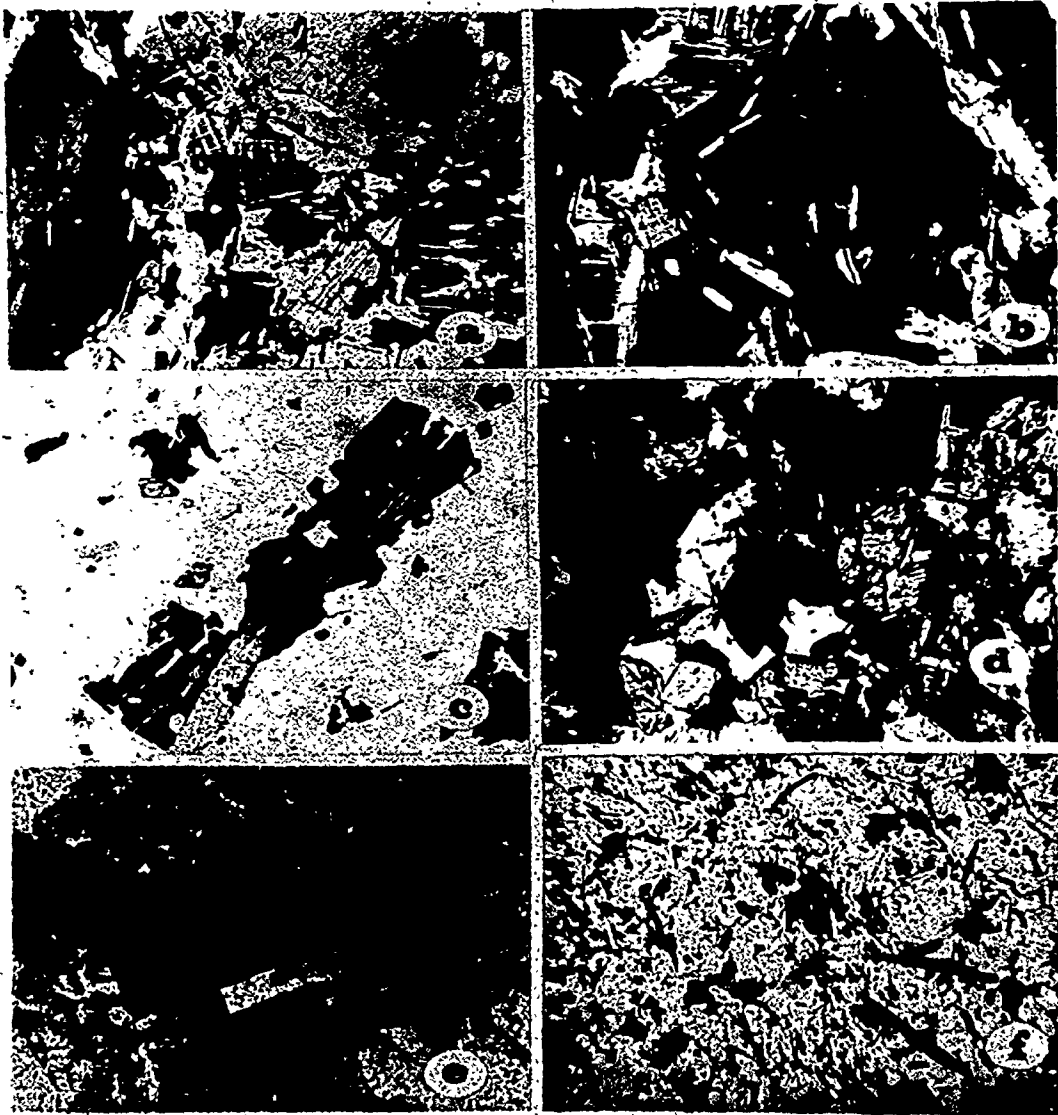
PLATE 11

Riebeckite Granite of Hadb-Aldyaheen

Ring Complex Thin Sections

- a) Twinned riebeckite crystal with amphibole cleavage; albite laths oriented along the margin of large quartz grain. (Cross nicols, X16)
- b) Riebeckite crystal enclosing albite laths, which are oriented along the margin, and microcline crystal. (Cross nicols, X25)
- c) Parallel growth of aegirine (gray) and riebeckite (black). (Cross nicols, X25)
- d) Euhedral aegirine crystals (dark gray). (Cross nicols, X16)
- e) Association of riebeckite with amphibole cleavage and aegirine. (Plane polarized light, X25)
- f) Aegirine as fibrous aggregates and dispersed wisps in the groundmass of the riebeckite granite from the contact zones. (Plane polarized light, X16)

PLATE .11



been reported by Jacobsen et al. (1958) in the riebeckite granite of Nigeria, such as pyrochlore, astrophyllite, thomsenolite, cryolite, were recognized in this granite.

Eight modal analyses of Table 8 plotted on the triangular diagram of Figure 13 are mostly within the adamellite field.

CHAPTER 4
PETROCHEMISTRY

4.1 General Statement

Chemical composition of 95 representative hand specimens of the four younger granitic plutons from the North East corner of Southern Hijaz quadrangle were determined by X-ray fluorescence. FeO was determined separately by wet chemical techniques. Complete analytical results are given in Appendix B, Tables 1, 2, 3, 4 and 5, and analytical procedures and results are summarized in Appendix A. Electronic computing techniques were employed, using a total of 11 major-element analyses, to devise i) CIPW molecular norms for all samples and ii) a differentiation index D.I., based on the total of normative minerals of quartz + orthoclase + albite + leucite + nepheline + kalsophilite (Thornton and Tuttle, 1960) and iii) a calculation of alkalinity index, A.I. based on the molecular proportion of $\text{Na}_2\text{O} + \text{K}_2\text{O}/\text{Al}_2\text{O}_3$ (Shand, 1944).

The purpose of analysing rocks of these four granitic plutons is four-fold: 1) classification of each pluton by their normative mineralogy and alkalinity index, 2) comparison of the abundances of major and trace elements

to published analyses of similar rock types in order to evaluate theories of petrogenesis previously proposed for similar granites, 3) construction of appropriate variation diagrams to determine co-relationships and possible generation of rock types by fractional crystallization, and 4) evaluation of recent hypotheses, applying subduction models to the western part of the Arabian Shield which includes the area studied.

4.2 Chemical Classification

Rocks of the four plutons have been classified after Streckeisen (1967) and O'Connor (1966) (Fig. 1, 2). The rocks have been classified also according to the degree of alumina saturation, using the molecular proportion ratio of $\text{Na}_2\text{O} + \text{K}_2\text{O}/\text{Al}_2\text{O}_3$ as the alkalinity index (Shand, 1949, 1952).

4.2.1 Albari granite

The Albari granite is within the granodiorite field of normative classification (Figs. 14, 15). This is consistent with the modal classification. The homogeneous nature of this pluton is evident for modes (Fig. 7) and norms. Molecular proportions of alkalis relative to alumina (A.I.) varies between 0.60 to 0.78 (Appendix B, Table 1b) and there is corundum in the norm. The Albari Pluton is peraluminous. CaO and $\text{Na}_2\text{O} + \text{K}_2\text{O}$ are used to calculate the alkali-lime index of Peacock (1931). The alkali-lime index of this granite is about 57% SiO_2 (Fig. 16) indicating a calc-alkalic affinity.

4.2.2 Alse-Hairah granite

Norms of the Alse-Hairah granite plot within the quartz-bearing monzonite and adamellite fields with 5 out of 8 samples in the adamellite field (Fig. 14). In general, this normative classification is consistent with the modal classification (Fig. 8) except for one sample. In the second ternary diagram (Fig. 15) this granite has a close cluster in the granite field. The alkalinity index (A.I.) varies between 0.82 to 0.88 (Appendix B, Table 2b), and corundum appears in the norm of most of the analysed samples. According to Shand (1948, 1952) the Alse-Hairah granite is peraluminous and more alkaline than the Albari granite.

4.2.3 Jabal Sayid Riebeckite granite

Norms of Jabal Sayid granite cluster in the adamellite field of Streckeisen's ternary diagram (Fig. 14). If the albite content of the plagioclase is added to the orthoclase content in the same diagram, samples plot along the quartz-orthoclase line of the alkali granite field. In all analysed samples the molecular proportion of total alkalis exceeds that of alumina. The alkalinity index (A.I.) of these rocks is between 1.02 to 1.17 (Appendix B, Table 3b), and the appearance of normative acmite in all the analysed samples is characteristic. Therefore, the riebeckite granite of Jabal Sayid is actually a soda rich peralkaline rock (Shand, 1949, 1952; Goldschmidt, 1954).

4.2.4 Hadb Aldyaheen ring complex

The rocks of the Hadb-Aldyaheen ring complex were classified in the field as biotite granite, microgranite, granite porphyry and riebeckite granite. Norms of analysed samples of the biotite granite are within the granodiorite field of Figure 14. The microgranite is within the adamellite and quartz-bearing monzonite fields. The majority of granite porphyry samples are within the adamellite field and only four samples are a granodiorite. The riebeckite granite is scattered between different fields with the majority within the adamellite field. Two are granodiorite and one is granite. Two samples which are from the outer contact zone between riebeckite granite and the country rocks are within the field of quartz-rich rocks.

By O'Conner's classification (Fig. 15) the biotite granite and microgranite are granites. Because normative anorthite is absent in all of the riebeckite granites of both Hadb-Aldyaheen and Jabal Sayid and most of the granite porphyry, they plot along the orthoclase-albite line at the side of the granite field. The alkalinity index (A.I.) of the biotite granite is between 0.79 to 0.83, comparable to the Alse-Hairah granite. This granite is characteristically peraluminous with corundum as a normative mineral. The microgranite alkalinity index is 0.96 to 0.99, with no corundum in the norm and the rocks are metaluminous. For the granite porphyry and the riebeckite granite, the alkalinity index is greater than one, from 1.02 to 1.14 and

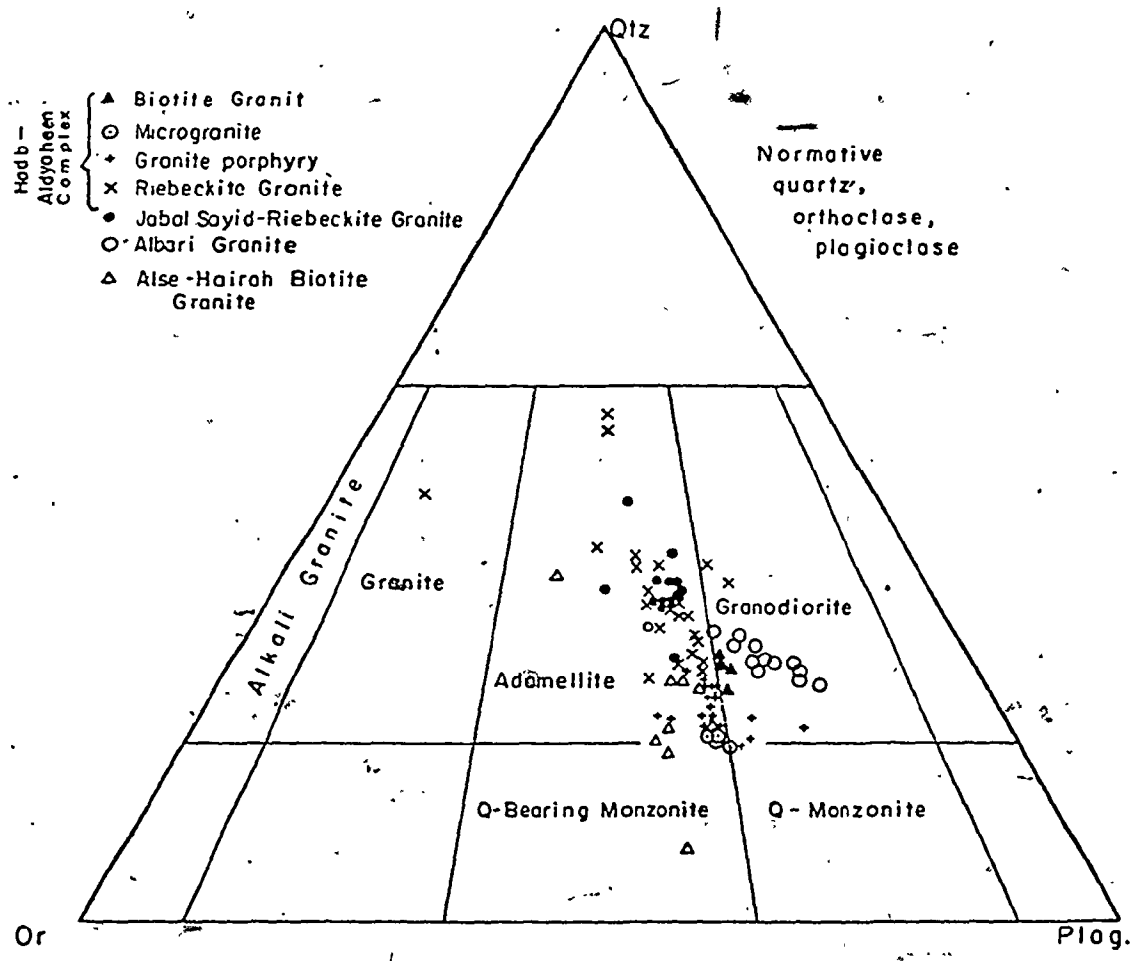


Figure 14. Normative classification of the granite rocks of the four plutons (modified after Streckeisen, 1967).

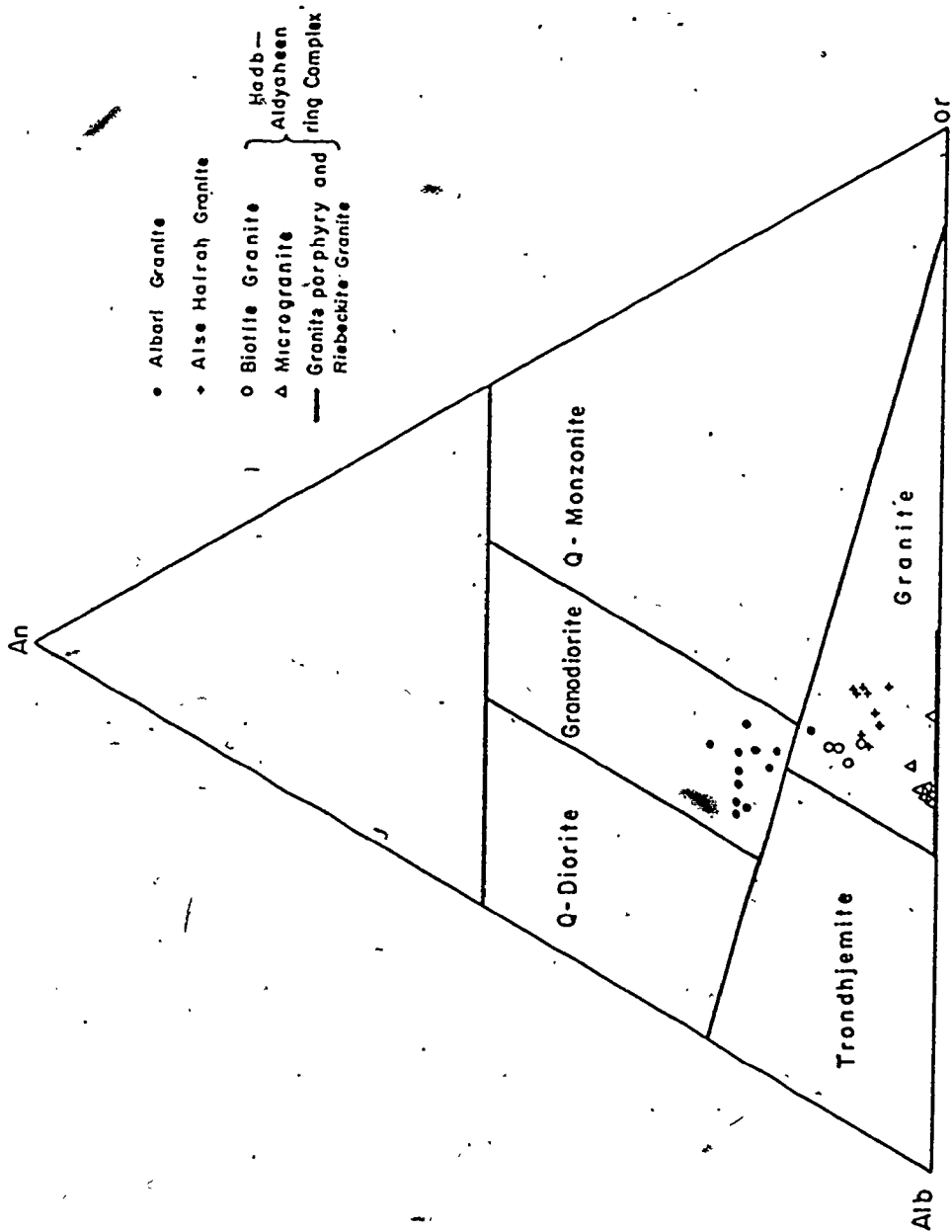


Figure 15. Normative classification of granitic rocks of Albari, Aise-Hairah and the Habb-Aldyaheen ring complex (after O'Connor, 1966).

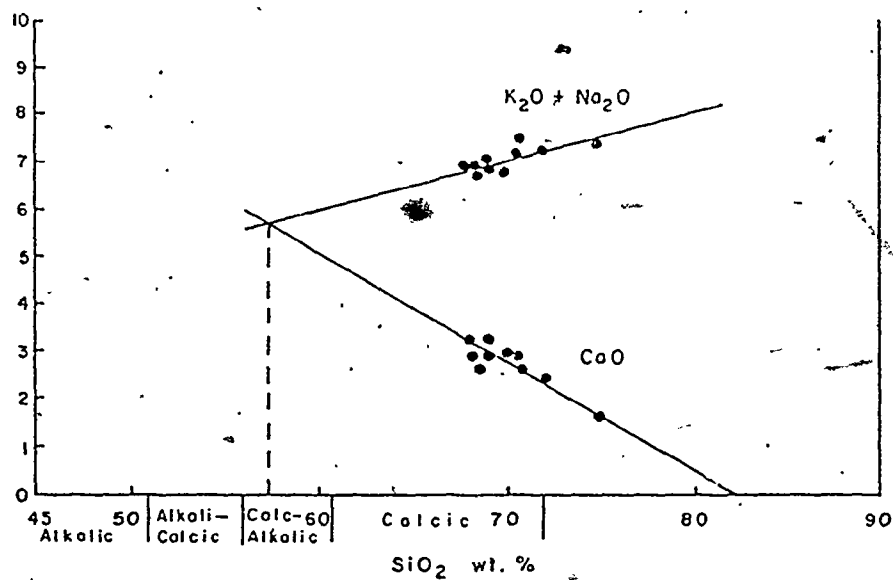


Figure 15. Alkali-lime index diagram for Albari granite (Peacock, 1931).

1.08 to 1.22 respectively. The presence of acmite and the absence of anorthite molecule in the norm of all samples of the granite porphyry and the riebeckite granite, is characteristic. Sodium metasilicate appears as a normative mineral in some of the granite porphyry and in all the riebeckite granite samples (see Appendix B, Tables 5, 6b). Both types of granite are characteristically peralkaline.

4.3 Major element abundances

4.3.1 Albari granite

Complete analyses of major and trace elements and calculated CIPW norms are given in Appendix B, Table 1b. The averages and ranges of these analyses are shown in Table 9.

Al_2O_3 (Av. 15.57%), Fe_2O_3 total (Av. 3.07%), MgO (Av. 0.092%) and CaO (Av. 2.88%) plots versus silica content (Fig. 17) have similar trends in which these elements decrease with the increase in silica. Average contents of Na_2O and K_2O are 3.95% and 3.05%, respectively. Plots of both elements against silica have a trend in which the K_2O increases and Na_2O slightly decreases with increase in silica content. The plots of $Na_2O + K_2O$ versus SiO_2 (Fig. 21) have a trend in which the total alkalis increase as a function of increasing silica content. Fe total, Mg and Ca were also plotted against the felsic index

($F = \frac{Na + K}{Na + K + Ca} \times 100$) (Simpson, 1954), the plots define

Table 9. Average and range of chemical compositions and CIPW norms of Albari granite (12 analyses) and the average biotite granodiorite of Nockolds (1954).

	Albari granite		Av. Biotite granodiorite
	Average	Range	(Nockolds, 1954)
SiO ₂	69.58	68.12 - 72.1	68.97
TiO ₂	0.27	0.18 - 0.36	0.45
Al ₂ O ₃	15.57	14.27 - 16.43	15.47
Fe ₂ O ₃	1.37	0.85 - 1.85	1.12
FeO	1.70	1.11 - 2.45	2.05
MnO	0.08	0.06 - 0.11	0.06
MgO	0.92	0.55 - 1.23	1.15
CaO	2.88	1.92 - 3.36	2.99
Na ₂ O	3.95	3.50 - 4.42	3.69
K ₂ O	3.05	2.51 - 3.69	3.16
P ₂ O ₅	0.13	0.09 - 0.16	0.19
L.O.I.	0.33	0.20 - 0.72	
Total	99.83		
Q	27.07	24.30 - 31.43	26.2
Or	18.10	14.87 - 22.13	18.9
Ab	33.57	29.88 - 37.49	31.4
An	13.54	9.08 - 16.17	14.2
Co	0.83	0.35 - 1.13	0.07
Hy	3.99	2.08 - 6.08	5.10
Mt	2.00	1.24 - 2.69	1.6
il	0.55	0.33 - 0.70	0.8
AP	0.32	0.22 - 0.38	0.4
Total			

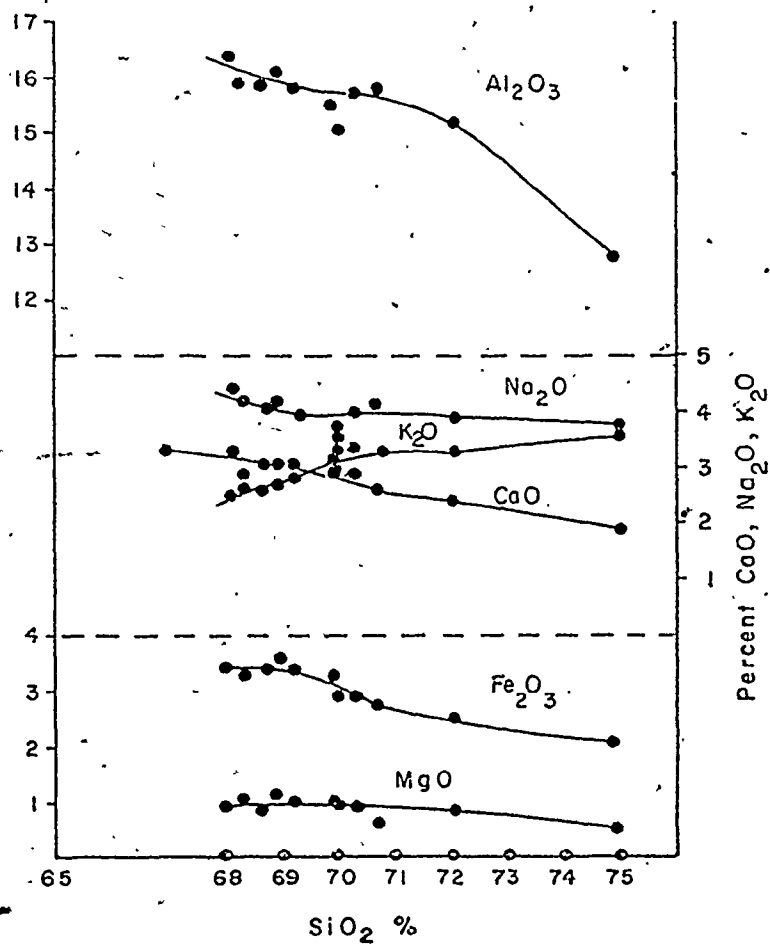


Figure 17. Harker silica-variation diagram for Albarr granite.

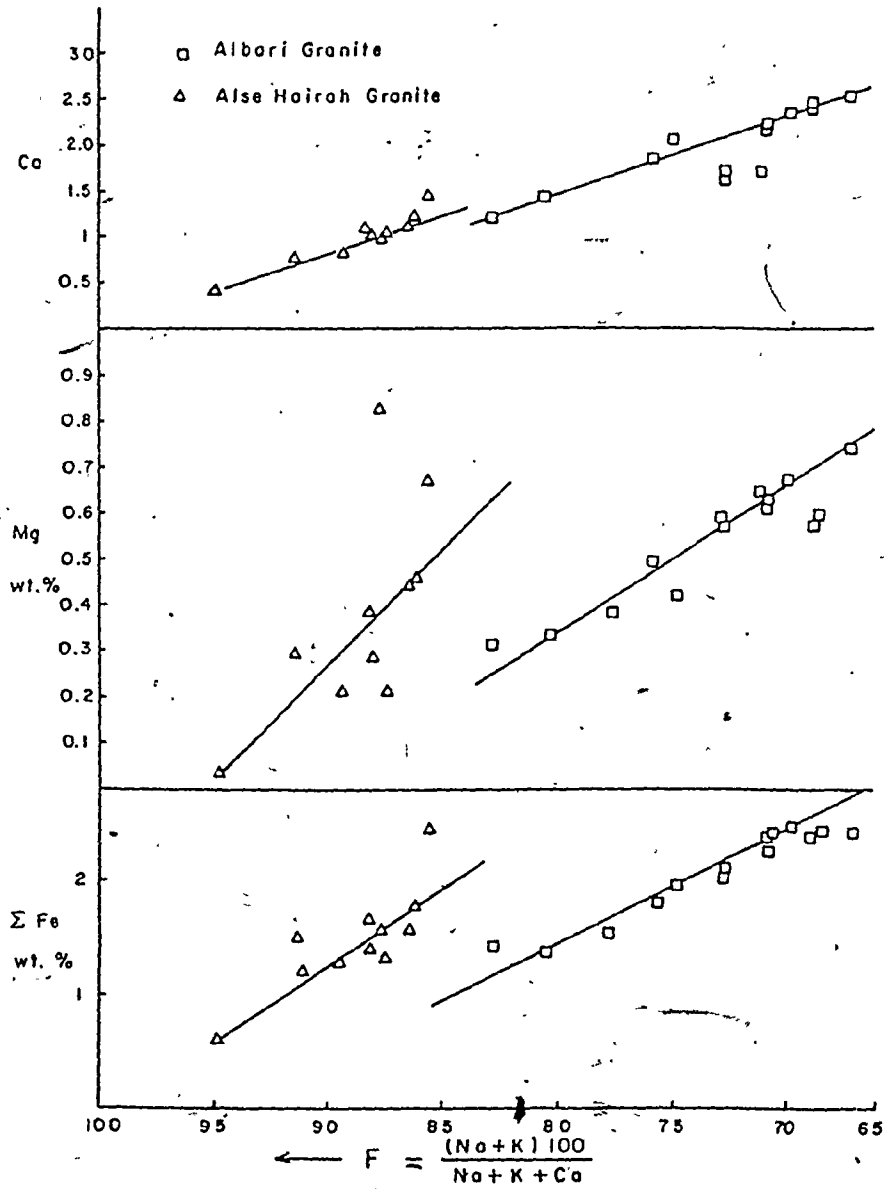


Figure 18. The felsic index (F) plotted against Fe total, Mg and Ca.

a trend in which these elements decrease with the increase in felsic index (Fig. 18). In Figures 22 and 23 the major oxides, SiO_2 , CaO , Fe_2O_3 total, Na_2O , K_2O and Al_2O_3 were plotted against the differentiation index (D.I.) of Thorton-Tuttle (1960). In these diagrams SiO_2 (Av. 69.58%) and K_2O both have positive correlation with the D.I., Na_2O remains approximately constant. CaO , Fe total and Al_2O_3 plots have a negative correlation with the D.I.

The averages of major oxides of Albari granite are similar to the average biotite granodiorite of Nockold (1954). The variation covers a range of SiO_2 values from 68 to 72 percent, and defines normal trends for increasing SiO_2 , felsic index and differentiation index were observed.

4.3.2 Alse-Hairah granite

Complete analyses of major elements and calculated CIPW norms are given in Appendix B, Table 2b. The averages and the ranges of these analyses are presented in Table 10.

Similar to the Albari granite, the variations in some of the major oxides are illustrated relative to silica content, felsic index (F) and the differentiation index (D.I.). In Figure 19 MgO (Av. 0.63%), Fe total (Av. 2.13%), K_2O (Av. 4.89%) and Al_2O_3 (Av. 14.95%) plots have a similar ill defined trend except for Al_2O_3 in which these elements decrease with the increase in SiO_2 content. The plots of CaO (Av. 1.34%) and Na_2O (Av. 4.43%) do not define a trend, and they remain approximately constant for increasing silica content.

Table 10. Average and range of chemical compositions and CIPW norms of Alse-Hairah granite (8 analyses) and the average adamellite of Nockolds (1954).

	Alse-Hairah granite		Average Adamellite (Nockolds, 1954)
	Average	Range	
SiO ₂	70.63	68.22 - 73.16	71.03
TiO ₂	.036	0.30 - 0.43	0.39
Al ₂ O ₃	14.95	13.92 - 15.91	14.31
Fe ₂ O ₃	1.78	1.40 - 2.32	0.95
FeO	0.35	0.06 - 0.76	1.96
MnO	0.05	0.05 - 0.07	0.06
MgO	0.63	0.34 - 1.24	0.75
CaO	1.34	1.02 - 1.59	1.89
Na ₂ O	4.43	4.06 - 4.71	3.33
K ₂ O	4.89	4.32 - 5.56	4.66
P ₂ O ₅	0.14	0.10 - 0.16	0.17
L.O.I.	0.33		
Total	99.88		
Q	22.92	17.96 - 28.39	27.7
Or	29.07	25.21 - 33.11	27.8
Ab	37.61	34.27 - 40.03	28.3
An	5.48	4.14 - 6.44	8.6
Co	0.33	0.23 - 0.89	0.5
Di	0.19	0.35 - 1.24	-
hy	1.51	0.28 - 3.34	4.1
Mt	0.48	0.34 - 1.76	1.4
il	0.55	0.21 - 0.82	0.8
Hm	1.46	0.21 - 2.34	-
Rut	0.07	0.11 - 0.29	-
AP	0.33	0.24 - 0.38	0.3
Total	100.00		

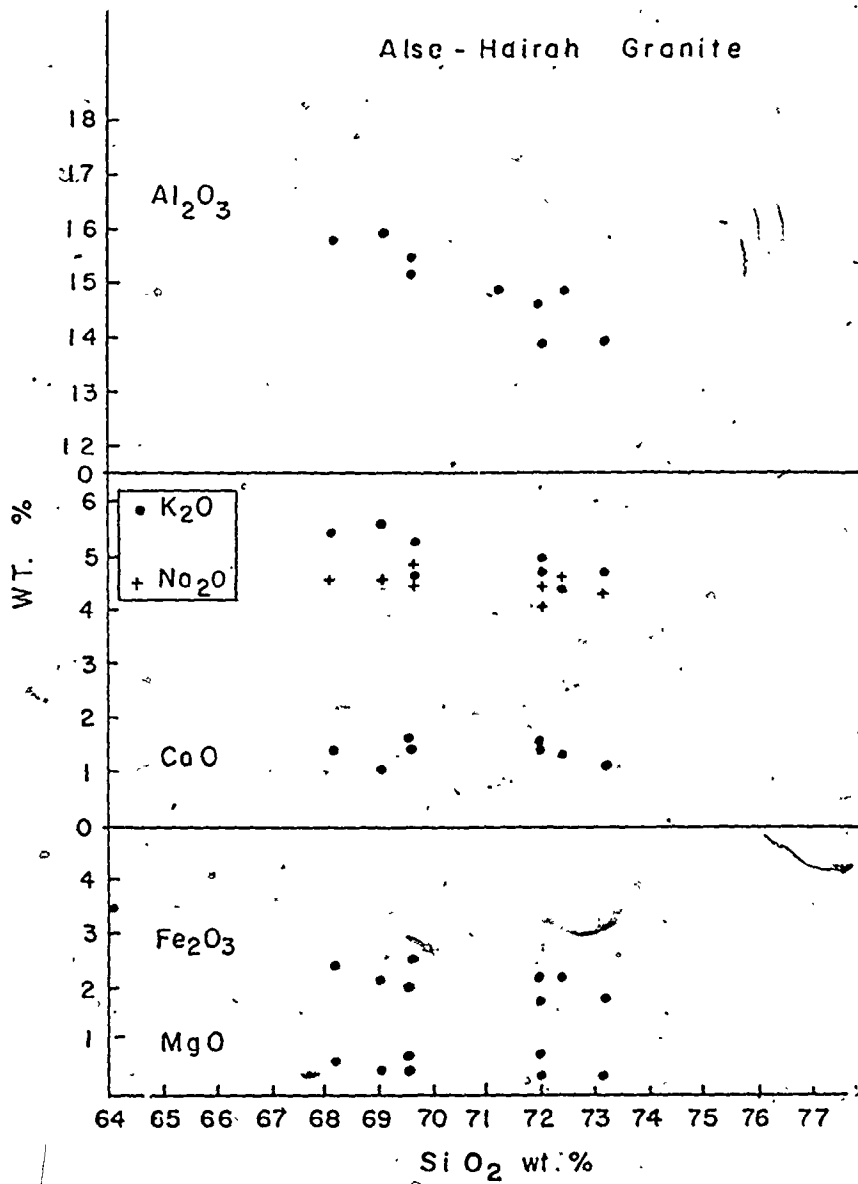


Figure 19. Harker silica-variation diagram of Alse-Hairah granite.

However, a total alkalis versus silica plot has a trend in which total alkalis decrease with the increase in SiO_2 content. In the second diagram (Fig. 18) where Fe total, Mg and Ca are plotted against the felsic index, the three elements have a negative correlation with the felsic index. In the third diagram (Fig. 22, 23) the major oxides are plotted against the D.I. In this diagram SiO_2 (Av. 70.63%) and K_2O have a positive correlation with the differentiation index. CaO , Fe total, Na_2O and Al_2O_3 all have negative correlation with D.I.

Averages of major oxides of this granite are similar to the average adamellite of Nockold's (1954), except for the Na_2O content which is greater in Alse-Hairah granite and CaO which is lower. As with the Albari granite, the variations in the major oxides versus silica, felsic index and differentiation index, have normal trends consistent with general trends of a differentiating granitic magma. However, the Alse-Hairah granite has a greater D.I. indicating a later stage of differentiation than Albari granite.

4.3.3 Jabal Sayid riebeckite granite

The major element oxide contents of 16 representative samples from Jabal Sayid granite are included in Appendix B, Table 3b. Their averages and ranges are in Table 11. These rocks are characterized by a consistently low CaO (Av. 0.18%) and MgO (Av. 0.006%) content. Plots of the major oxides

Table 11. Average and range of chemical compositions and CIPW norms of Jabal Sayid riebeckite granite and averages of similar granites from different sources.

	Jabal Sayid		(2) Riebeckite granite from Northern Nigeria Jacobsen (1958)	(3) Av. Riebeckite granite of Kaffe, Nigeria Borely (1975)
	Average	Range		
SiO ₂	75.51	74.6 - 76.47	74.35	73.65
TiO ₂	0.08	0.04 - 0.15	0.11	0.12
Al ₂ O ₃	10.99	10.55 - 11.43	11.69	12.21
Fe ₂ O ₃	2.92	1.60 - 3.89	1.54	1.42
FeO	0.69	0.03 - 1.76	1.05	1.09
MnO	0.04	0.01 - 0.007	0.04	0.05
MgO	0.006	0.00 - 0.04	0.23	<0.1
CaO	0.18	0.06 - 0.28	0.52	0.09
Na ₂ O	4.81	4.14 - 5.15	5.12	5.87
K ₂ O	3.98	3.61 - 4.81	4.45	4.01
P ₂ O ₅	0.02	0.00 - 0.03	0.02	<0.05
Q	33.63	29.79 - 39.45	29.57	27.25
Or	23.68	21.37 - 28.45	26.43	23.72
Ab	34.70	29.62 - 35.93	35.26	40.48
Ns	0.11	0.00 - 0.78	0.81	1.23
Di	0.29	0.00 - 1.13	0.35	0.39
Hy	0.70	0.00 - 3.09	1.82	1.5
Wol	0.19	0.00 - 0.50	-	-
Ac	5.13	4.40 - 7.1	3.59	3.34
Mt	0.71	0.00 - 1.83	0.42	0.39
il	0.15	0.08 - 0.29	0.13	0.23
Hm	0.68	0.00 - 1.83	-	-
AP	0.04	6.00 - 0.07	-	-

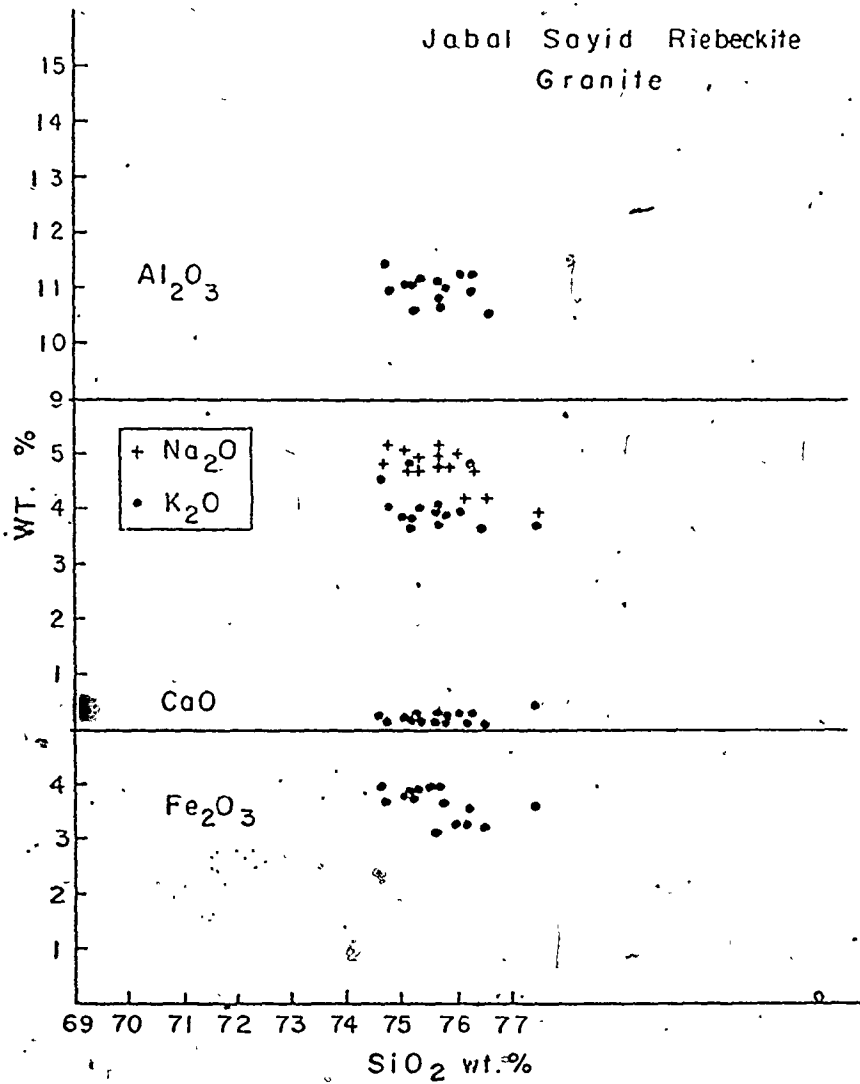


Figure 20. Harker silica-variation diagram of Jabal Sayid riebeckite granite.

- Albari Granite
 - △ Alse-Hairah Granite
 - Jabal Sayid Riebeckite Granite
- Hodab-Aldycheen complex
- ▲ Biotite Granite
 - ◇ Microgranite
 - + Granite porphyry
 - Riebeckite Granite

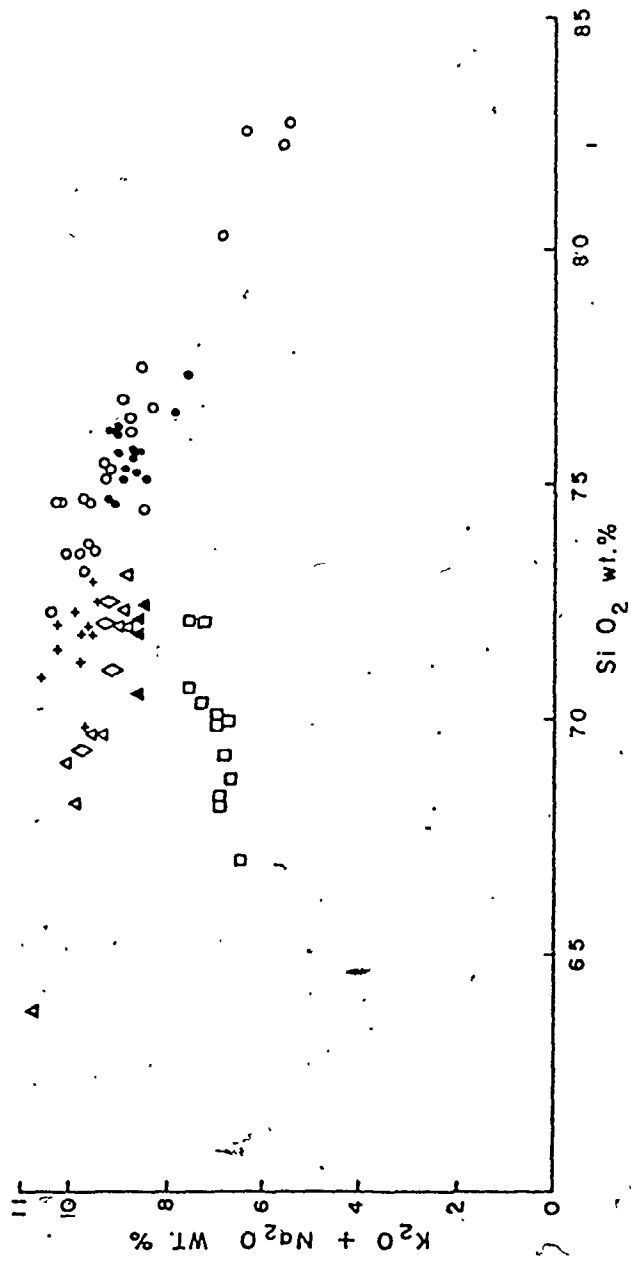


Figure 21. Total alkalies plotted against SiO₂ of granitic rocks from the four plutons.

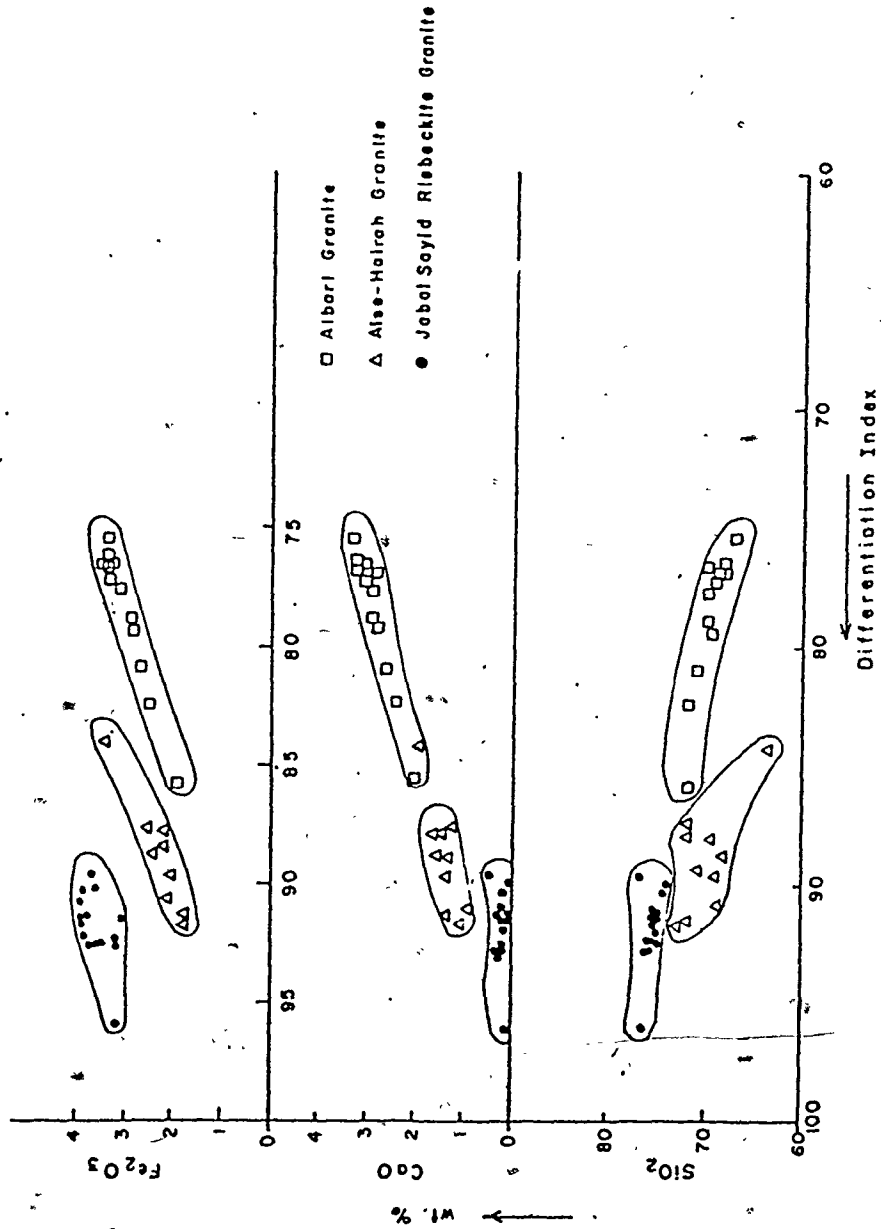


Figure 22. Variations in weight percentages of oxides, plotted against Thornton Tuttle differentiation index (D.I.).

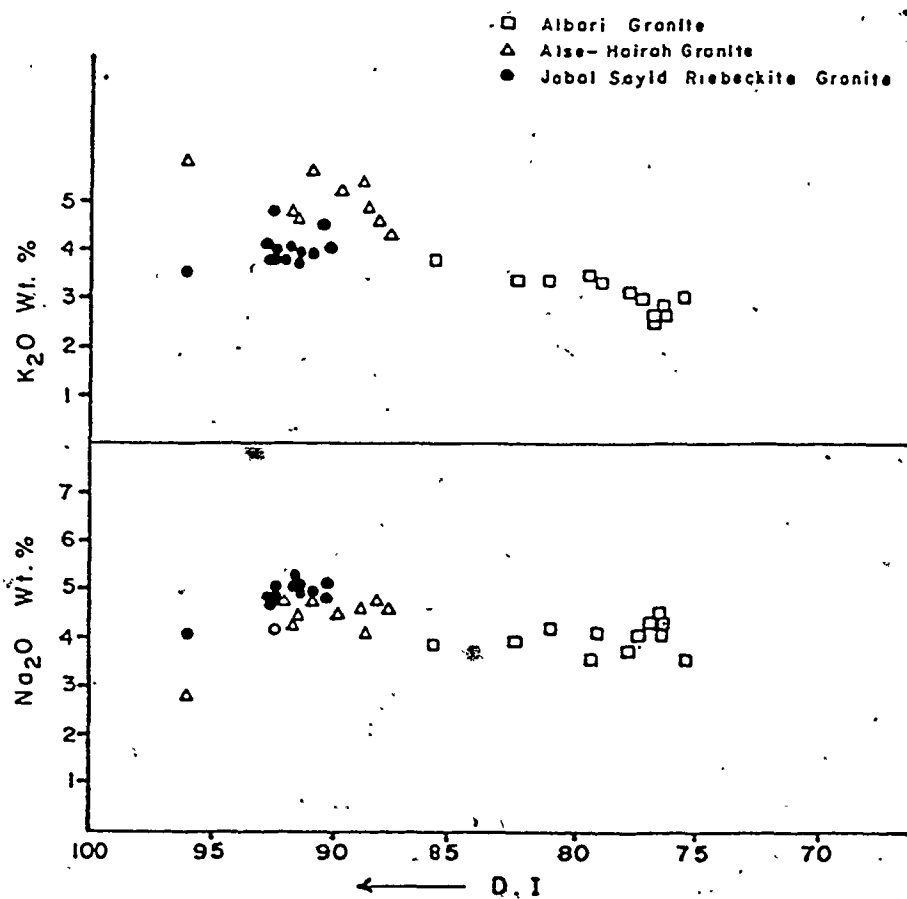


Figure 23. Variations in weight percentages of Na_2O and K_2O , plotted against Thornton-Tuttle differentiation index (D.I.).

versus silica (Fig. 20) define no trends and the points cluster between 74.6 and 76.5% SiO_2 content. Na_2O (Av. 4.81%) is generally large. K_2O (Av. 3.98%) is not particularly large for granite and there is a general excess of Na_2O over K_2O values. The plot of total alkalis against silica has a slight trend in which alkalis decrease with increase in silica. Relative to the differentiation index, SiO_2 (Av. 75.51%) and Al_2O_3 (Av. 10.99%) have a slight trend in which they increase slightly with the increase in D.I. CaO has no trend. Fe_2O_3 total (Av. 3.61%), Na_2O and K_2O plots (Figs. 22, 23) have similar trends in which there is a negative correlation with D.I. The major oxides are also plotted versus the Thornton-Tuttle differentiation index plus normative acmite (ac) and sodium metasilicate (ns) (Macdonald, 1969). In this diagram (Figs. 29, 30) none of the major oxides has a defined trend, although it seems that SiO_2 content increases slightly with an increase of $\text{DI} + \text{ac} + \text{ns}$.

Summary

Alkali abundances in these rocks are not abnormally great and the peralkaline nature is mainly because of the deficiency of alumina relative to alkalis. The rocks have characteristically minor Ca and Mg which would be only expected for pegmatitic rocks rather than igneous ones. However, the low content of CaO is reflected in the plagi-

class composition which rarely has more than 0.2% of the anorthite molecule. The minor MgO content is reflected in mafic minerals, soda-iron amphibole and pyroxene. In general, as a function of increasing SiO_2 , D.I. and D.I. + ac + ns, and major oxides do not vary systematically or have defined trends as would be expected if this rock formed by a fractional crystallization of granite magma.

Compared to the Nigerian peralkaline granite, the Jabal Sayid granite has greater SiO_2 , lesser Al_2O_3 , CaO, Na_2O , K_2O and MgO (Table 11).

4.3.4 Hadb-Aldyaheen ring complex

The major element abundances for the four members of the complex are illustrated relative to: silica content, differentiation index (D.I.), and D.I. + normative acmite (ac) + sodium metasilicate (ns).

i) Biotite granite

The averages and the ranges of the four analyses of this rock are in Table 12.

In the first diagram (Fig. 24), MgO (Av. 0.52%), Fe total (Av. 2.04%), CaO (Av. 1.59%) and Al_2O_3 (Av. 14.71%) plots versus SiO_2 . All have a similar slight trend in which they decrease with an increase of silica content. The average content of Na_2O and K_2O are 4.44 and 4.13%, respectively. K_2O slightly decreases while Na_2O remains approximately constant with an increase in silica content.

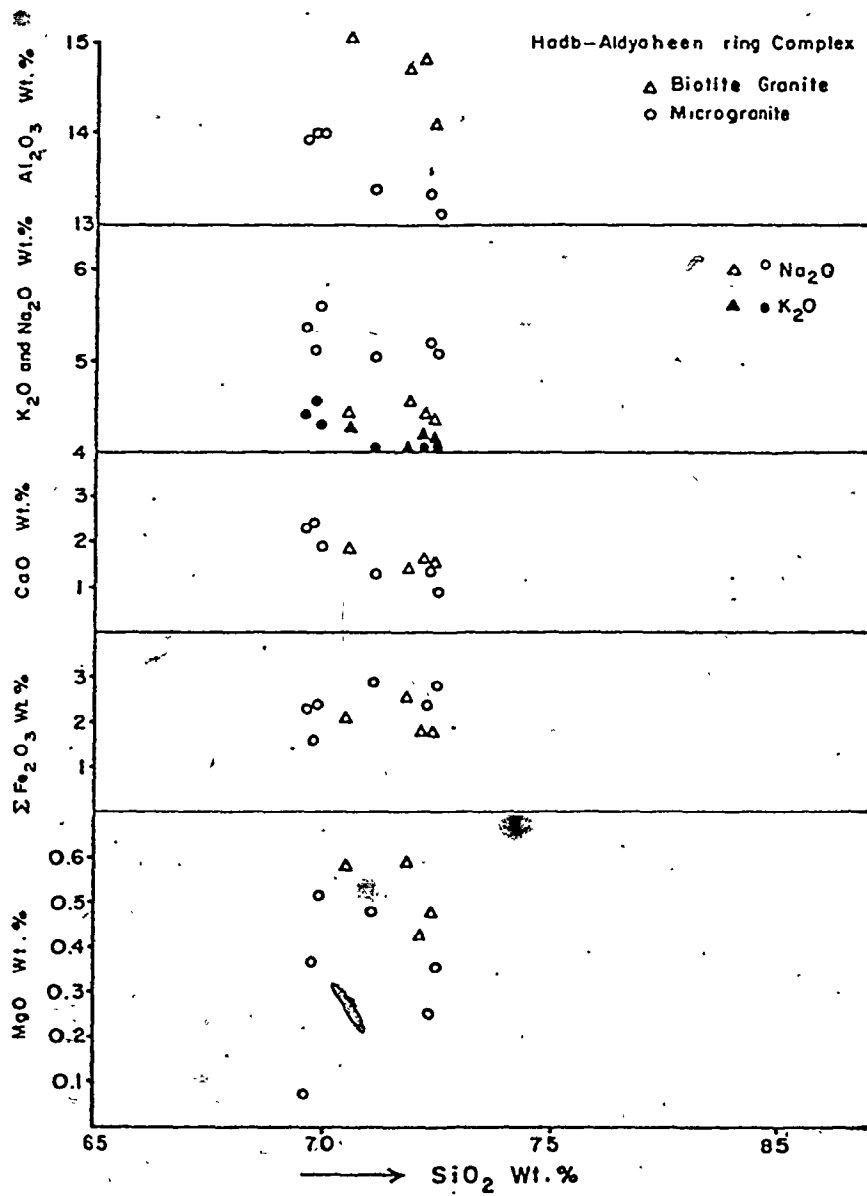


Figure 24. Harker silica-variation diagram of biotite granite, and micro granite of Hadb-Aldyaheen ring complex.

Table 12. Average and range of chemical compositions and CIPW norms of the biotite granite and the micro-granite of Hadb-Aldyaheen ring complex.

	Biotite granite (4 analyses)		Micro-granite (6 analyses)	
	Average	Range	Average	Range
SiO ₂	71.70	70.49 - 72.37	70.85	69.55 - 72.49
TiO ₂	0.26	0.23 - 0.30	0.28	0.24 - 0.32
Al ₂ O ₃	14.71	14.10 - 15.20	13.63	13.13 - 14.00
Fe ₂ O ₃	2.04	1.76 - 2.53	2.40	1.61 - 2.88
MnO	0.06	0.04 - 0.12	0.06	0.04 - 0.10
MgO	0.52	0.43 - 0.59	0.33	0.08 - 0.52
CaO	1.59	1.40 - 1.80	1.72	0.96 - 2.47
Na ₂ O	4.44	4.37 - 4.54	5.26	5.06 - 5.63
K ₂ O	4.13	4.02 - 4.24	4.27	4.04 - 4.56
P ₂ O ₅	0.08	0.05 - 0.11	0.07	0.04 - 0.10
Total	99.53			
Q	26.22	24.38 - 27.63	21.64	17.87 - 25.46
Or	24.57	23.75 - 25.25	25.57	24.24 - 27.47
Ab	37.74	37.28 - 38.41	45.08	43.46 - 46.42
An	7.38	6.38 - 8.28	0.82	0.16 - 1.74
Co	0.27	0.00 - 0.56	-	-
Di	0.10	0.00 - 0.35	2.07	0.44 - 3.45
Hy	1.26	1.04 - 1.47	-	-
Wo	-	-	1.99	0.16 - 4.14
Mt	0.48	0.00 - 0.26	1.47	0.00 - 2.6
il	0.42	0.15 - 0.57	0.47	0.22 - 0.62
Hm	1.44	0.66 - 1.75	0.76	0.00 - 1.18
SP	0.06	0.00 - 0.15	0.07	0.00 - 0.44
AP	0.19	0.12 - 0.26	0.17	0.10 - 0.19

Total alkalis versus silica have no well-defined trends. Figures 27, 28 are the variations of major oxides against D.I. In this diagram, CaO, Fe total and Al_2O_3 all have negative correlation with D.I. Na_2O and K_2O have no defined correlation and SiO_2 (Av. 71.7%) is the only oxide with a positive correlation with D.I.

Summary

The lack of clearly-defined trends for the major oxides relative to SiO_2 and D.I. is probably because of the limited number of chemical analyses of these rocks. The averages of major oxides of the granite is similar to the averages of Alse-Hairah granite. Also, compared to the average biotite granite associated with the peralkaline granites of Northern Nigeria (Jacobson, et al., 1958), this granite is different in every way. It contains more TiO_2 , Al_2O_3 , CaO, Fe total, MgO and less SiO_2 and K_2O and no tin mineralization associated with this granite.

ii) Microgranite

Averages and ranges of the analysed samples are given in Table 12.

The variations in major oxides relative to silica content (Fig. 24) indicate that MgO (Av. 0.33%), CaO (Av. 1.72%), Al_2O_3 (Av. 13.63%) Na_2O (Av. 4.44%) and K_2O (Av. 4.13%), all have a negative correlation with SiO_2 . Fe total (Av. 2.04%) is the only oxide with a rather weak

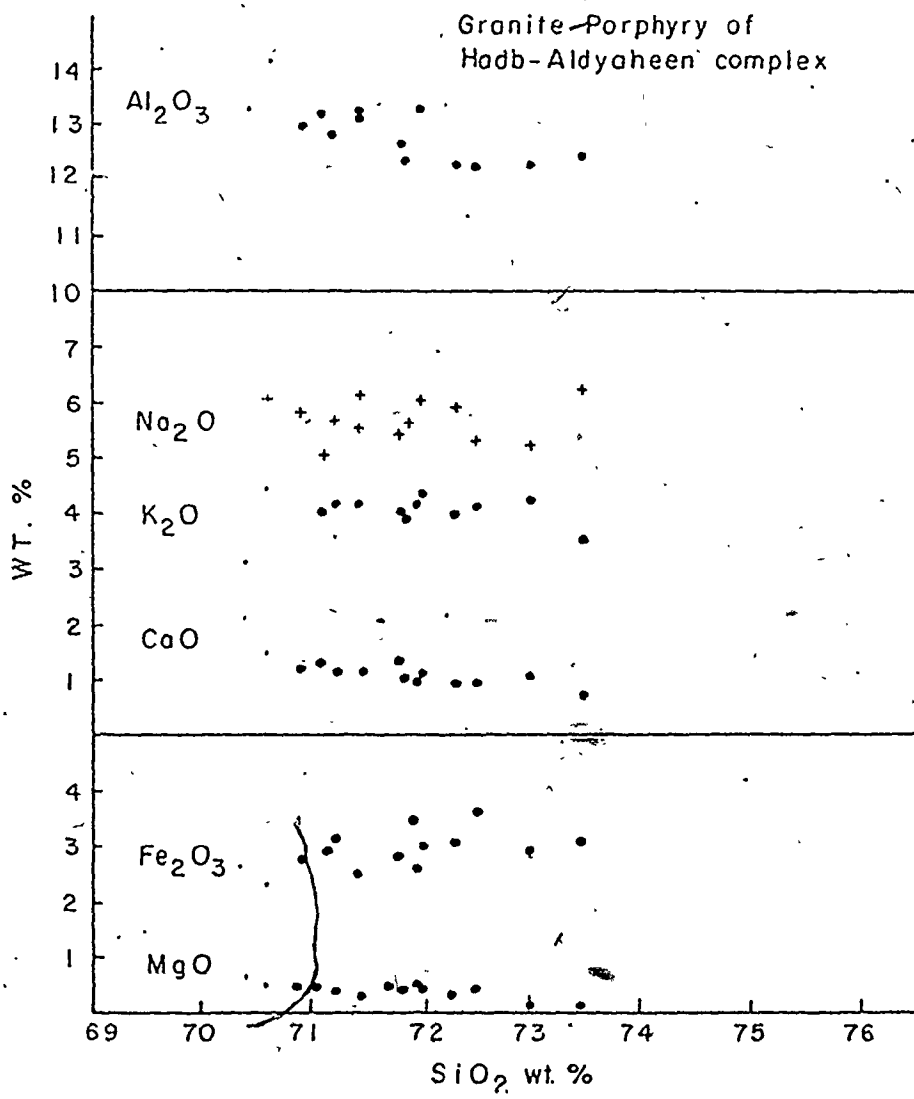


Figure 25. Harker silica-variation diagram of the granite porphyry of Hadb-Aldyaheen ring complex.

Table 13. Average and range of chemical compositions and CIPW norms of the granite porphyry of Hadd-Aldyaheen ring complex:

	Average*	Range
SiO ₂	71.82	70.48 - 73.48
TiO ₂	0.23	0.18 - 0.29
Al ₂ O ₃	12.79	12.27 - 13.76
Fe ₂ O ₃	2.91	2.46 - 3.59
MnO	0.06	0.05 - 0.11
MgO	0.34	0.14 - 0.49
CaO	1.17	0.73 - 1.99
Na ₂ O	5.81	5.20 - 6.82
K ₂ O	4.17	3.02 - 4.79
P ₂ O ₅	0.05	0.02 - 0.08
Total		
	**	
Q	21.94	18.45 - 25.53
Or	24.63	21.19 - 28.52
Ab	42.46	38.22 - 45.11
NS	0.26	0 - 0.81
Di	3.99	2.88 - 4.78
Hy	1.02	0.00 - 1.83
Ac	4.15	1.52 - 5.04
Mt	0.45	0.00 - 1.75
il	0.41	0.35 - 0.48
AP	0.12	0.05 - 0.17

* Average of 13 analyses

** Average of 11 analyses

positive correlation with an increase in silica content. A negative correlation has been observed for the total alkalis with SiO_2 . In Figure 27, 28 the major oxides were plotted against D.I.; SiO_2 (Av. 70.85%) and Fe total both have a similar positive correlation with D.I. CaO , Na_2O , K_2O and Al_2O_3 all have a similar weak negative correlation with D.I.

The variations of major oxides of this granite relative to silica content and D.I. are slight, and cover a range of SiO_2 contents from 69.55 to 72.49% SiO_2 . In general, they have a differentiation trend expected for a late stage granitic rock.

iii) Granite porphyry

The analytical results of major element oxides are given in Appendix B, Table 5b. The averages and the ranges are in Table 13.

In Figure 25 the major oxides are plotted versus silica, MgO (Av. 0.34%), CaO (Av. 1.17%) and Al_2O_3 (Av. 12.79%) all have a weak negative correlation with SiO_2 (Av. 71.82%). Fe total (Av. 2.91%), K_2O (Av. 4.17%) and Na_2O (Av. 5.81%) have no defined trends with increasing silica content. In Figure 21 the total alkalis are plotted against SiO_2 . There is a weak negative correlation. In the second diagram (Fig. 27, 28) the variations in major oxides are illustrated relative to D.I. All the oxides have either clustered or scattered data points without a

Table 14. Average and range of chemical compositions and CIPW norms of the riebeckite granite of Hadb-Aldyaheen ring complex.

	Average*	Range
SiO ₂	75.06	73.08 - 76.80
TiO ₂	0.07	0.04 - 0.14
Al ₂ O ₃	11.32	9.64 - 12.31
Fe ₂ O ₃	3.70	2.35 - 5.11
MnO	0.04	0.02 - 0.06
MgO	0.01	0.0 - 0.07
CaO	0.16	0.03 - 0.32
Na ₂ O	5.37	4.73 - 6.25
K ₂ O	3.96	3.76 - 4.39
P ₂ O ₅	0.02	0.00 - 0.04
Total	99.71	
Q	30.09	25.33 - 36.68
Or	23.7	22.32 - 25.89
Ab	36.26	25.09 - 41.34
NS	1.04	0.04 - 1.57
Di	0.52	0.06 - 1.31
Hy	3.52	1.19 - 6.01
Ac	4.56	4.41 - 4.82
il	0.14	0.06 - 0.27
AP	0.03	0.00 - 0.09

*Average of 15 analyses

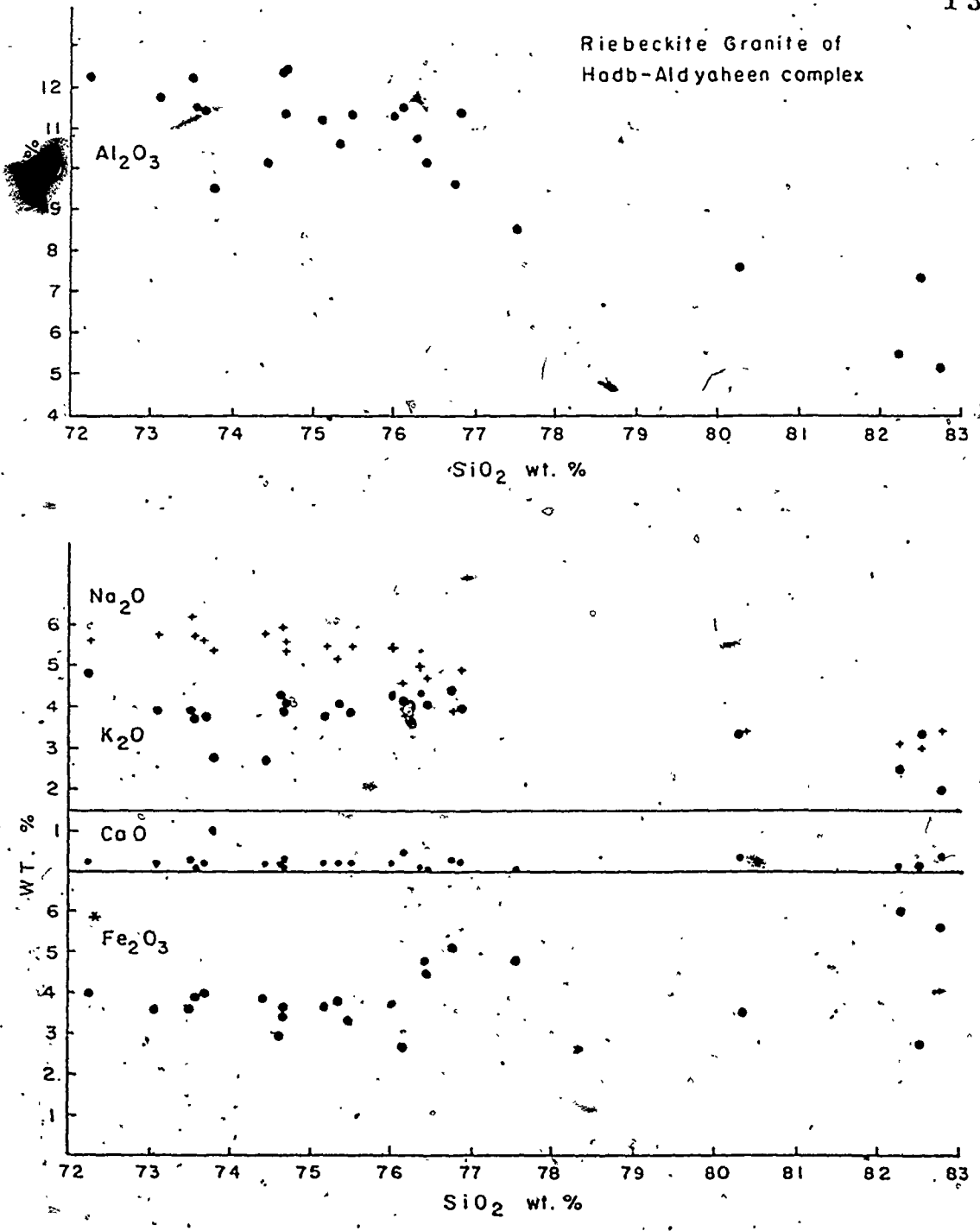


Figure 26. Harker silica-variation diagram of the riebeckite granite of Hadb-Aldyaheen ring complex.

defined trend. Data points for Na_2O and K_2O are more scattered than other major oxides. Fe total is the only oxide with a weak negative correlation with D.I. In the third diagram (Fig. 29, 30), SiO_2 , Fe total, Al_2O_3 and Na_2O plots against D.I. + ac + ns have a weak trend in which they slightly increase with an increase in D.I. + ac + ns. K_2O has no correlation. CaO is the only oxide showing a negative correlation with D.I. + ac + ns.

In general, the variations of major oxides is relatively more defined relative to D.I. + ac + ns, where scattered and clustered data points are observed relative to the differentiation index and silica content. In this granite the variations of major oxides become less systematic than the variations observed for the non-peralkaline granites.

iv) Riebeckite granite

The complete analysis of 25 samples are listed in Appendix B, Tables 6, 7b. The averages and ranges of 15 analysis, which are the most representative samples for this granite are in Table 14. The analyses which are excluded from the averages and the ranges have extreme differences in their major trace elements (Appendix B, Table 7b). These differences are mainly the result of abnormal modal abundances of quartz, aegirine relative to riebeckite, iron oxides and accessory minerals such as zircon and allanite. These samples are mainly from the contact zone between riebeckite granite and diorite country rocks or from the narrow dykes outside the western edge of the main ring complex.

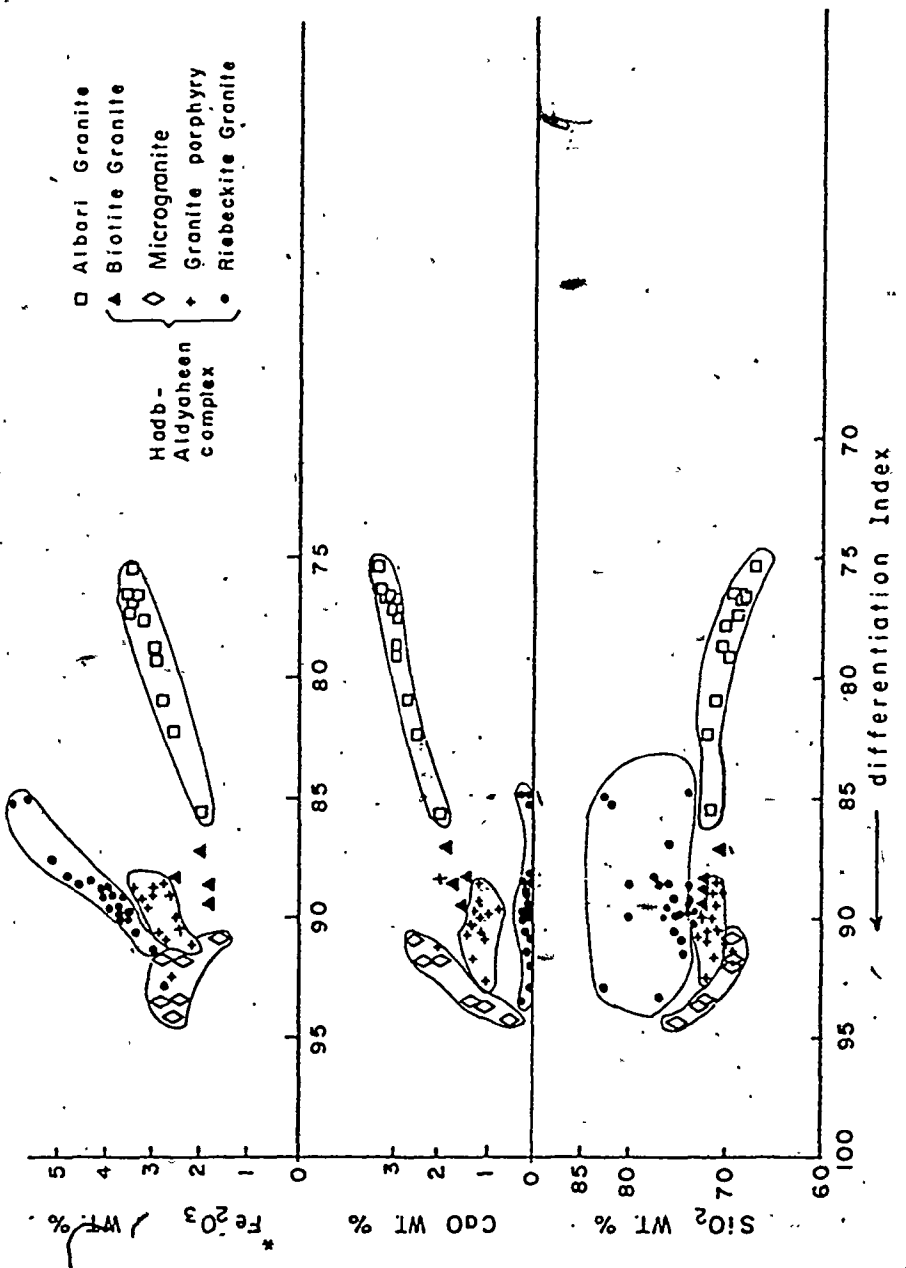


Figure 27. Variations in weight percentages of oxides, plotted against the Thornton-Tuttle differentiation index (D.I.).

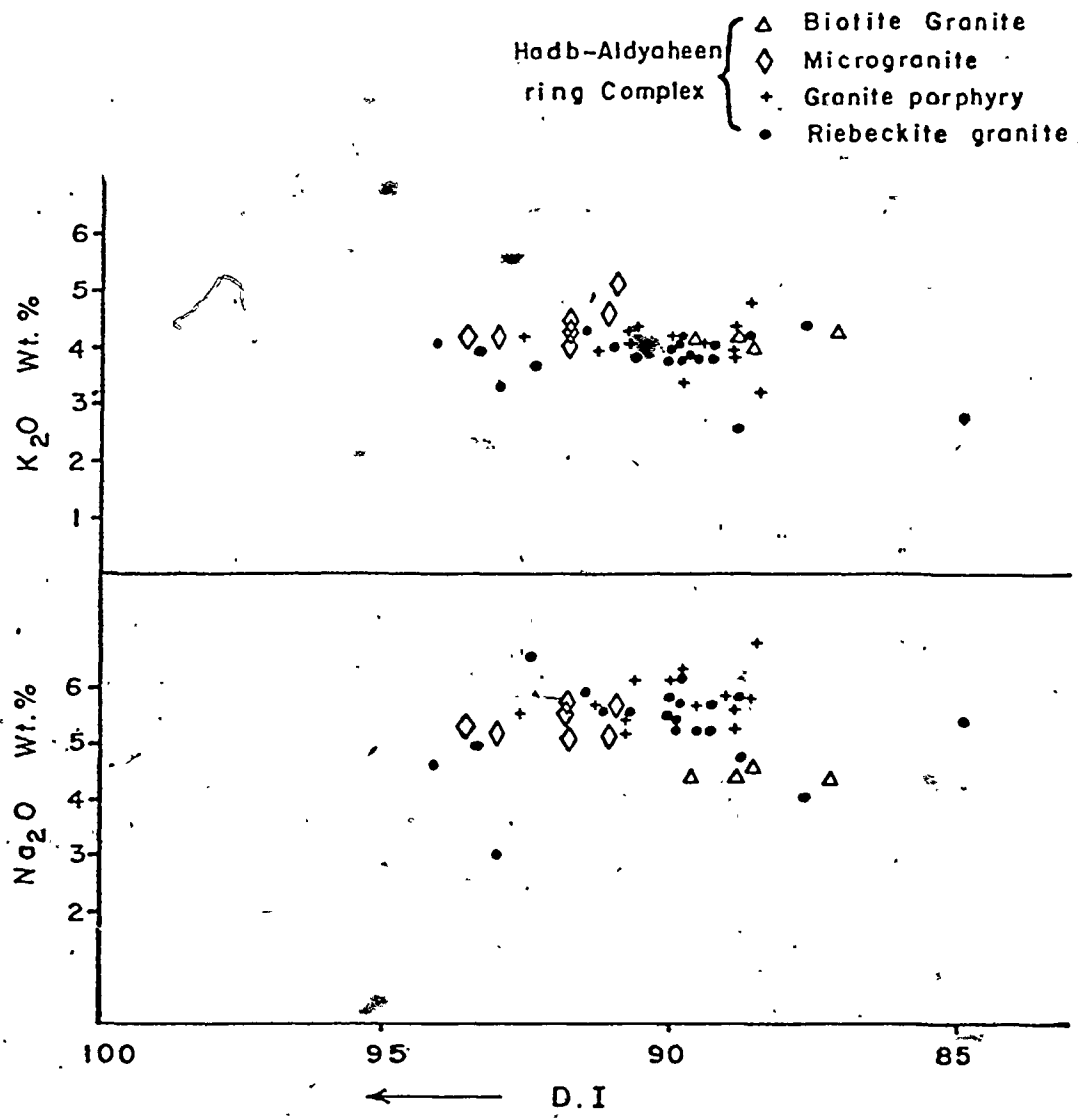


Figure 28. Variation in weight percentage of Na₂O and K₂O plotted against Thornton and Tuttle differentiation index.

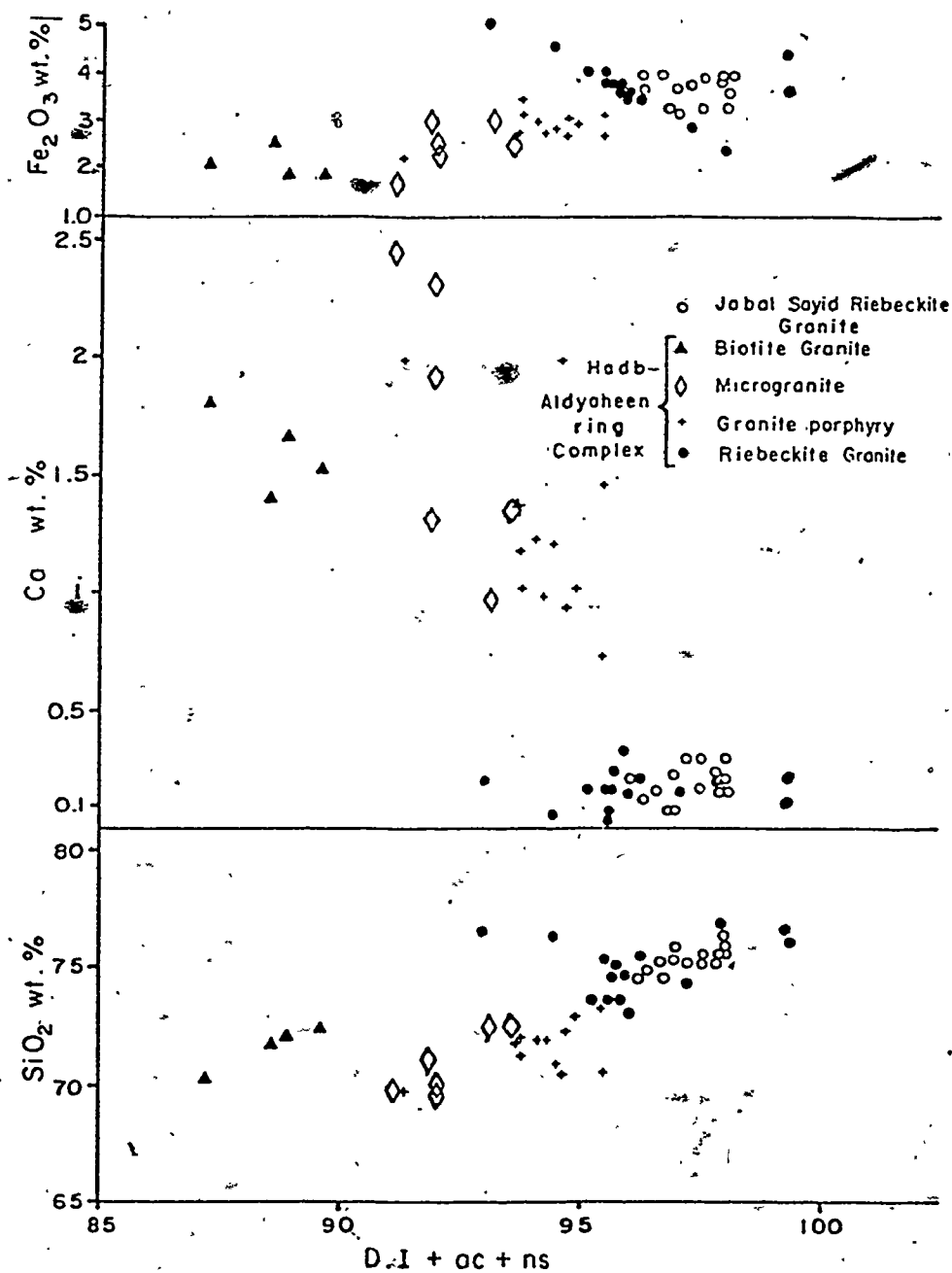


Figure 29. Variations in weight percentages of oxides, plotted against the Thornton-Tuttle differentiation index (D.I.) plus normative acmite (ac) and sodium metasilicate (ns) (Macdonald, 1969).

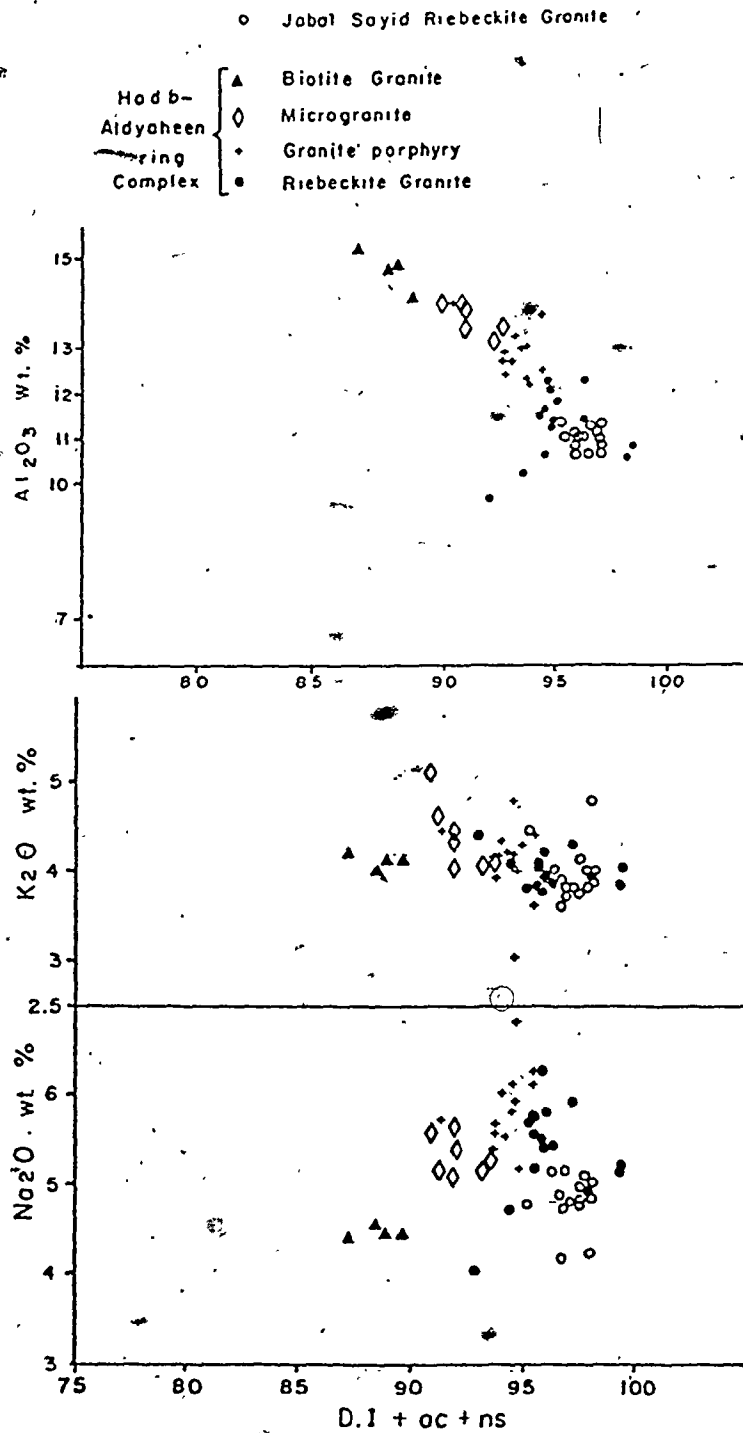


Figure 30. Variations in weight percentages of oxides, plotted against the Thornton-Tuttle differentiation index (D.I.) plus normative acmite (ac) and sodium metasilicate (ns) (Macdonald, 1969).

Major oxide content of all analysed samples of this granite are plotted versus silica content (Fig. 26). Thornton-Tuttle differentiation index (D.I.) and differentiation index plus normative acmite (ac) and sodium metasilicate (ns). Relative to silica content, Fe total (Av. 3.70%), CaO (Av. 0.16%) and K₂O (Av. 3.96%) does not have a defined correlation with SiO₂; only scattered points are observed. Na₂O (Av. 5.37%) and Al₂O₃ (Av. 11.32%) have fairly well defined trends in which these two elements decrease slightly as a function of increasing silica content. In the second variation diagram the major oxides are plotted against the D.I. (Figs. 27, 28). As a function of increasing D.I., none of the oxides has a defined trend, only scattered or clustered data points. Fe total is the only oxide with a defined negative correlation in which this oxide decreases sharply as a function of increasing D.I. In the third diagram the major oxides are plotted versus D.I. + ac + ns, Na₂O is the only oxide with a positive correlation, and Fe total Al₂O₃ with a negative correlation as a function of increasing D.I. + ac + ns. The rest of the oxides do not have a defined trend.

Summary

As in Jabal Sayid riebeckite granite, this rock is characterized by a deficiency of alumina content relative to the alkalis and minor abundances of Ca and Mg. As a function of increasing SiO₂ content, D.I. and D.I. +

ac + ns the major oxides do not vary systematically. The plots of data points are more scattered than any of the previously described granites, indicating a more erratic distribution of major elements:

4.4 Trace Element Abundances

4.4.1 General statement

Trace element analyses for Cr, Ba, Ni, Nb, Zr, Y, Sr and Rb were done on the same samples as were analysed for major oxides, using X-ray fluorescence (Appendix A). Ratios of Rb/Sr, K/Rb, K/Sr, Ba/Sr, Ba/Rb and Zr/Nb were calculated and complete results are in Appendix B. Averages and ranges of trace element abundances in each pluton are within the text as Tables 15, 16, 17, 18, 19 and 20.

The granitic rocks of the Albari and Alse-Hairah plutons have average or near average concentrations of these elements for granodiorite and granite. Whereas the Jabal Sayid and Hadb-Aldyaheen plutons except for the biotite granite of the latter, have trace element abundances quite different from an average granite (see Table 21).

4.4.2 Rubidium

The least Rb occurs in Albari granite which has an average of 92 ppm and in the Alse-Hairah granite which has an average of 198 ppm; it is most abundant in the peralkaline granite of Hadb-Aldyaheen ring complex and at Jabal Sayid 316 to 449 ppm respectively. The biotite granite

Table 15. Average and range of atomic abundances (ppm) of trace elements of Albari granite and the average abundances of granodiorite (Taylor, 1966).

	Albari granite		Granodiorite (Taylor, 1966).
	Average*	Range	
Cr	54	9 - 102	20
Ba	524	355 - 642	500
Ni	9	1 - 25	20
Nb	12	8 - 13	20
Zr	129	107 - 158	140
Y	23	12 - 29	30
Sr	462	318 - 631	450
Rb	92	63 - 148	120
Rb/Sr	0.21	0.1 - 0.47	
K/Rb	285	207 - 352	
K/Sr	58	35 - 96	
Ba/Sr	1.19	0.7 - 1.75	
Ba/Rb	5.89	3.76 - 7.08	
Zr/Nb	10.77	8.23 - 19.75	

*Average of 12 analyses.

Table 16. Average and range of atomic abundances (ppm) of trace elements of Alse-Hairah granite and the average abundances of granite (Taylor, 1966).

	Alse-Hairah granite		Granite (Taylor, 1966)
	Average*	Range	
Cr	38	6 - 145	4
Ba	625	416 - 904	600
Ni	19	2 - 73	0.5
Nb	21	16 - 24	20
Zr	214	153 - 295	180
Y	10	6 - 14	40
Sr	442	388 - 540	285
Rb	146	108 - 167	150
Rb/Sr	0.34	0.22 - 0.42	
K/Rb	289	230 - 414	
K/Sr	93	83 - 104	
Ba/Sr	1.39	1.05 - 1.67	
Ba/Rb	4.53	2.67 - 7.66	
Zr/Nb	10.56	7.65 - 16.56	

*Average of 8 analyses.

Table 17. Average and range of atomic abundances (ppm) of trace elements of the biotite granite and microgranite of Hadb-Aldyaheen ring complex.

	Biotite granite		Microgranite	
	Average*	Range	Average**	Range
Cr	12.50	7 - 25	16	7 - 37
Ba	703	590 - 867	536	412 - 653
Ni	7	2 - 13	15	7 - 24
Nb	18	15 - 22	72	30 - 161
Zr	194	169 - 245	843	280 - 2530
Y	20	16 - 23	94	32 - 271
Sr	441	376 - 511	294	205 - 407
Rb	198	192 - 206	279	237 - 306
Rb/Sr	0.45	0.40 - 0.50	1.03	0.60 - 1.50
K/Rb	173	167 - 183	128	112 - 145
K/Sr	79	69 - 89	128	84 - 147
Ba/Sr	1.58	1.46 - 1.69	1.89	1.43 - 2.45
Ba/Rb	3.56	2.90 - 4.52	1.95	1.35 - 2.44
Zr/Nb	10.77	9.56 - 11.27	10.88	7.85 - 15.71

*Average of 4 analyses

**Average of 6 analyses

Table 18. Average and range of atomic abundances (ppm) of trace elements of the granite porphyry of Hadb-Aldyaheen ring complex.

	Average*	Range
Cr	16	2 - 46
Ba	265	82 - 383
Ni	18	2 - 40
Nb	103	54 - 150
Zr	1336	337 - 2157
Y	169	45 - 302
Sr	138	78 - 178
Rb	316	224 - 397
Rb/Sr	2.42	1.5 - 3.7
K/Rb	113	83 - 158
K/Sr	263	184 - 382
Ba/Sr	2.08	1.05 - 2.27
Ba/Rb	0.86	0.28 - 1.35
Zr/Nb	13.05	6.24 - 21.84

*Average of 11 analyses..

Table 19. Average and range of atomic abundances (ppm) of trace elements of the riebeckite granite of Hadb-Aldyaheen ring complex.

	Average*	Range
Cr	11	1 - 35
Ba	16	0.00 - 46
Ni	14	0.00 - 55
Nb	67	15 - 160
Zr	1673	80 - 5080
Y	193	29 - 817
Sr	22	3 - 101
Rb	458	251 - 725
Rb/Sr	45	10 - 121
K/Rb	78	50 - 131
K/Sr	3585	886 - 11233
Ba/Sr	0.87	0.00 - 2.56
Ba/Rb	0.04	0.00 - 0.13
Zr/Nb	24.64	3.8 - 79

*Average of 13 analyses.

Table 20. Average and range of atomic abundances (ppm) of trace elements of Jabal Sayid Riebeckite granite.

	Average*	Range
Cr	44	2 - 220
Ba	5	1 - 15
Ni	32	1 - 116
Nb	126	63 - 193
Zr	1653	745 - 2683
Y	201	64 - 708
Sr	11	6 - 20
Rb	356	267 - 439
Rb/Sr	36	19 - 57
K/Rb	95	74 - 129
K/Sr	3426	1665 - 5700
Ba/Sr	0.52	0.00 - 3
Ba/Rb	0.01	0.00 - 0.07
Zr/Nb	14.28	5.55 - 21.64

*Average of 14 analyses.

(1) (2) Hadb-Algyaheen ring complex (3) (4)

	AV. Albari Granite (650 my)	AV. Aise-Hairah Granite	AV. Biotite Granite	AV. Micro-granite	AV. Granite	AV. Porphyry (573 my)	AV. Riebeckite (573 my)	AV. Riebeckite (505 my)	AV. Sayid	AV. Jabal	AV. Crust Taylor (1966)	AV. Basalt	AV. Syanite	AV. Granodiorite	AV. Granite
Cr	54	38	12	16	16	11	44	100	200	2	20	20	4		
Ba	425	625	703	536	265	16	5	425	250	1500	500	600			
Ni	9	19	7	15	18	14	32	75	150	5	20	0.5			
Nb	12	21	18	72	103	67	126	20	20	40	20	20			
Zr	129	214	194	843	1336	1548	1653	165	150	500	140	180			
Y	23	10	20	94	169	180	201	30	25	20	30	40			
Si	462	442	441	294	138	15	11	375	465	300	450	285			
Rb	92	146	198	279	316	449	356	90	30	110	120	150			
Rb/Sr	0.21	0.34	0.45	1.03	2.42	44	36	230							
K/Rb	285	289	173	128	113	80	95								
K/Sr	58	93	79	128	263	2808	3426								
Ba/Sr	1.19	1.39	1.58	1.89	2.08	0.96	0.52								
Ba/Rb	5.89	4.53	3.56	1.95	0.86	0.05	0.01								
Zr/Nb	10.77	10.56	10.77	10.42	13.05	24.38	14.28								
A.I.	0.64	0.84	0.80	0.98	1.08	1.18	1.11								

Table 21. Averages of trace element abundances of rocks of the four plutons compared to Taylor's (1966) averages.

and the microgranite of Hadb-Aldyaheen have average Rb contents of 198 and 279 ppm respectively which is an intermediate abundance.

Taylor (1966) has indicated the close association of Rb with K and their general positive correlation. This observation holds for Albari granite (Fig. 31). For Alse-Hairah granite and the biotite granite of Hadb-Aldyaheen ring complex, the correlation between K and Rb is negative. The preferential entry of Rb into biotite co-existing with feldspar, secondary enrichment of samples with K or varied fractionation within one type of melt, are among the factors which prevent a rigid relation between Rb and K in each sample. The relative enrichment of some of these granites compared to the others is probably caused by fractional crystallization and residual solutions, processes in which Rb is thought to be concentrated (Taylor, 1966).

The plot of K versus Rb for Jabal Sayid riebeckite granite has no defined trend (Fig. 31). In the same figure, K has a weak positive correlation with Rb for the microgranite and the riebeckite granite of the Hadb-Aldyaheen ring complex, but no defined trend was observed for the data points of the granite porphyry.

In general, there is a decrease in the average K/Rb from the oldest granite of Albari Av. 285 to the youngest peralkaline granites of Hadb-Aldyaheen ring complex and Jabal Sayid Av. 113 to 80, but this relation is by no means linear. This suggests that there has been no parental

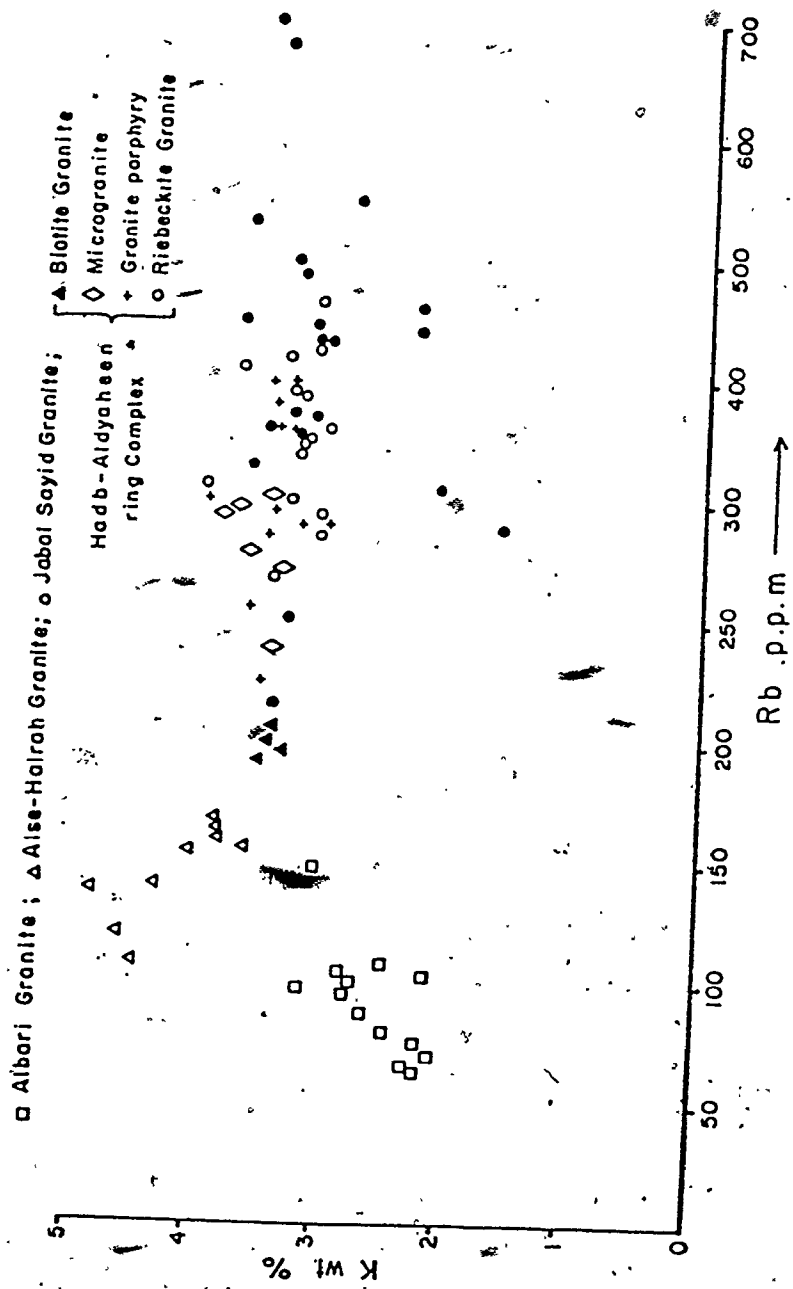


Figure 31. K (wt%), against Rb (ppm).

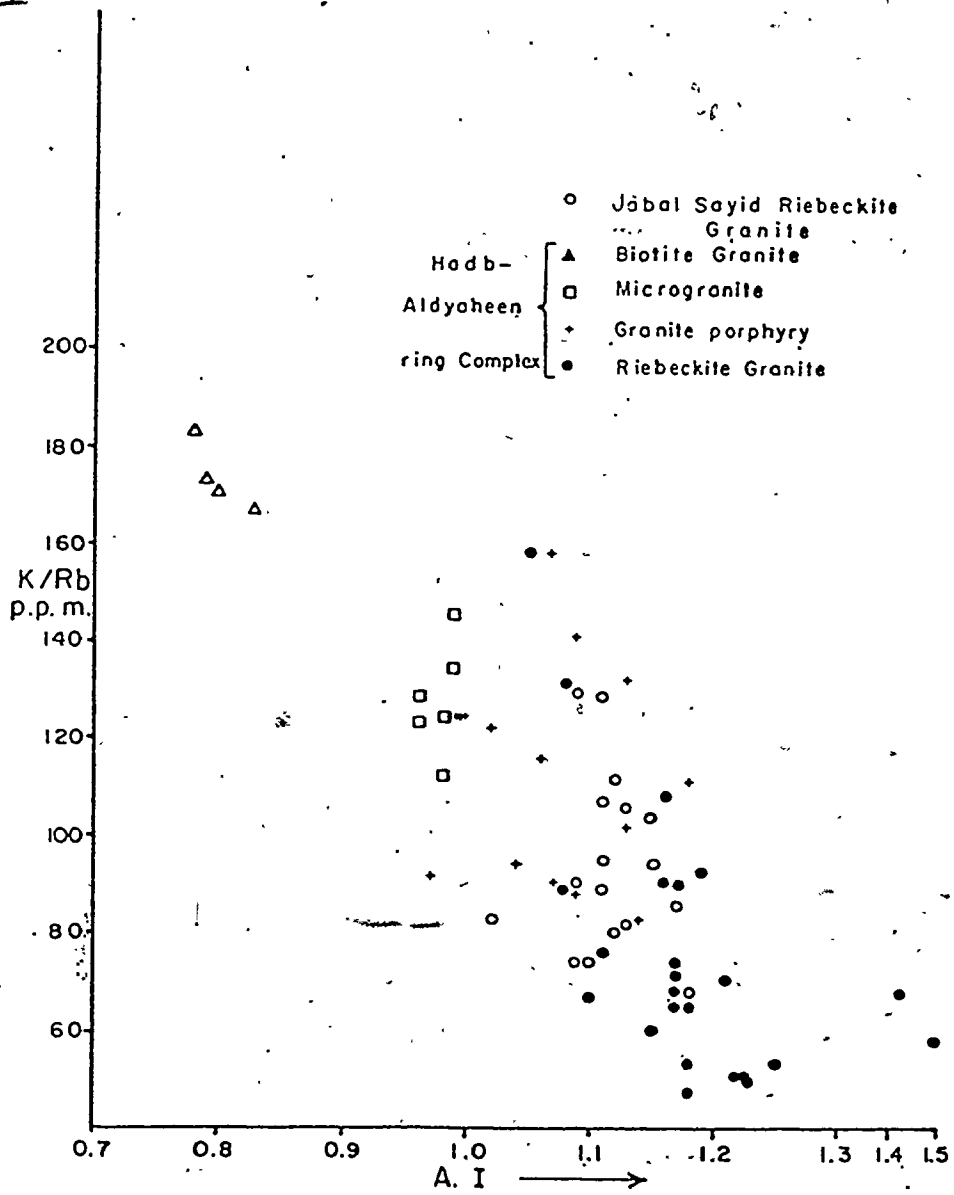


Figure 32. K/Rb plotted against alkalinity index (A.I.).

relationship between the non-peralkaline granites of Albari, Alse-Hairah, biotite granite of Hadb-Aldyaheen and the peralkaline granites of Hadb-Aldyaheen and Jabal Sayid. However the K/Rb of the non-peralkaline granites are comparable to those for normal granitic rocks.

For rocks of Hadb-Aldyaheen ring complex the K/Rb is 128 ppm in the microgranite to 113 ppm in the granite porphyry to 80 ppm in the riebeckite granite. This reduction of K/Rb could be taken to indicate the sequence of formation of the rocks forming the complex, which is in accordance with the field relationship.

The K/Rb of Jabal Sayid riebeckite granite Av. 95 ppm is fairly similar to average K/Rb of the riebeckite granite of Hadb-Aldyaheen ring complex suggesting a similar or common origin and history of crystallization.

The significant enrichment of Rb and the corresponding decrease of the K/Rb in the peralkaline granites of both Hadb-Aldyaheen and Jabal Sayid could be taken as indicative of crystallization from a magma which had undergone differentiation to the pegmatitic phase rather than the less extreme differentiation common in normal felsic igneous rocks. Similar proposals have been made by Taylor et al. (1956) for the Mourne and St. Austell granites. This interpretation should be used with caution as there is not enough evidence of enrichment of Rb by igneous differentiation as Rb has no clear correlation with either

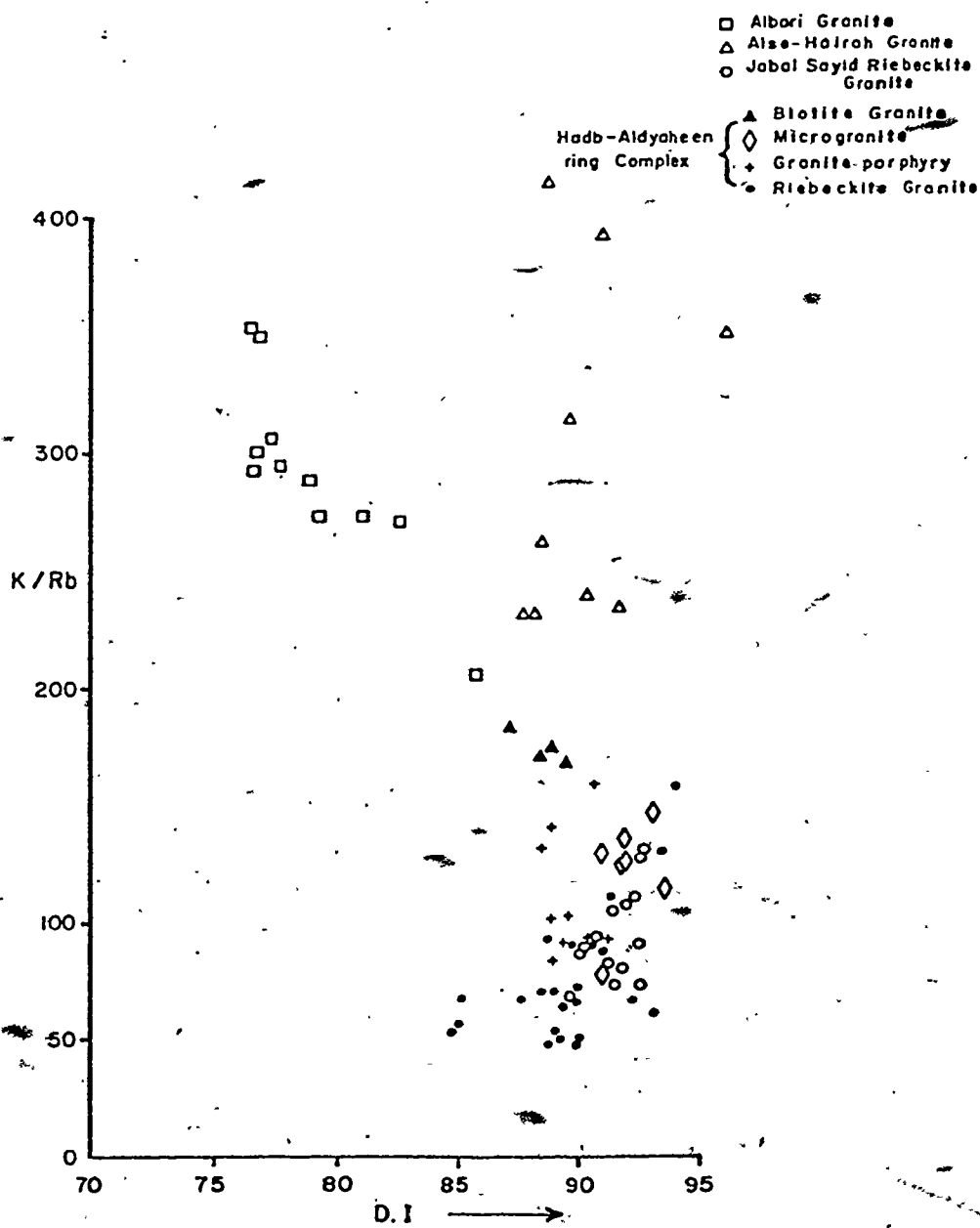


Figure 33. K/Rb plotted against differentiation index of Thornton and Tuttle (1960).

SiO₂ or K contents. K/Rb versus the A.I. (Fig. 32) has a weak trend in which the ratio decreases with increasing alkalinity index. This relation is in agreement with suggestion of Aleksyev (1970) for the Nigerian granite. The K/Rb versus the D.I. (Fig. 33) has two distinct general trends in which the K/Rb of the non-peralkaline granites has a negative correlation with D.I., whereas in the peralkaline granites the ratio has positive correlation.

4.4.3 Niobium

Nb is least abundant in the Albari granite averaging 12 ppm, which is less than average abundance in the crust and similar rock type quoted by Taylor (1966) (Table 21). The average content of the Nb in the Alse-Hairah granite and the biotite granite of Hadb-Aldyaheen ring complex is 21 and 18 ppm respectively and these abundances are within the range of published averages for younger granites from Africa and the Arabian Shield (Nasseef and Gass, 1977; Gass, 1977; Neary et al., 1976; Rooke, 1970). For the rocks forming Hadb-Aldyaheen ring complex, Nb content increases from an average of 72 ppm for the microgranite to an average of 103 ppm for the granite porphyry and decreases to 67 ppm for the riebeckite granite. Nb has its greatest average abundance of 126 ppm in Jabal Sayid riebeckite granite.

The variation in Nb abundances within a suite from a single type of non-peralkaline granites is relatively

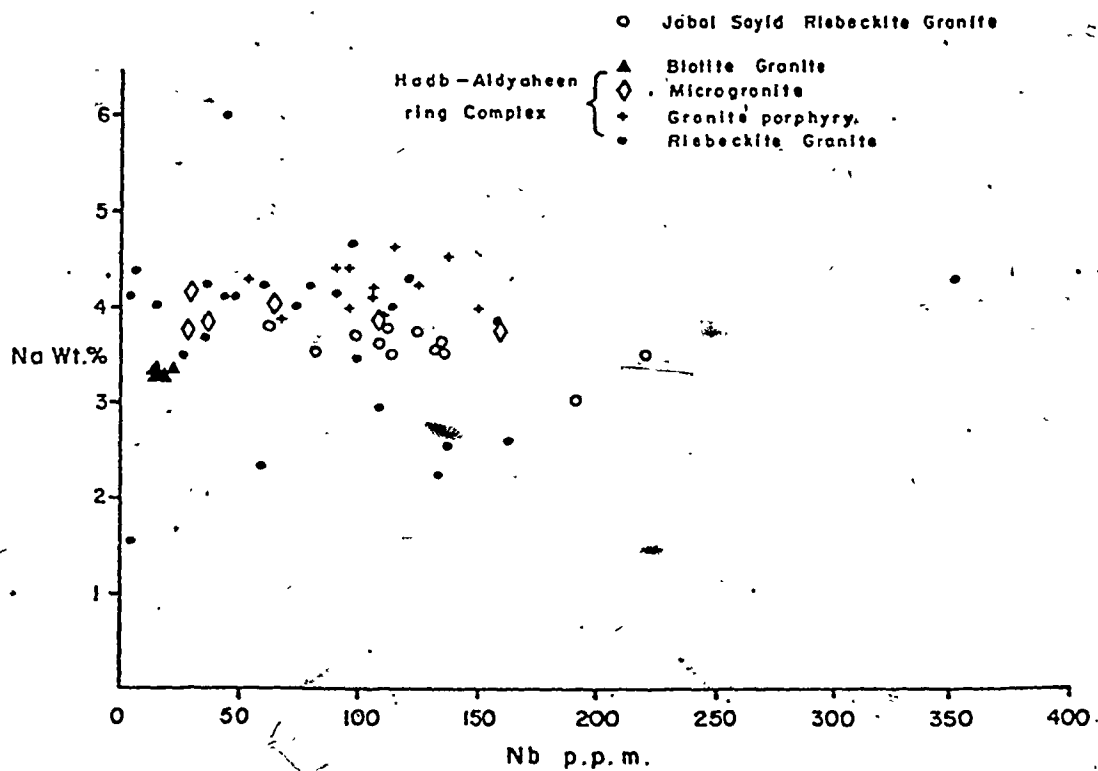


Figure 34. Na (wt %) against Nb (ppm).

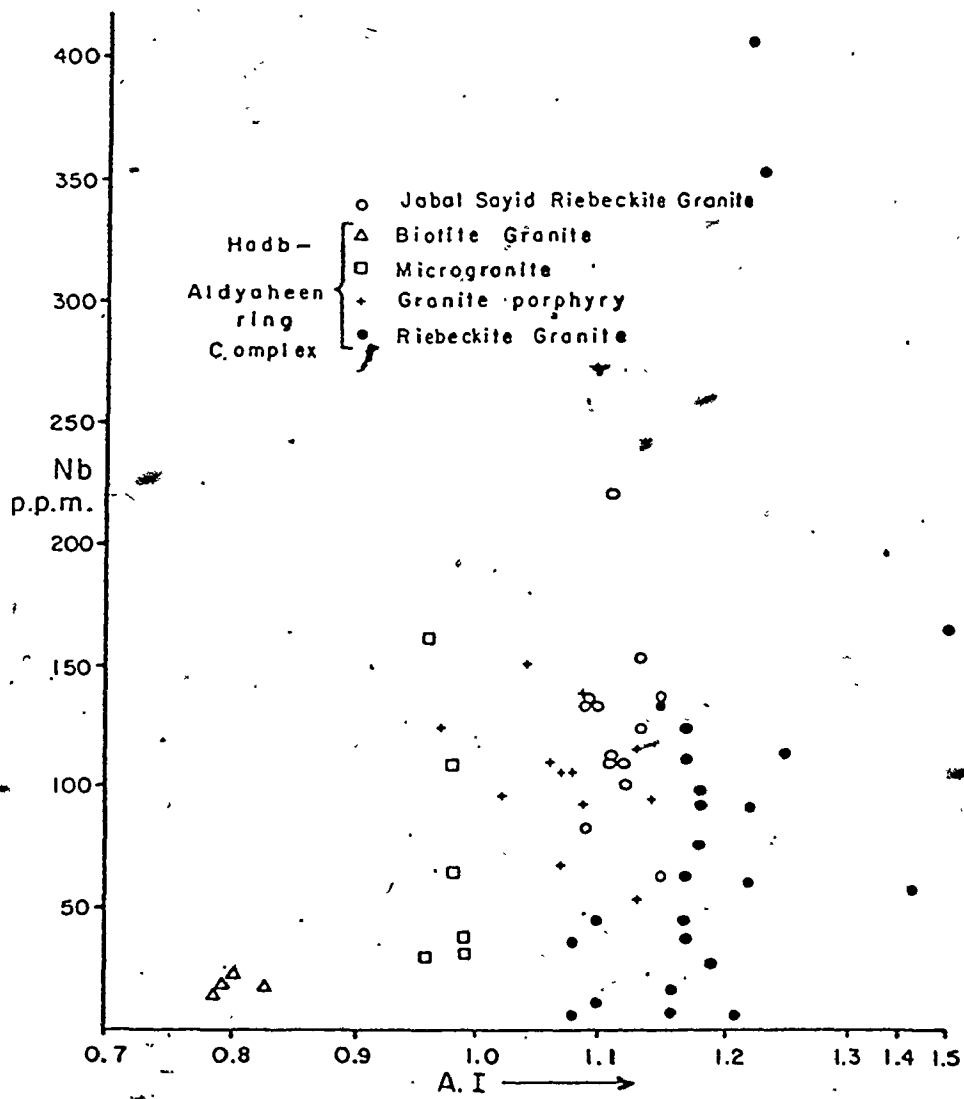


Figure 35. Nb (ppm) against the alkalinity index (A.I.).

small, in contrast with the large variations within the peralkaline granites, particularly the riebeckite granite of Hadb-Aldyaheen.

Pearce and Gale (1977) indicated that Nb content in granitic rocks that overly active subduction zones is commonly less than 15 ppm whereas continental granites are markedly enriched with 50 to 400 ppm niobium. Hence the minor content of Nb of the non-peralkaline granites of Albari, Alse-Hairah and the biotite granite of Hadb-Aldyaheen ring complex, suggests a magma type generated above a subduction zone whereas the peralkaline granites of Hadb-Aldyaheen and Jabal Sayid are a magmatic product of continental plate collision subsequent to the subduction.

Jacobson et al. (1958) conclude that there is a direct correlation between sodium and niobium content in the Younger Nigerian granites. This relation is not observed for the rocks of Hadb-Aldyaheen or the riebeckite granite of Jabal Sayid (Fig. 34). Aleksiyev (1970) concludes that for the Younger granites of Northern Nigeria, there is a direct correlation between the degree of alkalinity ($(Na + K/Al)$) or albitization and the trace element and rare earth abundances including Nb. Nb versus the alkalinity index (A.I.) (Fig. 35), for the rocks of Hadb-Aldyaheen ring complex and Jabal Sayid riebeckite granite, has no defined trend. However, there is a general increase in Nb content as a function of increasing A.I. from biotite

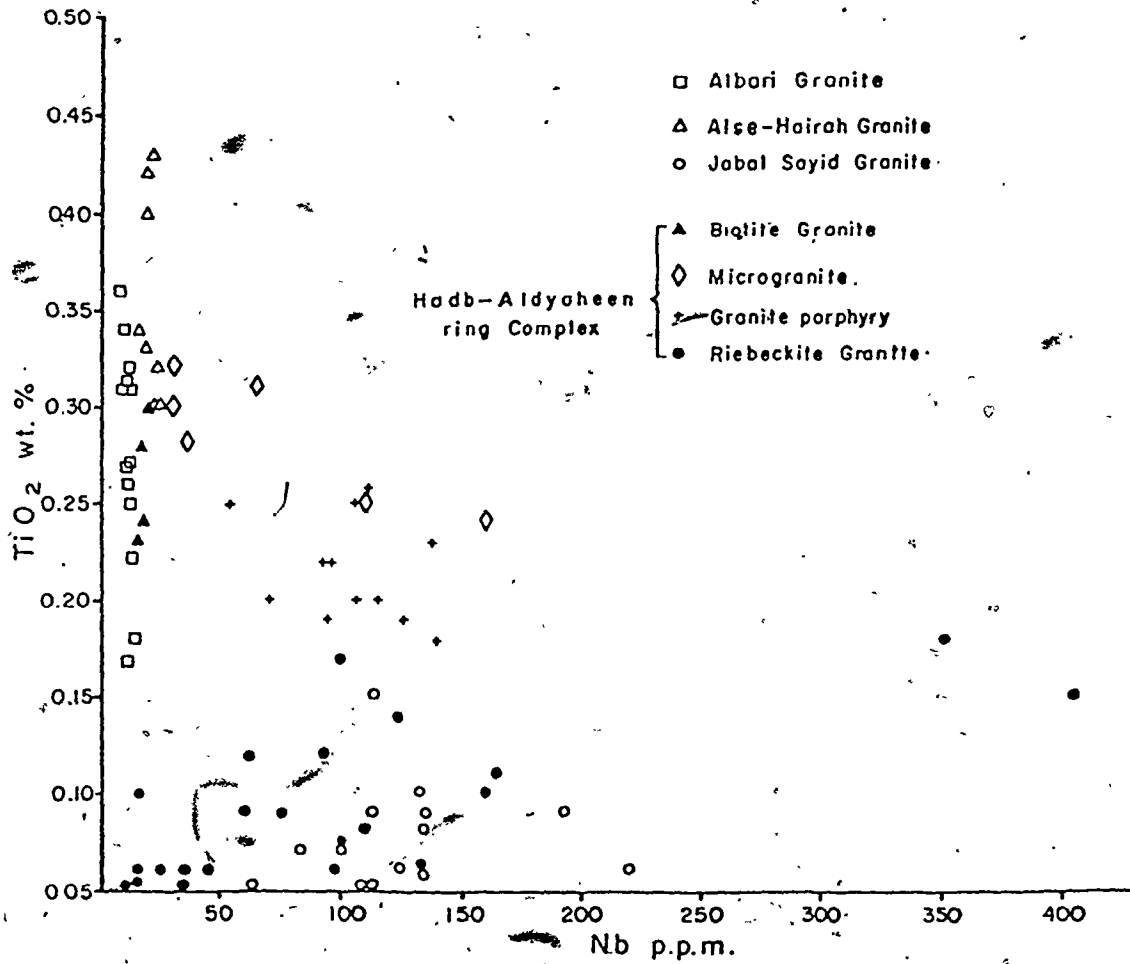


Figure 36. Nb (ppm) against TiO_2 (wt %).

granite to microgranite to granite porphyry to the riebeckite granite of Jabal Sayid. The riebeckite granite of Hadb-Aldyaheen has an alkalinity index greater than any of other types of granites in the area but the distribution of Nb in this rock is very erratic ranging from 15 to 400 ppm. Most of the lesser abundances are from samples collected either from the contact zones or from small bodies of riebeckite granite which intrude granite porphyry.

Nb content of the non-peralkaline granites of Albari, Alse-Hairah and biotite granite of Hadb-Aldyaheen, have no corresponding change with increase of TiO_2 content (Fig. 36). Whereas for peralkaline rocks there are scattered data points. However, Nb content of the microgranite and the granite porphyry has a weak negative correlation with TiO_2 . The scattered data point observed for the riebeckite granite of Jabal Sayid and Hadb Aldyaheen may suggest that, the Nb content of these rocks is not concentrated only in Ti minerals as it is suggested by Gerasimovskii et al. (1959) for the Lovozero alkalic massif, but also present in some other forms as complexes or in fine-grained minerals which could not be identified by microscopic work.

4.4.4 Zirconium

Zr is present in the non-peralkaline granites of Albari, Alse-Hairah and the biotite granite of Hadb-Aldyaheen, within the range of abundances of certain

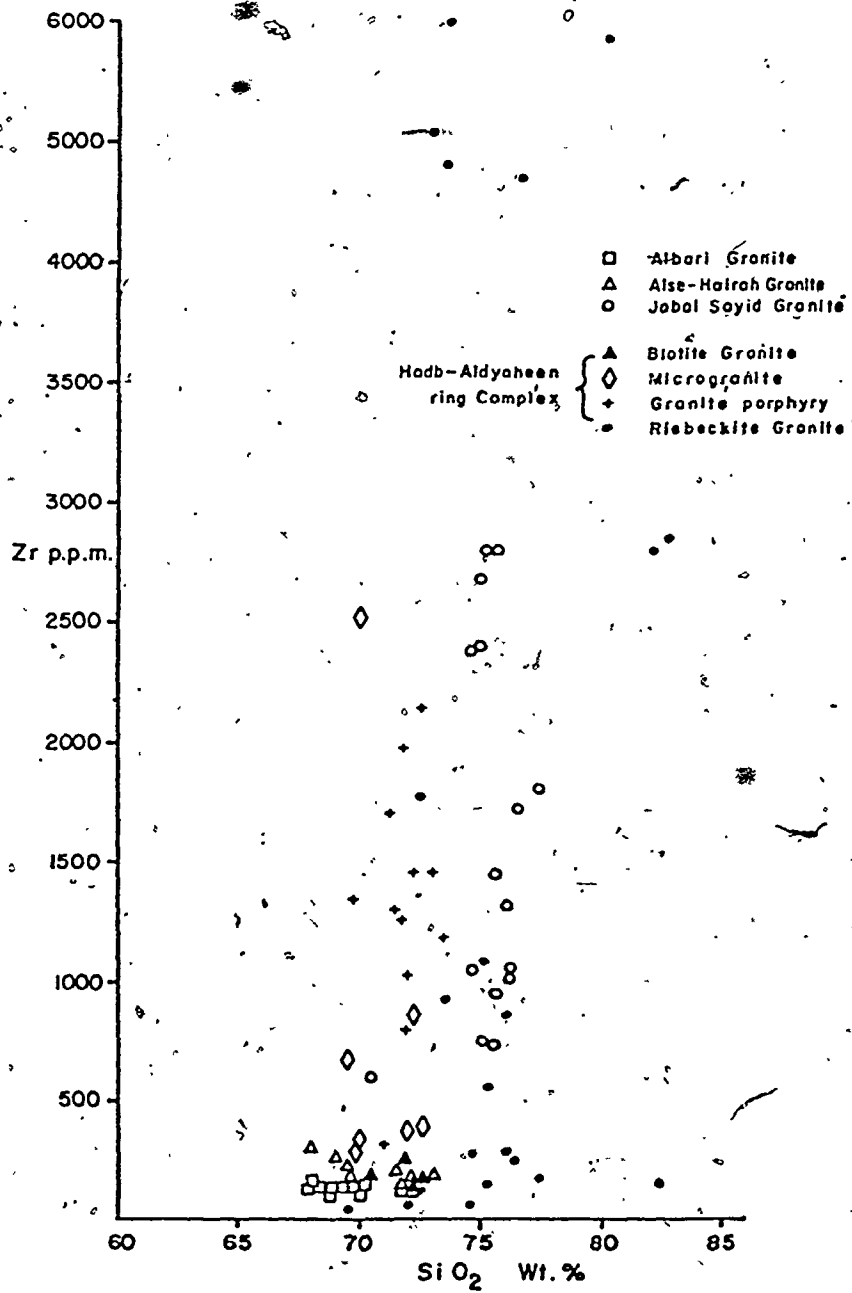


Figure 37. Zr (ppm) against SiO₂ (wt %).

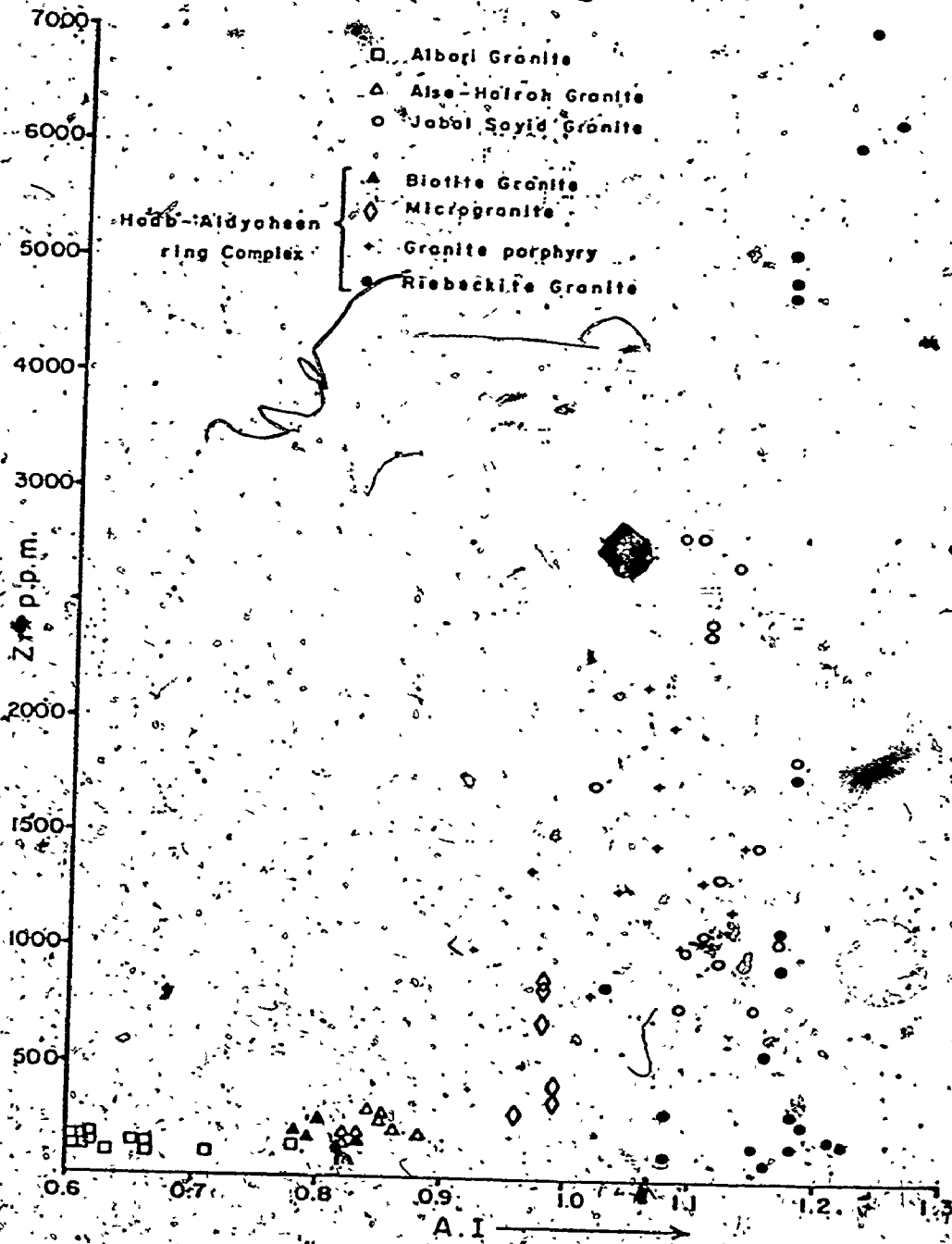


Figure 38. Zr (ppm) against the alkalinity index (A.I.).

published analyses of granites and granodiorite (Table 21). Among these rocks, Zr has its greatest concentration in the Alse-Hairah granite with an average of 214 ppm which has modal zircon. The Zr content of the microgranite of Hadb-Aldyaheen complex has an average of 843 ppm, but this rises abruptly to a maximum of 2000 ppm and an average of 1336 ppm in the granite porphyry and to a maximum of 5000 ppm in the riebeckite granite with an average of 1548 ppm. The average content of Zr of Jabal Sayid riebeckite granite is 1653 ppm which is very similar to the average of riebeckite granite of Hadb-Aldyaheen. Despite the relatively large Zr contents of the peralkaline granite, zircon crystals are rarely visible. Similar observation has been reported by Siedner (1965) for the Paresis felsic rocks, he suggested, that because of the solubility of zirconium in alkaline magmas, zircon did not crystallize to any marked extent. It is also interesting to note that rocks collected from the contact zones of the riebeckite granite of the Hadb-Aldyaheen ring complex, which usually contain more modal aegirine than rocks within the complex, have a greater Zr content. Gerasimovskii et al. (1962) note that zirconium could form a solid solution series with iron in aegirine. Butler and Thompson (1965) note that alkali amphiboles and alkali pyroxenes are conspicuous carriers of Zr and HF. Bowden (1966) concluded that under alkaline conditions, zirconium will not crystallize wholly as zircon but will

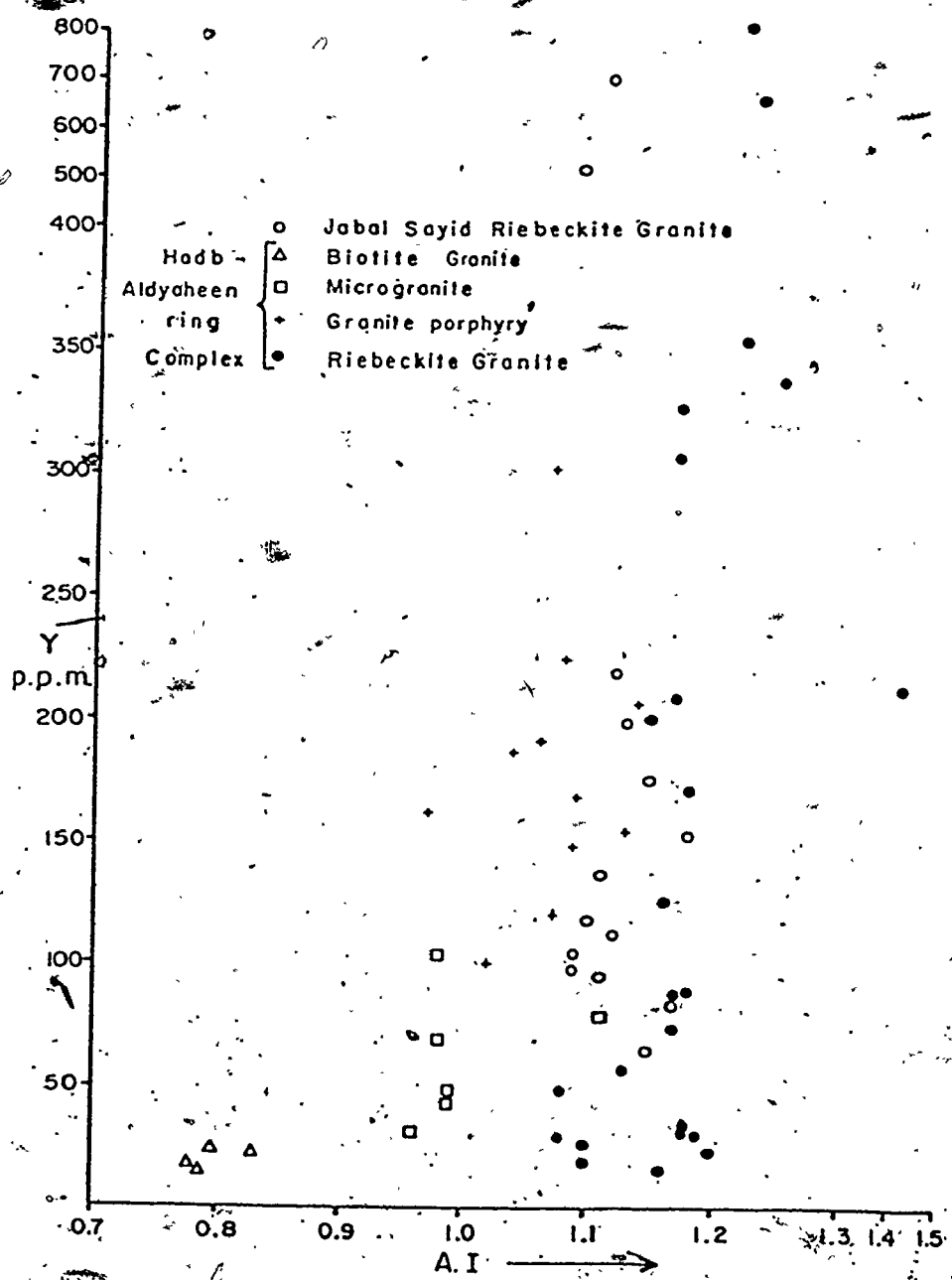


Figure 39. Y against the alkalinity index (A.I.).

be mainly incorporated in the lattice of mafic minerals.

Zr versus SiO_2 (Fig. 37) has a general trend in which Zr increases with increase of SiO_2 content. But the relation in Zr abundance within a suite of samples from a single pluton or from one pluton to another is by no means linear. Some samples of the peralkaline riebeckite granite have a minor Zr content similar to the non-peralkaline granites of Albari and Alse-Hairah plutons. Rocks of the Hadb-Aldyaheen ring complex, have a general increase in Zr following the trend of microgranite-granite porphyry-riebeckite granite. If Zr is mostly accumulated by magmatic differentiation in these rocks, this trend is in accordance with Goldschmid's hypothesis (1954) that Zr is enriched in alkaline residual magmas. Bowden (1965) and Aleksiyev (1970) have suggested that the Zr content of Nigerian Younger granites has a positive correlation with the corresponding apatitic coefficient expressed as the atomic ratio $[\text{Na}+\text{K}/\text{Al}]$; or degree of alkalinity. There are similar relationships in the rocks forming the Hadb-Aldyaheen ring complex and the riebeckite granite of Jabal Sayid (Fig. 38). Albari and Alse-Hairah granites data points were plotted for comparison.

4.4.5 Yttrium

Y is present in Albari granite and the biotite granite of Hadb-Aldyaheen within the average abundances

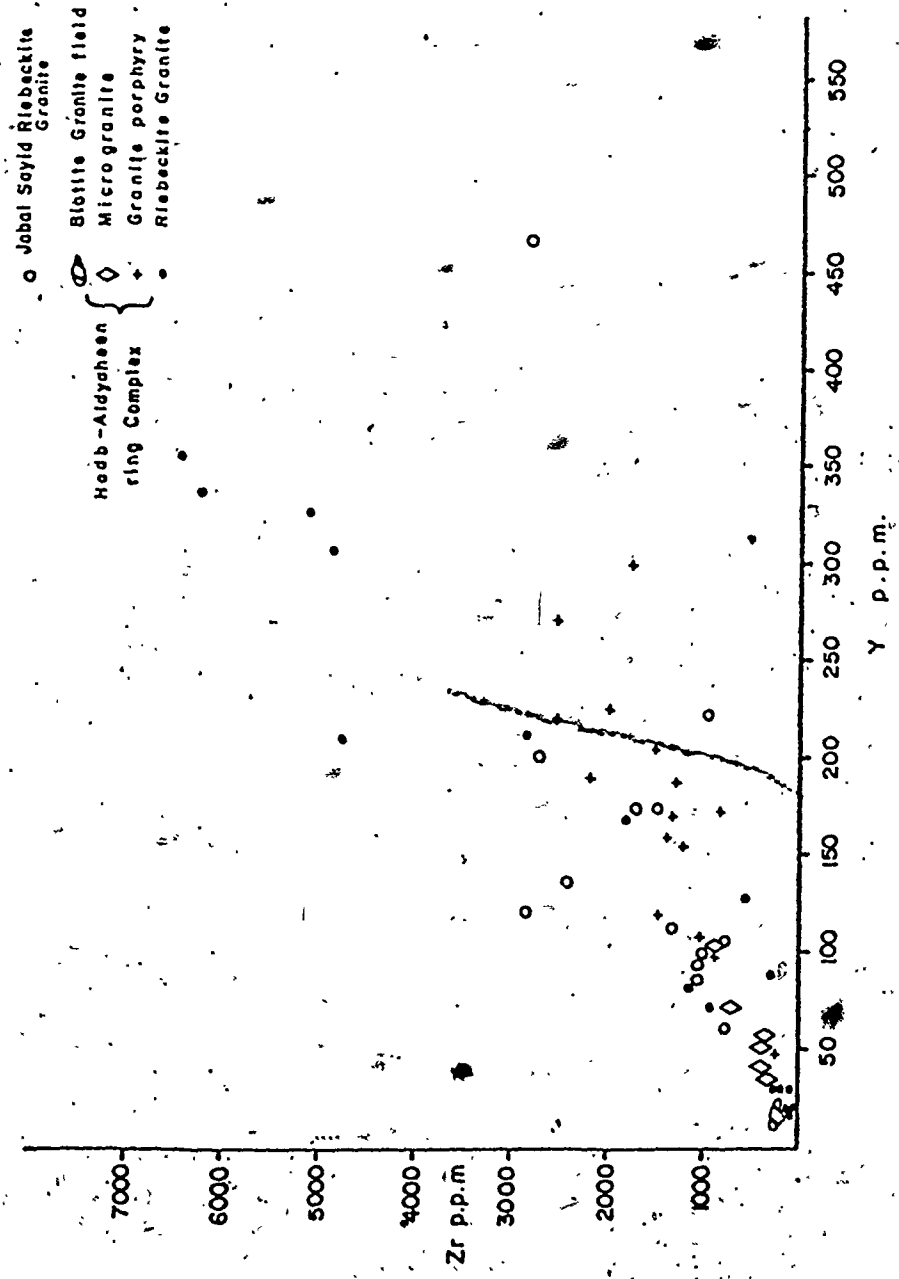


Figure 40. Zr against Y (ppm).

in similar rock types (Taylor, 1966). Its lesser concentration is in the Alse-Hairah granite, averaging 10 ppm. Rocks of Hadb-Aldyaheen ring complex and Jabal Sayid riebeckite granite have consistently greater Y than both crustal average and the granitic rocks quoted by Taylor (op. cit.) (Table 21). The abundance increases from an average of 94 ppm for the microgranite to an average of 169 ppm for the granite porphyry to an average of 193 ppm for the riebeckite granite and an average of 210 ppm for Jabal Sayid riebeckite granite. The increase in Y content from the non-peralkaline to peralkaline granites is by no means gradual. However, distribution of this element in the peralkaline granites is clearly erratic and does not have a correlation with other trace elements such as Nb, or the alkalinity index (Fig. 39). The plot of Y versus A.I. has scattered data points. In general it has a weak trend in which Y increases sharply with a small increase in A.I. Such correlation is in agreement with Aleksiyev (1970) for the Nigerian Younger granite and Yes'Kova and Yefimov (1970) for the Ural alkali granite, in which they indicate a relation between alkali-metasomatism or albitization, and the great content of Y and some other trace elements. Kovaleko et al. (1969) suggested that the Y content of the alkalic granites of Siberia is mainly accommodated by alkali amphiboles, aegirine and zircon. The plots of Zr versus Y for rocks of the Hadb-Aldyaheen ring complex and Jabal Sayid riebeckite granite, has a

defined trend in which Zr increases with increase of Y. However, overlapping between Zr contents from different rock types is apparent (Fig. 40).

4.4.6 Barium and Strontium

The average concentration of Ba and Sr is greatest in samples of the non-peralkaline granites of Albari, Alse-Hairah and Hadb-Aldyaheen ring complex and extremely depleted in peralkaline granites of Hadb-Aldyaheen and Jabal Sayid (Table 21). Sr commonly enters positions in plagioclase and its concentration is generally proportional to the amount of Ca. This relation is well shown in Figure 41, particularly for the non-peralkaline granites of Albari, Alse-Hairah and the biotite granite of Hadb-Aldyaheen. Variation in the abundance of Sr is very slight in the riebeckite granite of both Hadb-Aldyaheen and Jabal Sayid. This could be attributed to the minor Ca content of these rocks. The non-peralkaline granites and the granite porphyry of Hadb-Aldyaheen have a normal negative correlation between Sr and Rb (Fig. 42) in contrast with vertical correlation of the riebeckite granite of Hadb-Aldyaheen and Jabal Sayid in which Rb increases without any corresponding decrease in Sr content.

The behaviour of Ba is similar to that of Sr. Ba versus Sr for Albari granite has a well defined trend (Fig. 43) in which Ba decreases as a function of increasing Sr.

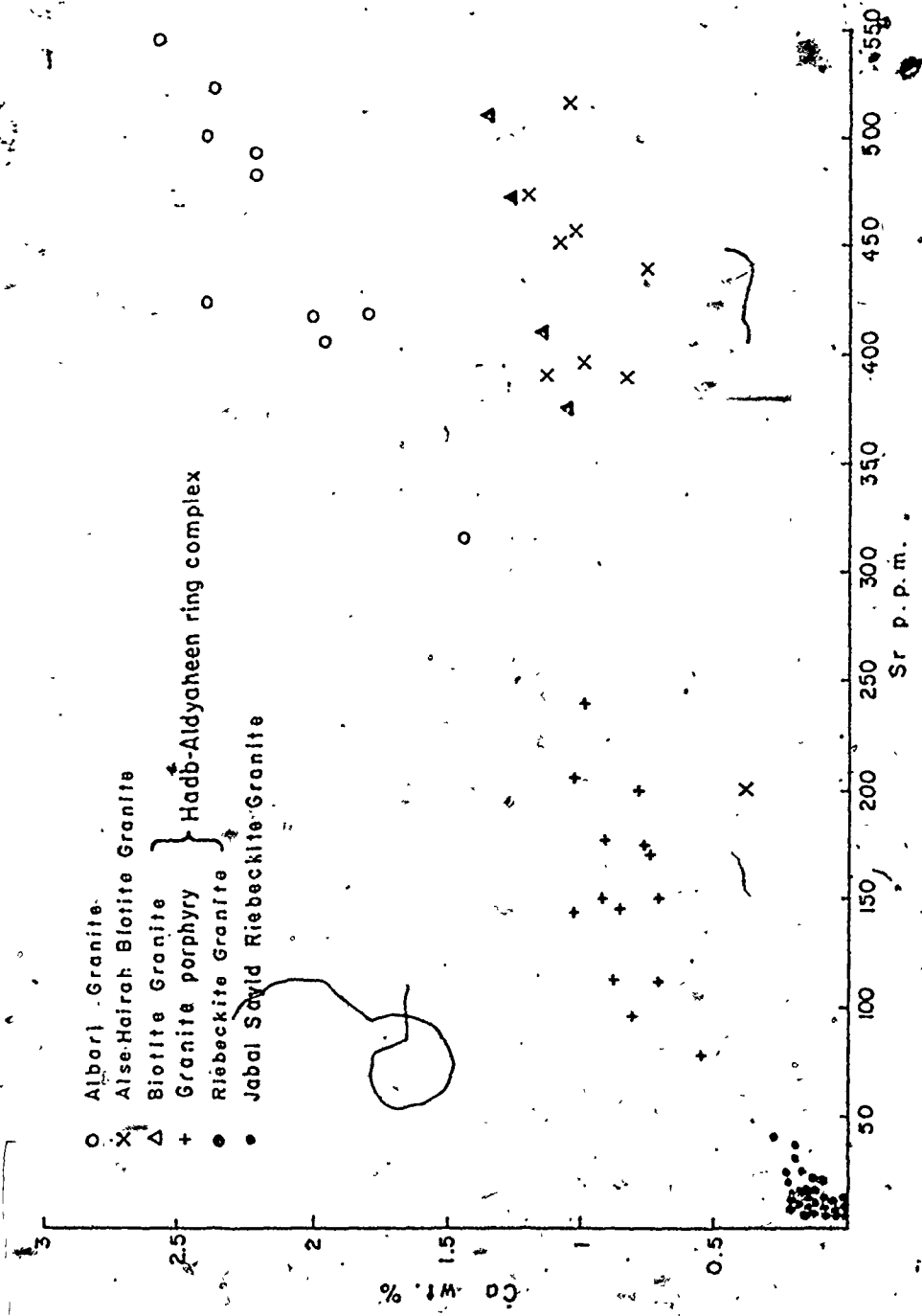


Figure 41. A diagram of the relationship between Ca and Sr in the granites of the four plutons.

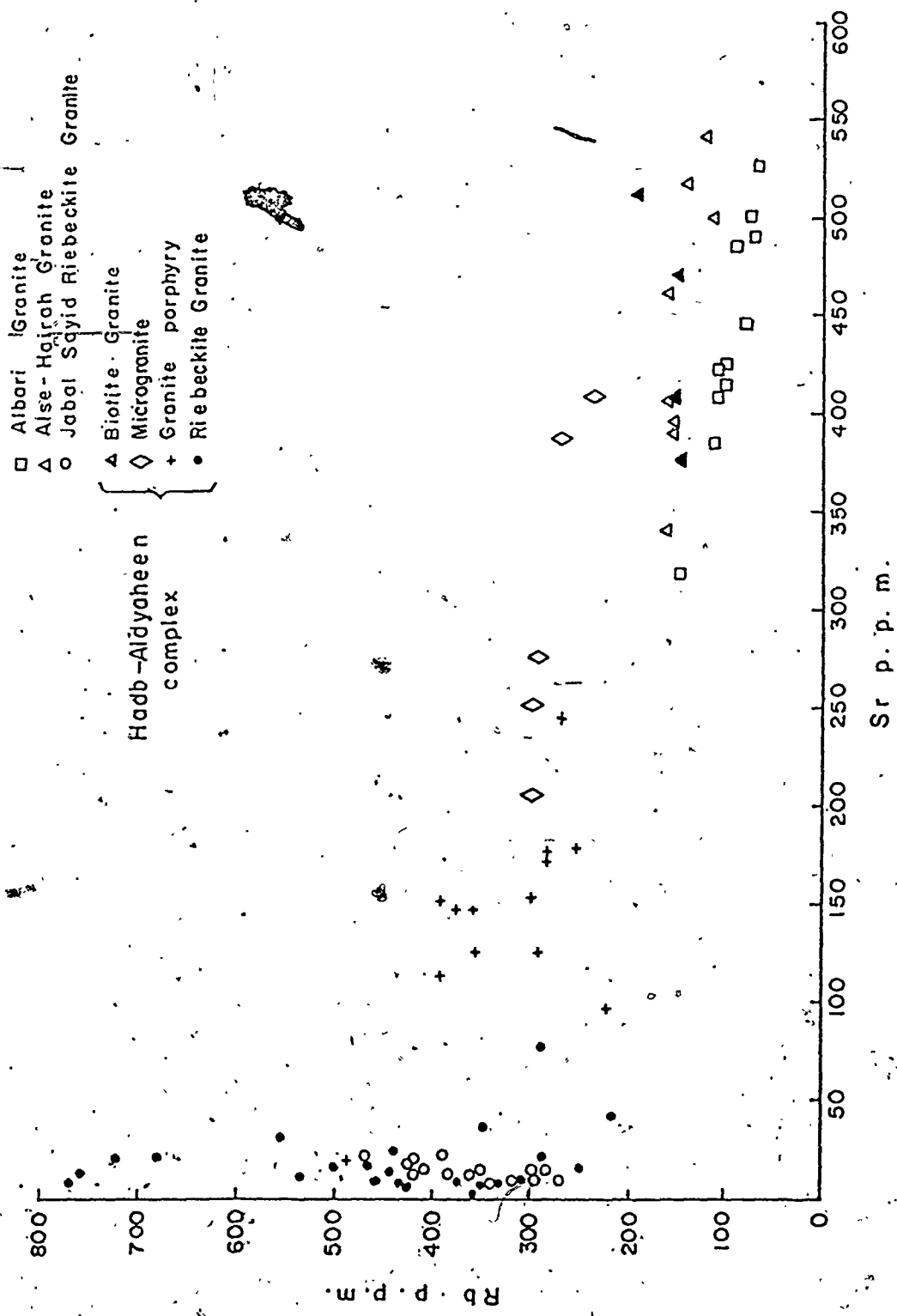


Figure 42. Rb against Sr for the granitic rocks of the four plutons.

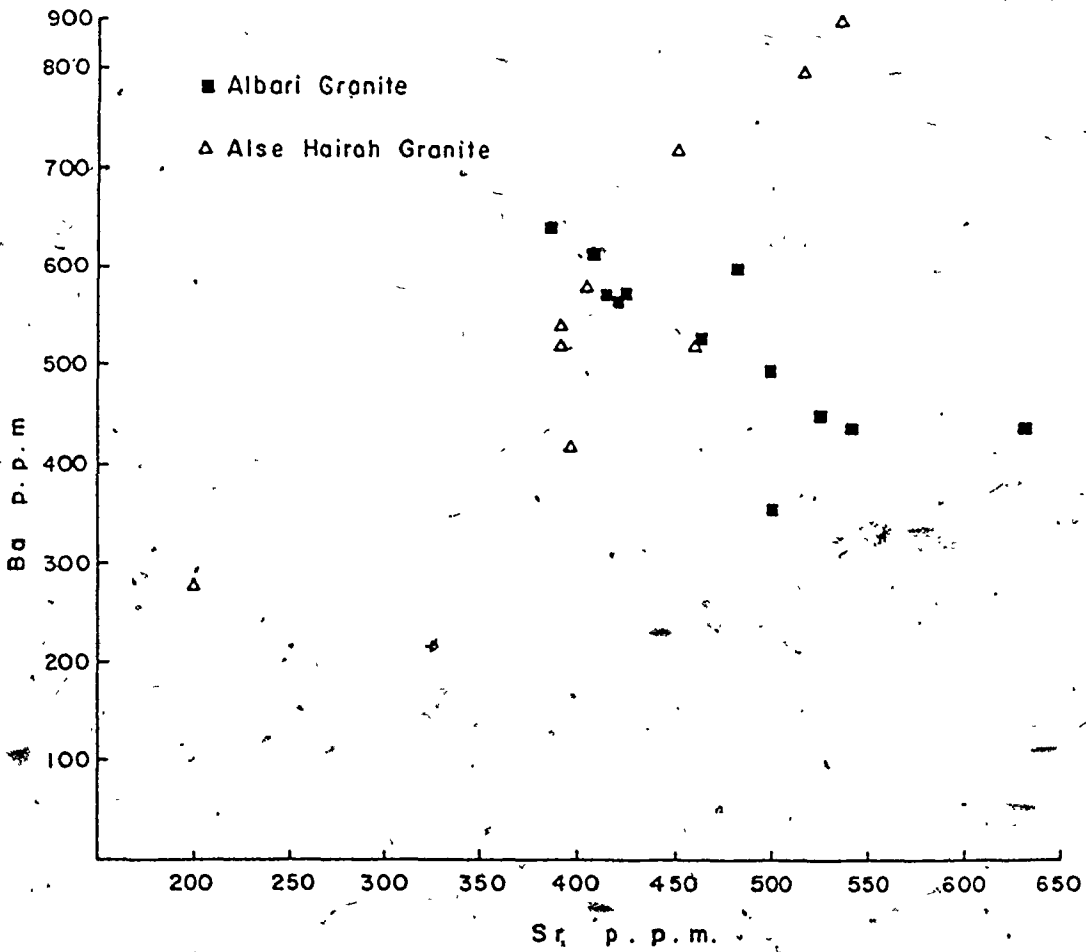


Figure 43. Ba/Sr of Albari and Alse-Hairah granites.

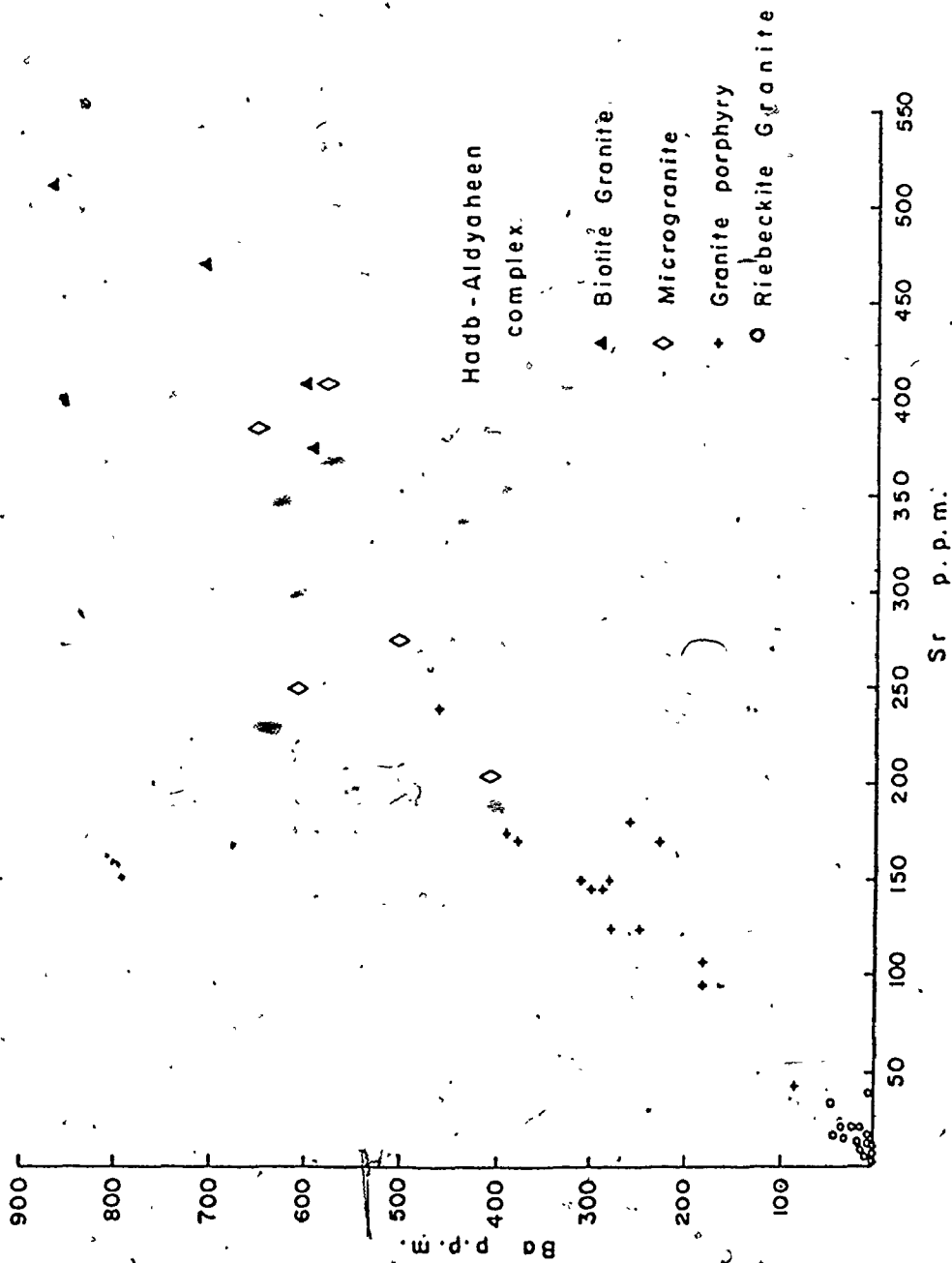


Figure 44. Ba/Sr of Habb-Aldyaheen ring complex rocks.

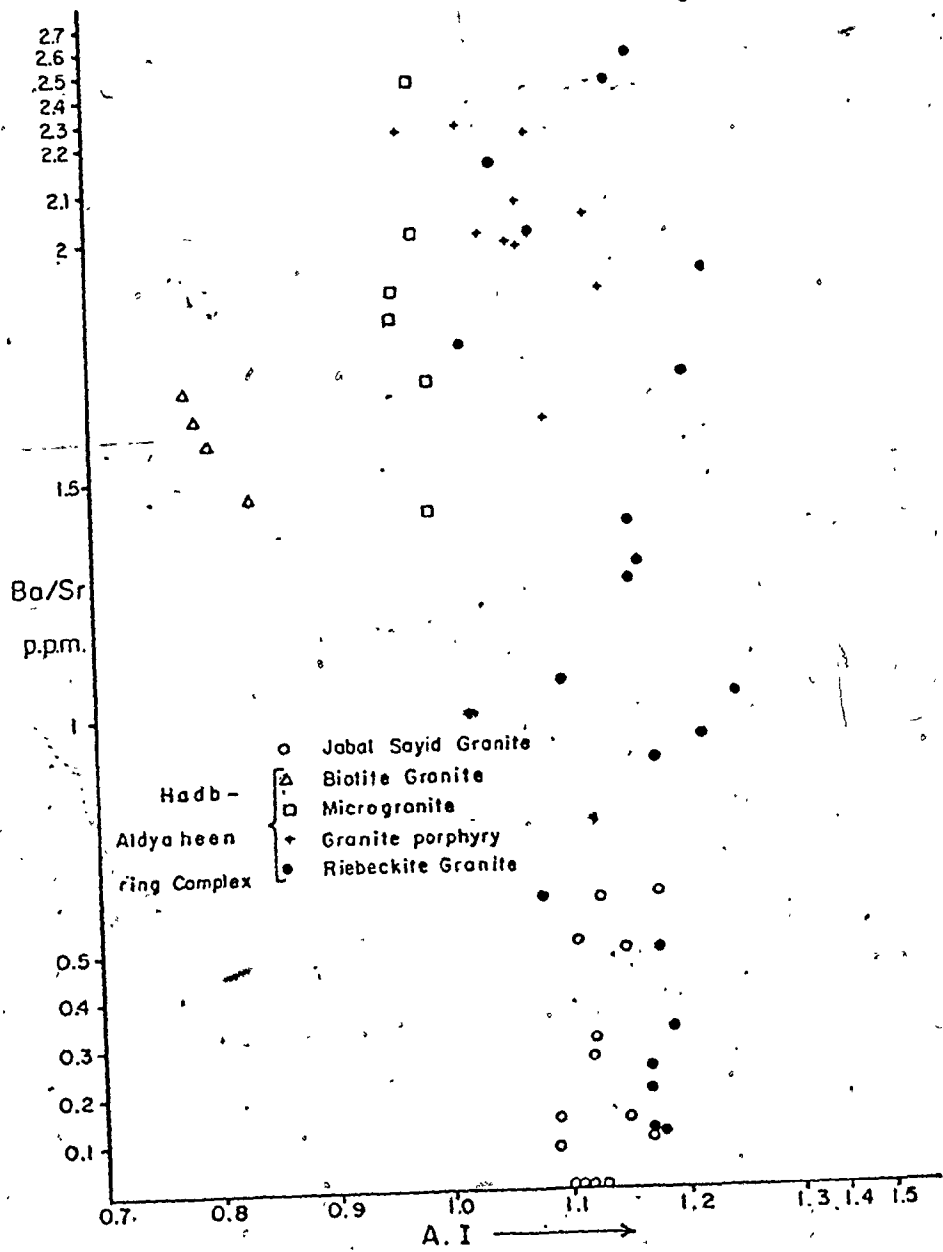


Figure 45. Ba/Sr against the alkalinity index (A.I.).

It has a positive correlation with Sr for Alse-Hairah granite. The same plot for the rocks of Hadb-Aldyaheen ring complex (Fig. 44) has a well defined trend in which Ba increases with the increase of Sr from riebeckite granite to granite porphyry to microgranite. The plots of Ba/Sr versus A.I. (Fig. 45) has no defined trend, only scattered data points whereas in the Nigerian Younger granite, Aleksiyev (1970) suggested a positive correlation between Ba/Sr and the degree of alkalinity.

Ba has a positive correlation with SiO_2 (Fig. 46) for Albari granite and scattered data points for Alse-Hairah and Hadb-Aldyaheen biotite granites. Sr has a negative correlation with SiO_2 for the non-peralkaline granites of Albari, Alse-Hairah and the biotite granite of Hadb-Aldyaheen. For the rocks of Hadb-Aldyaheen, Ba and Sr have a similar correlation with SiO_2 (Fig. 47) in which they decrease from the microgranite to granite porphyry to riebeckite granite with increasing SiO_2 .

Ba and Sr are only trace elements in the peralkaline granites which have a normal correlation relative to their common pair major element (Ca). Also they have a well defined trend relative to each other. This may indicate that the process which causes erratic distribution of other trace elements did not effect the distribution of Ba and Sr in the original magma. Their extreme depletion may be attributed to the extreme differentiation of the original magma (c.f. Marsh, 1975; Noble, 1972; Taylor et al., 1956).

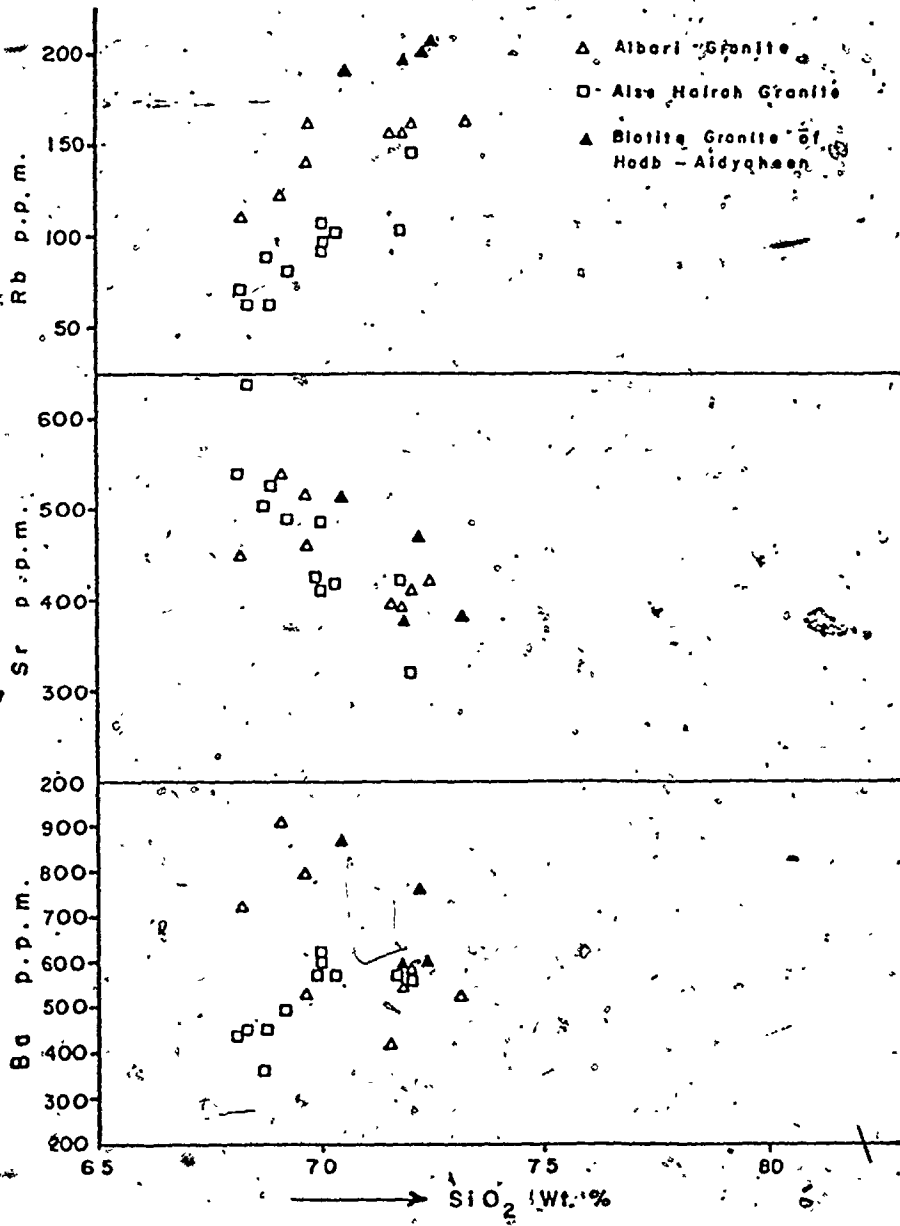
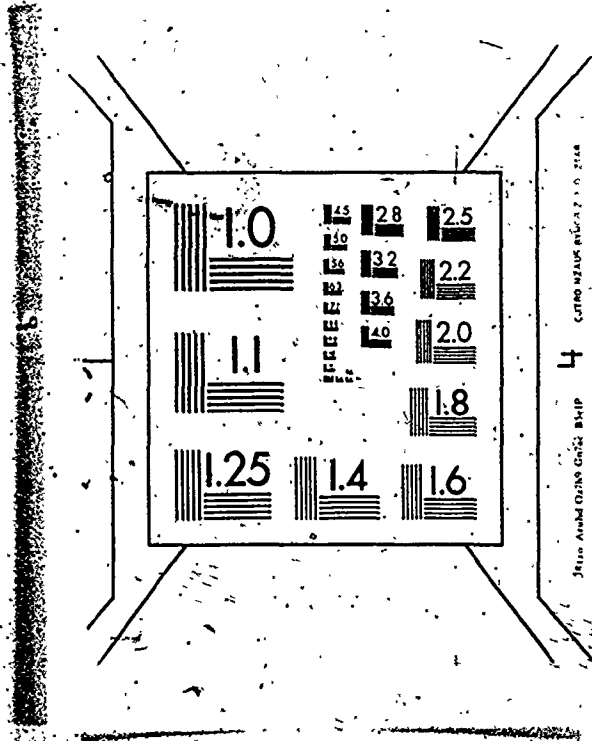


Figure 46. Ba, Sr and Rb (in ppm) against SiO₂ (wt %).

3 3

OF/DE



31 Jan Aviad Ozilo Chig: BHP
L CERNI N210K 11067 1 0 216

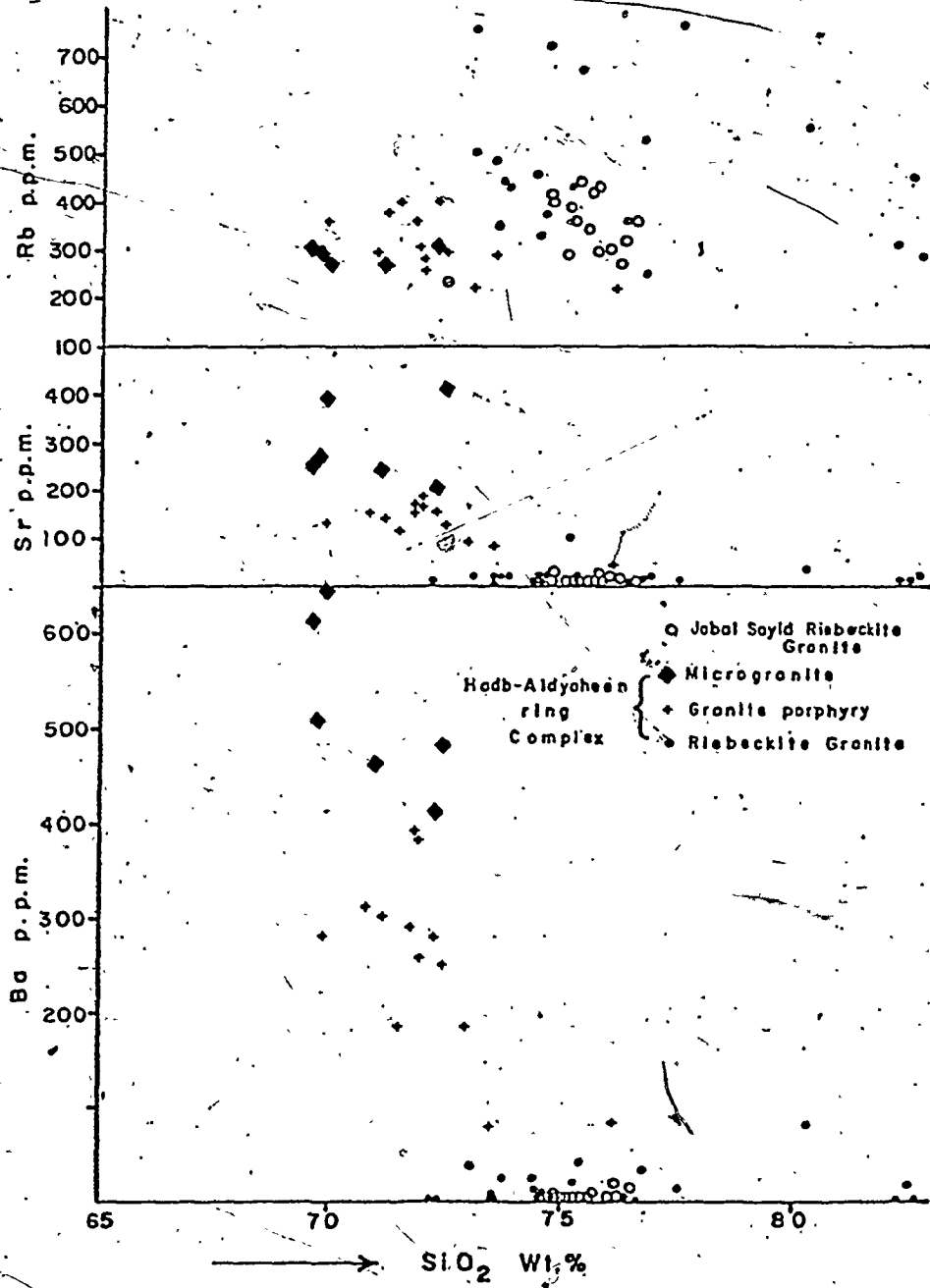


Figure 47. Ba, Sr and Rb (in ppm) versus SiO_2 (wt %).

Summary

1. Abundances and variations of trace elements in the non-peralkaline granites are normal and consistent with a differentiating granitic magma.
2. Peralkaline granites are significantly enriched in Nb, Zr, Y and Rb and depleted in Ba and Sr. Distribution of Nb, Zr, Y and Rb is erratic and does not have significant trends relative to paired major elements such as Rb against K, Nb against Ti or the alkalinity index. Ba and Sr are the only trace elements in these rocks which have a normal correlation relative to their common pair major element (Ca) and SiO_2 .

Yes'Kova and Yefimov (1970) suggested that large contents of Nb, Zr, Y, Rb and RE are always associated with alkali metasomatism. Depletion in Ba, Sr and Ca, and the enrichment in Rb have been considered by many workers (c.f. Marsh, 1975; Noble, 1972; Taylor, et al. 1956), as indicative of extreme fractionation in felsic rocks. Hence, it is possible that the peralkaline rocks of Hadb-Aldyaheen and Jabal Sayid are first products of extreme fractionation and subsequently modified by either contamination or alkali metasomatism or both.

3. There is no overlapping between the differentiation indices of the peralkaline granites of Hadb-Aldyaheen and Jabal Sayid and the non-peralkaline granites of Albari and Alse-Hairah. Also, there is a large difference in trace

element abundances between these two groups which can not be explained only as a result of magmatic differentiation. This suggests that neither the Hadb-Aldyaheen nor Jabal Sayid peralkaline granites need be regarded as particularly late stage differentiates amongst the Younger granites of the northeast corner of the Southern Hijaz quadrangle.

4. The distribution of trace elements in the peralkaline granites is possibly, as previously stated, caused by a metasomatic processes which was not only instrumental in formation of pure albite and almost pure microcline and soda-rich amphibole and pyroxene, but it also was able to effect the bulk of the rocks by enriching it in Nb, Y, Zr, and Rb.

CHAPTER 5

OXYGEN ISOTOPE AND FLUID INCLUSION STUDIES

5.1 Oxygen Isotope Relations

Analyses of oxygen isotopes of the whole rocks were done for fifteen samples, including granites of peralkaline composition from Hadb-Aldyahéen and Jabal Sayid together with granites of normal composition from the Hadb-Aldyaheen complex. The normal granites have an average $\delta^{18}\text{O}$ of 8.1‰, whereas the peralkaline granites have a $\delta^{18}\text{O}$ range from 10‰ to 16‰.

Taylor (1968) suggested that primary granite plutons generally have a narrow range of $\delta^{18}\text{O}$ values of ~8‰. Departures from primary values may occur by melting or assimilation of $\delta^{18}\text{O}$ -enriched material, or by exchange with a fluid reservoir. Taylor and Turi (1976) report $\delta^{18}\text{O}$ values of up to 16.4‰ for primary volcanic rocks where there is independent evidence for generation of magmas by melting or assimilation of sedimentary rocks, that would be $\delta^{18}\text{O}$ -enriched.

Igneous rocks may have departures from primary $\delta^{18}\text{O}$ values of ~8‰ by interaction with heated fluid reservoirs set into convective motion by the igneous heat source

Table 22. $\delta^{18}\text{O}$ whole rock in permille (SMOW)

	$\delta^{18}\text{O}\%$	Essential Mineralogy
JS 24,27	10.74*	Microcline, albite, quartz, riebeckite, aegirine.
JS 29	12.17	" " "
JS 46	14.62	" " "
HD 29	14.67	Microcline perthite, albite, quartz, aegirine, riebeckite, biotite
HD 37	14.79	" " "
HD 88	16.92	" " "
HD 87	13.81	Microcline, albite, quartz, riebeckite and aegirine
HD 41A	8.74	Microcline, albite, quartz, riebeckite and aegirine (contact zone)
HD 48	17.69	Microcline, albite, quartz, riebeckite and aegirine
HD 145B	6.19	Microcline, albite, quartz and aegirine (contact zone)
HD 22	8.26	Perthite, oligoclase, quartz and biotite
HD 27	7.94	" " "
HD 28	8.49	" " "
HD 52	7.86	" " "

*Z_o = ± 0.18%

(Taylor, 1968; Taylor, 1974; Wenner and Taylor, 1976; Muehlenbachs and Clayton, 1972). The magnitude of the depletion or enrichment from primary values of 8% depends on the $\delta^{18}\text{O}$ of the fluid reservoir, the temperature of exchange and the integrated water to rock ratio.

The anomalously heavy $\delta^{18}\text{O}$ values for the peralkaline granites may be accounted for by the aforementioned processes; i.e. melting or assimilation of high $\delta^{18}\text{O}$ precursors, and isotopic exchange with a fluid reservoir. Without data on mineral pair fractionations it is not possible to distinguish between these possibilities. The only other oxygen isotope study of peralkaline plutons is that by Borley et al. (1976) who reports normal $\delta^{18}\text{O}$ values of $8.1 \pm 0.2\%$ for the Kaffo albite-riebeckite peralkaline granite of Nigeria.

5.2 Fluid Inclusions

Quartz-fluorite veins are present in the peralkaline igneous rocks. The veins have a width in the centimetre to metre range, and lateral extent of tens of metres. Fluid inclusion studies were conducted on the minerals in an attempt to place quantitative limits on the physical and chemical properties of the hydrothermal solutions, from which the veins were precipitated (Methods, see Appendix A).

Results

Abundant primary and secondary fluid inclusions

are present in all the vein material examined. Primary inclusions range is from 80 μm to $<5 \mu\text{m}$: in some examples fluid had leaked from the larger cavities. Secondary fluid inclusions are present in planar arrays along healed microfractures. Measurements were made exclusively on primary fluid inclusions identified according to the criteria listed by Roedder (1967). These were all Ermakov type 4 inclusions, in which the liquid phase occupies greater than 50% of the total volume: inclusions homogenised in the liquid state. No inclusions were observed with two gaseous phases or with daughter minerals.

Filling temperatures for the quartz-fluorite veins are in the range of 300°C - 340°C , and fluid densities of the order of 0.8. These data may be interpreted with reference to the thermodynamic properties of aqueous systems, and aqueous alkali halide solutions, which are presented by Lemlein and Klevstov (1961). For a pure aqueous system of density 0.8 the boiling temperature is fixed at 250°C and 40 bars. The recorded data therefore imply that species are present in the solution which raise the boiling curve above that of pure water. A 10 wt. % NaCl aqueous solution has a boiling point fixed at 300°C and 80 bars, which may implicate a similar concentration of dissolved species in hydrothermal solutions from which the veins formed. Chemical analyses of many fluid inclusions have identified alkali halides as the most abundant dissolved species in solution (Roedder, 1972).

The filling temperatures represent the minimum temperature of vein formation. This is because a T increment is required to correct for fluid pressure. If the fluid pressure is assumed to be lithostatic rather than hydrostatic or some intermediate value, then the temperature correction for pressure would be +40°C at 2 km crustal depth, 500b; +100°C at 4 km, 1000b; and +150°C at 6 km, 1,500b (assuming a filling temperature of 300°C, and a 10 wt % NaCl aqueous solution).

CHAPTER 6

PETROGENESIS, TECTONICS, AND CONCLUSIONS

6.1 General Statement

Field, petrographic and chemical studies of younger granites in the northeast corner of the Southern Hijaz Quadrangle support their division into two main groups:

1) Non-peralkaline granites which include the Albari granite, Alse-Hairah granite and the biotite granite of Hadb-Aldyaheen.

2) Peralkaline granites which include the granite porphyry and the riebeckite granite of the Hadb-Aldyaheen ring complex and the riebeckite granite of Jabal Sayid.

The non-peralkaline granites are 600-650 my old. These granites are hypidiomorphic in texture, plagioclase ($An_{12}-An_{28}$), microperthite, quartz and biotite are the essential minerals. However, they are comparable to normal calc-alkaline granites (Nockolds, 1954) as to chemical composition and mineralogy.

The peralkaline granites are 500 to 550 my old and are high-level magmatic intrusions, the last granitic phase of the Pan-African thermal event (Brown, 1972) and the development of the Arabian Shield. Associated intrusions are pegmatite dykes containing radioactive minerals and

Table, 23. Averages of chemical compositions and CIPW norms of rocks forming Hadb-Aldyaheen ring complex and the riebeckite granite of Jabal Sayid.

	Biotite granite	Micro-granite	Granite Porphyry	Riebeckite granite	Riebeckite granite of Jabal Sayid
SiO ₂	71.70	70.85	71.82	75.06	75.51
TiO ₂	0.26	0.28	0.23	0.07	0.08
Al ₂ O ₃	14.71	13.63	12.79	11.32	10.99
ΣFe ₂ O ₃	2.04	2.40	2.91	3.70	3.61
MnO	0.06	0.06	0.06	0.04	0.04
MgO	0.52	0.33	0.34	0.01	0.006
CaO	1.59	1.72	1.17	0.16	0.18
Na ₂ O	4.44	5.26	5.81	5.37	4.81
K ₂ O	4.13	4.27	4.17	3.96	3.98
P ₂ O ₅	0.08	0.07	0.05	0.02	0.02
Q	26.22	21.64	21.94	30.09	33.63
Or	24.57	25.57	24.63	23.70	23.68
Ab	37.74	45.08	42.46	36.26	34.70
An	7.28	0.82	-	-	-
Ns	-	-	0.26	1.04	0.11
Co	0.27	-	-	-	-
Di	0.10	2.07	3.99	0.52	0.29
Hy	1.26	-	1.02	3.53	0.70
Wo	-	1.99	-	-	0.19
Ac	-	-	4.15	4.56	5.13
Mt	0.48	1.47	10.45	-	0.71
il	0.42	0.47	0.41	0.14	0.15
Hm	1.44	0.76	-	-	0.68
Sp	0.06	0.07	-	-	-
Ap	0.19	0.17	0.12	0.03	0.04

fluorite-bearing quartz veins. There is a notable absence of any contemporaneous more mafic plutons. The peralkaline rocks are hypidiomorphic to porphyritic. Riebeckite and aegirine are the principal mafic minerals which have crystallized late. Various workers (Kovalenko, et al., 1969; Bailey, 1969) regard the lower temperature paragenesis of riebeckite and aegirine with metamict zircon as indicating a hydrothermal or metasomatic origin. The plagioclase is almost pure albite and the K-spar is microcline (Or 96%) and microcline-perthite. Late growths and recrystallization of microcline and large quartz grains are evident.

These rocks have relatively large SiO_2 and total Fe; and relatively small Ca, Mg and Al abundances. Alkalis are not abnormally abundant for granitic rocks (Table 23) and in general major element oxides do not vary systematically with increasing SiO_2 , D.I., and D.I. + ac + ns. There is a significant enrichment in Nb, Zr, Y and Rb and depletion in Ba and Sr relative to crustal averages and to normal granites (Table 24). Distribution of most trace elements except Ba and Sr is erratic and has no trend relative to major element distribution. Also, there is no direct correlation between the contents of the trace elements and the alkalinity index (A.I.). Values of δO^{18} are + 10% to + 16%, which is considerably greater than the + 8% of the associated older non-peralkaline granites.

Table 24. Averages of trace element abundances of rocks forming Habb-Aldyaheen ring complex, and the riebeckite granite of Jabal Sayid compared to Taylor's (1966) averages.

	AV. Biotite Granite	AV. Micro- granite	AV. Granite Porphyry (573 my)	AV. Riebeck- ite G. (557 my)	AV. Jabal Sayid Riebeck- ite G. (505 my)	Crust (Taylor, 1966)	Syenite	Grano- diorite	Granite
Ba	703	536	265	16	5	425.	250	500	600
Nb	18	72	103	61	126	20	20	20	20
Zr	194	843	1336	1548	1653	165	150	140	180
Y	20	94	169	180	201	30	25	30	40
Sr	441	294	138	15	11	375	465	300	285
Rb	198	279	316	449	356	90	30	110	150
Rb/Sr	0.45	1.03	2.42	44	36	-	-	-	-
K/Rb	173	128	113	80	95	230	-	-	-
K/Sr	79	128	263	2808	3426	-	-	-	-
Ba/Sr	1.58	1.89	2.08	0.96	0.52	-	-	-	-
Ba/Rb	3.56	1.95	0.86	0.05	0.01	-	-	-	-
Zr/Nb	10.77	10.42	13.05	24.38	14.28	-	-	-	-
A.I.	0.80	0.98	1.08	1.18	1.11	-	-	-	-

The peralkaline granites therefore appear to be unrelated genetically to spatially related but older non-peralkaline granites of the northeast corner of the Southern Hijaz Quadrangle.

Peralkaline granites of the Arabian Shield and of the Southern Hijaz Quadrangle in particular, were compared to the Nigerian peralkaline granites of the once-contiguous African Shield, which have been well studied (Greenwood, 1951; Jacobson et al., 1958; Turner, 1963; Butler et al., 1962; Black, 1969; Bowden, Bowden et al., 1970; Fréeth, 1970; Brown and Bowden, 1973; Borely et al., 1976). They have the following differences summarized from Table 25.

1) Conventional differentiation trends with respect to major and trace elements are apparent for the Nigerian granites but not for the peralkaline granites of Southern Hijaz Quadrangle.

2) Nigerian granites have a complete and contemporaneous sequence from mantle fusion products to crustal melting products (Jacobson et al., 1958; Butler, 1962; Black, 1969; Bowden, 1970). There appear to be no mantle fusion products with peralkaline granites of the Southern Hijaz Quadrangle.

3) $^{18}\text{O}/^{16}\text{O}$ is + 10% to + 16% for the peralkaline granites of the Southern Hijaz Quadrangle but around + 8.1%, or similar to normal granites for the Nigerian peralkaline granites (Borley et al., 1976).

Table 25. Comparisons of the characteristic features

	Peralkaline granites of the North-east corner of the Southern Hijaz Quadrangle of the Arabian Shield	Peralkaline granites of Northern Nigeria
1. Age	Cambrian (500-570 my)	Mid-Jurassic (167-170 my)
2. Host rocks	Diorite and meta-volcano-sedimentary rocks of Precambrian age. Subduction zone rocks.	Gneissic-granitic basement complex of Precambrian age.
3. Igneous Sequence	Biotite granite, microgranite, granite porphyry, riebeckite-aegirine granite forming a ring complex, or small intrusions of riebeckite-aegirine granite.	Ca-amphibole-fayalite granite, granite porphyry, biotite albite granite (with tin mineralization) and riebeckite granite forming ring complexes and with gabbros.
4. Level of Emplacement	High level	High level intrusives associated with volcanic rocks (Rhyolite).
5. Mineralogy		
a) Essential minerals	Quartz, Albite (Ab 99%), Microcline (Or 94%), Microcline perthite, Riebeckite Aegirine and minor Biotite.	Similar (Ab 95%).
b) Accessories	Fluorite, Apatite, Spinel, Hematite, Magnetite, Ilmenite, Zircon and rare allanite.	Fluorite, Magnetite, Ilmenite, Monazite, Xenotime, Zircon, Thorite, Pyrochlore, Cryolite, Allanite and Astrophyllite.

cont...

Table 25 (cont.....)

6. Chemistry		
a) Major elements	Al ₂ O ₃ is low, MgO is extremely low, Cao generally less than one percent, Na ₂ O and K ₂ O are not particularly high for granites, slight excess of soda over potash. Acmite, sodium metasilicate appears in the norm, and no normative anorthite.	Similar
b) Trace elements	High content of Nb, Zr, Y and Rb. Low content of Ba and Sr. They have no correlation with the degree of alkalinity.	Same They have positive correlation with the alkalinity.
7. Alkalinity index	From 0.96 to 1.25.	From 0.9 to 1.15.
8. O ¹⁸ /O ¹⁶	High values (10-16%).	Similar to normal granites (8.1%).
9. Tectonic Feature	Post-tectonic, discordant to pre-existing structures, forming ring complexes or lacoliths.	Post-tectonic, discordant to pre-existing structures, forming individual or overlapping ring complexes.
10. Theories of origin	No previous hypothesis.	Produced by progressive melting of fayalite quartz monzonite under the influence of a linear zone of high heat flow from the mantle (Black, 1969; Bowden, 1970). Upper crustal melting (Bowden et al, 1970) followed by high level fractional crystallization (Fraeth, 1970).

cont.....

Table 25 (cont.....)

11. Differentiation Trend	Not well defined They appear to be genetically unrelated to the associated non-peralkaline younger granites.	Brown and Bowden, 1973, conclude that, simple partial melting of basement cannot give peralkaline magmas, and addition of alkali rich vapors to such a melt in order to furnish peralkaline magmas. Albitization is considered to have taken place close to the period of consolidation of the granite (Borley, et al., 1976).
		Well-defined. Ca-amphibole→biotite albite granite. Ca-amphibole granite→aegirine riebeckite granite→albite riebeckite granite. (Butler et al., 1962).

6.2 Tectonic Model

Plate tectonic models for the evolution of the Arabian Shield have been proposed (Greenwood and Brown, 1973; Al-Shanti and Mitchell, 1975; Greenwood, et al., 1976; Bakor, et al., 1976; Neary, et al., 1976; Nasseef and Gass, 1977; Gass, 1977; Marzouki and Fyfe, 1977; Marzouki, 1977; Frisch and Al-Shanti, 1977; Brown, 1978) and during a symposium on the evolution of the Arabian Nubian Shield held in Jeddah February 1978 at the Institute of Applied Geology, King Abdulaziz University, almost all workers compared the development of the Arabian Shield to Phanerozoic plate interaction. They especially commented on abundances in the Arabian Shield of granites, of mafic and ultramafic complexes as a possible ophiolitic suites. (Bakor, 1973; Neary, 1974; Garson and Shalaby, 1974; Bakor et al., 1976), mafic volcanic rocks and clastic sedimentary rocks deemed typical of accretionary and destructive plate margins. Most workers also agreed that magmas responsible for granites in the Arabian Shield were probably produced through partial melting of a subducted slab plus partial melting of the lower parts of continental crust.

The non-peralkaline granites of the Southern Hijaz Quadrangle are similar to younger calc-alkaline granites throughout the Arabian Shield (as described by Nasseef, 1971; Greenwood and Brown, 1973; Nasseef and Gass, 1977; Gass, 1977 and Marzouki and Fyfe, 1977.) and are

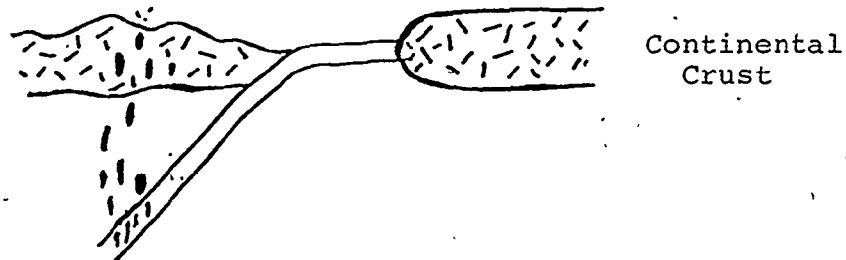
attributed to partial melting of lower crust above a subduction zone with some mixing of crustal material and andesitic magma derived from subducted material. By analogy the non-peralkaline granites of the Southern Hijaz Quadrangle are believed to have a similar origin. The chemistry of the two main types of this group, Albari and Alse-Hairah, suggests that the latter might belong to a different magma source, but most probably it represents a final differentiate of the former.

In spite of this consensus on the origin of the granitic rocks in the Arabian Shield, the current study suggests younger granitic rocks of peralkaline aspect, which are not associated with contemporaneous andesitic magmatism, require a variation on this origin and the following sequence of events is probable for peralkaline granites of the Southern Hijaz Quadrangle.

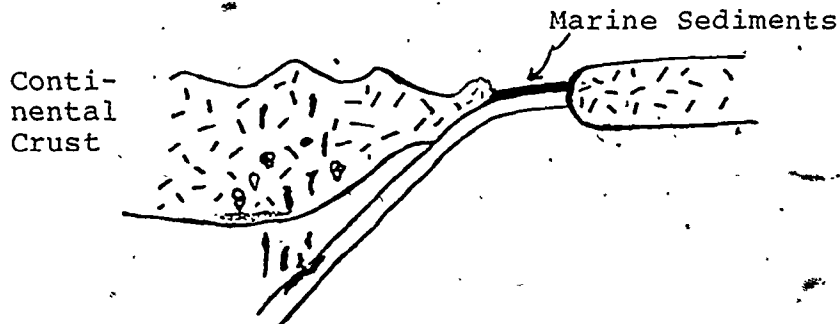
- 1) Subduction of oceanic crust beneath continental crust produces the voluminous andesites of the Arabian Shield (Fig. 48a).

- 2) Magmas of intermediate composition continue to intrude and extrude upon continental crust and to thicken it by underplating, adding plutons, and building large areas of volcanic accumulation (cf. Fyfe, 1978; Brown, 1977) (Fig. 48b).

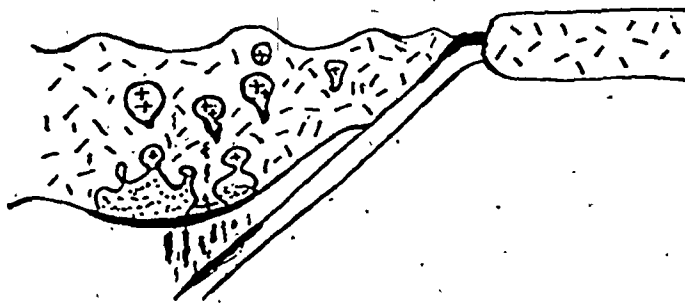
Crustal fusion at the base of thickened crust begins and its products mix with partial melts of subducted plate



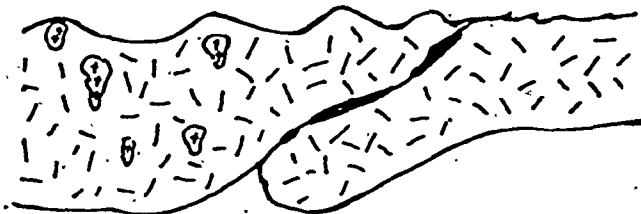
- a) Andesitic magma started to form from the descending ocean slab.



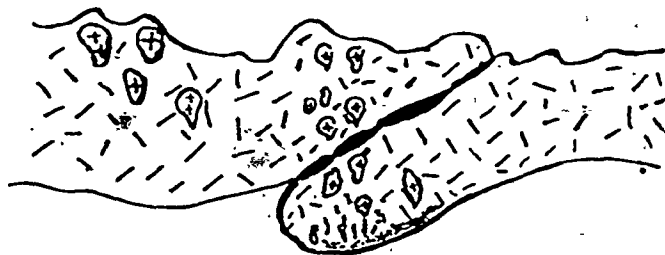
- b) Crustal loading and thickening. Marine sediments start to accumulate at the ocean crust.



- c) Because of heavy loading and high heat flow, the lower crust starts to melt to give the non-peralkaline granitic rocks; starting with the more basic and later will differentiate to give the more acidic.



- d) When the subducted layer is consumed, the continents will collide; some of the former ocean floor sediments will be trapped between the continents at the collision site.



- e) Overthickening of the partly subducted continental mass in the collision zone, leads to partial melting and the development of acidic granitic magma. Contamination by the trapped heavy sediments during the rise of the magma yields melt composition which is peralkaline.

Figure 48. A schematic model illustrating the tectonic environment and the generation of different granitic magmas.

to produce granitic magmas. These granitic magmas accumulate and rise to form plutons (Fyfe, 1970) (Fig. 48c). The $^{87}\text{Sr}/^{86}\text{Sr}$ systematics of these granites as presented by Greenwood et al. (1976) and Fléck (1978), indicate a heavy mantle imprint in their origin (cf. Armstrong, et al., 1977; Fyfe, 1978).

3) Subduction continues until all oceanic crust is underthrust and consumed and the continents collide (Fig. 48d). In this model we suggest that ocean sediments may be dragged under the stationary continental block and the total crustal thickness is approximately doubled. This is a Himalayan-type collision of continents which can produce granite magmas with large $^{87}\text{Sr}/^{86}\text{Sr}$ from the thickened crust (Hamet and Allegre, 1976; Dewey and Burke, 1973). Also, Brown and Hennessy (1978) have suggested that normal crust 30-40 km will not be sufficiently hot at its base to melt, and doubling the thickness of the crust will cause melting (Fig. 48e).

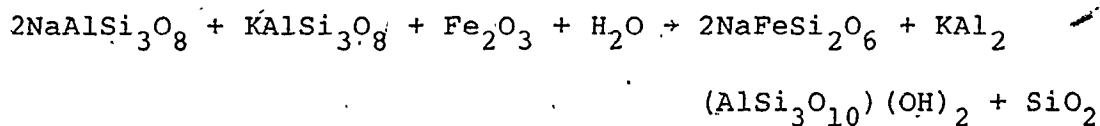
In essence, the thickened crust can produce a late granitic fraction which might be contaminated by trapped marine sediments such as chert, red marine clays which have a large Fe_2O_3 content and heavy oxygen content, or evaporites which similarly have a large heavy oxygen content as well as a distinct salinity (Fig. 48e). The considerable saline water content, heavy oxygen, large Fe_2O_3 content and probably anomalous radioactivity could contaminate a granitic magma to the point of peralkalinity.

There is no evidence of fractionation leading to peralkaline rock products in the thesis area, and it is unreasonable to resort to some peralkaline magma of unknown source as a final explanation. On the other hand, in support of the contention of contamination by Fe_2O_3 rich rocks producing peralkalinity, there is the work of Fyfe and Brown (1972) indicating that if a magma is derived from, or contaminated by, rocks rich in Fe_2O_3 , a peralkaline liquid may result. The following table lists microprobe analyses of glasses obtained in melting Fe_2O_3 rich crustal rocks. They have a peralkaline trend.

	T P	710°C 5 kilobars	740°C 5 kilobars	780°C 5 kilobars
SiO_2		74.88	73.62	73.05
Al_2O_3		13.78	13.53	12.84
Fe_2O_3		2.85	3.42	3.86
MgO		0.01	0.04	0.06
CaO		0.40	0.54	0.77
Na_2O		3.79	4.29	5.18
K_2O		4.24	4.48	4.14
MnO		0.01	0.02	0.01
TiO_2		0.04	0.06	0.09

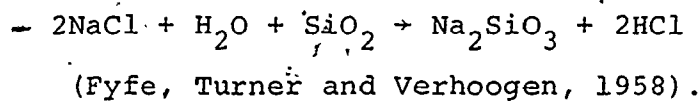
(Fyfe and Brown, 1972)

A possible reaction might be as follows:



Similarly contamination could be affected by contact of a granitic melt with hot saline solutions derived from trapped evaporites. Evaporites might well have been involved in the closing of the ocean basin and the eventual continental collision postulated in the present model.

A possible reaction might be as follows:



This latter process is now apparently operative at White Island, New Zealand (Giggenbach et al., 1977).

Unfortunately, the available information does not permit distinction between contamination by sediments or, contamination by hot saline solution. However, work in progress on the $^{18}\text{O}/^{16}\text{O}$ of individual minerals will hopefully resolve this problem.

At the present time there is no adequate explanation for the distribution of Nb, Zr, Y and Rb in the peralkaline rocks of the Southern Hijaz Quadrangle although accumulation by igneous fractionation seems improbable on the basis of the data. Concentration, or impoverishment of Ba and Sr, could be associated with partial melting of crustal rocks and subsequent contamination, or it might

be related to metasomatism by residual fluids during final crystallization or even shortly after crystallization. This late metasomatism is supported by fluid inclusion data as well as mineralogy and texture of the rocks which point to a low temperature recrystallization after primary crystallization of the contaminated granitic magma.

APPENDICES

APPENDIX A - METHODS

APPENDIX B - ELEMENT ABUNDANCES

APPENDIX C - MICROPROBE ANALYSES

APPENDIX A

METHODS

APPENDIX A
ANALYTICAL METHODS

1. X-ray Fluorescence Analysis

Unweathered bulk samples were crushed in a jaw crusher and then pulverized for 15 to 25 seconds in a Bleuler Mill. Powder and fused pellets were made from the powder of each sample according to the method of Norrish and Chappell (1967) and Norrish and Hutton (1969), respectively.

All analyses were carried out with a Philips PW1450 automated X-ray fluorescence spectrometer. Analytical conditions for all elements are presented in Table A1. The chemical compositions were obtained using the programme developed by Norrish and Hutton (1969) run on a Cyber 73 computer. The analyses are accurate to within 1% of the amount present for major elements except Na and to within 10% of the amount present for trace elements and Na.

2. Electron Microprobe Analysis

All analyses were carried out using M.A.C. (model 400) electron microprobe. The excitation voltage for all elements was 15 Kv. Initially the chemical compositions were obtained from Rucklidge's Probe Data Reduction

Table A1: Analytical Conditions for X-ray
Fluorescence Analysis

Element	Pellet	Radiation	Kv Ma	Line Measured	Crystal Used	Standard Used
Si			60 40		PET	
Ti			40 30		LiF-200	
Al		Cr			PET	
Fe					LiF 200	
Mn	fused	W				FS 72
Mg					ADP	
Ca				K α	GE	
K		Cr	60 40			
S					PET	
P					GE	
Na					TLAP	GA
Ba				L α		AGV
Sr	powder					AGV
Rb		W			LiF 200	GSP
Y				K α		VSN
Nb						VSN
Zr						AGV

run on a Cyber 73 computer. However, the majority of the analyses were obtained from the Magic programme (Colby, 1968) run on a PDP 11 computer. The analyses are accurate to within 5% of the amount present for the major elements and with a detection level of 0.05% of the total sample for minor elements.

3. Determination of FeO

All chemically analyzed whole rock samples of Albari, Alse-Hairah and Jabal Sayid granites were analyzed for FeO using the method of Wilson (1955). In this method 0.25g of sample plus 0.05g of ammonium metavanadate (AMV) were dissolved in 40% HF. The AMV quantitatively oxidizes the FeO in the sample. This solution is titrated against standardized ferrous ammonium sulfate solution (FAS). The excess AMV in the solution reacts quantitatively with the FAS. Therefore the amount of FeO in the sample is equal to the amount of initial AMV minus the amount of AMV titrated. The analyses are accurate to within 5% of the amount of FeO present. FeO values for Hadb-Aldyaheen granitic rocks were calculated according to Irvine and Baragar (1971) calculation.

4. Determination of Volatiles

The total volatiles for most of the chemically analysed samples were determined using the method of loss

on ignition (LOI). About 2g of sample was weighed, ignited at about 1100°C in a porcelain crucible, cooled in a desiccator and reweighed. The weight loss was assumed to be due to volatile loss (= LOI). The analyses are accurate to within 10% of the amount present.

5. Oxygen Isotope Methods

Fluorination

Introduction

Oxygen isotope abundance is derived from high precision mass spectrometric determination of isotopic composition of carbon dioxide (CO_2), which is a convenient gas to handle and lies in a clean part of the mass spectrum. Whole rock powder, silicate and metal oxide minerals are reacted with a fluorinating agent to extract oxygen, which is then converted to CO_2 . It is important that the extraction and conversion are reproducible and quantitative in order that kinetic isotope effect (KIE) do not swamp the small equilibrium fractionations which are to be measured.

A mass of mineral sample which is sufficient to yield about 100 micromoles of oxygen (O_2) is weighed into a steel container, and, together with a nickel reaction bomb, placed in a dry box for 24 hours. The precise mass used depends on the mineral type, but is generally about 10 gm.

The sample is loaded into the bomb in a dry box, because fluorinating agents react with atmospheric water to yield contaminant oxygen, and atmospheric water may be absorbed into nickel fluoride armor. The bombs are then sealed onto the vacuum extraction line, which is of conventional design, essentially as described by Taylor and Epstein (1962), but of all stainless steel construction, and with a vacuum capacity of 10^{-5} Torr.

Aliquots of purified bromine pentafluoride (BrF_5) are frozen down in vacuo into each of the four bombs, and reacted with the mineral at 550°C for 12 hours. Oxygen is separated from excess BrF_5 and other reaction products such as Br , BrF_3 , SiF_4 , etc. in a series of liquid nitrogen cold traps.

Oxygen is converted to CO_2 by reaction over a hot carbon rod with platinum catalyst. This procedure is done in a series of aliquots in order to avoid KIE, because, as for the oxygen extraction of fluorination, conversion of O_2 to CO_2 , follows the Rayleigh distillation equation; and large kinetic fractionations may occur unless the reaction goes to completion.

The CO_2 yield is measured in a mercury manometer and compared with the theoretical yield calculated from the mineral chemical formula. Isotopic results on any sample from which the yield was not $100\% \pm 1\%$, are treated with caution, and repeat runs conducted. The CO_2 is dried in

a 2-butoxyethanol solid carbon dioxide cold trap, and stored in stainless steel gas sample cylinders prior to mass spectrometry.

Mass Spectrometry

The instrument at UWO which is used for high precision isotopic analysis of CO_2 is a Micromass boze, Neir type 12 cm radius, 90° sector, double collecting mass spectrometer.

The abundance of carbon and oxygen isotopes are such that in CO_2 prepared from natural materials the relative proportions of the molecular species $m/e = 44, 45,$ and 46 are approximately 98.42%, 1.17%, and 0.40% respectively. The requirement of the mass spectrometer, therefore, is to measure ratios of about 1:100 ($45/44$) and 1:250 ($46/44 + 45$) with errors of less than 0.01%. (Beckinsale and others, 1973b).

CO_2 pressure in the sample and standard reservoirs are equalised to $>1\%$ using hollows and the CO_2 introduced into the spectrometer through two separate viscous leaks. The sample and standard are alternatively admitted to the ion source using magnetic changeover valves. m/e Ratios are calculated from 100 second counting periods, using a capacitor integrating system. (Beckinsale and others, 1973a).

The mass spectrometer is tuned firstly for the 46 ratio, from which the $\text{O}^{18}/\text{O}^{16}$ result is calculated. The 45 ratio is occasionally measured, primarily as a sensitive

check on the presence of water, and also for computing a small correction to the 46 ratio (Craig, 1957).

To convert results to the Standard Mean Ocean Water (SMOW) scale working standards CMV (18.54%) and Caltech Rose Quartz (8.24%), are used. A working standard is run approximately every 12 samples. Isotope ratios expressed relative to one standard (X) may be expressed relative to another standard (Y) using the expression

$$\delta(Sa-Y) = \delta(Sa-X) + \delta(X-Y) + 10^{-3} \delta(Sa-X)(X-Y)$$

where $\delta(Sa-Y)$ is the isotopic composition of the sample (Sa), relative to the standard (Y) etc., and all the values are in permil (Craig, 1961).

Errors which are attributable to fluorination and conversion amount to $\pm 0.09\%$: the mass spectrometer is accurate to $\pm 0.02\%$, giving a total error in the results of $\pm 0.1\%$. (Analyst, Dr. R. Kerrich).

6. Fluid Inclusion Studies

Analytical Methods

Double-polished plates of 50 to 1000 μm in thickness were prepared for microscopy on fluid inclusions. Filling temperature measurements were made using a Reichart Kofler microscope heating stage. Temperatures were recorded on a mercury thermometer calibrated against the fusion point of high purity substances located adjacent to the sample. A heating rate of $2^\circ\text{C}/\text{minute}$ was used throughout the homo-

genisation studies. Replicate measurements on individual inclusions were generally reproducible to $\pm 1^\circ\text{C}$. The overall accuracy of filling temperature data is about $\pm 5^\circ\text{C}$.

Determinations of fluid density were made from photomicrographs of geometrically regular inclusions using the method of Roedder (1967, p. 565). If the relative volumes of the gaseous and liquid phases are measured at room temperature, then the density of the originally homogeneous fluid may be calculated. (Analyst Dr. R. Kerrich).

APPENDIX B

ELEMENT ABUNDANCES

Major wt%, Trace ppm, Norms CIPW

Table 18. Albari granite

Sample #	Alb 9	Alb 11	Alb 13E	Alb 26	Alb 54	Alb 82	Alb 86	Alb 87	Alb 89	Alb 18	Alb 39B	Alb 77	Alb 34C	Alb * 58
SiO ₂	64.86	68.22	71.68	70.33	69.23	68.12	68.69	69.95	68.78	69.99	67.96	72.10	74.87	65.67
TiO ₂	0.27	0.31	0.22	0.25	0.31	0.32	0.31	0.27	0.34	0.26	0.36	0.18	0.17	0.005
Al ₂ O ₃	15.63	15.91	15.02	15.75	15.83	16.43	15.96	15.55	15.92	15.02	15.07	14.72	12.84	14.50
Fe ₂ O ₃	1.13	0.95	1.42	1.26	1.45	1.85	1.46	1.31	1.56	1.52	1.73	0.85	1.00	0.37
FeO	1.83	2.45	1.12	1.53	1.99	1.54	1.94	1.88	1.94	1.37	1.67	1.11	1.03	
MnO	0.06	0.10	0.06	0.07	0.09	0.10	0.10	0.07	0.11	0.08	0.07	0.06	0.05	0.05
HgO	0.94	1.06	0.61	0.66	1.00	0.98	0.95	1.04	1.10	0.95	1.23	0.55	0.52	0.03
CaO	2.91	2.92	2.45	2.65	2.99	3.32	3.18	2.96	3.00	2.88	3.36	1.92	1.62	1.06
Na ₂ O	4.00	4.25	3.91	4.15	3.92	4.42	4.06	3.68	4.28	3.50	3.51	3.75	3.59	5.19
K ₂ O	3.33	2.64	3.36	3.31	2.94	2.51	2.63	3.12	2.71	3.41	2.96	3.69	3.84	2.58
P ₂ O ₅	0.1	0.14	0.14	0.12	0.13	0.16	0.15	0.12	0.16	0.13	0.15	0.09	0.03	0.02
L.O.I.	0.23	0.62	0.21	0.31	0.20	0.26	0.26	0.24	0.20	0.49	0.72	0.22	0.21	0.51
Total	100.35	99.58	100.20	100.50	100.07	99.99	99.79	100.17	100.13	99.59	98.79	98.87	99.76	100.01
O	25.75	24.81	29.85	26.66	26.71	24.3	26.42	28.12	24.71	29.17	26.85	31.43	34.94	
Of	19.59	15.69	19.75	19.45	17.39	14.87	15.63	18.45	15.92	20.33	18.02	22.13	22.79	
Ab	33.59	36.31	32.82	35.00	33.21	37.49	34.55	31.15	36.00	29.88	30.59	32.2	30.61	
An	13.73	13.65	11.16	12.35	14.01	15.47	14.89	13.91	14.54	13.57	16.17	9.08	7.61	
Cor	0.47	1.13	1.01	0.80	1.07	0.79	1.01	1.02	0.84	0.65	0.35	0.84		
Di	-	-	-	-	-	-	-	-	-	-	-	-	0.22	
Hy	4.44	6.08	2.61	3.17	2.08	9.61	3.41	4.42	4.65	4.68	3.37	4.36	2.59	
Ht	1.64	1.39	2.04	1.82	2.1	2.69	2.13	1.90	2.26	2.22	2.58	1.24	1.46	
Il	0.55	0.58	0.43	0.47	0.59	0.61	0.59	0.51	0.69	0.5	0.7	0.33	0.32	
En														
Rut														
AP	0.24	0.36	0.33	0.28	0.31	0.38	0.36	0.28	0.40	0.31	0.37	0.22	0.07	
Cr	102	62	51	66	89	71	51	61	58	10	25	9	40	
Ba	573	440	564	567	492	355	601	453	616	642	556	374		
Ni	25	9	6	11	18	14	6	3	4	2	13	1	2	
Nb	12	12	12	12	11	12	11	10	10	8	13	11		
Sr	137	129	136	140	128	133	126	124	123	110	158	107	108	
Y	22	27	27	27	22	22	29	27	28	12	13	14	37	
Sr	424	631	419	416	494	540	501	484	525	407	385	318	223	
Rb	96	63	104	101	80	70	75	88	64	104	108	148	97	
Rb/Sr	0.23	0.10	0.25	0.24	0.16	0.13	0.15	0.18	0.12	0.26	0.28	0.47	0.43	
K/Rb	289	348	269	272	305	297	291	294	352	272	228	207	329	
K/Sr	65	35	67	66	49	39	44	54	43	70	68	96	143	
Ba/Sr	1.35	0.70	1.35	1.36	0.99	0.81	0.71	1.24	0.86	1.51	1.67	1.75	1.67	
Ba/Rb	5.97	6.98	5.42	5.61	6.15	6.26	4.73	6.83	7.08	5.92	5.94	3.76	3.86	
Zr/Nb	11.4	10.75	11.33	11.67	11.64	11.08	10.5	11.27	12.30	11.00	19.75	8.23	9.82	
D.I.	78.93	76.81	82.42	81.11	77.31	76.66	76.59	77.72	76.63	79.38	75.46	85.76	88.24	
A.I.	0.65	0.61	0.66	0.78	0.61	0.61	0.60	0.61	0.61	0.63	0.60	0.71	0.66	

*Muscovite granite

Table 2B. Alse-Hairah Granite

207

Sample #	Als 4	Als 7	Als 11B	Als 12	Als 14	Als 15	Als 29	Als 37	Als 46
SiO ₂	69.58	68.22	69.07	71.50	69.67	71.99	71.81	77.80	73.16
TiO ₂	0.33	0.42	0.34	0.30	0.43	0.30	0.40	0.10	0.32
Al ₂ O ₃	15.50	15.90	15.9	14.70	15.09	14.00	14.56	12.27	13.92
Fe ₂ O ₃	1.69	2.32	1.96	1.44	2.09	1.40	1.65	0.71	1.72
FeO	0.34	0.06	0.18	0.76	0.47	0.37	0.45	0.13	0.11
MnO	0.05	0.04	0.03	0.06	0.07	0.05	0.05	0.02	0.05
MgO	0.47	0.64	0.49	1.24	0.78	0.34	0.70	0.05	0.35
CaO	1.39	1.42	1.02	1.30	1.59	1.38	1.48	0.50	1.12
Na ₂ O	4.40	4.51	4.66	4.47	4.71	4.38	4.06	2.82	4.24
K ₂ O	5.22	5.41	5.56	4.32	4.63	4.59	4.84	5.84	4.61
P ₂ O ₅	0.13	0.14	0.14	0.15	0.16	0.10	0.14	0.04	0.13
L.O.I.	0.37	0.38	0.41	0.30	0.32	0.32	0.30	0.11	0.26
Total	99.47	99.46	99.78	100.45	100.01	99.22	100.44	100.39	99.99
Q	21.05	17.96	18.92	24.45	20.55	26.45	25.61	37.92	28.39
Or	21.12	32.26	33.11	25.21	27.48	27.47	28.58	34.42	27.32
Ab	37.55	38.58	38.88	38.09	40.03	37.47	34.27	23.76	35.98
An	6.07	6.11	4.14	5.38	6.39	4.63	6.44	2.21	4.58
Cor	0.34	0.33	0.39	0.59	-	-	0.23	0.49	0.25
Di	-	-	-	-	0.35	1.24	-	-	-
Hy	1.16	1.59	1.2	3.34	1.77	0.28	1.83	0.12	0.87
Mt	0.34	-	-	1.76	0.47	0.49	0.78	0.23	-
Il	0.61	0.21	0.45	0.60	0.82	0.58	0.77	0.19	0.32
Hm	1.46	2.34	1.97	0.21	1.77	1.08	1.13	0.56	1.72
Rut	-	0.29	0.11	-	-	-	-	-	0.15
AP	0.31	0.34	0.33	0.37	0.38	0.24	0.35	0.09	0.31
Cr	7	6	7	145	60	7	69	9	7
Ba	795	717	904	416	523	581	544	278	523
Ni	5	2	4	73	24	4	34	3	7
Nb	19	20	16	22	22	24	20	6	24
Zr	193	295	265	196	236	182	153	91	196
Y	7	12	6	9	14	13	6	-	11
Sr	514	447	540	395	460	405	390	201	388
Rb	138	108	118	156	167	160	155	138	163
Rb/Sr	0.27	0.24	0.22	0.39	0.36	0.40	0.40	0.70	0.40
K/Rb	314	414	392	230	230	238	261	352	234
K/Sr	84	100	86	91	83	94	104	242	98
Ba/Sr	1.55	1.6	1.67	1.05	1.14	1.43	1.39	1.38	1.35
Ba/Rb	5.76	6.64	7.66	2.67	3.13	3.63	3.51	2.01	3.2
Zr/Nb	10.15	14.75	16.56	8.91	10.73	7.58	7.65	15.17	8.17
D.I.	89.71	88.8	90.9	87.75	88.07	91.46	88.46	96.1	91.69
A.I.	0.83	0.84	0.85	0.82	0.85	0.88	0.82	0.89	0.86

Table 3B. Jabal Sayid Riebeckite Granite

Sample #	JS4	JS6	JS13	JS19	JS21	JS24	JS27	JS28	JS29	JS34	JS37A	JS40	JS44	JS46A	JS46B	JS47B
SiO ₂	75.68	75.58	74.50	75.59	76.47	75.37	75.26	75.05	74.68	75.12	76.16	75.16	76.24	75.56	77.42	70.51
TiO ₂	0.09	0.05	0.15	0.07	0.09	0.04	0.10	0.06	0.09	0.06	0.05	0.06	0.07	0.08	0.22	0.25
Al ₂ O ₃	10.98	11.16	11.43	11.32	10.55	10.85	11.13	11.07	10.98	10.60	10.96	11.02	11.27	10.64	8.85	12.91
Fe ₂ O ₃	2.76	3.89	3.17	3.02	3.00	3.62	3.60	3.44	1.84	3.78	3.27	3.29	2.45	3.67	3.87	2.30
P ₂ O ₅	0.48	0.03	1.74	0.20	0.22	1.53	1.29	0.38	1.76	0.08	0.25	0.38	0.74	0.27	0.77	0.35
MnO	0.07	0.05	0.05	0.04	0.01	0.04	0.05	0.05	0.05	0.04	0.03	0.05	0.04	0.05	0.06	0.05
MgO	10.04	-	-	0.01	-	-	-	-	0.03	-	-	-	-	-	0.06	0.42
CaO	0.22	0.13	0.20	0.28	0.07	0.06	0.15	0.22	0.10	0.16	0.14	0.28	0.28	0.19	0.48	1.49
M ₂ O	4.76	4.95	4.79	5.01	4.14	5.15	4.87	5.08	5.14	4.74	4.23	4.81	4.76	4.84	3.90	7.32
K ₂ O	3.80	4.04	4.46	3.98	3.61	3.68	3.93	3.83	4.01	3.67	4.81	3.80	4.15	3.91	3.71	2.41
P ₂ O ₅	0.01	0.02	0.03	0.02	0.03	-	-	0.01	0.01	0.02	0.02	0.02	0.02	0.02	0.01	0.02
L.O.I.	0.64	0.32	0.32	0.24	0.73	0.63	0.51	0.57	0.63	0.65	0.21	0.63	0.31	0.73	0.89	1.61
Total	99.90	100.2	99.92	100.18	98.90	99.14	99.91	99.75	99.32	98.91	100.12	98.49	100.32	99.95	99.14	99.45
O	34.29	32.84	29.79	32.8	32.45	33.6	32.53	32.56	31.53	35.34	34.46	33.93	33.33	34.36	42.12	19.27
Cr	22.62	23.9	26.46	23.53	11.73	22.07	23.36	22.82	24.01	22.07	28.45	22.71	24.52	23.29	22.29	14.53
Ab	35.57	34.95	34.04	36.09	14.00	35.85	35.58	35.91	34.61	34.7	28.62	35.93	34.86	33.22	25.28	56.05
Ms	-	-	-	-	0.71	-	-	-	0.78	-	-	-	-	-	-	0.33
Di	0.9	-	0.72	0.05	-	0.27	0.67	-	0.39	-	-	-	1.13	-	1.94	2.92
Hy	0.2	-	2.53	-	-	2.72	1.24	-	3.09	-	-	-	0.06	-	-	-
Wo1	-	0.22	-	0.5	0.07	-	0.45	-	-	0.31	0.24	0.53	-	0.34	0.06	1.57
Ac	4.4	6.15	5.81	5.57	0.77	4.7	5.17	6.54	5.39	5.39	5.46	4.61	4.77	7.10	7.28	6.79
Mt	1.83	0.12	0.25	0.57	0.49	-	1.26	1.22	-	0.22	0.76	1.23	1.16	0.81	0.58	-
Il	0.17	0.10	0.29	0.13	0.17	0.08	0.19	0.11	0.17	0.12	0.1	0.12	0.13	0.15	0.42	0.48
Hs	-	-	-	-	0.7	2.45	-	0.36	-	1.83	0.86	0.89	-	0.69	-	-
Ap	0.02	0.05	0.07	0.03	0.07	-	-	-	0.02	0.02	0.05	0.05	0.05	0.05	0.02	0.05
Gr	4	220	166	75	13	4	62	2	3	1	5	2	5	62	2	5
Ba	15	3	-	4	16	1	-	2	-	21	1	1	3	13	127	-
Ni	35	116	83	43	14	8	29	16	1	44	2	8	8	7	45	9
Nb	135	109	113	100	393	63	137	124	112	220	110	135	83	135	138	153
Kr	3797	953	2387	1320	1719	745	3798	2683	1037	2402	1059	749	1013	1458	3820	607
Y	528	219	136	112	172	64	118	199	85	708	95	104	94	176	152	101
Zr	15	11	11	13	9	7	14	10	20	9	7	12	7	6	18	189
Rb	426	419	414	299	382	294	439	386	389	285	312	353	267	344	463	188
Rb/Sr	28	38	38	23	40	42	31	39	19	32	45	29	38	57	26	1
K/Nb	74	80	89	111	83	104	74	82	86	107	128	90	129	94	67	106
K/Sr	2100	3055	3364	2566	3372	4371	2329	3180	1665	3389	5700	2633	4914	5400	1711	112
Ba/Sr	1	0.27	-	0.31	1.78	0.14	-	-	0.1	-	3	0.08	0.14	0.5	0.72	0.71
Ba/Nb	0.04	0.007	-	0.01	0.04	0.003	-	-	0.005	-	0.07	0.003	0.008	0.01	0.03	0.67
Zr/Nb	20.72	8.74	21.12	13.2	8.91	11.83	21.04	21.64	9.44	10.92	9.63	5.55	12.2	10.8	16.57	8.97
D.I.	92.48	91.69	90.38	92.42	95.98	91.53	91.47	91.30	90.15	92.11	92.54	92.58	92.70	90.87	84.65	87.86
A.I.	1.09	1.12	1.11	1.12	1.02	1.15	1.10	1.13	1.17	1.11	1.11	1.09	1.09	1.15	1.18	1.13

Table 4B. Biotite Granite and Microgranite of Hadd-
Aldyaheen Ring Complex

Sample #	Biotite granite				Micro-granite						
	HD22	HD27	HD28	HD52	HD53A	HD80	HD128	HD135	HD157	HD174	132B
SiO ₂	71.79	72.16	72.37	70.49	71.12	69.55	69.74	69.88	72.49	72.32	71.97
TiO ₂	0.30	0.23	0.24	0.28	0.24	0.31	0.30	0.32	0.28	0.25	0.17
Al ₂ O ₃	14.71	14.81	14.1	15.20	13.42	13.90	13.99	14.00	13.13	13.36	13.16
Fe ₂ O ₃	2.53	1.76	1.81	2.07	2.88	2.31	1.61	2.38	2.83	2.37	2.09
MnO	0.05	0.04	0.12	0.04	0.07	0.07	0.10	0.05	0.04	0.05	0.05
MgO	0.59	0.43	0.48	0.58	0.48	0.08	0.27	0.52	0.36	0.25	0.23
CaO	1.40	1.66	1.51	1.8	1.32	2.30	2.47	1.90	0.96	1.35	1.06
Na ₂ O	4.54	4.44	4.37	4.41	5.06	9.39	5.13	5.63	5.13	5.22	5.56
K ₂ O	4.02	4.15	4.14	4.24	4.04	4.93	4.56	4.33	4.14	4.13	5.09
P ₂ O ₅	0.09	0.07	0.05	0.11	0.08	0.08	0.07	0.10	0.04	0.06	0.04
L.O.I.	0.23	0.25	0.36	0.52	0.50	0.83	1.30	0.80	0.60	0.54	0.53
Total	100.25	99.93	99.55	99.74	99.21	99.24	99.54	99.91	100.00	99.90	99.95
Q	26.36	26.51	27.63	24.38	24.06	18.8	19.33	17.87	25.46	24.34	21.1
Or	23.75	24.59	24.67	25.25	24.24	26.64	27.47	25.85	24.58	24.62	30.25
Ab	38.41	37.66	37.28	37.61	43.46	46.42	44.26	48.14	43.64	43.64	44.57
An	6.36	7.80	6.69	8.28	1.45	0.63	1.74	0.16	0.38	0.64	-
SM	-	-	-	-	-	-	-	-	-	-	0.52
Co	0.56	0.16	-	0.35	-	-	-	-	-	-	-
Di	-	-	0.35	-	3.45	0.44	1.48	2.83	2.88	1.36	2.35
Ry	1.47	1.07	1.04	1.46	-	-	-	-	-	-	-
Wo	-	-	-	-	0.16	4.14	3.25	2.13	0.63	1.67	0.92
Ht	1.65	-	-	0.26	2.55	0.96	-	1.05	2.6	1.64	4.86
Il	0.57	0.15	0.41	0.54	0.44	0.6	0.22	0.62	0.54	0.42	0.32
Hm	0.66	1.73	1.75	1.62	-	1.18	1.64	1.12	-	0.61	-
Sp	-	0.15	0.07	-	-	-	0.44	-	-	-	-
AP	0.21	0.17	0.12	0.26	0.19	0.19	0.17	0.24	0.10	0.14	0.1
Cr	9	7	25	9	7	10	10	10	36	23	5
Ba	590	758	597	867	458	510	505	653	580	412	229
Ni	13	9	2	4	24	7	10	8	23	17	5
Nb	22	15	18	17	161	64	29	30	37	109	48
Zr	245	169	172	189	2530	669	280	334	387	856	369
Y	23	16	22	18	271	68	32	43	48	103	79
Sr	376	469	408	511	242	249	276	385	407	205	171
Rb	196	199	206	192	272	297	295	268	237	306	558
Rb/Sr	0.5	0.4	0.5	0.4	1.1	1.2	1.07	0.7	0.6	1.5	3.26
K/Rb	170	172	167	183	123	124	128	134	145	112	75.81
K/Sr	89	73	84	69	138	147	137	93	84	167	247
Ba/Sr	1.57	1.62	1.46	1.69	1.89	2.45	1.83	1.70	1.43	2.01	1.34
Ba/Rb	3.01	3.81	2.90	4.52	1.68	2.05	1.71	2.44	2.44	1.35	-
Zr/Nb	11.14	11.27	9.56	11.12	15.71	10.45	9.66	11.19	10.46	7.85	7.69
D.I.	88.52	88.76	89.58	87.24	91.76	1486	91.06	91.86	93.08	93.52	90.93
A.I.	0.80	0.79	0.83	0.78	8.96	0.98	0.96	0.99	0.99	0.98	1.11

Table 5B. Granite Porphyry of Hadb-Aldyaheen Ring.
Complex

Sample #	HD8	HD9	HD19A	HD29	HD30	HD37	HD66	HD88	HD100	HD125	HD150	HD170A	HD147	HD120B
SiO ₂	72.51	71.99	70.75	72.32	71.81	70.91	71.86	73.48	72.98	70.98	71.96	71.18	69.87	71.46
TiO ₂	0.26	0.22	0.29	0.19	0.18	0.25	0.25	0.20	0.2	0.25	0.22	0.20	0.19	0.23
Al ₂ O ₃	12.30	12.70	13.76	12.27	12.68	12.98	12.38	12.48	12.59	13.02	13.26	12.88	14.03	13.22
Fe ₂ O ₃	3.59	2.97	2.53	3.03	2.74	2.75	3.40	3.09	2.91	2.58	2.62	3.10	2.23	2.46
MnO	0.06	0.05	0.05	0.05	0.06	0.06	0.05	0.05	0.05	0.11	0.06	0.06	0.04	0.05
MgO	0.34	0.42	0.40	0.28	0.39	0.40	0.34	0.17	0.14	0.44	0.49	0.37	0.6	0.24
CaO	0.94	1.22	1.46	0.93	1.37	1.21	1.02	0.73	1.08	1.98	0.98	1.17	1.98	1.16
Na ₂ O	5.24	5.97	6.11	5.91	5.39	6.81	5.61	6.25	5.20	6.82	5.50	5.65	5.71	6.13
K ₂ O	4.12	4.36	4.39	3.98	4.09	4.79	3.88	3.59	4.27	3.02	4.20	4.15	3.95	4.19
P ₂ O ₅	0.05	0.06	0.07	0.02	0.04	0.06	0.07	0.05	0.03	0.08	0.06	0.07	0.09	0.05
L.O.I.	0.32	0.13	0.18	0.17	0.26	0.55	0.25	0.10	0.63	0.13	0.24	0.27	0.33	0.45
Total	99.73	100.09	99.99	99.15	99.01	99.77	99.10	100.19	99.78	98.92	99.59	99.09	99.02	99.69
Q	18.45	19.43		23.82	23.29	19.64	23.18	24.39	25.53		22.55	21.07		20.02
Or	23.08	25.62		23.76	24.47	28.52	23.19	21.19	25.45		24.98	24.81		25.95
Ab	38.22	43.84		41.37	42.98	49.41	42.56	44.16	39.77		45.11	43.65		45.01
An														
Na		0.18		0.81		0.78		0.72						0.36
Di	3.65	4.78		3.91	4.36	4.77	4.02	2.88	4.05		3.43	4.62		3.52
Hy	1.83	1.61		1.54	1.19	1.46	1.57	1.27				0.73		
Ac	3.35	4.95		4.94	2.81	5.1	4.8	4.91	4.05		1.52	4.15		5.09
Ht	0.74				1.06		0.16	0.38	0.46		1.75	0.41		
Il	0.47	0.42		0.36	0.35	0.48	0.48	0.38	0.38		0.42	0.38		0.44
Ap	0.11	0.14		0.05	0.1	0.14	0.17	0.17	0.07		0.14	0.17		0.12
Mn														
SPh														
Cr	83	46		34	25	6	7	2	3		7	6	73	5
Ba	247	260		283	290	308	390	82	185		383	298	283	186
Ni	40	27		27	24	5	15	14	2		14	21	39	11
Nb	110	92		94	150	54	106	119	67		96	106	125	138
Zr	2157	1028		1457	1261	337	1982	1180	1463		810	1723	1353	1296
Y	191	148		206	187	56	225	154	120		101	302	162	168
Sr	125	178		150	145	151	175	78	94		169	144	126	113
Rb	296	256		397	359	302	289	291	224		284	380	357	395
Rb/Sr	2.4	1.5		2.6	2.5	2.0	1.7	3.7	2.4		1.7	2.6	2.8	3.5
K/Rb	116	141		83	94	132	111	102	158		123	91	92	88
R/Sr	274	203		221	234	264	184	382	377		207	240	260	308
Ba/Sr	1.98	1.46		1.89	2.00	2.04	2.23	1.05	1.97		2.27	2.07	2.25	1.65
Ba/Rb	0.83	1.02		0.71	0.81	1.02	1.35	0.28	0.83		1.35	0.78	0.79	0.47
Zr/Nb	19.61	11.17		15.5	8.41	6.24	18.69	10.26	21.84		8.44	15.25	10.82	9.39
D.I.	79.75	88.89	90.57	88.95	90.75	88.57	88.92	89.74	90.75	88.45	92.64	89.53	91.29	89.48
A.I.	1.06	1.09	1.08	1.14	1.04	1.13	1.08	1.13	1.07	1.10	1.02	1.07	0.97	1.11

Table 6B. Riebeckite Granite of Habb-Aldyaheen Ring Complex

Sample

Sample #	HD5A	HD6	HD17	HD33	HD41A	HD41B	HD48	WD51	HD72	HD87	HD93	HD132A	HD141	HD152	HD53B
SiO ₂	76.41	74.64	76.74	74.65	75.14	73.64	73.08	76.80	76.37	75.44	73.56	75.29	73.51	76.14	74.52
TiO ₂	0.05	0.04	0.08	0.09	0.06	0.12	0.14	0.04	0.06	0.06	0.06	0.10	0.05	0.08	0.03
Al ₂ O ₃	10.46	12.19	9.64	11.35	11.21	11.45	11.76	11.40	10.15	11.36	11.56	10.61	12.22	10.80	12.31
Fe ₂ O ₃	4.34	3.75	5.11	3.40	3.65	3.99	3.57	2.35	4.49	3.35	3.88	3.79	3.61	3.51	2.78
MnO	0.03	0.04	0.06	0.06	0.04	0.02	0.05	0.03	0.04	0.05	0.04	0.06	0.04	0.05	0.02
HgO	-	0.04	0.02	-	-	-	-	0.06	-	-	-	-	-	0.07	-
CaO	0.10	0.07	0.19	0.32	0.15	0.16	0.15	0.19	0.05	0.20	0.03	0.16	0.22	0.21	0.15
Na ₂ O	5.15	5.56	3.96	5.43	5.52	5.71	5.77	4.94	4.73	5.48	5.74	5.19	6.25	5.18	5.93
K ₂ O	3.84	3.98	4.39	4.17	3.76	3.78	3.95	3.96	4.06	3.85	3.77	4.06	3.88	4.04	4.33
P ₂ O ₅	-	0.02	0.02	0.02	-	0.01	0.02	-	0.01	-	-	0.02	0.01	0.02	0.04
L.O.I.	0.11	0.22	0.34	0.32	0.37	0.54	0.52	0.32	0.14	0.21	0.37	0.55	0.30	0.23	0.14
-Total	100.49	100.55	99.95	99.81	99.91	99.41	98.99	100.1	100.00	99.99	99.01	99.81	100.09	100.33	100.25
Q	34.33	26.33	36.68	29.82	30.84	28.37	27.19	33.26	35.06	30.79	28.19	32.88	25.33	32.63	26.46
Or	22.53	23.50	25.89	24.77	22.32	22.59	23.7	23.46	24.00	22.80	22.59	24.17	22.98	23.90	25.48
Ab	32.10	41.22	25.09	35.34	38.99	38.28	39.09	36.68	29.62	37.08	39.01	32.2	41.34	33.01	39.56
Ms	-	0.14	0.74	1.30	1.14	1.21	1.17	0.04	1.23	0.99	1.18	1.57	1.53	-	1.28
Di	-	0.19	0.73	1.31	0.67	0.66	0.56	0.83	0.16	0.89	0.14	0.06	0.09	0.38	0.43
Hy	-	4.06	6.01	2.61	3.48	3.89	3.16	1.19	5.27	2.82	4.26	3.68	3.29	-	2.23
Ac	9.80	4.43	4.56	4.62	4.53	4.74	4.82	4.47	4.52	4.52	4.55	4.66	4.49	9.48	4.41
Mc	-	-	-	-	-	-	-	-	-	-	-	-	-	-	-
1	0.08	0.08	0.15	0.17	0.11	0.23	0.27	0.08	0.11	0.11	0.10	0.19	0.1	0.13	0.06
HM	0.94	-	-	-	-	-	-	-	-	-	-	-	-	-	-
AP	-	0.05	0.05	0.05	-	0.02	0.05	-	0.02	-	-	0.05	0.02	0.05	0.09
CF	25	10	1	35	1	9	5	3	3	3	15	2	1	7	7
Ba	5	2	19	-	17	41	32	-	46	-	20	-	9	14	14
Ni	20	18	4	7	25	15	7	-	32	8	55	11	11	-	-
Nb	15	110	75	45	61	123	35	26	15	37	160	98	98	6	6
Zr	801	4757	285	1088	4838	5080	278	244	565	920	167	1769	1769	62	62
Y	29	209	89	83	307	327	48	30	128	73	817	171	171	16	16
Sr	7	10	21	101	13	16	16	3	36	4	21	18	18	10	10
Rb	374	534	725	432	445	501	251	363	353	351	679	492	492	333	333
Rb/Sr	53	53	34	43	34	31	17	121	10	88	32	27	27	33	33
K/Rb	89	68	47	73	71	65	131	93	90	89	50	65	65	108	108
K/Sr	4743	3650	1648	3120	2415	2050	2056	11333	886	7825	1605	1789	1789	3590	3590
Ba/Sr	0.71	0.20	0.90	-	1.31	2.56	2.00	-	1.28	-	0.95	0.50	0.50	1.40	1.40
Ba/Rb	0.01	0.003	0.034	-	0.04	0.08	0.13	-	0.13	-	0.03	0.02	0.02	0.04	0.04
Zr/Nb	5	43.25	3.8	24.18	79.3	41.3	7.9	9.38	37.67	24.86	1.04	18.05	18.05	10.33	10.33
D.I.	89.51	91.05	87.66	89.93	90.07	89.25	89.98	93.39	88.68	90.66	89.78	89.25	89.65	89.82	91.1
A.I.	1.21	1.08	1.17	1.18	1.17	1.17	1.17	1.08	1.19	1.16	1.17	1.22	1.18	1.19	1.16

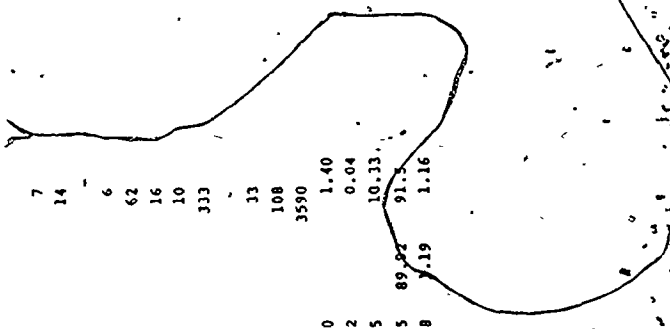


Table 6B... (Cont.)

Sample #	Sample										
	HD4	HD62	HD14	HD112	HD139	HD145	HD154	HD95	HD10	HD162	HD20A
SiO ₂	82.53	82.76	72.25	82.25	80.27	74.42	73.76	77.49	69.60	76.13	72.32
TiO ₂	0.06	0.11	0.12	0.09	0.15	0.18	0.34	0.1	0.03	0.07	0.04
Al ₂ O ₃	7.44	5.23	12.27	5.49	7.6	10.17	9.52	8.59	15.49	11.54	13.39
Fe ₂ O ₃	2.72	5.62	3.98	5.97	3.5	3.86	4.8	4.75	2.74	2.71	2.58
MnO	0.01	0.07	0.02	0.09	0.09	0.05	0.03	0.03	0.02	0.01	0.02
MgO	-	-	-	-	0.02	0.05	-	-	-	-	0.06
CaO	0.04	0.31	0.20	0.07	0.27	0.14	1.01	0.06	0.12	0.39	0.27
Na ₂ O	3.03	3.52	4.85	3.14	3.43	5.81	5.41	2.06	8.11	4.63	6.51
K ₂ O	3.29	1.97	5.61	2.52	3.35	2.73	2.77	6.43	3.51	4.12	3.71
P ₂ O ₅	-	0.01	0.02	-	0.02	0.01	0.01	0.08	0.01	0.03	0.03
L.O.I.	0.51	0.27	0.47	0.23	0.41	1.13	1.20	0.22	0.12	0.25	0.21
Total	99.63	99.87	99.79	99.83	99.10	98.55	98.85	99.85	100.05	99.88	99.14
Q	53.3	57.44	23.81	56.09	49.39	34.12	33.87	42.12	11.05	33.17	21.48
Or	19.62	11.69	28.86	14.95	20.06	16.56	16.73	38.17	20.82	24.44	22.10
Ab	20.13	16.00	36.36	14.26	20.71	38.1	34.28	8.17	60.36	36.55	48.74
NS	0.13	2.00	1.41	1.67	0.75	1.56	1.47	0.95	0.81	-	0.43
Di	0.18	1.33	0.78	0.31	1.1	0.58	4.53	-	0.48	0.57	1.03
Hy	1.97	6.64	3.79	7.93	2.83	3.72	3.00	5.7	1.97	0.57	1.52
Ac	4.55	4.68	4.72	4.62	4.84	4.99	5.44	4.65	4.44	2.44	4.50
Ht	-	-	-	-	-	-	-	-	-	1.06	-
il	0.11	0.21	0.23	0.17	0.29	0.35	0.66	0.19	0.06	0.13	0.08
AP	-	0.02	0.05	-	0.05	0.02	0.02	0.19	0.02	0.07	0.07
Cr	68	-	2	2	-	-	-	2	24	3	23
Ba	17	5	1	1	81	27	25	12	< 1	86	< 1
Ni	35	6	3	10	15	46	22	-	10	15	39
Nb	133	164	93	59	406	352	114	15	45	100	10
Zr	156	2843	136	2794	5910	9200	6209	184	38	865	67
Y	200	146	30	213	354	673	337	21	20	172	26
Sr	7	9	6	29	14	14	22	7	6	40	17
Rb	455	289	761	311	551	464	437	767	434	216	129
Rb/Sr	65	14	85	52	19	33	20	110	72	5	8
K/Rb	60	57	53	68	50	49	53	70	67	158	235
K/Sr	3914	820	4467	3500	959	1621	1045	7629	4867	855	-
Ba/Sr	2.43	0.25	0.11	0.16	2.79	1.93	1.14	1.71	0.17	2.15	0.06
Ba/Rb	-	-	0.001	-	-	-	-	0.0	0.003	0.4	-
Zr/Nb	1.17	17.35	1.46	47.36	14.56	26.14	54.46	36.80	0.84	8.65	6.70
D.I.	93.05	85.12	89.02	85.3	90.15	88.78	84.87	88.46	92.22	94.16	92.38
A.I.	1.15	1.51	1.18	1.43	1.22	1.23	1.25	1.21	1.10	1.05	1.10

APPENDIX C

MICROPROBE ANALYSES

Analyst R.L. Barnett

TABLE 1C

PLAGIOCLASES

	Samples Alb. 10, 26 (Albari granite)							
	1		1		2		2	
	Core	Rim	Core	Rim	1	Core	Inter- mediate	Rim
SiO ₂	56.79	61.02	60.14	63.93	59.17	55.11	57.05	60.86
Al ₂ O ₃	26.98	24.07	24.54	22.29	25.20	27.72	26.50	24.09
Fe ₂ O ₃	0.08	0.05	0.1	0.04	0.13	0.12	0.11	0.09
CaO	9.70	6.00	6.61	3.81	7.30	10.32	8.68	5.78
Na ₂ O	5.36	8.47	8.10	9.61	7.53	5.48	6.53	8.17
K ₂ O	0.20	0.22	0.26	0.27	0.31	0.20	0.24	0.16
BaO	0.99	0.13	0.08	0.05	0.13	0.05	0.12	0.04
Total	99.20	99.97	99.82	99.99	99.73	99.02	99.22	99.10
Ab	49.43	70.91	67.79	80.73	63.95	48.49	58.87	71.35
Or	1.14	1.30	1.56	1.56	1.84	1.09	1.35	0.81
An	49.43	27.79	30.65	17.71	34.21	50.42	41.78	27.64

TABLE 2C

PLAGIOCLASES

Samples Als 4	(Alse-Hairah granite)								
	1	2 Core	2 Rim	3 Core	3 Rim	4 Rim	4 Int I	4 Int II	5 Center
SiO ₂	64.89	66.24	65.41	68.12	64.45	64.52	64.58	64.71	64.58
Al ₂ O ₃	21.08	20.88	20.65	19.64	21.67	21.72	21.32	21.38	21.50
Fe ₂ O ₃	0.16	0.19	0.21	0.13	0.23	0.27	0.32	0.39	0.30
CaO	2.69	2.14	2.24	0.29	3.37	3.42	3.14	3.05	3.47
Na ₂ O	10.00	10.57	10.45	11.62	9.18	9.50	9.77	9.05	8.87
K ₂ O	0.43	0.41	0.30	0.20	0.54	0.75	1.05	1.36	1.23
BaO	0.08	0.05	0.21	0.07	0.10	0.07	0.11	0.09	0.09
Total	99.32	100.48	99.33	100.07	99.54	100.25	100.29	100.02	100.04
Ab	85.90	87.88	88.22	97.66	80.65	79.89	80.15	77.87	76.47
Or	1.33	2.33	1.57	1.04	2.99	4.18	5.59	7.73	6.95
An	12.77	9.79	10.21	1.30	16.36	15.93	14.26	14.40	16.58

TABLE 4C

PLAGIOCLASES

Sample HD171	(Microgranite Hadb-Aldyaheen)							
	1	3 Rim	3 Core	4	5	6	7	8
SiO ₂	68.88	68.44	67.16	68.19	68.52	67.55	67.97	69.93
Al ₂ O ₃	19.38	19.42	19.53	19.16	19.73	19.57	19.95	19.95
Fe ₂ O ₃	0.14	0.13	0.00	0.09	0.00	0.08	0.07	0.11
CaO	0.03	0.11	0.16	0.03	0.19	0.34	0.61	0.34
Na ₂ O	11.39	11.96	11.93	11.71	11.13	11.91	11.27	9.13
K ₂ O	0.16	0.16	0.07	0.14	0.11	0.11	0.14	0.48
BaO	0.05	0.07	0.10	0.05	0.06	0.09	0.01	0.04
Total	100.04	100.28	98.95	99.36	99.73	99.75	100.02	99.98
Ab	98.95	98.62	98.9	49.1	84.4	97.86	96.34	94.82
Or	0.92	0.87	0.38	0.76	0.63	0.59	0.79	3.22
An	0.13	0.51	0.72	0.13	0.93	1.55	2.86	1.96

TABLE 5C

PLAGIOCLASESSample HD9 (Granite Porphyry of Hadb-Aldyaheen)

	<u>1</u>	<u>2</u>	<u>3</u>	<u>4</u>	<u>5</u>	<u>6</u>
SiO ₂	68.62	69.20	69.01	68.98	69.56	68.98
Al ₂ O ₃	18.33	18.97	18.96	18.80	18.92	18.86
Fe ₂ O ₃	0.77	0.82	0.90	0.89	0.59	0.84
CaO	0.55	0.03	0.05	0.04	0.03	0.03
Na ₂ O	11.05	11.21	11.49	11.13	11.27	11.31
K ₂ O	0.20	0.16	0.13	0.21	0.23	0.20
BaO	0.07	0.09	0.13	0.09	0.10	0.05
Total	99.10	100.48	100.67	100.15	100.69	100.26
Ab	98.54	98.93	98.96	98.71	98.51	98.78
Or	1.11	0.93	0.80	1.10	1.35	1.08
An	0.35	0.14	0.24	0.19	0.14	0.14

TABLE 6C
PLAGIOCLASES

Sample HD10	(Riebeckite granite of Hadb-Aldyaheen)						
	1	2	3	4	5	6	7
SiO ₂	68.54	68.29	68.58	67.55	68.97	68.26	68.29
Al ₂ O ₃	18.56	18.51	18.56	18.67	18.29	18.63	18.19
Fe ₂ O ₃	0.94	1.11	1.10	0.96	1.15	1.21	1.29
CaO	0.02	0.02	0.02	0.03	0.02	0.03	0.04
Na ₂ O	10.93	10.62	11.05	10.74	11.17	10.98	10.68
K ₂ O	0.17	0.16	0.16	0.22	0.11	0.13	0.14
BaO	0.11	0.09	0.05	0.05	0.10	0.11	0.14
Total	99.26	98.80	99.52	98.22	99.82	99.35	98.76
Ab	98.88	98.90	98.95	98.52	99.26	99.08	98.97
Or	1.01	0.98	0.94	1.34	0.63	0.78	0.83
An	0.11	0.12	0.11	0.14	0.11	0.14	0.20

TABLE 7C

PLAGIOCLASES

 Sample HD 26 (Riebeckite Granite of Hadb-Aldyaheen)

	<u>1</u>	<u>2</u>	<u>3</u>	<u>4</u>	<u>5</u>	<u>6</u>
SiO ₂	68.02	68.45	67.98	68.61	68.98	68.41
Al ₂ O ₃	18.30	18.82	18.89	18.71	18.71	18.71
Fe ₂ O ₃	1.12	1.02	0.97	1.01	0.98	1.04
CaO	0.03	0.02	0.02	0.02	0.02	0.02
Na ₂ O	12.11	11.75	12.19	11.99	12.14	11.91
K ₂ O	0.14	0.24	0.18	0.14	0.28	0.19
BaO	0.03	0.05	0.05	0.07	0.03	0.09
Total.	99.72	100.35	100.29	100.54	101.16	100.36
Ab	99.11	98.57	98.94	99.13	98.42	98.87
Or	0.76	1.33	0.96	0.77	1.48	1.03
An	0.13	0.10	0.11	0.10	0.10	0.10

TABLE 8C

MICROGLINESample HD10 (Riebeckite granite of Hadb-Aldyaheen)

	<u>.1</u>	<u>2</u>	<u>3</u>	<u>4</u>	<u>4</u>	<u>5</u>	<u>6</u>
SiO ₂	64.34	64.29	65.96	64.81	65.12	65.73	65.22
Al ₂ O ₃	17.93	18.15	17.63	17.76	18.16	18.00	17.93
Fe ₂ O ₃	0.74	0.38	0.71	0.85	0.65	0.73	0.76
MgO	0.03	0.01	-	0.02	-	-	0.07
CaO	-	-	-	-	-	-	-
Na ₂ O	0.46	0.71	0.57	0.48	0.72	1.04	0.54
K ₂ O	16.39	15.64	15.98	16.35	16.27	15.35	16.02
Total	99.89	99.18	100.85	100.26	100.92	100.85	100.54
Or	96.13	93.79	94.94	95.61	93.52	91.06	94.97
Ab	3.87	6.21	5.06	4.39	6.48	8.94	5.03

TABLE 9C

MICROCLINE

Sample HD26	(Riebeckite granite of Hadb-Aldyaheen)					
	1	2	3	4	5	6
SiO ₂	65.62	65.55	64.77	65.33	66.45	65.44
Al ₂ O ₃	17.76	17.49	17.19	17.79	17.38	17.56
Fe ₂ O ₃	0.75	0.64	0.70	0.67	0.71	0.81
MgO	0.03	0.07	0.04	0.03	0.04	0.04
CaO	-	-	-	-	-	-
Na ₂ O	0.71	0.72	0.55	0.67	0.72	0.76
K ₂ O	15.56	15.59	16.10	15.58	15.14	15.24
Total	100.43	100.06	99.34	100.07	100.43	99.85
Or	93.75	93.23	95.00	93.75	93.06	93.11
Ab	6.25	6.77	5.00	6.25	6.94	6.89

TABLE 11C

Plagioclase Baths in Quartz and in Microcline

Sample JS.40	(Riebeckite granite of Jabal Sayid)								
	Plag in Qtz			Plag in Microcline					
	1	2	3	1	2	3	4	5	6
SiO ₂	68.84	69.30	69.61	68.57	68.32	68.26	58.36	69.43	68.87
Al ₂ O ₃	18.71	19.05	18.73	19.06	18.89	19.39	19.21	19.42	19.05
Fe ₂ O ₃	1.00	0.97	0.95	0.93	0.79	0.01	0.09	0.05	0.82
MgO	0.04	0.02	0.02	0.00	0.00	0.05	0.06	0.03	0.03
CaO	0.00	0.00	0.01	0.00	0.00	0.00	0.03	0.00	0.00
Na ₂ O	11.13	10.76	10.60	11.25	11.22	11.27	11.90	11.28	11.00
K ₂ O	0.10	0.18	0.14	0.14	0.18	0.06	0.05	0.09	0.17
Total	99.81	100.29	99.46	99.95	99.40	99.63	99.70	100.30	99.91
Ab	99.45	98.86	99.07	99.18	98.90	99.73	99.61	99.45	98.88
Or	0.55	1.14	0.87	0.82	1.10	0.27	0.26	0.55	1.12
An	0.00	0.00	0.06	0.00	0.00	0.00	0.13	0.00	0.00

TABLE 12C

Plagioclase Laths in Quartz

Sample JS.41 (Riebeckite granite of Jabal Sayid)

	<u>1</u>	<u>2</u>	<u>3</u>	<u>4</u>	<u>5</u>	<u>6</u>
SiO ₂	69.54	68.07	68.79	68.79	68.28	68.75
Al ₂ O ₃	18.86	18.81	19.03	19.00	18.73	18.89
Fe ₂ O ₃	0.90	0.98	0.47	0.90	0.95	0.89
MgO	0.02	0.00	0.02	0.05	0.04	0.01
CaO	0.02	0.02	0.02	0.01	0.00	0.01
Na ₂ O	10.27	10.86	12.16	10.79	11.40	10.61
K ₂ O	0.10	0.10	0.16	0.09	0.12	0.11
Total	99.70	98.86	100.66	99.60	99.52	99.27
Ab	99.25	99.29	99.04	99.40	99.32	99.28
Or	0.63	0.59	0.86	0.54	0.67	0.66
An	0.12	0.11	0.10	0.06	0.00	0.06

TABLE 13C

Plagioclase Laths in MicroclineSample JS.41(Riebeckite granite of Jabal Sayid)

	<u>1</u>	<u>2</u>	<u>3</u>	<u>4</u>	<u>5</u>
SiO ₂	68.84	69.14	68.07	69.11	68.82
Al ₂ O ₃	19.08	19.20	19.38	19.53	18.80
Fe ₂ O ₃	0.39	0.26	0.03	0.01	0.80
MgO	0.04	0.01	0.01	0.03	0.00
CaO	0.01	0.00	0.00	0.00	0.02
Na ₂ O	10.71	11.12	11.00	11.07	11.06
K ₂ O	0.18	0.15	0.05	0.06	0.14
Total	99.25	99.88	98.55	99.80	99.65
Ab	98.86	99.12	99.69	99.64	99.06
Or	1.08	0.88	0.31	0.36	0.82
An	0.06	0	0	0	0.11

TABLE 14C

Plagioclases in Groundmass Associated with Hematite

Sample JS.41C	(Riebeckite granite of Jabal Sayid)					
	1	2	3	4	5	6
SiO ₂	67.80	68.73	67.79	69.73	68.67	69.30
Al ₂ O ₃	19.18	18.42	18.54	18.74	18.83	19.33
Fe ₂ O ₃	0.26	0.81	1.16	1.02	0.83	0.40
MgO	0.04	0.02	0.02	0.04	0.02	0.04
CaO	0.01	0.01	0.01	0.00	0.01	0.00
Na ₂ O	11.17	10.56	10.75	11.05	10.52	11.36
K ₂ O	0.37	0.16	0.14	0.11	0.14	0.14
Total	98.82	98.72	98.41	100.69	99.02	100.46
Ab	97.83	98.95	99.08	99.36	99.07	99.70
Or	2.12	0.99	0.85	0.64	0.87	0.30
An	0.05	0.06	0.06	0.00	0.06	0.00

TABLE 15C

MICROCLINE

Sample JS.13 (Riebeckite granite of Jabal Sayid)

	<u>1</u>	<u>2</u>	<u>3</u>	<u>4</u>	<u>5</u>	<u>6</u>
SiO ₂	65.03	64.96	64.60	65.08	64.96	64.57
Al ₂ O ₃	17.80	18.02	18.16	17.43	17.54	17.40
Fe ₂ O ₃	6.46	0.70	0.53	0.93	0.85	0.86
MgO	-	-	-	0.03	0.23	0.04
CaO	-	-	-	-	-	-
Na ₂ O	0.35	0.26	0.40	0.41	0.84	0.48
K ₂ O	16.28	16.25	15.88	16.43	16.25	16.43
Total	99.92	100.19	99.57	100.33	100.68	99.79
Or	96.92	97.73	96.29	96.51	92.74	95.88
Ab	3.08	2.27	3.71	3.59	7.26	4.12

TABLE 16C

MICROCLINE

Sample JS.41 (Riebeckite granite of Jabal Sayid)

	<u>1</u>	<u>2</u>	<u>3</u>	<u>4</u>	<u>5</u>
SiO ₂	64.58	65.11	64.67	65.14	64.09
Al ₂ O ₃	17.96	18.03	18.17	18.34	18.39
Fe ₂ O ₃	-	-	-	-	0.08
MgO	0.04	0.03	0.02	0.05	0.02
K ₂ O	16.76	17.04	16.02	15.66	15.98
Na ₂ O	0.18	0.20	0.35	0.25	0.32
Total	99.52	100.42	99.23	99.44	98.82
Or	98.34	98.37	96.87	97.65	97.14
Ab	1.66	1.63	3.13	2.35	2.86

BIBLIOGRAPHY

- Aleksiyev, E.I. 1970. Genetic significance of the rare-earth elements in the younger granites of Northern Nigeria and the Cameroons. *Geochemistry International*, 127-132. Tran. from *Geokhimiya*, No. 2, pp. 192-198, 1970.
- Al-Shanti, A.M.S., Mitchell, A.H.G. 1976. Late Precambrian subduction and collision in the Al-Amar Idsas region, Arabian Shield, Kingdom of Saudi Arabia. *Tectonophysics*, 30, pp. 41-43.
- Armstrong, R.L., Taubeneck, W.H. and Hales, O.P., 1977. Rb-Sr and K-Ar geochronology of Mesozoic granitic rocks and their Sr isotopic composition, Oregon, Washington, and Idaho. *Geol. Soc. Am. Bull.* 88, pp. 397-411.
- Bailey, D.K. and MacDonald, R. 1969. Alkali feldspar fractionation trends and the derivation of peralkaline liquids. *Am. J. Sci.* 267, pp. 242-248.
- _____ 1966. The system $\text{Na}_2\text{O}-\text{Al}_2\text{O}_3-\text{Fe}_2\text{O}_3-\text{SiO}_2$ at 1 atmosphere and the petrogenesis of alkaline rocks. *J. Petrol.* 7, pp. 114-170.
- Balashov, Yu. A. 1963. Regularities in the distribution of the Rare Earths in the Earth's Crust. *Geochemistry*, 2, pp. 107-122.

- Bakor, A.R., Gass, I.G. and Neary, C.R. 1976. Jabal Al-Wask, Northwest Saudi Arabia: An eocambrian back-arc ophiolite; *Earth Planetary Sci. Letters* 30, pp. 1-9.
- Barth, T.F.W., 1962. *Theoretical Petrology*, Wiley, New York.
- Barker, D.S., Long, L.E., Hoops, G.K. and Hodges, F.N. 1977. The petrogly and Rb-Sr isotope geochemistry of intrusions in the Diablo Plateau, northern Trans-Pecos magmatic Province, Texas and New Mexico. *Geol. Soc. Am. Bull.* 88, pp. 1437-1446.
- Bateman, P.C. and Dodge, F.C.W. 1970. Variations of major chemical constituents across the Central Sierra Nevada Batholith. *Geol. Soc. America Bull.* 81, pp. 409-420.
- Black, R. and Girdo, M. 1970. Late Paleozoic to recent igneous activity in west Africa and its relationship to basement structure. In African magmatism and tectonics. (Clifford, T.N. and Gass, I.G., eds.). Oliver and Boyd, pp. 185-210.
- Borley, G.D., R.D. Beckinsale, P. Suddaby and J.J. Durham. 1976. Variations in composition and $\delta^{18}\text{O}$ values within the Kaffo albite-riebeckite granite of Liruëi complex, younger granites of Nigeria. *Chemical Geology*, 18, pp. 297-308.
- Bowden, P. 1966. Zirconium in younger granites of Northern Nigeria. *Geochim. Cosmochim. Acta*, 30, pp. 985-993.

- Bowden, P. 1970. Origine of the Younger Granites of Northern Nigeria. *Contrib. Mineral. Petrol.* 25, pp. 153-162.
- _____ and Breemen, O.V. 1970. Isotopic and chemical studies on younger granites from Northern Nigeria. In African Geology. Dessauvague, T.F.J. and Whiteman, A.J. (Eds.). Univ. of Ibadan. pp. 105-122.
- Brown, G.C., Fyfe, W.S. 1970. The production of granitic melt during ultrametamorphism. *Contrib. Mineral. and Petrol.* 28, pp. 310-318.
- _____. 1973. Evolution of granite magmas at destruction plate margins. *Nature Physical Science*, 241, pp. 26-28.
- _____ and Bowden, P. 1973. Experimental Studies concerning the Genesis of the Nigerian younger granites. *Contr. Mineral. and Petrol.* 40, pp. 131-139.
- _____. 1978. Calc-alkaline magma genesis: The Pan-African contribution to crustal growth. In: Evolution and Mineralization of the Arabian-Nubian Shield (Symposium), Institute of Applied Geology, King Abdulaziz University, Jeddah, Saudi Arabia (in press).
- _____. 1977. Mantle origin of Cordilleran granites. *Nature*. 265, pp. 21-24.
- _____ and Hennessy, J. 1978. The initiation and thermal diversity of granitic magmatism. *Phil. Trans. R. Soc. Lond. A*, 1978 (in press).

- Brown, G.F. and Jackson, R.O. 1960. The Arabian Shield, Proc. Internat. Geol. Cong., 21st Copenhagen Rept. Pt. 9, 69-77.
- Brown, G.F., Jackson, R.O., Bogue, R.G., and Maclean, W.H. 1962. Geologic map of the southern Hijaz Quadrangle, Kingdom of Saudi Arabia. U.S.G.S. Misc. Geol. Inv. Map I-210A.
- _____. 1972. Tectonic map of the Arabian Peninsula (1:4,000,000). Saudi Arabian Dir. Gen. Mineral Resources, Arabian Peninsula Map AP.2.
- _____ and Coleman, R.G. 1972. The tectonic framework of the Arabian Peninsula; Internat. Geol. Cong., 24th Montreal Rept., 3, pp. 300-305.
- Brown, G.M. 1963. Melting relations of tertiary granitic rocks in Skye and Rhum. Mineral. Mag. 33, pp. 533-562.
- Butler, J.R. and Smith, A.Z. 1962. Zirconium, niobium and certain other trace elements in some alkali igneous rocks. Geochim. Cosmochim. Acta 26, pp. 945-953.
- _____, Bowden, P. and Smith, A.Z. 1962. K/Rb ratios in the evolution of the younger granites of Northern Nigeria. Geochim. Cosmochim. Acta, 26, pp. 89-100.
- _____, and Thompson, A.G. 1965. Zirconium hafnium ratios in some igneous rocks. Geochim. Cosmochim. Acta. 29, pp. 167-175.

- Carmichael, I.S.E., Turner, F.J., Verhoogen, J. 1974.
Igneous Petrology. McGraw Hill, New York. 739 p.
- Chapman, R.W. 1942. Ring structures of the Pliny region,
New Hampshire. Geol. Soc. Am. Bull. 53, pp. 1533-
1568.
- Clifford, T.N. 1970. The structural framework of Africa.
In: African Magmatism and Tectonics (Clifford
, T.N. and Gass, I.G., eds.). Oliver and Boyd.
- Cobbing, E.J. and Pitcher, W.S. 1972. The coastal batholith
of central Peru. Jour. Geol. Soc. London, 128,
pp. 421-460.
- Deer, W.A., Howie, R.A. and Zussman, J. 1966. An introduc-
tion to the rock forming minerals. Longman, 528 p.
- Demine, A.M. and Khitarov, D.N. 1958. Geochemistry of
potassium, rubidium and thallium in application
to problems in petrology. Geochemistry 5, pp. 721-
734.
- Dewey, J.F. and Burke, K.C.A. 1973. Tibetan, Variscan,
and PreCambrian basement reactivation: products
of continental collision. J. Geol. 81, pp. 683-
692.
- Edgar, A.D. 1977. A comment on apacity revisited: pattern
recognition in the chemistry of nepheline syanite
rocks by Dagbert et al. Geochim. Cosmochim. Acta
41, pp. 439-440.

Essawy, M.A. 1972. Petrogenesis of alkaline rhyolites and microgranites from Samadai-Tunduba area, Eastern Desert. Ann. Geol. Survey of Egypt. II, pp. 239-250.

Fleck, R.J., Coleman, R.G., Cornwall, H.R., Greenwood, W.R., Hadely, D.G., Prinz, W.C., Ratte, J.C. and Schmidt, D.L. 1976. Potassium-Argon geochronology of the Arabian Shield, Kingdom of Saudi Arabia. Geol. Soc. Am. Bull. 87, pp. 9-21.

Freeth, S.J. 1970. The petrogenesis of the younger granites of Northern Nigeria and Southern Nigeria. In African Geology. Dessauvage, T.F.J. and Whiteman, A.J. (Eds.). University of Ibadan. pp. 121-126.

Friesch, W. and Al-Shanti, A. 1977. Ophiolite belts and the collision of island arcs in the Arabian Shield. Tectonophysics, 43. pp. 293-306.

Fyfe, W.S., Turner, F.J., Verhoogen, J. 1958. Metamorphic reaction and metamorphic facies. Geol. Soc. Am. Memoir 73; 259 pp.

Fyfe, W.S. 1970. Some thoughts on granitic magmas, in G. Newall and N. Rast (eds.), Mechanics of Igneous Intrusion. Gallery Press, Liverpool, pp. 201-216.

_____, and Brown, G.C. 1972. Granites Past and Present. Jour. of Earth Sci. 8, pp. 249-260.

_____. 1973. The generation of batholiths. Tectonophysics. 17, pp. 273-283.

- Fyfe, W.S. and McBirney, A.R. 1975. Subduction and the structure of andesitic volcanic belts. *Am. Journ. of Sci.* 275A, pp. 285-297.
- _____, 1977. Cordilleran granites: production of geosphere mixing. Comment on G.C. Brown's "Mantle Origin of Cordilleran Granite". *Nature* (in press).
- _____, 1978. The tectonic significance of granite magmatism. In: *Evolution and Mineralization of the Arabian Nubian Shield (Symposium)*. Institute of Applied Geology, King Abdulaziz University, Jeddah, Saudi Arabia (in press).
- Garson, M.S. and Shalaby, I.M. 1974. PreCambrian-Lower Paleozoic plate tectonics and metallogenesis in the Red Sea region. In: *Symposium on Metallogeny and Plate Tectonics*. Geol. Assoc. Canada, Mineralogy Assoc. Canada, Mtg., 1974, St. John's Newfoundland.
- Gass, I.G. 1977. The evolution of the Pan-African crystalline basement in NE Africa and Arabia. *J. Geol. Soc. Lond.* 134, pp. 129-138.
- Gerasimovskii, V.T. 1956. Geochemistry and mineralogy of nepheline syenite intrusions. *Geochemistry*, 5, pp. 494-510.
- _____, Kakhana, M.M., Rodionova, L.M. and Venkina, V.A. 1959. On the geochemistry of niobium and tantalum in the Lovozero alkalie massif. *Geochemistry*, 7, pp. 803-812.

- Gerasimovskii, V.T., Tuzova, A.M. and Shevaleyvskii, J.D.
1962. Zirconia-hafnia ratio in minerals and rock
of the Lovozero massif. *Geochemistry* 6, pp. 585-
592.
- Giggenbach, W.F. and Glasby, G.P. 1977. New Zealand D.S.I.R.
Bull. 218, pp. 121-126.
- Gilluly, J. 1969. Oceanic sediment volumes and continental
drift. *Science*, 166, pp. 992-994.
- Goldsmith, R. 1971. Mineral resources of the Southern
Hijaz quadrangle, Kingdom of Saudi Arabia, Saudi
Arabian Dir. Gen. Mineral. Resources Bull. 5,
62 pp.
- _____ and Koutner, J.H. 1971. Geology of the Madh-
Adh-Dhahab-Umm Ad-Damar Area, Kingdom of Saudi
Arabia, Saudi Arabian Dir. Gen. Mineral Resources
Bull. 6, 19 pp.
- Greenwood, W.R. and Brown, G.F. 1973. Petrology and chemical
analysis of selected plutonic rocks from the Arabian
Shield, Kingdom of Saudi Arabia, Saudi Arabian Dir.
Gen. Mineral Resources, Bull. 9, 9 pp.
- _____, Hadley, D.G. and Schmidt, D.C. 1973. Tecto-
nostratigraphic subdivision of precambrian rocks
in the southern part of the Arabian Shield (abs.).
Geol. Soc. Am. Abstracts with Programs, v. 5, p. 643.

- Greenwood, W.R., Hadley, D.G., Anderson, R.E., Fleck, R.J. and Schmidt, D.C. 1976. Late proterozoic cratonization in southwestern Saudi Arabia. Phil. Trans. R. Soc. Lond. A. 280, 517-527.
- Greenwood, R. 1951. Younger intrusive rocks of Plateau Province, Nigeria, compared with alkali rocks of New England. Geol. Soc. Am. Bull. 62, pp. 1151-1178.
- Hanson, G.N. 1978. The application of trace elements to the petrogenesis of igneous rocks of Granitic composition. Earth Planetary Sci. Lett. 38, pp. 26-44.
- Hyndman, D.W. 1972. Petrology of igneous and metamorphic rocks. International Series in the Earth and Planetary Sciences, New York. McGraw-Hill, 533 p.
- Irvine, T.N. and Baragar, W.R.A. 1971. A guide to the chemical classification of the common volcanic rocks. Canad. Jour. Earth Sci. 8, pp. 523-548.
- Jacobson, R.R.E., Macleod, W.N. and Black, R. 1958. Ring complexes in the Younger granite province of Northern Nigeria. Mem. Geol. Soc. Lond. 1, 72 p.
- Kempe, D.R.C. 1973. The petrology of Warsak alkaline granites, Pakistan, and their relationship to other alkaline rocks of the region. Geol. Mag. 110 (No. 5), pp. 385-495.

Korringa, M.K. and Noble, D.C. 1972. Genetic significance of chemical, isotopic, and petrographic features of some peralkaline salic rocks from the Island of Pantellria. *Earth Planet. Sci. Lett.*, 17, pp. 258-262.

Kovalenko, V.I., Znamenskaya, A.S., Popolitov, E.I., and Abramova, S.R. 1969. Distribution of the rare earth elements and yttrium in minerals of alkalic granitoids. *Geochemistry*, pp. 790-798. Trans. from *Geokhimiya*, no. 8, pp. 997-1006.

Lemlein, C.G. and P.V. Klevstov. 1961. Relations among the principal thermodynamic parameters in part of the system $H_2O-NaCl$. *Geochemistry*, 2, pp. 148-158.

Macdonald, R. 1969. The petrology of alkaline dykes from the Tugtutoq area, south-Greenland. *Geol. Soc. Denmark Bull.*, v. 19, pp. 257-282.

MacCarthy, T.S. and Hasty, R.A. 1976. Trace element distribution patterns and their relationships to the crystallization of granitic melt. *Geochim. Cosmochim. Acta*, 40, pp. 1351-1358.

Marsh, J.S. 1976. Distribution of Ca in highly fractionated peralkaline magmas. *Earth and Planetary Science Letters*, 31, pp. 153-160.

Marzouki, F. and Fyfe, W.S. 1977. Pan-African Plates: additional evidence from igneous events in Saudi Arabia. *Contr. Mineral and Petrol.* 60, pp. 219-224.

- Mason, B. 1966. Principles of Geochemistry. 3rd Ed. Toppan Co., Ltd., Japan. 329 p.
- Molnar, P. and Tapponnier, P. 1977. The collision between India and Eurasia. *Sci. Amer.* 236, pp. 30-42.
- Muehlenbachs, K. and R.N. Clayton. 1972. Oxygen isotope geochemistry of submarine greenstones. *Canadian Jour. Ear. Sci.* 9, pp. 471-478.
- Nasseef, A.Q. 1971. The geology of northeastern At-Taif area, Saudi Arabia. Unpubl. Ph.D. Thesis, University of Leeds.
- _____, and Gass, I.G. 1977. Granitic and metamorphic rocks of the Taif area, western Saudi Arabia. *Geol. Soc. Am. Bull.* 88, pp. 1721-1730.
- Neary, C.R., Gass, I.G. and Cavanagh, B.J. 1976. Granitic association of northwestern Sudan. *Geol. Soc. Am. Bull.* 87, 1501-1512.
- Noble, D.G., Korringa, M.K., Hedge, C.E. and Riddle, G.O. 1972. Highly differentiated subalkaline rhyolite from Glass Mountain, Mono County California. *Geol. Soc. Am. Bull.* 83, 1179.
- Nockolds, S.R. 1954. Average chemical composition of some igneous rocks. *Geol. Soc. Am. Bull.* 65, pp. 1007-1032.
- _____, and Allen, R. 1953. The geochemistry of some igneous rock series. *Geochim. Cosmochim. Acta.* 4, pp. 105-142.

- Nockolds, S.R. and Allen, R. 1954. The geochemistry of some igneous rock series. *Geochim. Cosmochim. Acta.* 5, pp. 245-285.
- Norish, K. and Chappell, J. 1967. X-ray fluorescence spectrography, In: Zussman, J., Ed., Physical Methods in Determinative Mineralogy, Academic Press, London, pp. 161-214.
- _____ and Hutton, J.T. 1969. An accurate x-ray spectrographic method for the analysis of a wide range of geological samples. *Geochim. Cosmochim. Acta.* 33, pp. 431-453.
- O'Connor, J.T. 1966. A classification for quartz-rich igneous rocks based on feldspar ratios; in *Geol. Surv. Res. 1965; U.S. Geol. Surv. Prof. Paper* 525-B, pp. 79-84.
- Peacock, M.A. 1931. Classification of igneous rocks. *Jour. Geol.* 39, pp. 54-67.
- Pearce, J.A. and Cann, J.R. 1977. Identification of ore-deposition environment from trace-element geochemistry of associated igneous host rocks. In: Volcanic Processes in Ore Genesis, Spec. Publ. Inst. Min. and Metall. Geol. Soc. London, pp. 14-24.
- Pitcher, W.S. 1974. The Mesozoic and Cenozoic batholiths of Peru. *Pacific Geology*, 8, pp. 51-62.
- Poldervaart, A. 1956. Zircon in rocks. 2. Igneous rocks. *Am. J. Sci.* 254, pp. 521-554.

- Radain, A.A. and Kerrich, R. 1978. Peralkaline granites in the Western part of the Arabian Shield, Saudi Arabia. In: Evolution and Mineralization of the Arabian-Nubian Shield (Symposium). Institute of Applied Geology, King Abdulaziz University, Jeddah, Saudi Arabia (in press).
- Ramberg, H. 1970. Model studies in relation to intrusion of plutonic bodies, In: Mechanisms of Igneous Intrusion, Ed., Newall, G. and Rast, N., Geol. Jour. Spec. Issue 2, Liverpool, Gallery Press, pp. 261-286.
- Ringwood, A.E. 1955. The principles governing trace element distribution during magmatic crystallization. Geochim. Cosmochim. Acta 7, 189-202, 242-254.
- Roedder, E. 1967. Fluid inclusions as samples of ore fluids. In: H.L. Barnes (Ed.), The Geochemistry of Hydrothermal Ore Deposits. Holt, Rinehart and Winston, New York, pp. 515-574.
- _____. 1972. Chapter J.J. Composition of Fluid Inclusions. In: Data of Geochemistry, Sixth Edition. Geol. Survey, Professional Paper 440-JJ.
- Rooke, J.M. 1970. Geochemical variations in African granitic rock and their structural implications. In: Clifford, T.N. and Gass, I.G. (Eds.) African Magmatism and Tectonics. Oliver & Boyd, Edinburgh, 355-417.

- Schmidt, D.L., Hadley, D.G., Greenwood, W.R., Coleman, R.G., Gonzalez, L. and Brown, G.F. 1973. Stratigraphy and tectonism of the southern part of the pre-cambrian Shield of Saudi Arabia. Saudi Arabian Dir. Gen. Mineral Res. Bull. 8, 13 p.
- Shackleton, R.M. 1976. Pan-African Structures. Phil. Trans. Roy. Soc. London. Ser A280, pp. 491-497.
- Shand, S.J. 1949. Eruptive Rocks. New York, John Wiley & Sons, Inc., 488 p.
- Siedner, G. 1965. Geochemical features of a strongly fractionated alkali igneous suite. Geochim. Cosmochim. Acta, 29, 113-137.
- Simpson, E.S.W. 1954. On the graphical representation of differentiation trends in igneous rocks. Geol. Mag. 91, pp. 238-244.
- Streckeisen, A.L. 1967. Classification and nomenclature of igneous rocks (final report of inquiry); N. Jahrb. Mineral. Abh, 197, pp. 144-240.
- Tauson, L.V. 1967. Geochemical behaviour of rare elements during crystallization and differentiation of granitic magma. -Geochem. Int. 4, pp. 1067-1075.
- Taylor, S.R., Emeleus, C.H. and Exley, C.S. 1956. Some anomalous K/Rb ratios in igneous rocks and their petrological significance. Geochim. Cosmochim. Acta, 10, pp. 224-229.
- Taylor, S.R. 1966. The application of trace element data to problems in petrology. Physics and Chemistry of the Earth, v. 5, 133-213.

- Taylor, H.P. 1968. The oxygen isotope geochemistry of igneous rocks. *Contributions to Mineralogy and Petrology*, 19, pp. 1-71.
- _____ 1974. The application of oxygen and hydrogen isotope studies to problems of hydrothermal alteration and ore deposition. *Econ. Geol.* 69, pp. 843-883.
- _____ and B. Turi. 1976. High-¹⁸O igneous rocks from the Tuscan magmatic province, Italy. *Contributions to Mineralogy and Petrology*, 55, pp. 33-54.
- _____ 1977. Water/rock interactions and the origin of H₂O in granitic batholiths. *Jl. Geol. Soc. Lond.* 133, pp. 509-558.
- _____ 1978. Oxygen and hydrogen isotope studies of plutonic granitic rocks. *Earth. Planet. Sci. Lett.*, 38, pp. 177-210.
- Teng, H.C. and Strong, D.F. 1976. Geology and geochemistry of the St. Lawrence peralkaline granite and associated fluorite deposits, Southeast Newfoundland. *Canad. J. Earth Sci.*, vol. 13, No. 10, pp. 1374-1385.
- Thornton, C.P. and Tuttle, O.F. 1960. Chemistry of igneous rocks. I. Differentiation index. *Am. Jour. Sci.*, v. 258, pp. 664-684.
- Turner, D.C. 1963. Ring-structures in the Sara-Fier Younger granite complex, Northern Nigeria. *J. Geol. Soc. Lond.* 119, pp. 345-366.

- Tuttle, O.F. and Bowen, N.L. 1958. Origin of granite in the light of experimental studies in the system $\text{NaAlSi}_3\text{O}_8$ - KAlSi_3O_8 - SiO_2 - H_2O . Geol. Soc. Am. Mem. 74, 153 pp.
- Wager, L.R. and Mitchell, R.L. 1951. *The distribution of trace elements during strong fractionation of basic magma. Geochim. Cosmochim. Acta. 1, pp. 129-208.
- Wenner, D.B. and H.P. Taylor. 1976. Oxygen and hydrogen isotope studies of a precambrian granite-rhyolite terrane, St. Francois Mountains, southeastern Missouri. Geological Soc. Amer. Bull. 87, pp. 1587-1598.
- Wilson, A.D. 1955. A new method for determination of ferrous iron in rocks and minerals. Great Britain Geol. Surv. Bull. 9, pp. 56-58.
- Wright, J.B. 1969. A simple alkalinity ratio and its application to questions of non-orogenic granite genesis. Geol. Mag. 106 (No. 4), pp. 370-384.
- Yes'kova, E.M. and Yefimov, A.F. 1970. Distribution of rare elements in the apofessive alkalic meta-somatites of the Urals. Geochemistry International 5. Tran. From Geokhimiya, No. 9, pp. 1027-1041, 1970.